ZooKeys 904: 1–22 (2020)
doi: 10.3897/zookeys.904.37609
http://zookeys.pensoft.net

RESEARCH ARTICLE

A peer-reviewed open-access journal
ZooKeys
Launched to accelerate biodiversity research

A new species of *Boholina* (Crustacea, Copepoda, Calanoida) and a first record for stygobiotic calanoid fauna from a cave in Thailand

Chaichat Boonyanusith[1], Koraon Wongkamhaeng[2], Sujeephon Athibai[3]

1 *School of Biology, Faculty of Science and Technology, Nakhon Ratchasima Rajabhat University, Nakhon Ratchasima 30000, Thailand* **2** *Department of Zoology, Faculty of Science, Kasetsart University, Bangkok 10900, Thailand* **3** *Applied Taxonomic Research Center and Department of Biology, Faculty of Science, Khon Kaen University, Khon Kaen 40002, Thailand*

Corresponding author: *Chaichat Boonyanusith* (chaichat.b@nrru.ac.th)

Academic editor: *Danielle Defaye* | Received 22 June 2019 | Accepted 6 December 2019 | Published 16 January 2020

http://zoobank.org/59C0DE82-EFA1-4A20-B2E4-3BE6F8220AA3

Citation: Boonyanusith C, Wongkamhaeng K, Athibai S (2020) A new species of *Boholina* (Crustacea, Copepoda, Calanoida) and a first record for stygobiotic calanoid fauna from a cave in Thailand. ZooKeys 904: 1–22. https://doi.org/10.3897/zookeys.904.37609

Abstract

A new species of Calanoida belonging to the genus *Boholina* Fosshagen & Iliffe, 1989 was found in a freshwater pool within a cave of the Satun province, South Thailand. It is the first record of the genus and of a stygobiotic representative of calanoid fauna in this country. The new species is most similar to *B. crassicephala* Fosshagen & Iliffe, 1989, based on position of genital pores, structures of P4 and P5 in both sexes, relative length of subapical spine vestige on the male right P5, and shape of the male left P5 endopods. However, this new species is distinguished from its known congeners by: (1) relatively longer distal outer spines on the male right P5 exopods, (2) smaller endopods of the male left P5 and (3) elongated apical spines on the distal exopodal segment of the female P4 and P5. Furthermore, the distinctive characteristic of the Thai *Boholina* is the presence of inner minute seta on the distal segment of the male right P5 exopod. Detailed descriptions of the new species and a key to all six known species of the genus *Boholina* is provided.

Keywords

anchialine cave, cave-dwelling copepod, Pseudocyclopidae, Satun Province, Southeast Asia

Introduction

The study of the Copepoda diversity in Southeast Asia is progressing rapidly due to an intensive program coordinated by Prof. La-orsri Sanoamuang and her colleagues. During 12 years of intensive sampling of cave-dwelling copepods in Thailand and Vietnam, many new Cyclopoida and Harpacticoida have been presented to science (Brancelj et al. 2010; Watiroyram et al. 2012, 2015a, 2015b, 2017; Boonyanusith et al. 2013, 2018a, 2018b; Watiroyram and Brancelj 2016; Karanovic et al. 2017; Watiroyram 2018a, 2018b; Sanoamuang et al. 2019). Among Cyclopoida, two endemic genera from Thailand and Vietnam were established, including *Siamcyclops* Boonyanusith, Sanoamuang & Brancelj, 2018, and *Pseudograeteriella* Sanoamuang, Boonyanusith & Brancelj, 2019 (Boonyanusith et al. 2018b; Sanoamuang et al. 2019).

Various calanoid copepods showing plesiomorphic features, belonging to the families Boholinidae, Ridgewayiidae (now both synonyms of the family Pseudocyclopidae) and Epacteriscidae were discovered from several anchialine environments in tropical and subtropical waters around the world (e.g., Fosshagen and Iliffe 1989, 1991, 2004a, 2004b; Fosshagen et al. 2001; Jaume and Humphreys 2001; Boxshall and Jaume 2003, 2012; Suárez-Morales and Iliffe 2007; Figueroa 2011; Moon and Soh 2014). However, stygobiotic Calanoida have never been recorded in Thailand to date.

During the investigation of cave-dwelling Copepoda in the Satun province, South Thailand, a representative of Calanoida was collected from a freshwater pool within a cave. Based on the unique characteristic of a grasping organ on the males' left P5, the cuticular pointed projection on the caudal rami (Fosshagen and Iliffe 1989), and the presence of an additional element on the inner margin of the males' right P5 exopod, a new species of the genus *Boholina* Fosshagen & Iliffe, 1989 was identified representing the first record of the genus and of the stygobiotic representative of calanoid species in Thailand.

According to Fosshagen and Iliffe (1989), the family Boholinidae and the genus *Boholina* were established on the basis of two new species collected from a brackish pool in San Vicente cave on Bohol Island in the Philippines. To date, five species are recognised in this genus, only known from East and Southeast Asia (Fig. 1); they are *B. crassicephala* Fosshagen & Iliffe, 1989, and *B. purgata* Fosshagen & Iliffe, 1989, recorded from a pool in the San Vicente Cave on Bohol Island in the Philippines, *B. munaensis* Boxshall & Jaume, 2012 from a spring in Lawou Cave on Muna Island in Indonesia, *B. parapurgata* Boxshall & Jaume, 2012 from sinkholes on the coast of Muna Island, Indonesia, and *B. ganghwaensis* Moon & Soh, 2014 from the burrows of *Cleistostoma dilatatum* (De Haan, 1833) in the inter-tidal mudflat of Ganghwa Island, western Korea (Fosshagen and Iliffe 1989; Boxshall and Jaume 2012; Moon and Soh 2014). More recently, the families Boholinidae and Ridgewayiidae were synonymised in the family Pseudocyclopidae by the morphology-based phylogenetic work of Bradford-Grieve et al. (2014).

In Thailand, six specimens of *Boholina* were collected from a freshwater pool within a cave. This type locality is in an area that has recently been designated as a UNESCO global geopark.

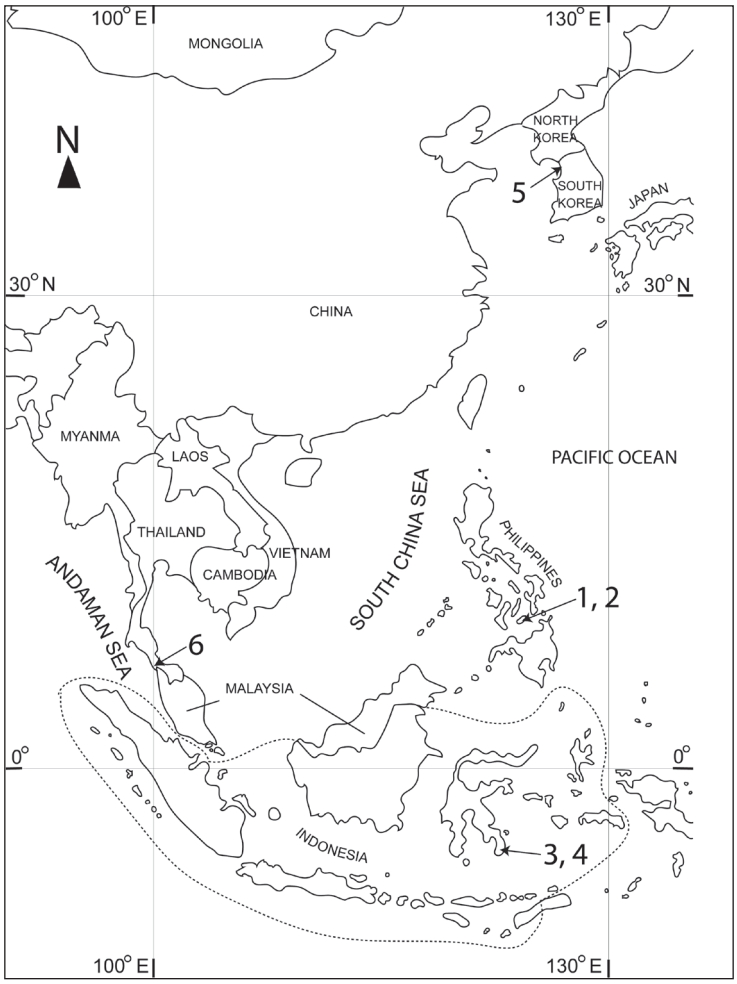

Figure 1. Distribution of the representatives of the genus *Boholina*: **1** *B. crassicephala* **2** *B. purgata* **3** *B. parapurgata* **4** *B. munaensis* **5** *B. ganghwaensis* **6** *B. laorsriae* sp. nov.

Materials and methods

Samples were collected from a pool in Khay Cave of Satun province, South Thailand (Fig. 2) by hand net with a mesh size of 60 μm. They were placed in a plastic bottle with a 4 % formaldehyde solution as a fixative. In the laboratory, specimens were sorted under a stereomicroscope and stored in 70 % ethanol. They were placed in a mixture of glycerol and 70 % ethanol (ratio ~1:10 v/v) for 30 minutes before the morphological examination. Examination of habitus was done on the male and female specimens, which were placed in a drop of glycerol between a pair of coverslips on slide. Specimens were then dissected and mounted on slides using glycerol as a mounting medium. The examination was made with a Nikon ECLIPSE E200 compound light microscope at a magnification of ×1000. Habitus and dissected body parts were drawn using a drawing tube at-

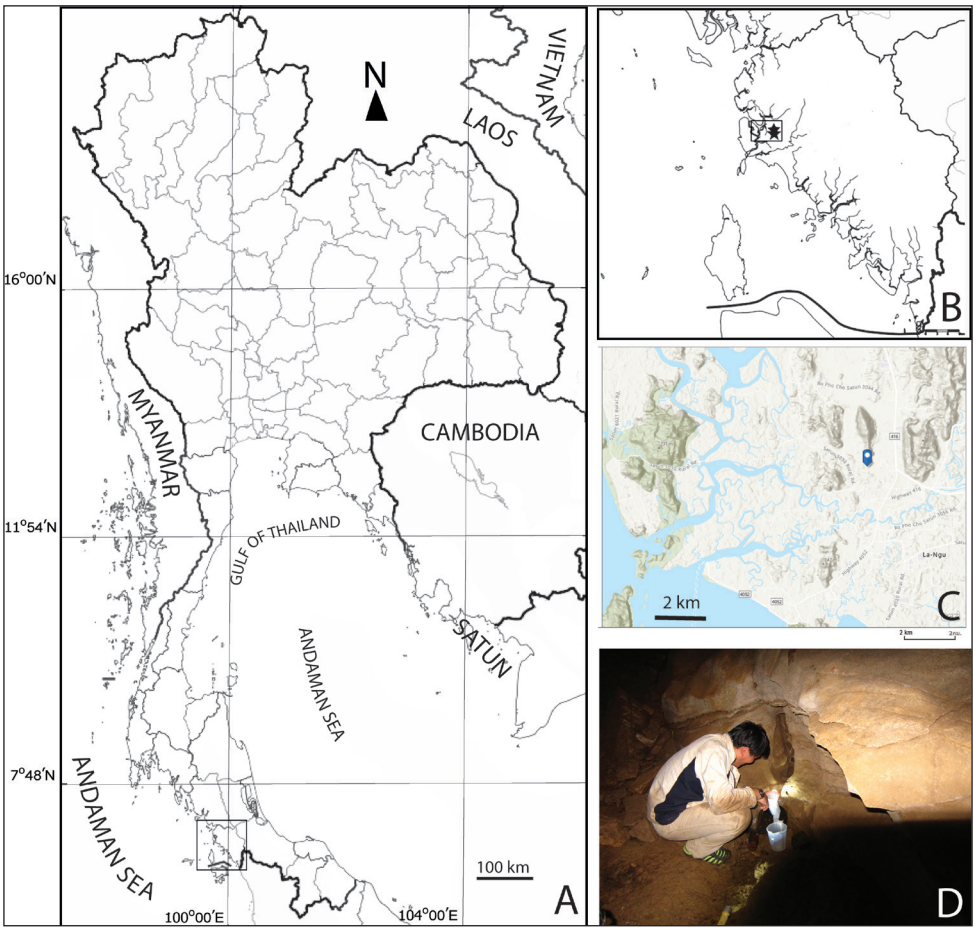

Figure 2. Geographical location and details of sampling site: **A** map of Thailand and location of Satun province **B** sampling location of cave in Satun province (indicated by a star) **C** topography of area around the hill in which the cave is located **D** sampling point in cave.

tached to a compound microscope, and the final versions of illustrations were prepared by Adobe Illustrator CC 2017. Description follows Huys and Boxshall (1991). The following descriptive abbreviations are used throughout the text and figures:

Endp	endopod;
Exp	exopod;
Endp/Exp-1 (2, 3)	proximal (middle, distal) segment of rami;
ae	aesthetasc;
I	spine;
P1–P5	swimming legs 1–5.

Type material has been deposited at the Princess Maha Chakri Sirindhorn National History Museum, Prince of Songkla University, Songkhla, Thailand (**PSUNHM**).

Taxonomy

Order Calanoida G.O. Sars, 1903
Family Pseudocyclopidae Giesbrecht, 1893
Genus *Boholina* Fosshagen & Iliffe, 1989

***Boholina laorsriae* sp. nov.**
http://zoobank.org/E1E3D8D5-7B4E-4DD8-86F8-AAC296A21649
Figs 3–6 [female]; Figs 7, 8 [male]

Material examined. *Holotype*: THAILAND • ♀ (adult), 0.73 mm long; Satun Province, Khay Cave; 6°53'40"N, 99°46'44"E, 17 m a.s.l.; 17 December 2014; C. Boonyanusith leg.; hand net; completely dissected and mounted on two slides in glycerol and sealed with nail vanish; PSUZC-PK2004-01–02. ***Allotype*:** THAILAND • ♂ (adult), 0.67 mm long, collection data as for holotype; PSUZC-PK2004-03. ***Paratypes*:** THAILAND • 1 ♀ (adult) and 1 ♂ (adult); same data as for holotype; PSUZC-PK2004-04–05.

Additional material. THAILAND • 2 ♂♂ (adult); same data as for holotype; preserved in 70% ethanol; retained in collection of the first author (CB).

Etymology. The species is named after Prof. Dr. La-orsri Sanoamuang (Khon Kaen University) in honour of her great and invaluable contribution on the knowledge of the planktonic fauna in Thailand. The name of species is a feminine noun in genitive singular.

Type locality. The Khay Cave is in La-Ngu district, Satun province, ca. 760 km south of Bangkok (Thailand) (Fig. 2A). The cave is in an isolated, limestone hill of the Nakhon Sri Thammarat Mountain range, at an elevation of 17 m a.s.l, ca. 6.5 km from the Andaman Sea, (Fig. 2A–C). The cave has two entrances. The first one is located ca. 3 m over the hill floor and the second is at the base of the hill. Beyond the entrance is a horizontal gallery, which is ca. 20 m high. Occasionally, the gallery is inundated by freshwater during the rainy season. There is no permanent route connecting water in the cave and the sea; however, ca. 40 years ago, the cave was probably inundated by the sea water during the rising up of the sea water level (personal communication). The type locality is a small pool hidden under the cave wall with a small opening (Fig. 2D). It is ca. 10 m far from the first entrance and is seasonally filled by rain. The water temperature was 24.6 °C, pH 8.93, conductivity 450 μS cm^{-1}, DO 5.7 mg L^{-1}, and salinity 0.2 ppt.

Diagnosis. *Female*: Pseudocyclopidae. Fourth and fifth pedigerous somites completely fused. Postero-lateral corners of cephalosome and first three pedigerous somite rounded. Genital double-somite barrel-shaped, ornamented with hyaline membrane all around the posterior margin; hyaline membrane with large medial notch ventrally. Genital pores paired, located ventrolaterally. Hyaline membrane of preanal somite expanded dorso-medially to form trapezoidal double-pointed flap. Caudal ramus with triangular pointed projection on distal margin. Antennule relative short, not reaching

beyond distal margin of prosome. Apical spine on female P4 Exp-3 elongated, ca. 3 × as long as outer terminal spine. Apical spine on female P5 Exp-3 ca. 1.8 × as long as outer terminal spine. ***Male*:** The left P5 Exp-3 highly transformed, bearing three irregular lobes; Endp oval-shaped, much shorter than right P5 Endp, ca. 1.6 × as long as wide. The male right P5 Exp with minute inner spiniform seta; distal outer spine elongated, ca. 3.4 × as long as proximal outer one and ca. 2.7 × as long as apical spine; subapical spine vestige ca. 0.7 × as long as apical spine.

Description of adult female. Body (Fig. 3A) with a total length of 0.68 and 0.73 mm (measured from anterior margin of cephalosome to tip of projection of caudal rami, mean: 0.71 mm; $N = 2$). Prosome 5-segmented, elliptical, ca. 70 % of body length and 2.5 × as long as urosome, with greatest width at posterior end of first pedigerous somite; greatest width ca. 43 % of prosome length. Cephalosome and first three pedigerous somites free; postero-lateral corners rounded. Fourth and fifth pedigerous somites completely fused (Fig. 3A); postero-lateral corners rounded, symmetrical. Naupliar eye not discernible. Urosome 4-segmented, comprising genital double-somite, two free abdominal somites and very short anal somite (Fig. 3A–D). Genital double-somite barrel-shaped, ca. 45 % of urosome length, with greatest width at mid-length of double-somite, with hyaline membrane all around the posterior margin; hyaline membrane with large medial notch ventrally. Genital pores paired, located ventrolaterally (Fig. 3C). First and second free abdominal somites subequal in length, bearing hyaline membrane; hyaline membrane of the first free abdominal somite with serrulate margin, that of the second expanded dorso-medially to form a trapezoidal double-pointed flap, representing a pseudoperculum. Anal somite very short, telescoped within the preceding urosomite (Fig. 3B, D).

Caudal rami (Fig. 3D) subrectangular, ca. 1.8 × as long as wide (measured from base to level of insertion of setae V), with triangular pointed-projection on distal margin dorsally (Fig. 3B); projection 0.4 × as long as ramus length; caudal seta II to VII present, caudal seta I absent; seta II spiniform, with setules along inner margin; seta III plumose, approx. mid-length of seta IV; seta IV shorter than seta V, with breaking planes and plumose; seta V longest, with breaking plane and plumose, sub-equal to urosome length; seta VI slim and plumose. Seta VII inserted dorso-medially near insertion of seta V and seta VI (Fig. 3D). Length ratio of caudal setae to ramus length, from seta II to seta VII: 0.6 : 2.3 : 4.3 : 5.5 : 3.7 : 1.0. Length ratio of caudal setae from seta II to seta VII: 1.0 : 3.7 : 6.9 : 8.9 : 6.0 : 1.5.

Rostrum (Fig. 3E) weakly developed and V-shaped; base broad, completely fused to anterior margin of cephalic shield and tapering to rounded tip between bases of antennules, with two sensillae at middle third of rostrum.

Antennule (Fig. 4A–C) symmetrical, 24-segmented, reaching to distal margin of prosome; ancestral segments II-IV and ancestral segments XXVII–XXVIII completely fused, representing evident segments 2 and 24, respectively. Segments 8 and 9 partly fused, with remnant of ancestral articulation of ancestral segment X and XI, penultimate and ultimate segments sub-equal in length. Armature formula as follows (Roman numeral corresponds to ancestral segment): 1+ae (I), 6+ae (II–IV), 2+ae (V), 2 (VI), 2+ae (VII), 2 (VIII), 2+ae

(IX), 2+2ae (X–XI), 1 (XII), 1+ae (XIII), 1+ae (XIV), 1+ae (XV), 1+ae (XVI), 1 (XVII), 1+ae (XVIII), 1 (XIX), 1 (XX), 1+ae (XXI), 1 (XXII), 1 (XXIII), 2 (XXIV), 2+ae (XXV), 2 (XXVI), 5+ae (XXVII–XXVIII).

Antenna (Fig. 4D) biramous. Coxa short, bearing one spinulose seta on distomedial corner. Basis with two sub-equal setae on distomedial corner. Exp 9-segmented, apical segment small, setal formula 1, 1, 1, 1, 1, 1, 1, 1, 3. Endp 2-segmented; proximal segment bearing two setae on medial margin, setae inserted in the same place; distal segment bilobed, bearing three medial setae and six apical setae on medial lobe, with seven apical setae on distal lobe.

Mandible (Fig. 4E) with sclerotised gnathobase comprising ten cuspid or simple teeth and one small dorsal seta on cutting edge of coxal gnathobase. Mandibular palp biramous; basis with four setae on inner margin. Exp 5-segmented, ultimate segment minute, setal formula 1, 1, 1, 1, 2. Endp 2-segmented; proximal segment with four setae on distomedial corner; distal segment with ten apical setae.

Maxillule (Fig. 5A) with praecoxal arthrite bearing nine marginal, spinulose spines and one seta on anterior surface, and four setae on posterior surface. Coxal epipodite with nine apical setae; two proximal ones spinulose, other plumose; coxal endite with four apical setae. Basis fused to exopod, proximal and distal endites armed with four and five apical setae, respectively; basal exite with knob-like appearance and one vestigial seta. Exp with ten setae along apical and outer margin. Endp 3-segmented, proximal and middle segments partly fused, setal formula 4, 4, 7.

Maxilla (Fig. 5B) 6-segmented, comprising praecoxa, coxa, basis and 4-segmented Endp. Praecoxa partly fused to coxa, proximal and distal praecoxal endites with five and three apical setae, respectively. Coxa with two endites, each armed with three apical setae. Basis with large basal endite, armed with four strong apical setae; one of which ornamented with spinule row at mid-length of seta. Endp 4-segmented, setal formula 2, 2, 2, 3; ultimate segment with two long and one short setae.

Maxilliped (Fig. 5C) 8-segmented, comprising syncoxa, basis, and 6-segmented Endp. Syncoxa with four syncoxal endites, setal formula 1, 2, 2, 3; seta on first endite spinulose, basal seta on second endite strong, spinulose; distal endite with one long seta and two short, slender setae. Basis with three medial setae, with row of spinules on anterior surface. Endp with setal formula 2, 4, 4, 3, 3+1, 4; basal seta on first endopodal segment spinulose.

P1–P4 (Fig. 6A–D) biramous, comprising coxa, basis, and 3-segmented rami. Intercoxal sclerite trapezoidal. Coxa rectangular, with seta on distomedial corner. Basis of all swimming legs with lateral seta but lacking in P2; lateral seta inserted on posterior surface. Basis of P1 with robust seta on distomedial corner, with finger-like process on posterior surface arising near base of Exp; process reaching distal margin of Endp-1. Outer distal corner of all endopodal segments drawn out into triangular projection; projection relatively large in P1 and P2. P1 Endp-1 without any outer seta. Outer distal corner of P1 Exp-2 drawn out into spoon-like process, ornamented with spinules along outer margin. Outer distal corner of Exp-1 and Exp-2 of P2–P4 extended, forming 2-pointed sclerotised expansion, distal pointed process larger than proximal one.

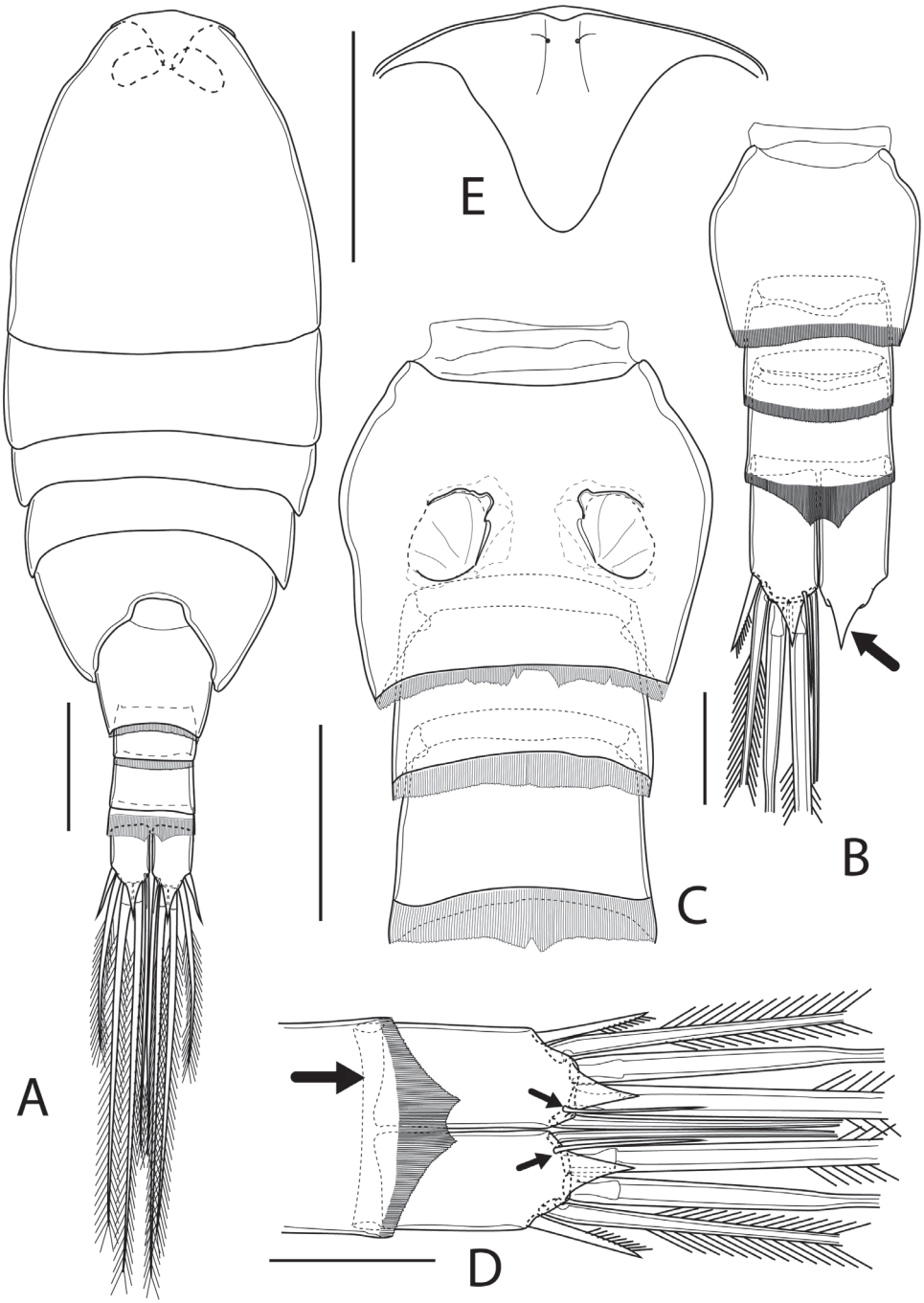

Figure 3. *Boholina laorsriae* sp. nov. female: **A** habitus, dorsal view **B** urosome, dorsal view **C** genital double-somite, ventral view **D** caudal rami, dorsal view **E** rostrum, frontal view. Scale bars: 100 μm (**A**); 50 μm (**B–E**).

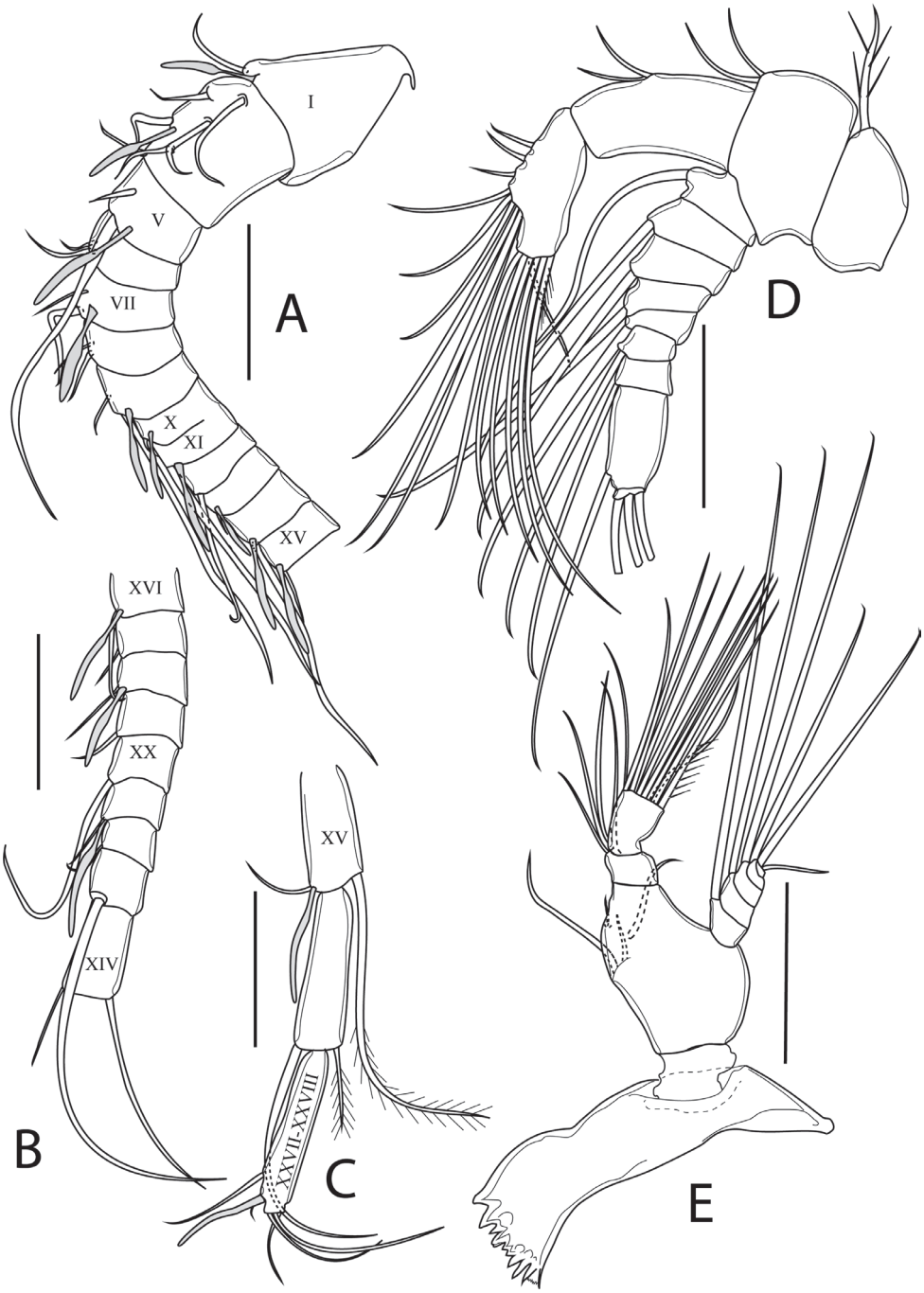

Figure 4. *Boholina laorsriae* sp. nov. female: **A** segments 1–12 of antennule **B** segments 13–21 of antennule **C** segments 22–24 of antennule **D** antenna **E** mandible. Scale bars: 50 μm. Roman numerals on antennule correspond to ancestral segments.

Figure 5. *Boholina laorsriae* sp. nov. female: **A** maxillule **B** maxilla **C** maxilliped. Scale bars: 50 μm.

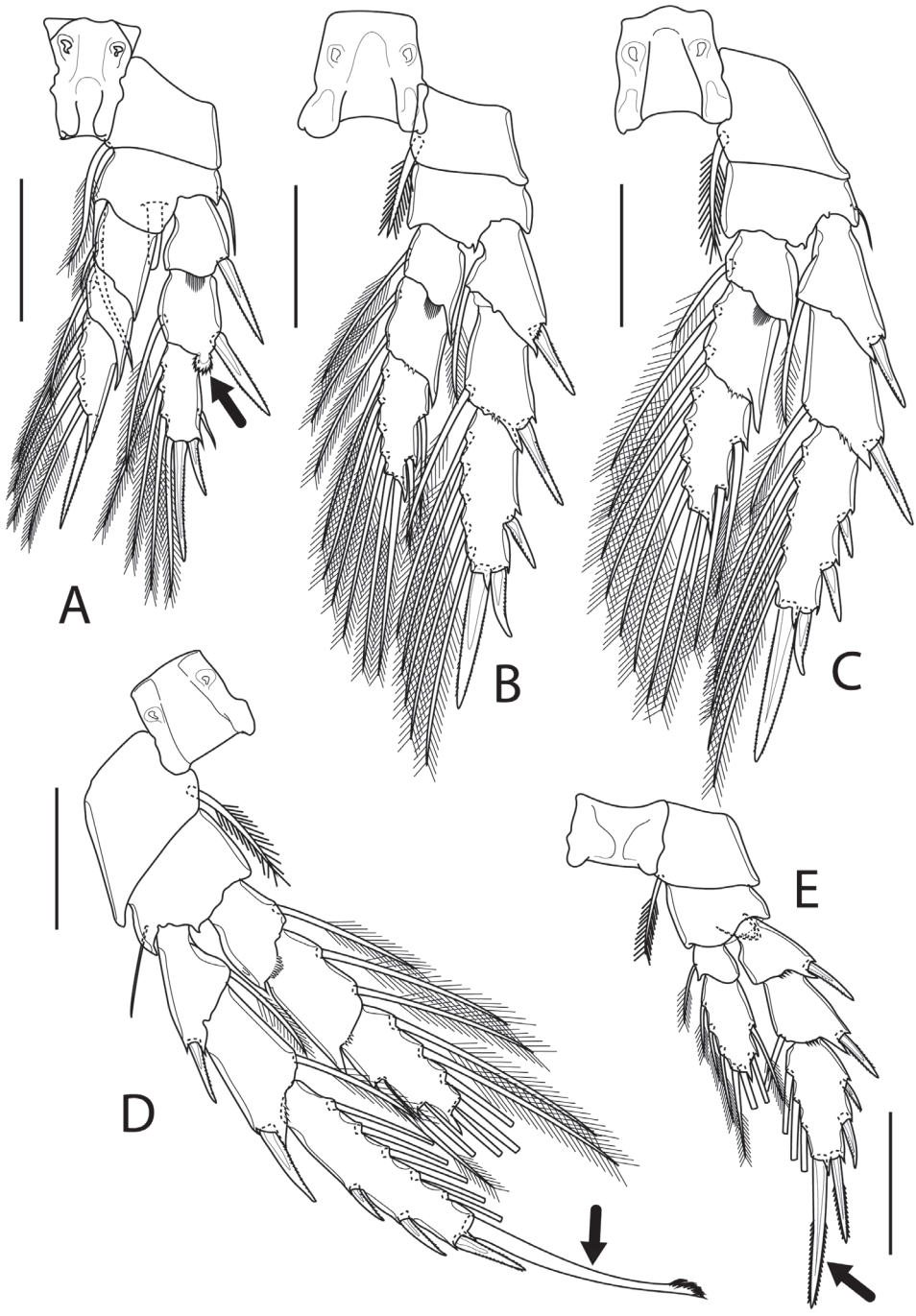

Figure 6. *Boholina laorsriae* sp. nov. female: **A** P1 **B** P2 **C** P3 **D** P4 **E** P5. Scale bars: 50 μm.

Outer spine of Exp-3 of all swimming legs relatively short. P4 Exp-3 ca. 3.2 × as long as wide, with elongated, smooth apical spine, as long as segment bearing it and ca. 3 × as long as outer terminal spine, with row of curved spinules at its tip. Armature of swimming legs as presented in Table 1.

P5 (Fig. 6E) biramous, with 3-segmented Exp and 2-segmented Endp; armament as in Table 1. Coxa and basis as in P3 and P4. Exp-3 ca. twice as long as wide, with apical and outer terminal spines on its tip; apical spine elongated, ca. 1.8 × as long as outer terminal spine, ca. 1.2 × as long as Exp-3 length. Endp much shorter than Exp, reaching level of articulation of Exp-2; Endp-1 as long as wide, without pointed process on outer distal corner; Endp-2 ca.2.6 × as long as wide, with small, pointed process on outer distal corner.

Description of adult male. Body with a total length of 0.65 and 0.67 mm (measured from anterior margin of cephalosome to tip of the projection of caudal rami; mean: 0.66 mm; $N = 2$). Habitus smaller and slenderer than in female (Fig. 7A). Prosome 5-segmented, as in female, ca. 70 % of body length and 2.5 × as long as urosome, with greatest width at posterior end of first pedigerous somite; greatest width ca. 47 % of prosome length. Cephalosome and first three pedigerous somites similar to those in female. Naupliar eye not discernible. Urosome 5-segmented; comprising genital somite, three free abdominal somites and very short anal somite. Genital somite slightly asymmetrical, ca. 25 % of urosome length; posterior margin with hyaline membrane dorsally. First three free abdominal somites similar in length, each with hyaline membrane all around posterior margin; hyaline membrane on third free abdominal somite as in female. Anal somite very short, telescoped within the preceding somite, as in female (Fig. 7B).

Caudal rami (Fig. 7B) relatively shorter than in female, ca. 1.8 × as long as wide. Armament and ornamentation as in female.

Antennule (Fig. 7C–E) asymmetrical. Left antennule non-geniculate, 24-segmented, setal formula as in female. Right antennule geniculate, 22-segmented; armature formula as follows (Roman numeral corresponds to ancestral segment): 1+ae (I), 6+ae (II–IV), 2+ae (V), 2 (VI), 2+ae (VII), 2 (VIII), 2+ae (IX), 1+ae (X), 1+ae (XI), 1(XII), 1+ae (XIII); 1 spiniform seta+ae (XIV), 1+ae (XV), 1+ae (XVI), 1 (XVII), 1 obtuse, fused spine +1+ae (XVIII), 1 obtuse, fused spine +2 (XIX), 1 (XX), 2+ae; one seta spiniform (XXI–XXIII), 4+ae (XXIV–XXV), 2 (XXVI), 5+ae (XXVII–XXVIII).

Table 1. Armament of female thoracic legs P1–P5 in *Boholina laorsriae* sp. nov. (Roman numerals represent number of spines; Arabic numerals represent number of setae).

Swimming leg	Coxa	Basis	Exopod	Endopod
P1	0-1	1-1	I-0; I-1; II, I, 4	0-1; 0-1; 0, I+1, 3
P2	0-1	0-0	I-1; I-1; II, I, 5	0-1; 0-2; 2, 2, 4
P3	0-1	1-0	I-1; I-1; III, I, 5	0-1; 0-2; 2, 2, 4
P4	0-1	1-0	I-1; I-1; III, I, 5	0-1; 0-2; 2, 2, 3
P5	0-1	1-0	I-0; I-1; III, I, 3	0-1; 2, 2, 3

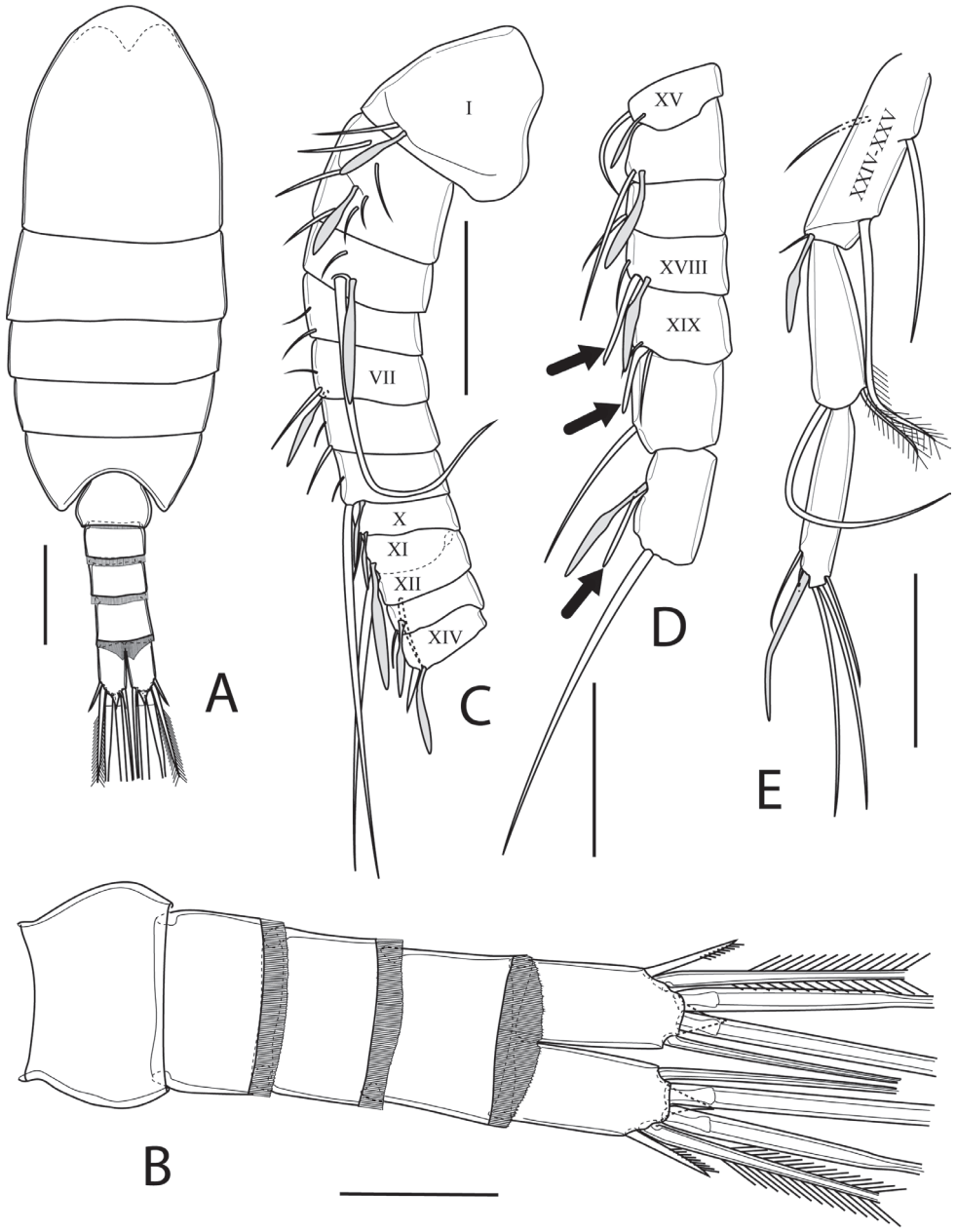

Figure 7. *Boholina laorsriae* sp. nov. male: **A** habitus, dorsal view **B**: urosome, ventral view **C** segments 1–12 of antennule **D** segments 13–19 of antennule **E** segments 20–22 of antennule. Scale bars: 100 μm (**A**); 50 μm (**B–E**). Roman numerals on antennule correspond to ancestral segments.

Antenna, mandible, maxillula, maxilla, maxilliped, and P1–P4 as in female.

P5 (Fig. 8A, B) biramous, asymmetrical. Coxae and intercoxal sclerite fused, forming a common base. Basis rectangular, with outer seta on posterior surface. Left leg biramous, with 3-segmented Exp and 1-segmented Endp; Exp-1 with a long robust outer spine; Exp-2 modified, with a long robust outer spine; Exp-3 highly transformed, bearing several flexible and irregular lobes; outer lobe bearing finger-like appendage; middle lobe prominent, bearing scoop-like appendage; inner lobe, with two elements; innermost (uppermost) one curved, strong seta; other one curved, gutter-like, with serrated concave margin at its cutting edge; Endp flat, oval-shaped, ca. 1.6 × as long as wide. Right leg biramous, with 1-segmented Exp and 1-segmented Endp. Exp with two outer spines, inner spiniform seta, and apical spine, plus spine vestige located subapically on anterior surface; distal outer spine elongated, ca. 3.4 × as long as proximal outer one, ca. 2.7 × as long as apical spine; subapical and apical spines machete-shaped, subapical spine vestige ca. 0.7 × as long as apical spine; apical spine ca. 0.4 × as long as distal outer spine; inner spiniform seta minute, located at level of insertion of proximal outer spine; Endp as long as Exp, ca. 3 × as long as wide, armed with two sub-equal spines.

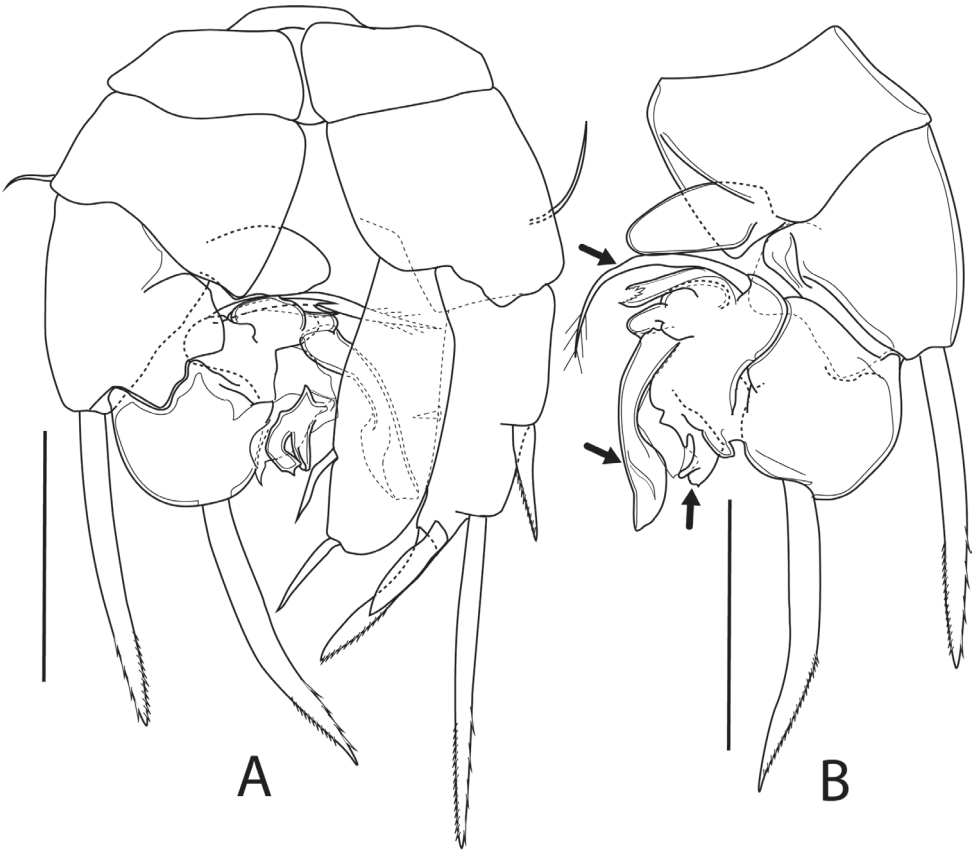

Figure 8. *Boholina laorsriae* sp. nov. male: **A** P5 caudal view **B** left rami of P5. Scale bars: 50 μm.

Differential diagnosis. The new species was confidently identified to the genus *Boholina* based on the combination of the following characteristics mentioned by Fosshagen and Iliffe (1989):

(1) fourth and fifth pedigerous somites fused,
(2) rostrum with a rounded tip,
(3) genital pores paired and separate,
(4) caudal rami with cuticular pointed projection distally,
(5) distal outer corner of all endopodal segments of P1 forming a triangular pointed projection,
(6) P1 Endp-3 without outer seta,
(7) P4 Exp-3 with modified apical spine,
(8) female P5 with a 2-segmented Endp,
(9) male left P5 Exp-3 modified to unique characteristic grasping organ, and
(10) female and male with 4- and 5-segmented urosome, respectively; anal somite very short and sometimes concealed within the preceding somite.

Examination of the structure of the genital double-somite, of P4 and P5 in both males and females, the relative length of subapical spine vestige on the male right P5 and the shape of the male left P5 Endp revealed that the new species is most similar to *B. crassicephala,* which had previously been described from a pool in a cave of Bohol Island, the Philippines. Several characters are shared by both species, especially the structure of the male P5. However, there are also remarkable differences (Table 2). The characteristics which obviously distinguish *Boholina laorsriae* sp. nov. from *B. crassicephala* are as follows:

i) Apical spine of the female P5 Exp-3 is ca. 1.8 × as long as outer terminal spine in the new species, but it is sub-equal to the outer terminal spine found in *B. crassicephala*.
ii) Exopodal segment of the male right P5 has medial minute seta in the new species; however, it is absent in *B. crassicephala*.
iii) Distal outer spine on exopodal segment of the male right P5 is relatively long, and the distal outer spine is ca. 2.9 × as long as the proximal one; however, in *B. crassicephala*, the spine on exopodal segment of the male right P5 is relative shorter and the distal outer spine is ca. 1.9 × as long as the proximal one.
iv) The male left P5 Endp is relatively smaller in the new species than that of *B. crassicephala*.

The Thai *Boholina* can be easily distinguished from *B. purgata*, *B. parapurgata,* and *B. ganghwaensis* by the characteristics of the widely separated genital pores, relatively longer subapical spine vestige on the male right P5 when compared to the length of apical spine, the higher length ratio of the apical spine to the outer terminal spine in the female P5 Exp-3 and the elongated apical spine of the female P4 Exp (Table 2). The genital double-somite of the new species is barrel-shaped, while it is globular in *B. munaensis*. Additionally, the ii) characteristic is unique for the Thai *Boholina*. Based on

Table 2. Morphological comparison of the six species of genus *Boholina*. Abbreviations: GDS, genital double-somite; CR, caudal rami; A2, antenna; Mb, mandible; Mx, maxillule (*measured from figures of the original description).

Character	*B. ganghwaensis*	*B. parapurgata*	*B. munaensis*	*B. purgata*	*B. crassicephala*	*B. laorsriae* sp. nov.
Female						
Body length (mm)	1.03–1.29	0.93–1.11	0.70–0.77	0.73–0.79	0.75–0.85	0.68–0.73
Posterior lateral corner of second and third pedigerous somites	Pointed	Pointed	Rounded	Pointed	Rounded	Rounded
Genital pores on GDS	Either side of ventralmidline	Either side of ventralmidline	Ventrolaterally	Either side of ventralmidline	Ventrolaterally	Ventrolaterally
Hook–like process on genital pore plate	Yes	No	No	No	No	No
Length/width ratio of CR	1.6	1.5	1.5	1.6*	1.8*	1.8
Distal two segments of A2 Exp	Separated	Separated	Separated	Fused	Fused?	Separated
Number of setae on distal endopodal segment of Mb	11	10	10	10	10	10
Setal formula of Mb Exp	1,1,1,1,2	0.1,1,1,2	0,1,1,1,2	1,1,1,1,2	1,1,1,1,2	1,1,1,1,2
Basis and first endopodal segment of Mx	Partly fused	Fused	Fused	Fused	Fused	Separated
Length ratio of apical and outer terminal spines of P4 Exp–3	1.6*	1.5	1.9	1.5	2.5	3.0
Length/width ratio of distal endopodal segment of P5	2.5	2.6	2.6	1.8*	1.6*	2.6
Length ratio of apical and outer terminal spine of P5 Exp–3	1.0	0.8	1.4	0.8*	1.2*	1.8
Length ratio of apical spineand P5 Exp–3	0.9	0.9	0.8	0.8*	1.0*	1.2
Male						
Body length (mm)	0.87–0.93	0.66–0.71	0.68	0.64–0.73	0.70–0.77	0.65–0.67
Length ratio of left and right Endp of P5	1.1*	0.8*	0.5	0.7*	0.8*	0.45
Length/width ratio of right P5 Endp	3.2	3.6	3.5*	2.6*	2.7*	3.0
Right P5 Endp with large inner spiniform process	No	No	Yes	No	No	No
Right P5 Endp armature	2 slender spines	2 sigmoid spines	Absent	2 slender spines	2 slender spines	2 slender spines
Length ratio of two outer exopodal spines on right P5	1.5	1.8	1.3	1.7*	1.7*	3.4
Relative length of subapical spine compared to apical spine on left P5 Exp	Less than 0.5 ×	Less than 0.5 ×	More than 0.5 ×	Less than 0.5 ×	More than 0.5 ×	More than 0.5 ×

the characteristics used in Moon and Soh (2014) accompanied by additional ones, the morphological characteristics of the six species are presented in Table 2.

Remarks. Only six specimens were collected from a pool and the new species was not encountered in the other eight caves visited in this research project. Freshwater Cyclopoida belonging to the genera *Thermocyclops, Metacyclops,* and *Mesocyclops,* as well as harpacticoids of the genus *Schizopera* and of the family Ectosomatidae were also collected from the type locality.

Key to the adult of *Boholina*

Boxshall and Jaume (2012) provided key to adults of the genus based on the four described species. In this paper, two more species from Korea and Thailand are added in the key.

1 Female genital double-somite globular-shaped, as long as wide; male right P5 Endp unarmed, with large inner spinous process.... ***B. munaensis*** **Boxshall & Jaume, 2012**

– Female genital double-somite barrel-shaped, longer than wide; male right P5 Endp armed with 2 elements, without large inner spinous process **2**

2 Female genital pores located ventrolaterally; postero-lateral corners of second and third pedigerous somites rounded in both sexes; male right P5 Exp with relatively large spine vestige; spine vestige longer than half length of apical spine **3**

– Female genital pores located close together on either side of body midline; postero-lateral corners of second and third pedigerous somites pointed in both sexes; male right P5 Exp with relatively small spine vestige; spine vestige shorter than half length of apical spine..... **4**

3 Apical spines on female P5 sub-equal in length; male right P5 Exp without inner spiniform seta; male left P5 Enp large, as long as right P5 Endp .... ***B. crassicephala*** **Fosshagen & Illife, 1989**

– Inner apical spines on female P5 ca. 1.6 × as long as outer one; male right P5 Exp with inner spiniform seta; male left P5 Enp small, much shorter than right P5 Endp..... ***B. laorsriae*** **sp. nov.**

4 Apical spine on female P5 Exp-3 longer than outer terminal spine; gonoporal plate without small hook-like process..... **5**

– Apical spine on female P5 Exp-3 slightly shorter than outer terminal spine (0.96 x); gonoporal plate with small hook-like process.... ***B. ganghwaensis*** **Moon & Ho, 2014**

5 Male right P5 Endp ca. 2.6 × as long as wide, bearing two slender spines; distal endopodal segment of female P5 Endp ca. 1.8 × as long as wide; outer terminal spine on female P5 Exp-3 shorter than segment bearing it .... ***B. purgata*** **Fosshagen & Illife, 1989**

– Male right P5 Endp ca. 3.6 × as long as wide, bearing two sigmoid spines; distal endopodal segment of female P5 Endp ca. 2.6 × as long as wide; outer terminal spine on female P5 Exp-3 longer than segment bearing it .... ***B. parapurgata*** **Boxshall & Jaume, 2012**

Discussion

Calanoid copepods are ubiquitous in marine, brackish, and fresh waters, comprising 44 families and approximately 330 genera (Walter and Boxshall 2019). However, compared to the diversity of cave-dwelling Cyclopoida and Harpacticoida, stygobiotic Calanoida is less diverse in terms of numbers of species. In Southeast Asia, seven stygobiotic calanoid species have been previously recorded from caves in Vietnam, the Philippines, and Indonesia, including *Boholina* (four species, excluding the new species described here), *Hadodiaptomus* Brancelj, 2005 (one species), and *Nannodiaptomus* Dang & Ho, 2001 (two species) (Brancelj 2005; Boxshall and Jaume 2012; Tran and Brancelj 2017). Of these, only representatives of *Boholina* were described from anchialine caves.

The genus *Boholina* clearly shows affinities to the families Ridgewayiidae and Pseudocyclopidae, by the presence of several plesiomorphic characters in the antennule, antenna, mouthparts, and swimming legs. Nearly all species of *Boholina* were collected from anchialine caves: this habitat is different from a benthic environment in shallow water where the two families have frequently been found (Fosshagen and Iliffe 1989). Recently, the families Boholinidae and Ridgewayiidae were synonymised in the family Pseudocyclopidae, and the genus *Boholina* is sister to the clade of the genera *Ridgewayia, Stygoridgewayia, Hondurella, Placocalanus,* and *Pseudocyclops*, based on a morphology-based cladistic analysis of Bradford-Grieve et al. (2014). From a geographical point of view, *Boholina* has been recorded only from East and Southeast Asian countries along the western coast of the Pacific Ocean (Fig. 1). This suggests an Asian origin of the genus. The assumption is supported by the fact that its most closely related genera (*Ridgewayia*, *Stygoridgewayia*, *Placocalanus,* and *Pseudocyclops*) can also be found in this region. The only genus that has yet to be found in Asia is *Hondurella*, which was only obtained from Utila Island of Honduras in the Caribbean basin (Suárez-Morales and Iliffe 2007).

The geographical distribution of the new species is slightly different from those of all other species of *Boholina*, as it was collected from a freshwater pool within a cave located very far from the sea (ca. 6.5 km) compared with those of *B. crassicephala* and *B. purgata* (200 m), *B. parapurgata* and *B. munaensis* (700 m), and *B. ganghwaensis* (inter-tidal mudflat). The occurrence of the new species in a cave located so far from the coast is the same as that of *Stygoridgewayia*, which were collected from bores/wells located up to 450 km inland from the coast in the Cape Range Peninsula and Pilbara region, Western Australia (Tang et al. 2008). Tang et al. (2008) hypothesised that the occurrence of *Stygoridgewayia* in subterranean waters is due to secondary colonisation of freshwater after the regression of the epicontinental sea which inundated a large part of the land. From this geographical viewpoint, we postulate that the ancestor of the present-day population of Thai *Boholina* could have penetrated the cave in either the Cretaceous or Miocene periods. The assumption was postulated as the geological evidence shows that the sedimentary rocks in the area of the present-day Satun province and north-western Malay Peninsula were formed under the ancient sea for a very

long time, spanning the Late Cambrian and Triassic periods, before uplifting of the area in Cretaceous, and the Quaternary sediments in the area below 10 m a.s.l. were interpreted as deposits of the epicontinental sea in the Holocene (The Malaysian and Thai Working Groups 2009).

Based on structure (i.e., degree of modification) of mouthparts, especially with respect to the mandible, maxilla, and maxilliped, feeding habits were suggested for several taxa of the families Epacteriscidae, Ridgewayiidae, and Pseudocyclopidae (e.g., Fosshagen 1968; Fosshagen et al. 2001; Jaume and Humphreys 2001; Fosshagen and Iliffe 2003, 2004a, 2004b, 2007; Suárez-Morales and Iliffe 2007). The absence of the conspicuous modification of the raptorial feeding habit in the mandible, maxilla, and maxilliped in Thai *Boholina* and its congeners suggests that they are particle feeders. The characters that indicate particle-feeding habits in *Boholina* and in several ridgewayiids, such as *Ridgewayia*, *Brattstromia*, *Exumellina,* and *Stargatia* are are as follows: 1) the mandible bears numerous small teeth on the cutting-edge of the gnathobase and the endopod is well-developed, with four and more than nine setae on proximal and distal segments, respectively, and 2) the maxilla and maxilliped are armed with normal plumose setae. In the raptorial feeders, like epacteriscids and some ridgewayiids, such as *Exumella, Palmeriella,* and *Normancavia*, the general modifications of these three appendages include: 1) an enlargement of the teeth, especially the ventralmost teeth, and the reduction of the endopod, and 2) the transformation of setae on the distal part of the maxilla and maxilliped to stout, elongate, spinous setae or the reduction of setae on both the maxilla and maxilliped.

Even if many calanoid taxa in the superfamily Pseudocyclopoidea Giesbrecht, 1893 were collected from anchialine caves, it is likely that there is no specific adaption/modification in relation to the cave habitat in this family. Such a morphological adaptation or modification generally corresponds to the zones of the water column in which the copepod lives. Based on the relative length of the antennule, we suggest that the genus *Boholina* is a hyperbenthic form, because it has relatively short antennules (not extending beyond prosome) as in most epacteriscids. In the genera *Exumellina* and *Stargatia*, which were collected in the water column of anchialine caves, the antennules extend beyond the prosome (Fosshagen and Iliffe, 1998, 2003). In our opinion, only the reductions of the eyes and outer seta on P1 Endp are adaptations of *Boholina* corresponding with life in caves, as Brancelj and Dumont (2007) suggested for the freshwater stygobiotic Calanoida.

Acknowledgements

This research was supported by a grant from the Office of the Higher Education Commission, Thailand (2558A13562002) and was funded by the Government of Thailand's Grants to Khon Kaen University (KKU) (Project code 561302). The authors gratefully thank Dr. Danielle Defaye, Dr. Anton Brancelj, and an anonymous reviewer for their useful comments on the manuscript.

References

Boonyanusith C, Brancelj A, Sanoamuang L (2013) First representatives of the genus *Fierscyclops* Karanovic, 2004 (Copepoda, Cyclopidae) from South East Asia. Journal of Limnology 72 (Supplement 2): 275–289. https://doi.org/10.4081/jlimnol.2013.s2.e13

Boonyanusith C, Saetang T, Wongkamheng K, Maiphae S (2018a) *Onychocamptus* Daday, 1903 from Thailand, with descriptions of two new species and two new records (Crustacea, Copepoda, Harpacticoida, Laophontidae). ZooKeys 810: 45–89. https://doi.org/10.3897/zookeys.810.29253

Boonyanusith C, Sanoamuang L, Brancelj A (2018b) A new genus and two new species of cave-dwelling cyclopoids (Crustacea, Copepoda) from the epikarst zone of Thailand and up-to-date keys to genera and subgenera of the *Bryocyclops* and *Microcyclops* groups. European Journal of Taxonomy 431: 1–30. https://doi.org/10.5852/ejt.2018.431

Boxshall GA, Jaume D (2003) *Iboyella,* a new genus of epacteriscid copepod (Copepoda: Calanoida: Epacteriscidae) from Cuba. Organisms Diversity & Evolution 3: 85–92. https://doi.org/10.1078/1439-6092-00062

Boxshall GA, Jaume D (2012) Three new species of copepods (Copepoda: Calanoida and Cyclopoida) from anchialine habitats in Indonesia. Zootaxa 3150: 36–58. https://doi.org/10.11646/zootaxa.3150.1.2

Bradford-Grieve JM, Boxshall GA, Blanco-Bercial L (2014) Revision of basal calanoid copepod families, with a description of a new species and genus of Pseudocyclopidae. Zoological Journal of the Linnean Society 171: 507–533. https://doi.org/10.1111/zoj.12141

Brancelj A (2005). *Hadodiaptomus dumonti* n. gen., n. sp., a new freshwater stygobiotic calanoid (Crustacea: Copepoda: Calanoida) from Vietnam (South Asia) and a new member of the subfamily Speodiaptominae Borutzky, 1962. Hydrobiologia 534: 57–70. https://doi.org/10.1007/s10750-004-1321-4

Brancelj A, Dumont HJ (2007) A review of the diversity, adaptations and groundwater colonization pathways in Cladocera and Calanoida (Crustacea), two rare and contrasting groups of stygobionts. Fundamental and Applied Limnology 168/1: 3–17. https://doi.org/10.1127/1863-9135/2007/0168-0003

Brancelj A, Watiroyram S, Sanoamuang L (2010) The first record of cave-dwelling Copepoda from Thailand and description of a new species: *Elaphoidella namnaoensis* n. sp. (Copepoda, Harpacticoida). Crustaceana 83: 779–793. https://doi.org/10.1163/001121610X502894

Figueroa DF (2011) Phylogenetic analysis of *Ridgewayia* (Copepoda: Calanoida) from the Galapagos and of a new species from the Florida: keys with a reevaluation of the phylogeny of Calanoida. Journal of Crustacean Biology 31: 153–165. https://doi.org/10.1651/10-3341.1

Fosshagen A (1968) Marine biological investigations in the Bahamas. 4. Pseudocyclopidae (Copepoda, Calanoida) from the Bahamas. Sarsia 32: 39–62. https://doi.org/10.1080/00364827.1968.10411121

Fosshagen A, Boxshall BG, Iliffe TM (2001) The Epacteriscidae, a cave-living family of calanoid copepods. Sarsia 86: 245–318. https://doi.org/10.1080/00364827.2001.10425520

Fosshagen A, Iliffe TM (1989) *Boholina*, a new genus (Copepoda: Calanoida) with two new species from an anchialine cave in the Philippines. Sarsia 74: 201–208. https://doi.org/10.1080/00364827.1989.10413429

Fosshagen A, Iliffe TM (1991) A new genus of calanoid copepod from an anchialine cave in Belize. Bulletin of Plankton Society of Japan Special Volume (1991): 339–346.

Fosshagen A, Iliffe TM (1998) A new genus of the Ridgewayiidae (Copepoda, Calanoida) from an anchialine cave in the Bahamas. Journal of Marine Systems 15: 373–380. https://doi.org/10.1016/S0924-7963(97)00071-7

Fosshagen A, Iliffe TM (2003) Three new genera of Ridgewayiidae (Copepoda, Calanoida) from anchialine caves in the Bahamas. Sarsia 88: 16–35. https://doi.org/10.1080/00364820308465

Fosshagen A, Iliffe TM (2004a) New epacteriscids (Copepoda, Calanoida) from anchialine caves in the Bahamas. Sarsia 89:117–136. https://doi.org/10.1080/00364820410004981

Fosshagen A,Iliffe TM (2004b) A new species of cave-living calanoid copepod from Grand Bahama. Sarsia 89:346–354. https://doi.org/10.1080/00364820410002613

Fosshagen A, Iliffe TM (2007) New species of epacteriscids (Copepoda, Calanoida) from anchialine caves in the Caicos Islands and the Bahamas. Marine Biology Research 3: 73–92. https://doi.org/10.1080/17451000701274571

Huys R, Boxshall GA (1991) Copepod Evolution. The Ray Society, London, 468 pp.

Jaume D, Humphreys WF (2001) A new genus of epacteriscid calanoid copepod from an anchialine sinkhole on northwestern Australia. Journal of Crustacean Biology 21: 157–169. https://doi.org/10.1163/20021975-99990114

Karanovic T, Koomput K, Sanoamuang L (2017) Two new *Thermocyclops* species (Copepoda, Cyclopoida) from Thailand, with notes on the genus phylogeny inferred from 18S and ITS sequences. Zoologischer Anzeiger-A Journal of Comparative Zoology 269: 26–47. https://doi.org/10.1016/j.jcz.2017.07.003

Moon SY, Soh HY (2014) A new species of *Boholina* (Copepoda, Calanoida, Boholinidae) from Ganghwa Island in western Korea. Journal of the Marine Biological Association of the United Kingdom 94: 537–545. https://doi.org/10.1017/S002531541300177X

Sanoamuang L, Boonyanusith C, Brancelj A (2019) A new genus and new species of stygobitic copepod (Crustacea: Copepoda: Cyclopoida) from Thien Duong Cave in Central Vietnam, with a redescription of *Bryocyclops anninae* (Menzel, 1926). Raffles Bulletin of Zoology 67: 189–205.

Suárez-Morales E, Iliffe, TM (2007). A new genus of Ridgewayiidae (Copepoda: Calanoida) from a karstic cave of the western caribbean. Journal of Crustacean Biology 27: 339–350. https://doi.org/10.1651/S-2720.1

Tang D, Barron H, Goater S (2008) A new genus and species of Ridgewayiidae (Copepoda: Calanoida) from subterranean waters of northwestern Australia. Journal of Crustacean Biology 28: 551–563. https://doi.org/10.1651/07-2869R.1

The Malaysian and Thai Working Groups (2009) Geology of the Bukit Batu Puteh-Satun Transect Area along the Malaysia-Thailand borders. Percetakan Zainon Kassim Sdn. Bhd. Perak Darul Ridzuan,111 pp.

Tran DL, Brancelj A (2017) Amended diagnosis of the genus *Nannodiaptomus* (Copepoda, Calanoida), based on redescription of *N. phongnhaensis* and description of a new species from caves in central Vietnam. Zootaxa 4221: 467–473. https://doi.org/10.11646/zootaxa.4221.4.3

Walter TC, Boxshall GA (2019) World of Copepods database. Calanoida. Accessed at: http://www.marinespecies.org/copepoda/aphia.php?p=taxdetails&id=1100 on 2019-04-07

Watiroyram S (2018a) Two new species of the genus *Bryocyclops* Kiefer, 1927 (Copepoda: Cyclopoida: Cyclopidae) from southern Thailand. Raffles Bulletin of Zoology 66:149–169.

Watiroyram S (2018b) *Bryocyclops asetus* sp. n. and the presence of *Bryocyclops musicola* (Menzel, 1926) from Thailand (Crustacea, Copepoda, Cyclopoida, Cyclopidae). ZooKeys 793: 29–51. https://doi.org/10.3897/zookeys.793.25005

Watiroyram S, Brancelj A (2016) A new species of the genus *Elaphoidella* Chappuis (Copepoda, Harpacticoida) from a cave in the south of Thailand. Crustaceana 89: 459–476. https://doi.org/10.1163/15685403-00003536

Watiroyram S, Brancelj A, Sanoamuang L (2012) A new *Bryocyclops* Kiefer (Crustacea: Copepoda: Cyclopoidae) from karstic caves in Thailand. Raffles Bulletin of Zoology 60: 11–21.

Watiroyram S, Brancelj A, Sanoamuang L (2015a) A new cave-dwelling copepod from northeastern Thailand (Cyclopoida: Cyclopidae). Raffles Bulletin of Zoology 63: 426–437.

Watiroyram S, Brancelj A, Sanoamuang L (2015b) Two new stygobiotic species of *Elaphoidella* (Crustacea: Copepoda: Harpacticoida) with comments on geographical distribution and ecology of harpacticoids from caves in Thailand. Zootaxa 3919: 81–99. https://doi.org/10.11646/zootaxa.3919.1.4

Watiroyram S, Sanoamuang L, Brancelj A (2017) Two new species of *Elaphoidella* (Copepoda, Harpacticoida) from caves in southern Thailand and a key to the species of Southeast Asia. Zootaxa 4282: 501–525. https://doi.org/10.11646/zootaxa.4282.3.5

ZooKeys 904: 23–33 (2020)
doi: 10.3897/zookeys.904.47189
http://zookeys.pensoft.net

RESEARCH ARTICLE

A peer-reviewed open-access journal
ZooKeys
Launched to accelerate biodiversity research

Three new species of *Meleonoma* Meyrick from Yunnan, China (Lepidoptera, Gelechioidea, Xyloryctidae)

Aihui Yin[1], Yan Zhi[2], Yanpeng Cai[1]

1 *Morphological Laboratory, Guizhou University of Traditional Chinese medicine, Guiyang 550025, Guizhou, China* **2** *Laboratory Animal Center, Guizhou Medical University, Guiyang, Guizhou, 550025, China*

Corresponding author: *Yanpeng Cai* (CYP815@hotmail.com)

Academic editor: *E. J. van Nieukerken* | Received 9 October 2019 | Accepted 18 December 2019 | Published 16 January 2020

http://zoobank.org/1998E984-40D6-4B23-BC36-C0D90BB78BBA

Citation: Yin A, Zhi Y, Cai Y (2020) Three new species of *Meleonoma* Meyrick from Yunnan, China (Lepidoptera, Gelechioidea, Xyloryctidae). ZooKeys 904: 23–33. https://doi.org/10.3897/zookeys.904.47189

Abstract

Three new species of *Meleonoma* Meyrick, 1914 (Gelechioidea, Xyloryctidae) from China, Yunnan Province, *Meleonoma plicata* **sp. nov.**, *M. scalprata* **sp. nov.** and *M. taeniata* **sp. nov.**, are described and illustrated. A key to *Meleonoma* species known from China is provided.

Keywords

Key, morphology, moth, taxonomy

Introduction

This paper is a continuation of our taxonomic studies of the Chinese *Meleonoma* Meyrick, 1914. The last contribution of ours to this subject was a description of two new species from China with a review of its taxonomic history (Yin and Cai 2019), and yet, the examination of newly received specimens collected from Yunnan Province brought another three new species, *Meleonoma plicata* sp. nov., *M. scalprata* sp. nov. and *M. taeniata* sp. nov., which are described and illustrated here. Adding the three Japanese species recently published by Kitajima and Sakamaki (2019), the total number of *Meleonoma* species has thus increased to 43, with 19 occurring in China. A checklist of the Chinese *Meleonoma* prior to this study can be found in Yin and Cai (2019).

Little is known about their biology. The larvae of some species, such as *M. tamraensis* Park, 2016 and *M. flavilineata* Kitajima & Sakamaki, 2019, are case-bearers. The cases are usually semi-oblong or cylindrical, and built from dead broad leaves and fragments of moss and stems of Poaceae (Kitajima and Sakamaki 2019).

As summarized in Yin and Cai (2019), a well-defined taxonomic position of the genus *Meleonoma* has not been proposed yet. In the absence of recent phylogenetic research, we continue to follow Kim et al. (2016), tentatively placing *Meleonoma* in the Xyloryctidae.

Material and methods

The examined specimens were collected from Yunnan Province in southwestern China in 2018. The descriptive terminology of the anatomical structures generally follows Wang (2006a) and Kristensen (2003). Photographs of adults were taken using a Canon EOS 6D Mark II camera plus an EF 100 mm f/2.8L MACRO IS USM lens with the help of EOS Utility 3.10.20 software. Images of genitalia were captured using a Leica DM4 B upright microscope and photomontage was performed with Leica Application Suite X imaging software. All type specimens are deposited in the Morphological Laboratory, Guizhou University of Traditional Chinese Medicine, Guiyang 550025, Guizhou, China.

Taxonomy

Genus *Meleonoma* Meyrick, 1914

Meleonoma Meyrick, 1914: 255. Type species: *Cryptolechia stomota* Meyrick, 1910a, by original designation.

= *Acryptolechia* Lvovsky, 2010: 378. Type species: *Cryptolechia malacobyrsa* Meyrick, 1921. Synonymised by Lvovsky (2015).

Diagnosis. See Yin and Cai (2019: 80).

Key to *Meleonoma* species from China

1 Male genitalia with an oval process arising from junction of valva and sacculus ..... ***M. foliata* Li, 2004**

– Male genitalia without any process arising from junction of valva and sacculus **2**

2 Costa of valva with a sclerotized process **3**

– Costa of valva smooth, without any process **4**

3 Phallus with an irregularly shaped large cornutus.....***M. echinata* Li, 2004**
– Phallus heavily wrinkled and covered with numerous tiny spines distally (Fig. 4).....***M. plicata* sp. nov.**
4 Ventral margin of valva with rounded hairy prominence or sclerotized tooth-shaped or thornlike process.....**5**
– Ventral margin of valva smooth, without any prominence or process.....**10**
5 Ventral margin of valva with rounded hairy prominence near base.....**6**
– Ventral margin of valva with sclerotized tooth-shaped or thornlike process...**7**
6 Saccus broader and shorter, triangular in shape; phallus without any sclerotized spine or cornutus in male genitalia. Ductus bursae long and nonsclerotized; signum spine-shaped in female genitalia.....
.....***M. flavimaculata* (Christoph 1882)**
– Saccus narrower and longer, linguiform in shape; phallus with a group of sclerotized sclerites near apex in male genitalia. Ductus bursae short, lateral sides sclerotized basally; signum irregularly rounded, with toothlike spines in female genitalia.....***M. peditata* (Wang 2006b)**
7 Valva with large heavily sclerotized thornlike process along median part of ventral margin .....***M. margisclerotica* Wang, 2016**
– Valva with small spinelike process on ventral margin **8**
8 Valva with small spinelike process ventroapically.....
.....***M. torophanes* (Meyrick 1935)**
– Valva with small spinelike process at about middle of ventral margin.....**9**
9 Uncus long and slender, rodlike; sacculus somewhat triangular in shape, dorsal and ventral margins straightly converging into slightly pointed apex, without any extra process.....***M. pardalias* Meyrick, 1931**
– Uncus short, lanciform; sacculus somewhat trapezoid in shape, dorsal and ventral margins each bearing a sclerotized process respectively .....
.....***M. malacobyrsa* (Meyrick 1921)**
10 Uncus sclerotized, long and slender, rodlike, apex acute.....**11**
– Uncus membranous, short, not rodlike.....**18**
11 Saccus short and broad, widely rounded at apex **12**
– Saccus triangular or funnel-shaped, tapered or at least narrowly rounded at apex.....**13**
12 Phallus with numerous extremely small spines distally.....
.....***M. meyricki* Lvovsky, 2015**
– Phallus without cornutus or any other spine.....
.....***M. malacognatha* Li & Wang, 2002**
13 Forewing mostly blackish brown, broadly and densely scattered with orange yellow forming irregular streaks and blotches, or only sparsely diffused with yellow.....**14**
– Forewing mostly yellow, more or less mixed with brown, with or without brown fascia or patch on apical half.....**15**

14 Forewing broadly and densely scattered with orange yellow forming irregular streaks and blotches. Sacculus with several short spines distally and no extra process; phallus with a curved band-shaped plate distally ..... ***M. apicispinata* Wang, 2016**

– Forewing only sparsely diffused with yellow. Sacculus with a long bladelike process distally; phallus with three small teeth distally ..... ***M. projecta* Yin, 2019**

15 Valva small, oblong and pointing downward, median surface covered with long and thick setae ..... ***M. polychaeta* Li, 2004**

– Valva generally broad, knife-shaped and uplifted, median surface covered with thin long hairs **16**

16 Basal half of valva densely covered with long hairs on median surface ..... ***M. facunda* (Meyrick 1910b)**

– Basal half of valva only sparsely covered with long hairs on median surface.... **17**

17 Dorsal margin of sacculus with one process at end; phallus straight, with one rodlike sclerite extending from middle to apex (Fig. 5)..... ***M. scalprata* sp. nov.**

– Sacculus with two sclerotized processes at end of dorsal and ventral margins respectively; phallus hooked in distal 1/4, without any sclerite ..... ***M. foliiformis* Yin, 2019**

18 Uncus triangular; sacculus without any process; phallus forming an 8-shaped bandlike structure distally (Fig. 7)..... ***M. taeniata* sp. nov.**

– Uncus cone-shaped; sacculus with three processes; phallus with one short cornutus in vesica ..... ***M. facialis* Li & Wang, 2002**

***Meleonoma plicata* sp. nov.**
http://zoobank.org/FEF920AC-F5FD-4DDF-936B-4DC7D43F5035
Figs 1, 4

Material examined. ***Holotype:*** China • ♂; Yunnan Province, Puer City, Lianhua Village; alt. 1300 m, 20 May 2018; Yan Zhi leg.; YAH19068.

Diagnosis. This new species, *M. foliiformis*, *M. malacobyrsa* and *M. scalprata* share many characters in both appearance and male genitalia, which implies that these four species might belong to the same lineage within *Meleonoma*. In appearance, they all have a relatively large wingspan; similar composition of body color (primarily yellow and brown); similar pattern of coloration of forewings (mostly yellow, more or less mixed with brown near base, a brown fascia from costa obliquely to slightly before tornus, a somewhat triangular brown patch at apex). In male genitalia, they all share the following characters: valva large and broad with median surface densely covered with long hairs; sacculus broad, nearly triangular or trapezoid with various sclerotized processes. However, *M. plicata* can be easily distinguished from the others by the following character combination: forewing with basal 1/3 densely mixed with blackish brown speckles; dorsal margin of valva with a small finger-shaped process at distal 1/6, ventral margin smooth, without any process; dorsal margin of sacculus with a large

Figures 1–3. *Meleonoma* species, morphology **1** adult of *M. plicata* sp. nov., holotype, male (gen. slide no. YAH19068) **2** adult of *M. taeniata* sp. nov., holotype, male (gen. slide no. YAH19071) **3** adult of *M. scalprata* sp. nov., paratype, female (gen. slide no. YAH19070). Scale bars: 2.50 mm.

fingerlike process at end; phallus with an oblique portion in distal 1/3 heavily wrinkled and covered with numerous tiny spines.

Description. ***Head:*** vertex and front pale gray, mixed with yellow bilaterally; labial palpus long and recurved, extending well beyond vertex, with smooth scales, yellow, segment 1 mixed with dark brown on outer surface, segment 2 blackish brown distally and extending to middle of ventral margin; segment 3 about 3/4 length of segment 2; antenna with scape blackish brown on dorsal surface and yellow on ventral surface, with flagellum ringed, alternately blackish brown and yellow, except almost pure pale yellow on ventral surface of basal half flagellomeres; scales of proboscis yellow.

Thorax: tegula and mesonotum blackish brown mixed with yellow; legs whitish yellow, tibiae and tarsi scattered with blackish brown speckles on outside. Forewing (Fig. 1): length 5.8 mm ($N = 1$), about 3.6 × as long as wide, yellow, basal 1/3 quite densely mixed with blackish brown speckles; a blackish brown fascia extending from basal 3/5 of costa obliquely to slightly before tornus, with inner margin slightly arched outward, outer margin somewhat serrated irregularly; cell with two dim black dots, one set at middle, other at middle of fold; apex forming a somewhat triangular patch, blackish brown, mixed with yellow along apex and termen; other yellow parts sparsely scattered with blackish brown scales; cilia yellow except blackish brown on tornus; ventral surface yellowish brown. Hindwing (Fig. 1): translucent grayish brown, gradually darkening towards apex; cilia grayish.

Male genitalia (Fig. 4): uncus with base short, slightly dilated bilaterally, with other part quite long and slender, slightly curved, apex acute; gnathos mostly membranous, with

lateral arms arched outward; tegumen near bell-shape, lateral arms about same width, posterior margin slightly concave at middle, anterior margin shallowly concave into parenthesis-shape; valva gradually widening to middle from a narrow base, with ventral margin broadly arcuate in distal half into rounded apex, median surface densely covered with long hairs; costa nearly straight, strongly sclerotized except only weakly so in distal 1/6, with a small finger-shaped process protruded outward at distal 1/6; transtilla short and weakly sclerotized, covered with rows of long hairs, protruded forward medially; sacculus broad, nearly triangular, with basal 2/3 of dorsal margin joined with valva, a large fingerlike process at end of dorsal margin, distal half of ventral margin slightly serrated, somewhat protruded, densely covered with long hairs and as well on central area of sacculus; saccus funnel-shaped narrowly rounded at apex; juxta arcuate; phallus moderately sclerotized, cigar-shaped, with an oblique portion in distal 1/3 heavily wrinkled and covered with numerous tiny spines.

Female genitalia: unknown.

Biology. Nothing is known about the larva. The adult was collected at night in May.

Distribution. Known only from the type locality (Southwest China: Yunnan Province).

Etymology. The specific name is derived from the Latin adjective *plicatus* (wrinkled, folded), referring to the heavily wrinkled distal part of the phallus in male genitalia.

***Meleonoma scalprata* sp. nov.**

http://zoobank.org/CCA1F194-3A1D-4FF6-A2C9-2936B97702AF

Figs 3, 5, 6

Material examined. ***Holotype:*** China • ♂; Yunnan Province, Puer City, Lianhua Village; alt. 1300 m, 20 May 2018; Yan Zhi leg.; YAH19069. ***Paratype:*** 1 ♀, same collection data as for preceding; YAH19070.

Diagnosis. This new species belongs to the lineage comprising *M. foliiformis*, *M. malacobyrsa* and *M. plicata*. The new species can be easily distinguished from the others by the following combination of characters: forewing with basal half mixed with blackish brown speckles; both dorsal and ventral margins of valva smooth, without any process; dorsal margin of sacculus with an inconspicuous beak-shaped process at end; phallus with one rodlike sclerite originating from middle and extending to apex.

Description. ***Head:*** vertex pale gray, mixed with yellow bilaterally, front pale yellowish gray; labial palpus long and recurved, extending well beyond vertex, with smooth scales, yellow, segment 1 mixed with blackish brown on outer surface, segment 2 blackish brown distally and extending vaguely to middle of ventral margin; segment 3 about half length of segment 2; antenna with scape blackish brown on dorsal surface and yellow on ventral surface, with flagellum ringed, alternately blackish brown and yellow, except almost pure yellow on ventral surface of about basal half flagellomeres; scales of proboscis pale yellow.

Thorax: tegula yellow, very sparsely mixed with blackish brown laterally; mesonotum yellow, mixed with blackish brown and more strongly so on posterior half; legs whitish yellow, tibiae and tarsi scattered with blackish brown speckles on outside. Fore-

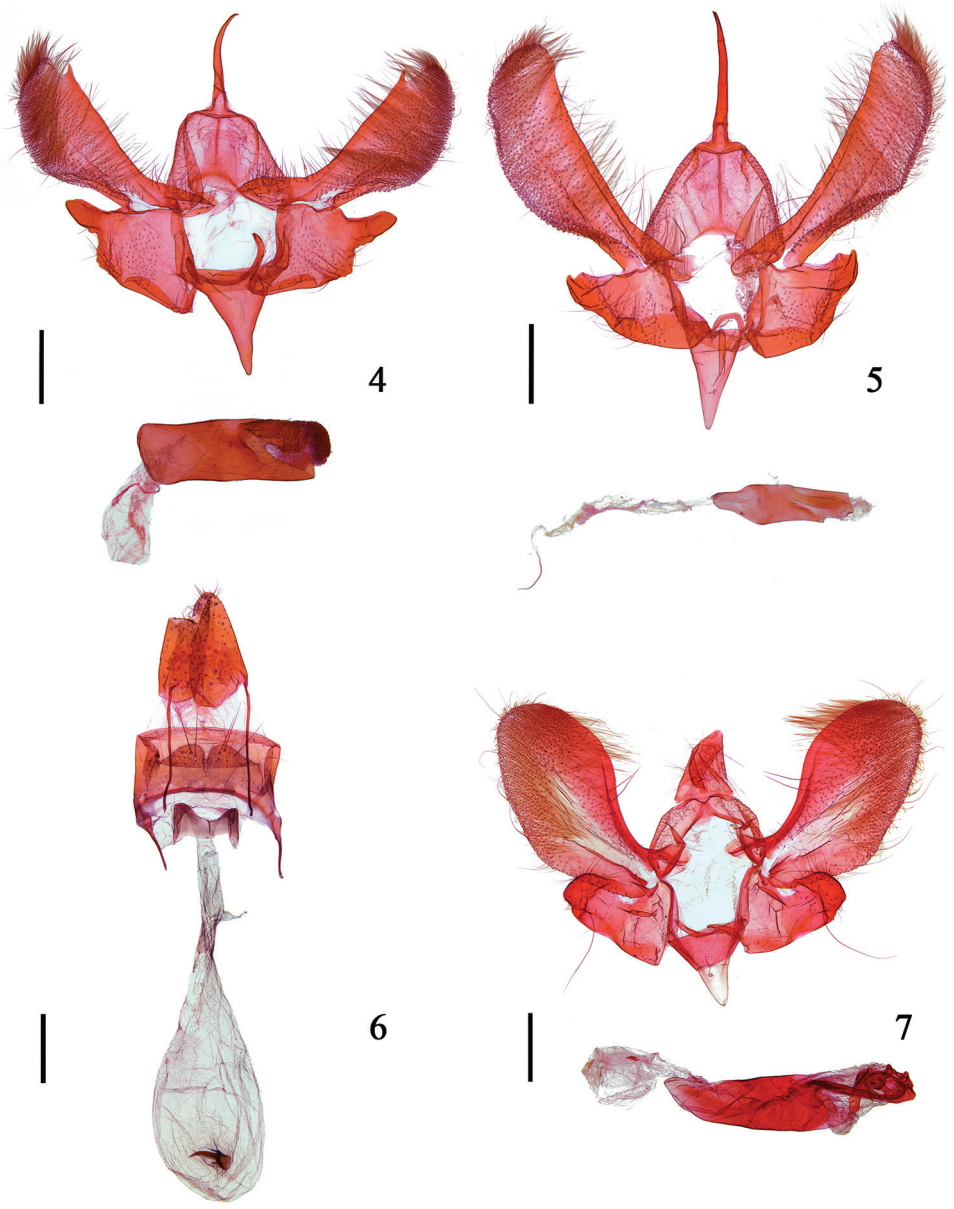

Figures 4–7. *Meleonoma* species, morphology **4** male genitalia of *M. plicata* sp. nov., holotype, phallus illustrated separately (gen. slide no. YAH19068) **5** male genitalia of *M. scalprata* sp. nov., holotype, phallus illustrated separately (gen. slide no. YAH19069) **6** female genitalia of *M. scalprata* sp. nov., paratype (gen. slide no. YAH19070) **7** male genitalia of *M. taeniata* sp. nov., holotype, phallus illustrated separately (gen. slide no. YAH19071). Scale bars: 0.25 mm.

wing (Fig. 3): length 5.4–5.6 mm (N = 2), about 3.3 × as long as wide, yellow, basal half mixed with blackish brown speckles; a narrow blackish brown fascia extending from basal 3/5 of costa obliquely to slightly before tornus, slightly wider anteriorly; cell

with two very dim black dots, one set at end, other at middle of fold; apex forming a somewhat narrow triangular patch, blackish brown, mixed with yellow along apex and termen; other yellow parts sparsely scattered with blackish brown scales; cilia yellow except grayish brown on tornus; ventral surface dark yellowish brown. Hindwing (Fig. 3): translucent grayish brown, gradually darkening towards apex; cilia grayish brown.

Male genitalia (Fig. 5): uncus with base short, dilated bilaterally into inverted T-shape, with other part quite long and slender, rodlike, apex acute; gnathos mostly membranous, with lateral arms slightly curved, a bit more sclerotized in basal half than distal half; tegumen nearly inverted V-shaped, lateral arms gradually narrowed to apex, posterior margin slightly concave at middle, anterior margin relatively shallowly concave into parenthesis-shape; valva somewhat in shape of table knife, gradually widening to basal 1/4 from a narrow base, with ventral margin arcuate in distal 1/5 into rounded apex, median surface densely covered with long hairs; costa strongly sclerotized, nearly straight, scattered with long hairs; transtilla covered with rows of long hairs, protruded forward medially, distal portion rounded; sacculus broad, nearly triangular, with basal half of dorsal margin joined with valva, dorsal margin with an inconspicuous beak-shaped process at end, ventral margin slightly more sclerotized, with a very shallow arcuate emargination from about middle to distal 1/4, with long hairs covering median portion and as well as central area of sacculus; saccus funnel-shaped, narrowly rounded at apex; juxta widely U-shaped; phallus moderately sclerotized, nearly cylindrical in shape, narrower in basal 1/3, with one rodlike sclerite originating from middle and extending to apex.

Female genitalia (Fig. 6): papillae anales large and broad, setose; apophyses posterioris about 3 times length of apophysis anteriores; eighth tergum entirely sclerotized; eighth sternite with granules posteriorly, posterior margin narrowly concave at middle, forming two semiovate plates with long setae; lamella antevaginalis moderately sclerotized, capital M-shaped; ductus bursae entirely membranous; ductus seminalis originating from about middle of ductus bursae; corpus bursae large, ovate, entirely membranous; signum machete-shaped, with one extra small spine on each side near base.

Biology. Nothing is known about the larva. The adults were collected at night in May.

Distribution. Known only from the type locality (Southwest China: Yunnan Province).

Etymology. The specific name is derived from the Latin adjective *scalpratus* (knife-shaped), referring to the machete-shaped signum in female genitalia.

Meleonoma taeniata sp. nov.

http://zoobank.org/7190435D-430A-46A3-B99B-778AEEDCB020
Figs 2, 7

Material examined. ***Holotype:*** China • ♂; Yunnan Province, Puer City, Lianhua Village; alt. 1300 m, 21 May 2018; Yan Zhi leg.; YAH19071.

Diagnosis. This new species is similar to *M. torophanes* superficially, but it can be distinguished from the latter by having one large earthy yellow V-shaped mark on forewing; uncus triangular; ventral margin of valva smooth, without any spine; sacculus with distal

1/4 sclerotized forming a thickened plate, without any extra process; phallus forming an 8-shaped bandlike structure distally. Whereas the latter has two large light-yellow marks on forewing; uncus lanciform; valva with a short spine ventroapically; sacculus forming a narrow process distally; phallus with a hairbrush-shaped sclerite attached with short spines.

Description. ***Head:*** vertex and front pale earthy yellow mixed with dark brown; labial palpus long and recurved, extending well beyond vertex, with smooth scales, pale earthy yellow, outer surface of segment 1 dark brown, of segment 2 dark brown distally and extending vaguely to distal 2/3, of segment 3 slightly tinged with dark brown at middle, inner surface of segment 2 dark brown distally; segment 3 slightly shorter than segment 2; antenna with scape dark brown on dorsal surface and pale earthy yellow on ventral surface, with flagellum alternately dark brown and yellow on dorsal surface, except middle 1/3 flagellomeres almost pure dark brown, ventral surface pale earthy yellow; scales of proboscis pale earthy yellow.

Thorax: tegula and mesonotum dark brown mixed with pale earthy yellow; legs pale earthy yellow, forelegs somewhat segmented with wide dark brown rings, mid and hindlegs with tibiae and tarsi scattered with dark brown speckles on outside. Forewing (Fig. 2): length 5.5 mm (N = 1), about 3.6 × as long as wide, dark brown; cell with three indistinct black dots, one set at middle, one at end and one at middle of fold; a broad somewhat V-shaped mark with two ends extending from about basal 1/2 and 4/5 of costa respectively, and converging slightly before tornus, earthy yellow in color, and sparsely tinged with yellowish brown and dark brown scales; apex and termen narrowly edged with pale earthy yellow; cilia earthy yellow mixed with pale brown; ventral surface light brown. Hindwing (Fig. 2): translucent light grayish brown, gradually darkening towards apex; cilia light grayish brown.

Male genitalia (Fig. 7): uncus membranous, triangular in shape, with long setae on dorsal surface; gnathos absent; tegumen inverted U-shaped, lateral arms long, about same width, posterior margin with a shallow V-shaped notch at middle, anterior margin deeply concave; valva broad, gradually widening to basal 2/5 from a relatively narrow base, with distal 3/5 nearly same width, apex broadly rounded, densely covered with long hairs on median surface, but asetose in an elongate membranous area at center; costa moderately sclerotized, broadly arched forming a shallow notch; transtilla round, narrow at base, swollen distally, asetose, protruded forward medially; sacculus broad, trapezoid, with dorsal margin joined with valva at base, with distal 1/4 strongly sclerotized forming a distinct thickened plate that sparsely covered with long setae on both outer and median surfaces, dorsal and ventral margins nearly parallel; saccus short, funnel-shaped narrowly rounded at apex; juxta bifurcated, weakly joined at base; phallus moderately sclerotized, rodlike, narrow at base, gently thickened to basal 2/3, heavily sclerotized in distal 1/3, forming a bandlike structure similar to Arabic numeral "8" in shape.

Female genitalia: unknown.

Biology. Nothing is known about the larva. The adult was collected at night in May.

Distribution. Known only from the type locality (Southwest China: Yunnan Province).

Etymology. The specific name is derived from the Latin adjective *taeniatus* (bandlike), referring to the bandlike structure of the phallus in male genitalia.

Acknowledgements

This project was supported by the National Natural Science Foundation of China (No. 31760630, No. 31760629), Guizhou Provincial Department of Education Youth Science and Technology Talent Growth Project (黔教合KY字[2017]175) and the Science and Technology Project of Guiyang (No. [2017]5-25).

References

Caradja A, Meyrick E (1935) Materialien zu einer Microlepidopteren-Fauna der chinesischen Provinzen Kiangsu, Chekiang und Hunan. R. Friedländer & Sohn, Berlin, 96 pp. [2 pls]

Christoph HT (1882) Neue Lepidopteren des Amurgebietes. Bulletin de la Société impériale des naturalists de Moscou 57(1): 5–47.

Kim S, Kaila L, Lee S (2016) Evolution of larval mode of life of Oecophoridae (Lepidoptera: Gelechioidea) inferred from molecular phylogeny. Molecular Phylogenetics and Evolution 101: 314–335. https://doi.org/10.1016/j.ympev.2016.05.015

Kitajima Y, Sakamaki Y (2019) Three new species of the genus *Meleonoma* Meyrick (Lepidoptera: Oecophoridae) from Japan. Lepidoptera Science 70(2): 33–46.

Kristensen NP (2003) Skeleton and muscles: adults. In: Kristensen NP (Ed.) Lepidoptera, Moths and Butterflies, 2 Morphology, physiology and development. Handbook of Zoology 4(36): 39–131. De Gruyter, Berlin, New York.

Li HH, Wang SX (2002) A study on the genus *Meleonoma* Meyrick from China, with descriptions of two new species (Lepidoptera: Cosmopterigidae). Acta Entomologica Sinica 45(2): 230–233.

Li HH, Wang XP (2004) New species of *Meleonoma* Meyrick (Lepidoptera: Cosmopterigidae) from China. Entomotaxonomia 26(1): 35–40.

Lvovsky AL (2010) New genus of broad-winged moths of the family Cryptolechiidae (Lepidoptera, Gelechioidea) from Southeastern Asia. Entomological Review 90: 255–258. https://doi.org/10.1134/S0013873810020119

Lvovsky AL (2015) Composition of the subfamily Periacminae (Lepidoptera, Lypusidae) with descriptions of new and little known species of the genus *Meleonoma* Meyrick, 1914 from South, East, and South-East Asia. Entomological Review 95(6): 766–778. https://doi.org/10.1134/S0013873815060111

Meyrick E (1910a) Notes and descriptions of Indian Micro-Lepidoptera. Records of the Indian Museum 5(4): 217–232. https://doi.org/10.5962/bhl.part.10499

Meyrick E (1910b) Descriptions of Indian Micro-Lepidoptera. Journal of the Bombay Natural History Society 20: 143–168.

Meyrick E (1914) Exotic Microlepidoptera 1(8): 225–256.

Meyrick E (1921) Exotic Microlepidoptera 2(13): 385–416.

Meyrick E (1931) Exotic Microlepidoptera 4(6): 161–192.

Park KT, Park YM (2016) Two new species of the genus *Meleonoma* Meyrick (Lepidoptera, Lypusidae) from Korea. Journal of Asia-Pacific Biodiversity 9: 485–488. https://doi.org/10.1016/j.japb.2016.07.006

Wang SX (2006a) Oecophoridae of China (Insecta: Lepidoptera). Science Press, Beijing, 258 pp. [15 col. pls]

Wang SX (2006b) The *Cryptolechia* Zeller (Lepidoptera: Oecophoridae) of China (III): Checklist and descriptions of new species. Zootaxa 1195: 1–29. https://doi.org/10.11646/zootaxa.1330.1.4

Yin AH, Cai YP (2019) Two new species of the genus *Meleonoma* Meyrick from China (Lepidoptera, Gelechioidea, Xyloryctidae). ZooKeys 871: 79–87. https://doi.org/10.3897/zookeys.871.35738

Yin AH, Wang SX (2016) Two new species in the genus *Meleonoma* Meyrick (Lepidoptera: Oecophoridae) from Taiwan. Entomotaxonomia 38(1): 24–28.

ZooKeys 904: 35–62 (2020)
doi: 10.3897/zookeys.904.47354
http://zookeys.pensoft.net

RESEARCH ARTICLE

A peer-reviewed open-access journal
ZooKeys
Launched to accelerate biodiversity research

A new *Megophrys* Kuhl & Van Hasselt (Amphibia, Megophryidae) from southeastern China

Bin Wang[1], Yan-Qing Wu[2], Jun-Wei Peng[3], Sheng-Chao Shi[1], Ning-Ning Lu[1], Jun Wu[1,2]

1 *CAS Key Laboratory of Mountain Ecological Restoration and Bioresource Utilization and Ecological Restoration Biodiversity Conservation Key Laboratory of Sichuan Province, Chengdu Institute of Biology, Chinese Academy of Sciences, Chengdu 610041, China* **2** *Nanjing Institute of Environmental Sciences, Ministry of Ecology and Environment of China, Nanjing 210042, China* **3** *Xianju Biodiversity Development Company Limited, Taizhou 317300, China*

Corresponding author: *Jun Wu* (wujun@nies.org), *Bin Wang* (wangbin@cib.ac.cn)

Academic editor: *A. Herrel* | Received 16 October 2019 | Accepted 22 November 2019 | Published 16 January 2020

http://zoobank.org/1F338DB9-5D94-406B-A7C9-E4EAEDFDE503

Citation: Wang B, Wu Y-Q, Peng J-W, Shi S-C, Lu N-N, Wu J (2020) A new *Megophrys* Kuhl & Van Hasselt (Amphibia, Megophryidae) from southeastern China. ZooKeys 904: 35–62. https://doi.org/10.3897/zookeys.904.47354

Abstract

A new species of the genus *Megophrys* from Zhejiang Province, China is described. Molecular phylogenetic analyses supported the new taxon as an independent clade nested into the *Megophrys* clade and sister to *M. lishuiensis*. The new species could be distinguished from its congeners by a combination of the following morphological characteristics: (1) small size (SVL 31.0–36.3 mm in male and 41.6 mm in female); (2) vomerine ridge present and vomerine teeth absent; (3) tongue not notched behind; (4) a small horn-like tubercle at the edge of each upper eyelid; (5) tympanum distinctly visible, rounded; (6) two metacarpal tubercles in hand; (7) relative finger lengths: II < I < IV < III; (8) toes with rudimentary webbing at bases; (9) heels overlapping when thighs are positioned at right angles to the body; (10) tibiotarsal articulation reaching tympanum to eye when leg stretched forward; (11) an internal single subgular vocal sac in male; (12) in breeding male, the nuptial pads with black nuptial spines on the dorsal bases of the first and second fingers.

Keywords

Taxonomy, new species, molecular phylogenetic analysis, morphology, Zhejiang Province, China

Introduction

Megophryidae Bonaparte, 1850 (Amphibia: Anura) is a large Asian toad family which was divided into three subfamilies, i.e., Leptobrachiinae Dubois, 1983, Leptolalaginae Delorme, Dubois, Grosjean & Ohler, 2006 and Megophryinae Bonaparte, 1850 (Delorme et al. 2006). The generic and/or subgeneric classifications in Megophryinae have been under debates for a long time (Tian and Hu 1983; Dubois 1987 "1986"; Lathrop 1997; Rao and Yang 1997; Dubois and Ohler 1998; Jiang et al. 2003; Delorme et al. 2006; Frost et al. 2006; Fei and Ye 2009, 2012, 2016; Chen et al. 2017; Mahony et al. 2017; Liu et al. 2018; Munir et al. 2018) though recent phylogenetic studies clustered all recognised species of Megophryinae into one big clade (e.g., Chen et al. 2017; Mahony et al. 2017; Li et al. 2018). Mahony et al. (2017) classified all members of Megophryinae into a single genus *Megophrys* Kuhl & Van Hasselt, 1822 including seven subgenera (*Megophrys*, *Xenophrys* Günther, 1864, *Panophrys* Rao & Yang, 1997, *Atympanophrys* Tian & Hu, 1983, *Ophryophryne* Boulenger, 1908, *Pelobatrachus* Beddard, 1908 (1907), and *Brachytarsophrys* Tian & Hu, 1983) based on molecular phylogenetics and morphological comparisons. Partly based on this point, Frost (2019) placed all recognised species of Megophryinae into the genus *Megophrys* but with no subgeneric classifications.

The genus *Megophrys* is widely distributed from eastern China through the eastern and southern Himalayas, throughout mainland Indochina and the islands of the Sunda shelf in Indonesia and parts of the Philippines (Frost 2019). It currently contains 92 recognised species (Frost 2019), and noticeably, 37 species were described in the last decade (See species list of *Megophrys* in Frost 2019). The genus is suggested to harbour both cryptic diversity and highly localised species diversification (Chen et al. 2017; Mahony et al. 2017, 2018; Liu et al. 2018). For example, in the genus, just in China, 41 cryptic species were suggested by molecular phylogenetic analyses in Liu et al. (2018), and six of them were subsequently described (Li et al. 2018; Wang et al. 2019). To present, 48 *Megophrys* species have been described in China. Obviously, we still need to verify that undescribed taxa and conduct deep investigations for exploring underestimated diversity in this group especially based on detailed morphological comparisons, molecular phylogenetics and bioacoustics data.

During our field surveys in the Xianju County, Zhejiang Province, China, some *Megophrys* specimens were collected from the montane forests. Molecular phylogenetic analyses and morphological comparisons support that it is distinctly different from its *Megophrys* congeners. Therefore, we describe it herein as a new species.

Materials and methods

Specimens

Seven adult males, two adult females, and six tadpoles of the new taxon (for voucher information see Suppl. material 1: Table S1 and Suppl. material 2: Table S2) were

collected from the mountain streams of Xianju County, Zhejiang Province, China (Fig. 1). The stages of tadpoles were identified following Gosner (1960). After taking photographs, they were euthanised using isoflurane, and the specimens were then fixed in 75% ethanol. Tissue samples were taken and preserved separately in 95% ethanol prior to fixation. Specimens were deposited in Chengdu Institute of Biology, Chinese Academy of Sciences (**CIB, CAS**).

Molecular data and phylogenetic analyses

Four male, two female, and three tadpole specimens of the new taxon were included in the molecular analyses (for voucher information see Table 1). For phylogenetic analyses, two topotypes of *M. kuatunensis* and two topotypes of *M. boettgeri* from Wuyi Mountain, Fujian Province, China (the common type locality of these species; Fig. 1) were also collected and sequenced (for voucher information see Table 1).

Total DNA was extracted using a standard phenol-chloroform extraction protocol (Sambrook et al. 1989). Two fragments of the mitochondrial genes 16S rRNA and cytochrome oxidase subunit I (COI) were amplified. For 16S, the primers P7 (5'-CGCCTGTTTACCAAAAACAT-3') and P8 (5'-CCGGTCTGAACTCAGATCACGT-3') were used following Simon et al. (1994), and for COI, Chmf4 (5'-TYTCWACWAAYCAYAAAGAYATCGG-3') and Chmr4 (5'-ACYTCRGGRTGRCCRAARAATCA-3') were used following Che et al. (2012). Gene fragments were amplified under the following conditions: an initial denaturing step at 95 °C for 4 min; 36 cycles of denaturing at 95 °C for 30 sec, annealing at 52 °C (for 16S)/47 °C (for COI) for 40 sec and extending at 72 °C for 70 sec. Sequencing was conducted using an ABI3730 automated

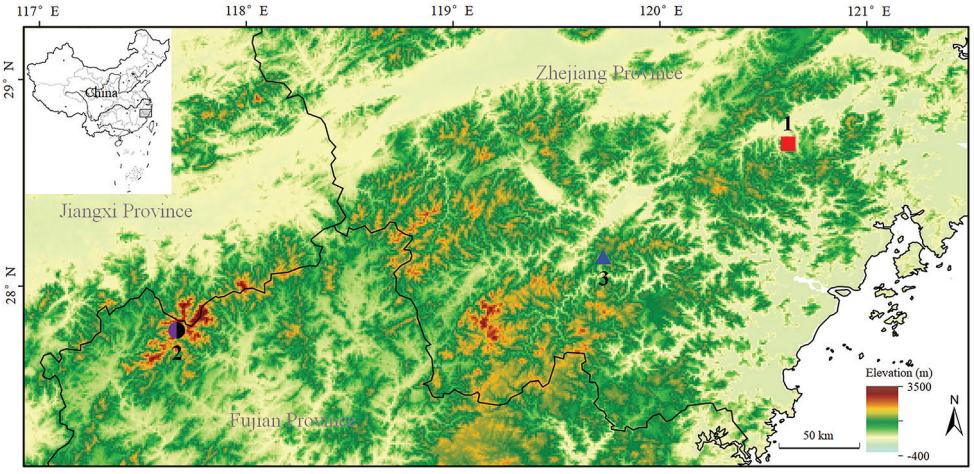

Figure 1. Localities for specimens used in this study. 1, the type locality of *Megophrys xianjuensis* sp. nov., Xianju County, Zhejiang Province, China; 2. the common type locality of *M. boettgeri* (black) and *M. kuatunensis* (purple), Wuyi Mountain, Nanping County, Fujian Province, China; 3, the type locality of *M. lishuiensis*, Lishui City, Zhejiang Province, China.

Table 1. Localities, voucher information, and GenBank accession numbers for molecular samples used in this study.

Species	Voucher number	Locality	GenBank accession number	
			16S	COI
Megophrys aceras	KIZ025467	Khao Nan National Park, Nakhon Si Thammarat, Thailand	KX811925	KX812159
M. acuta	SYS a001957	Heishiding Nature Reserve, Guangdong Prov., China	KJ579118	–
M. auralensis	NCSM 79599	Aural, Kampong Speu, Cambodia	KX811807	–
M. baluensis	ZMH A13125	Gunung Kinabalu National Park, Kogopan Trail, Malaysia	KJ831310	–
M. baolongensis	KIZ019216	Baolong, Chongqing City, China	KX811813	KX812093
M. binchuanensis	KIZ019441	Mt. Jizu, Yunnan Prov., China	KX811849	KX812112
M. binlingensis	KIZ025807	Mt. Wawu, Sichuan Prov., China	KX811852	KX812115
M. boettgeri	Tissue ID: YPXJK033	Mt. Wuyi, Fujian Prov., China	KX811814	KX812104
	CIBWY18082307	Mt. Wuyi, Fujian Prov., China	MN563762	MN563778
	CIBWY18082603	Mt. Wuyi, Fujian Prov., China	MN563763	MN563779
M. brachykolos	ROM 16634	Hong Kong, China	KX811897	KX812150
M. carinense	Tissue ID: YPX20455	Dayao Shan, Guangxi Prov., China	KX811811	KX812057
M. cheni	SYS a001427	Jinggang Shan, Jiangxi Prov., China	KJ560391	–
M. chuannanensis	CIB20050081	Hejiang, Sichuan Prov., China	KM504261	–
M. daweimontis	KIZ048997	Dawei Shan, Yunnan Prov., China	KX811867	KX812125
M. dongguanensis	SYS a001972	Mt. Yinping, Guangdong Prov., China	MK524098	MK524129
M. dringi	UNIMAS 8943	Gunung Mulu National Park, Sarawak, Malaysia	KJ831317	–
M. edwardinae	FMNH 273694	Bintulu, Sarawak, Malaysia	KX811918	KX812050
M. elfina	ZMMU ABV-00454	Bidoup Mountain, Lam Dong, Vietnam	KY425379	–
M. fansipanensis	VNMN 2018.01	Lao Cai, Sa Pa, Vietnam	MH514886	–
M. feae	KIZ046706	Huangcaoling, Yunnan Prov., China	KX811810	KX812056
M. flavipunctata	SDBDU2009.297	East Khasi Hills dist., Meghalaya	KY022307	MH647536
M. gerti	ITBCZ 1108	Nui Chua National Park, Ninh Thuan, Vietnam	KX811917	KX812161
M. gigantica	SYSa003933	Wuliang shan, Yunnan Prov., China	MH406775	MH406235
M. glandulosa	KIZ048439	Husa, Yunnan Prov., China	KX811762	KX812075
M. hansi	KIZ010360	Phong Dien Nature Reserve, Thua Thien Hue, Vietnam	KX811913	KX812155
M. himalayana	SDBDU2009.75	East Siang dist., Arunachal Pradesh, India	KY022311	–
M. hoanglienensis	VNMN 2018.02	Lao Cai, Sa Pa, Vietnam	MH514889	–
M. huangshanensis	KIZ022004	Mt. Huang, Anhui Prov., China	KX811821	KX812107
M. intermedia	ZFMK 87596	U Bo, Phong Nha-Ke Bang NP, Vietnam	HQ588950	–
M. jingdongensis	KIZ-LC0805067	Huanglianshan, Yunnan Prov., China	KX811872	KX812131
M. jinggangensis	KIZ07132	Chashan Forest Farm, Jiangxi Prov., China	KX811840	KX812108
M. jiulianensis	SYS a002107	Mt. Jiulian, Jiangxi Prov., China	MK524099	MK524130
M. kalimantanensis	MZB. Amph 21482	Tanah Bumbu, Kalimantan Selatan, Borneo, Indonesia	MG993554	–
M. kobayashii	UNIMAS 8148	Gunung Kinabalu National Park, Sabah, Malaysia	KJ831313	–
M. kuatunensis	CIBWY18082407	Mt. Wuyi, Fujian Prov., China	MN563764	MN563780
	CIBWY18082408	Mt. Wuyi, Fujian Prov., China	MN563765	MN563781
	SYS a001579	Mt. Wuyi, Fujian Prov., China	KJ560376	–
M. lancip	MZB:Amp:22233	–	KY679891	–
M. leishanensis	CIBLS20171101001	Mt. Leigong, Guizhou Prov., China	MK005310	MK005306
M. ligayae	ZMMU NAP-05015	Palawan, Philippines	KX811919	KX812051
M. lini	SYS a002370	Suichuan Co., Jiangxi Prov., China	KJ560412	–
M. lishuiensis	CIBWYF00169	Lishui City, Zhejiang Prov., China	KY021418	–
	CIBWYF00170	Lishui City, Zhejiang Prov., China	KY113084	–
	CIBWYF11011	Lishui City, Zhejiang Prov., China	KY113085	–
M. major	SYSa002961	Zhushihe, Yunnan Prov., China	MH406728	MH406180
M. mangshanensis	KIZ021786	Nanling National Forest Park, Guangdong Prov., China	KX811790	KX812079
M. maosonensis	KIZ016045	Xiaoqiaogou Nature Reserve, Yunnan Prov., China	KX811780	KX812080
M. medogensis	KIZ06621	Beibeng, Xizang Prov., China	KX811767	KX812082
M. microstoma	KIZ048799	Xiaoqiaogou Nature Reserve, Yunnan Prov., China	KX811914	KX812156
M. minor	KIZ01939	Qingcheng Shan, Sichuan Prov., China	KX811896	KX812145
M. montana	LSUMZ 81916	Sukabumi, Java, Indonesia	KX811927	KX812163
M. monticola	SDBDU 2011.1047 [h]	Darjeeling dist., West Bengal, India	KX894679	–
M. mufumontana	SYS a006391	Mt. Mufu, Hunan Prov., China	MK524105	MK524136

Species	Voucher number	Locality	GenBank accession number	
			16S	COI
M. nankiangensis	CIB ZYC517	Nanjiang, Sichuan Prov., China	KX811900	–
M. nankunensis	SYS a004498	Mt. Nankun, Guangdong Prov., China	MK524108	MK524139
M. nanlingensis	SYS a001959	Nanling Nature Reserve, Guangdong Prov., China	MK524111	MK524142
M. nasuta	KIZ019419	Malaysia	KX811921	KX812054
M. obesa	SYS a002272	Heishiding Nature Reserve, Guangdong Prov., China	KJ579122	–
M. ombrophila	KRM18	Mt. Wuyi, Fujian Prov., China	KX856404	–
M. omeimontis	KIZ025765	Mt. E'mei, Sichuan Prov., China	KX811884	KX812136
M. oreocrypta	BNHS 6046	West Garo Hills dist., Meghalaya	KY022306	–
M. pachyproctus	KIZ010978	Beibeng, Xizang Prov., China	KX811908	KX812153
M. palpebralespinosa	KIZ011603	Pu Hu Nature Reserve, Thanh Hoa, Vietnam	KX811888	KX812137
M. parva	SYSa003042	Zhushihe, Yunnan Prov., China	MH406737	MH406189
M. periosa	BNHS 6061	West Kameng dist., Arunachal Pradesh, India	KY022309	MH647528
M. popei	SYS a000589	Naling Nature Reserve, Guangdong Prov., China	KM504251	–
M. sangzhiensis	Tissue ID: YPX11006	Badagongshan Nature Reserve, Hunan Prov., China	KX811856	KX812117
M. shapingensis	KIZ014512	Liziping Nature Reserve, Sichuan Prov., China	KX811904	KX812060
M. spinata	KIZ016100	Mt. Leigong, Guizhou Prov., China	KX811864	KX812119
M. stejnegeri	KU 314303	Pasonanca Natural Park, Zamboanga, Philippines	KX811922	KX812052
M. synoria	FMNH 262778	O'Reang, Mondolkiri, Cambodia	KY022198	–
M. tuberogranulata	Tissue ID: YPX10987	Badagongshan Nature Reserve, Hunan Prov., China	KX811823	KX812095
M. wawuensis	KIZ025799	Wawu Shan, Sichuan Prov., China	KX811902	KX812062
M. wugongensis	SYS a002610	Wugongshan Scenic Area, Jiangxi Prov., China	MK524114	MK524145
M. wuliangshanensis	KIZ046812	Huangcaoling, Yunnan Prov., China	KX811881	KX812129
M. wushanensis	KIZ045469	Guangwu Mountain, Sichuan Prov., China	KX811838	KX812094
M. xianjuensis sp. nov.	CIBXJ190505	Xianju Co., Zhejiang Prov., China	MN563753	MN563769
	CIBXJ20190801	Xianju Co., Zhejiang Prov., China	MN563754	MN563770
	CIBXJ20190802	Xianju Co., Zhejiang Prov., China	MN563755	MN563771
	CIBXJ20190803	Xianju Co., Zhejiang Prov., China	MN563756	MN563772
	CIB20180514008	Xianju Co., Zhejiang Prov., China	MN563757	MN563773
	CIBXJ190503	Xianju Co., Zhejiang Prov., China	MN563758	MN563774
	CIBXJT19050702	Xianju Co., Zhejiang Prov., China	MN563759	MN563775
	CIBXJT19050703	Xianju Co., Zhejiang Prov., China	MN563760	MN563776
	CIBXJT19050704	Xianju Co., Zhejiang Prov., China	MN563761	MN563777
M. zhangi	KIZ014278	Zhangmu, Xizang Prov., China	KX811765	KX812084
Leptobrachium boringii	Tissue ID: YPX37539	Emei Shan, Sichuan Prov., China	KX811930	KX812164
L. oshanensis	KIZ025778	Emei Shan, Sichuan Prov., China	KX811928	KX812166

DNA sequencer in Shanghai DNA BioTechnologies Co., Ltd. (Shanghai, China). New sequences were deposited in GenBank (for GenBank accession numbers see Table 1).

For molecular analyses, the available sequence data for all related species of the genus *Megophrys* were downloaded from GenBank, mainly from previous studies (Chen et al. 2017; Mahony et al. 2017; Liu et al. 2018; Wang et al. 2019; for GenBank accession number see Table 1). For phylogenetic analyses, corresponding sequences of one *Leptobrachella oshanensis* and one *Leptobrachium boringii* were downloaded (for GenBank accession number see Table 1) and used as outgroups according to Chen et al. (2017).

Sequences were assembled and aligned using the Clustalw module in BioEdit v. 7.0.9.0 (Hall 1999) with default settings. Alignments were checked by eye and revised manually if necessary. To avoid bias in alignments, GBLOCKS v. 0.91.b (Castresana 2000) with default settings was used to extract regions of defined sequence conservation from the length-variable 16S gene fragments. Non-sequenced fragments were defined as missing loci.

Phylogenetic trees were reconstructed for the concatenated data of the mitochondrial genes. Phylogenetic analyses were conducted using maximum likelihood (ML) and Bayesian Inference (BI) methods, implemented in PhyML v. 3.0 (Guindon et al. 2010) and MrBayes v. 3.12 (Ronquist and Huelsenbeck 2003), respectively. To avoid under- or over-parameterisation (McGuire et al. 2007), the best partition scheme and the best evolutionary model for each partition were chosen for the phylogenetic analyses using PARTITIONFINDER v. 1.1.1 (Robert et al. 2012). For this analysis, 16S rRNA and COI genes were defined, and Bayesian Inference Criteria (BIC) was used. As a result, the analyses suggested that the best partition scheme was 16S/COI gene, and selected GTR+I+G model as the best model for all partitions. For the ML tree, branch supports were drawn from 10,000 non-parametric bootstrap replicates. In BI analyses, two runs each with four Markov chains were run for 60 million generations with sampling every 1000 generations. The first 25% of generations were removed as the "burn-in" stage followed by calculation of Bayesian posterior probabilities and the 50% majority-rule consensus of the post burn-in trees sampled at stationarity. Finally, genetic distance was calculated with the pairwise uncorrected *p*-distance model between the new taxon and its congeners by 16S rRNA gene using MEGA v. 6.06 (Tamura et al. 2013).

Morphological comparisons

Nine adult specimens of the new taxon and the holotype and seven paratypes of *M. lishuiensis* were measured (for voucher information see Suppl. material 1: Table S1). The terminology and methods followed Fei et al. (2009). Measurements were taken with a dial calliper to 0.1 mm. In total, 22 morphometric characters of adult specimens were measured:

ED eye diameter (distance from the anterior corner to the posterior corner of the eye);
FIIIL third finger length (distance from base to tip of finger III);
FIIL second finger length (distance from base to tip of finger II);
FIL first finger length (distance from base to tip of finger I);
FIVL fourth finger length (distance from base to tip of finger IV);
FL foot length (distance from tarsus to the tip of fourth toe);
HAL hand length (distance from the posterior end of the inner metacarpal tubercle to the distal tip of finger III);
HDL head length (distance from the tip of the snout to the articulation of jaw);
HDW maximum head width (greatest width between the left and right articulations of jaw);
IND internasal distance (minimum distance between the inner margins of the external nares);
IOD interorbital distance (minimum distance between the inner edges of the upper eyelids);
LAL length of lower arm and hand (distance from the elbow to the distal end of the finger III);

LW lower arm width (maximum width of the lower arm);
SL snout length (distance from the tip of the snout to the anterior corner of the eye);
SNT distance from the tip of the snout to the naris;
SVL snout-vent length (distance from the tip of the snout to the posterior edge of the vent);
TFL length of foot and tarsus (distance from the tibiotarsal articulation to the distal end of the Toe IV);
THL thigh length (distance from vent to knee);
TL tibia length (distance from knee to tarsus);
TW maximal tibia width;
TYD maximal tympanum diameter;
UEW upper eyelid width (greatest width of the upper eyelid margins measured perpendicular to the anterior-posterior axis).

For seven tadpoles of the new taxon (for voucher information see Suppl. material 2: Table S2), eleven morphometric characters were measured:

BH maximum body height;
BW maximum body width;
IOD interocular distance (minimum distance between eye);
MW mouth width (distance between two corners of mouth);
SL snout length (distance from the tip of the snout to the anterior corner of the eye);
SS snout to spiraculum (distance from spiraculum to the tip of the snout);
SVL snout-vent length;
TAH tail height (maximum height between upper and lower edges of tail);
TAL tail length (distance from base of vent to the tip of tail);
TBW maximum width of tail base;
TOL total length (distance from the tip of the snout to the tip of tail).

In order to reduce the impact of allometry, a size-corrected value from the ratio of each character to SVL was calculated and then log-transformed for the following morphometric analyses. One-way analysis of variance (ANOVA) was used to test the significance of differences on morphometric characters between different sexes as well as between different species. The significance level was set at 0.05. Furthermore, to show the spatial distribution of each species on the morphometric characters, principal component analyses (PCA) were performed. These analyses were carried out in R (R Development Core Team 2008).

We compared morphological characters of the new taxon with other *Megophrys* species. Comparative data were obtained from the literature for 92 species of the genus (Table 2). In addition, for comparison, we examined the type and/or topotype materials for *M. lishuiensis*, *M. boettgeri*, and *M. kuatunensis* (for voucher numbers see Table 1 and Suppl. material 1: Table S1).

Table 2. References for morphological characters for congeners of the genus *Megophrys*.

Species	Literature obtained
M. aceras Boulenger, 1903	Taylor 1962
M. acuta Wang, Li & Jin, 2014	Li et al. 2014
M. ancrae Mahony, Teeling & Biju, 2013	Mahony et al. 2013
M. auralensis Ohler, Swan & Daltry, 2002	Ohler et al. 2002
M. baluensis (Boulenger, 1899)	Boulenger 1899
M. baolongensis Ye, Fei & Xie, 2007	Ye et al. 2007
M. binchuanensis Ye & Fei, 1995	Ye and Fei 1995
M. binlingensis Jiang, Fei & Ye, 2009	Fei et al. 2009
M. boettgeri (Boulenger, 1899)	Fei et al. 2012
M. brachykolos Inger & Romer, 1961	Inger and Romer 1961
M. carinense (Boulenger, 1889)	Fei et al. 2009
M. caudoprocta Shen, 1994	Fei et al. 2012
M. cheni (Wang & Liu, 2014)	Wang et al. 2014
M. chuannanensis (Fei, Ye & Huang, 2001)	Fei et al. 2012
M. damrei Mahony, 2011	Mahony 2011
M. daweimontis Rao & Yang, 1997	Fei et al. 2012
M. dongguanensis Wang & Wang, 2019	Wang et al. 2019
M. dringi Inger, Stuebing & Tan, 1995	Inger et al. 1995
M. edwardinae Inger, 1989	Inger 1989
M. elfina Poyarkov, Duong, Orlov, Gogoleva, Vassilieva, Nguyen, Nguyen, Nguyen, Che & Mahony, 2017	Poyarkov et al. 2017
M. fansipanensis Tapley, Cutajar, Mahony, Nguyen, Dau, Luong, Le, Nguyen, Nguyen, Portway, Luong & Rowley, 2018	Tapley et al. 2018
M. feae Boulenger, 1887	Fei et al. 2009
M. feii Yang, Wang & Wang, 2018	Yang et al. 2018
M. flavipunctata Mahony, Kamei, Teeling & Biju, 2018	Mahony et al. 2018
M. gerti (Ohler, 2003)	Ohler 2003
M. gigantica Liu, Hu & Yang, 1960	Fei et al. 2012
M. glandulosa Fei, Ye & Huang, 1990	Fei et al. 2012
M. hansi (Ohler, 2003)	Ohler 2003
M. himalayana Mahony, Kamei, Teeling & Biju, 2018	Mahony et al. 2018
M. hoanglienensis Tapley, Cutajar, Mahony, Nguyen, Dau, Luong, Le, Nguyen, Nguyen, Portway, Luong & Rowley, 2018	Tapley et al. 2018
M. huangshanensis Fei & Ye, 2005	Fei et al. 2012
M. insularis (Wang, Liu, Lyu, Zeng & Wang, 2017)	Wang et al. 2017a
M. intermedia Smith, 1921	Rao and Yang 1997
M. jingdongensis Fei & Ye, 1983	Fei et al. 2012
M. jinggangensis (Wang, 2012)	Wang et al. 2012
M. jiulianensis Wang, Zeng, Lyu & Wang, 2019	Wang et al. 2019
M. kalimantanensis Munir, Hamidy, Matsui, Iskandar, Sidik & Shimada, 2019	Munir et al. 2019
M. kobayashii Malkmus & Matsui, 1997	Malkmus and Matsui 1997
M. koui Mahony, Foley, Biju & Teeling, 2017	Mahony et al. 2017
M. kuatunensis Pope, 1929	Fei et al. 2012
M. lancip Munir, Hamidy, Farajallah & Smith, 2018	Munir et al. 2018
M. leishanensis Li, Xu, Liu, Jiang, Wei & Wang, 2018	Li et al. 2018
M. lekaguli Stuart, Chuaynkern, Chan-ard & Inger, 2006	Stuart et al. 2006
M. liboensis (Zhang, Li, Xiao, Li, Pan, Wang, Zhang & Zhou, 2017)	Zhang et al. 2017
M. ligayae Taylor, 1920	Taylor 1920
M. lini (Wang & Yang, 2014)	Wang et al. 2014
M. lishuiensis (Wang, Liu & Jiang, 2017)	Wang et al. 2017b
M. longipes Boulenger, 1886	Taylor 1962
M. major Boulenger, 1908	Mahony et al. 2018
M. mangshanensis Fei & Ye, 1990	Fei et al. 2012
M. maosonensis Bourret, 1937	Bourret 1937
M. medogensis Fei, Ye & Huang, 1983	Fei et al. 2012
M. megacephala Mahony, Sengupta, Kamei & Biju, 2011	Mahony et al. 2011
M. microstoma (Boulenger, 1903)	Fei et al. 2012
M. minor Stejneger, 1926	Fei et al. 2012
M. montana Kuhl & Van Hasselt, 1822	Kuhl & Van Hasselt 1822
M. monticola (Günther, 1864)	Mahony et al. 2018

Species	Literature obtained
M. mufumontana Wang, Lyu & Wang, 2019	Wang et al. 2019
M. nankiangensis Liu & Hu, 1966	Fei et al. 2012
M. nankunensis Wang, Zeng &. Wang, 2019	Wang et al. 2019
M. nanlingensis Lyu, Wang, Liu & Wang, 2019	Wang et al. 2019
M. nasuta (Schlegel, 1858)	Taylor 1962
M. obesa Wang, Li & Zhao, 2014	Wang et al. 2014
M. ombrophila Messenger & Dahn, 2019	Munir et al. 2019
M. omeimontis Liu, 1950	Fei et al. 2009
M. oreocrypta Mahony, Kamei, Teeling & Biju, 2018	Mahony et al. 2018
M. oropedion Mahony, Teeling & Biju, 2013	Mahony et al. 2013
M. pachyproctus Huang, 1981	Fei et al. 2009
M. palpebralespinosa Bourret, 1937	Fei et al. 2012
M. parallela Inger & Iskandar, 2005	Inger and Iskandar 2005
M. parva (Boulenger, 1893)	Fei et al. 2009
M. periosa Mahony, Kamei, Teeling & Biju, 2018	Mahony et al. 2018
M. popei (Zhao, Yang, Chen, Chen & Wang, 2014)	Zhao et al. 2014
M. robusta Boulenger, 1908	Mahony et al. 2018
M. rubrimera Tapley, Cutajar, Mahony, Chung, Dau, Nguyen, Luong & Rowley, 2017	Tapley et al. 2017
M. sangzhiensis Jiang, Ye & Fei, 2008	Jiang et al. 2008
M. serchhipii (Mathew & Sen, 2007)	Mathew and Sen 2007
M. shapingensis Liu, 1950	Fei et al. 2009
M. shuichengensis Tian & Sun, 1995	Fei et al. 2009
M. shunhuangensis Wang, Deng, Liu, Wu & Liu, 2019	Wang et al. 2019
M. spinata Liu & Hu, 1973	Fei et al. 2009
M. stejnegeri Taylor, 1920	Taylor 1920
M. synoria (Stuart, Sok & Neang, 2006)	Stuart et al. 2006
M. takensis Mahony, 2011	Mahony 2011
M. tuberogranulata Shen, Mo & Li, 2010	Fei et al. 2012
M. vegrandis Mahony, Teeling, Biju, 2013	Mahony et al. 2013
M. wawuensis Fei, Jiang & Zheng, 2001	Fei et al. 2012
M. wugongensis Wang, Lyu & Wang, 2019	Wang et al. 2019
M. wuliangshanensis Ye & Fei, 1995	Fei et al. 2012
M. wushanensis Ye & Fei, 1995	Fei et al. 2012
M. zhangi Ye & Fei, 1992	Fei et al. 2012
M. zunhebotoensis (Mathew & Sen, 2007)	Mathew and Sen 2007

Bioacoustics notes

The advertisement calls of the new taxon from Xianju County, Zhejiang Province, China were recorded in the field. SONY PCM-D50 digital sound recorder was used to record within 20 cm of the calling individuals. The sound files in wave format were resampled at 48 kHz with sampling depth 24 bits. The sonograms and waveforms were generated by WaveSurfer software (Sjöander and Beskow 2000) from which all parameters and characters were measured. Ambient temperature was taken by a digital hygrothermograph.

Results

Phylogenetic analyses

Aligned sequence matrix of 16S+COI contained 1104 bps. ML and BI trees of the mitochondrial DNA dataset presented almost consistent topology, though relationships of some lineages were unresolved (Fig. 2). All individuals of the new taxon were

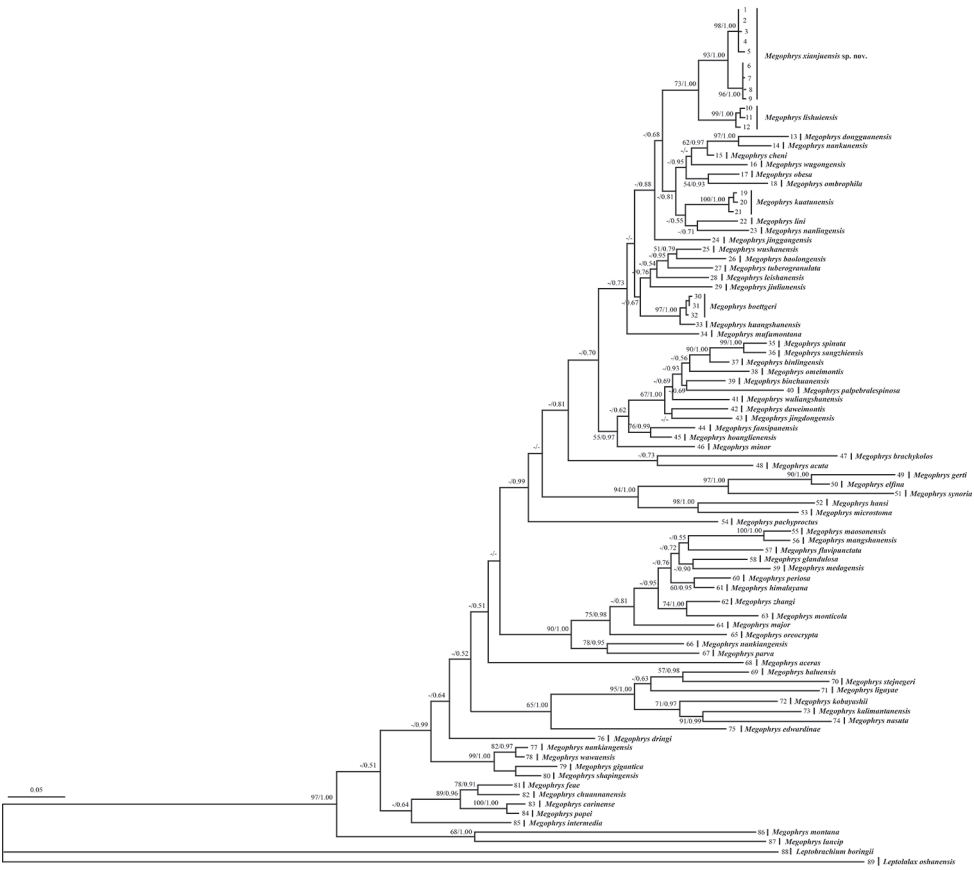

Figure 2. Maximum Likelihood tree of the genus *Megophrys* reconstructed based on the 16S rRNA and COI gene sequences. ML bootstrap support/Bayesian posterior probability was denoted beside each node. Samples 1-89 refer to Table 1.

clustered into one clade which was independently nested into the *Megophrys* clade and sister to the *M. lishuiensis* clade. Genetic distances on 16S gene with uncorrected *p*-distance model between specimens of the new taxon were less than 0.7% (ranging from 0.0% to 0.6%), being lower than most interspecific genetic distances in the genus *Megophrys* (0.4%–19.3%; Suppl. material 3: Table S3). Genetic distance between the new taxon and its closely-related species *M. lishuiensis* is 2.8%, higher than that between many substantial species, for example, *M. wushanensis* vs. *M. baolongensis* (2.1%), *M. baolongensis* vs. *M. tuberogranulata* (1.5%), *M. sangzhiensis* vs. *M. binlingensis* (1.7%), and *M. omeimontis* vs. *M. jingdongensis* (2.1%).

Morphometric analyses

The results of one-way ANOVA showed that in the new taxon, the male group was significantly different from the female group on SVL and the ratio of ED and IND to SVL

(p-value < 0.05). Therefore, morphometric analyses between the new taxon and *M. lishuiensis* were conducted separately for male and female. In PCA, the total variation of the first two principal components was 56.2% in male and 74.9% in female respectively. In both male and female, the new taxon could be distinctly separated from its phylogenetically sister species *M. lishuiensis* on the two-dimensional plots of PC1 vs. PC2 (Fig. 3). The results of one-way ANOVA indicated that the new taxon was significantly different from *M. lishuiensis* on many morphometric characters (all p-values < 0.05; Table 3). More detailed descriptions of results from morphological comparisons between the new taxon and its congeners were presented in the following sections for describing the new species.

Taxonomic accounts

Megophrys xianjuensis sp. nov.

http://zoobank.org/8CFD24E0-1ABD-4642-B9C1-FFA1D80262C2
Figures 1–9

Type material. ***Holotype*.** CIBXJ190503 (Fig. 4A, B, E, G, I), adult male, from Shenxianju scenic area, Danzhu Township, Xianju County, Zhejiang Province, China (28.677483N, 120.594888E, 350 m a. s. l.), collected by Bin Wang on 7 May 2019.

Table 3. Morphometric comparisons between the adult specimens of *Megophrys xianjuensis* sp. nov. and *M. lishuiensis*. Units are in mm. See abbreviations for the morphological characters in Materials and methods section.

Character	*Megophrys xianjuensis* sp. nov. (MX)				*M. lishuiensis* (ML)				*P*-value from ANOVA		
	Males (N = 7)		Female (N = 2)		Males (N = 6)		Female (N = 2)				
	Range	Mean ± SD	Range	Mean ± SD	Range	Mean ± SD	Range	Mean ± SD	Male vs. female in MX	MX vs. ML in male	MX vs. ML in female
SVL	31.0–36.3	33.1 ± 1.8	32.8–41.6	37.2 ± 6.2	30.5–34.7	32.5 ± 1.6	37.6–40.4	39.0 ± 1.9	0.119	0.633	0.728
HDL	9.4–10.5	9.9 ± 0.4	10.1–10.8	10.4 ± 0.5	9.4–10.3	9.8 ± 0.4	9.9–11.4	10.6 ± 1.1	0.365	0.916	0.705
HDW	10.6–11.5	11.1 ± 0.3	10.7–12.9	11.8 ± 1.5	10.6–11.6	10.9 ± 0.3	12.1–12.1	12.1 ± 0.02	0.361	0.813	0.561
SL	3.8–4.7	4.2 ± 0.3	3.6–5.2	4.4 ± 1.1	4.1–4.5	4.3 ± 0.2	4.3–4.4	4.3 ± 0.1	0.318	0.569	0.510
SNT	1.9–2.5	2.2 ± 0.2	1.8–2.5	2.1 ± 0.5	2.0–2.5	2.3 ± 0.2	2.4–2.7	2.6 ± 0.2	0.165	0.177	0.177
IND	3.2–3.7	3.4 ± 0.2	3.2–3.6	3.4 ± 0.3	3.1–4.0	3.5 ± 0.4	4.2–4.2	4.2 ± 0.01	0.045*	0.470	0.121
IOD	2.3–3.3	2.8 ± 0.4	2.8–2.9	2.8 ± 0.1	2.4–2.8	2.5 ± 0.1	2.8–3.1	2.9 ± 0.2	0.345	0.140	0.959
UEW	2.3–2.9	2.7 ± 0.2	2.7–3.4	3.1 ± 0.5	2.6–3.6	3.2 ± 0.3	3.7–3.7	3.7 ± 0.02	0.807	0.004**	0.047*
ED	3.3–4.0	3.6 ± 0.3	2.9–4.0	3.4 ± 0.8	3.8–4.6	4.1 ± 0.2	4.1–4.6	4.3 ± 0.3	0.002**	0.002**	0.046*
TYD	1.8–2.2	2.0 ± 0.1	1.7–2.7	2.2 ± 0.6	1.9–2.5	2.1 ± 0.2	2.2–2.3	2.3 ± 0.1	0.571	0.044*	0.962
LAL	14.2–17.2	15.3 ± 1.0	13.7–19.2	16.5 ± 3.9	14.6–15.7	15.2 ± 0.4	17.5–17.6	17.5 ± 0.04	0.279	0.792	0.767
HAL	7.6–9.2	8.2 ± 0.6	7.8–10.0	8.9 ± 1.5	8.0–8.8	8.4 ± 0.3	8.7–9.3	9.0 ± 0.4	0.489	0.220	0.021*
LW	2.1–2.7	2.5 ± 0.2	2.0–2.6	2.3 ± 0.4	2.4–3.1	2.8 ± 0.2	2.4–2.4	2.4 ± 0.01	0.062	0.042*	0.879
FIL	2.5–3.1	2.9 ± 0.2	2.8–3.9	3.4 ± 0.78	2.4–3.0	2.7 ± 0.2	2.8–3.6	3.2 ± 0.5	0.488	0.644	0.602
FIIL	2.7–3.5	3.0 ± 0.3	3.0–4.0	3.5 ± 0.78	2.5–3.3	2.9 ± 0.3	3.0–3.2	3.1 ± 0.2	0.675	0.975	0.151
FIIIL	4.4–6.2	4.9 ± 0.6	4.8–5.9	5.4 ± 0.8	4.9–5.7	5.2 ± 0.2	5.3–5.8	5.6 ± 0.3	0.622	0.111	0.949
FIVL	2.9–4.1	3.3 ± 0.2	3.0–4.4	3.6 ± 1.0	3.2–3.9	3.5 ± 0.2	3.2–3.6	3.4 ± 0.3	0.726	0.110	0.471
THL	13.8–16.0	14. ± 0.8	13.1–17.6	15.3 ± 3.2	13.7–14.7	14.2 ± 0.4	15.7–16.3	16. 0 ± 0.4	0.177	0.646	0.996
TL	14.5–16.1	15.0 ± 0.5	13.0–17.8	15.4 ± 3.4	14.3–15.5	15.0 ± 0.3	16.4–16.7	16.5 ± 0.2	0.019*	0.558	0.628
TW	2.8–4.4	3.4 ± 0.6	2.9–3.3	3.1 ± 0.3	3.9–4.4	4.1 ± 0.2	4.0–4.7	4.3 ± 0.5	0.124	0.004**	0.050
TFL	18.0–21.5	19.5 ± 1.14	19.3–23.5	21.4 ± 3.0	18.6–20.4	19.7 ± 0.7	21.0–22.4	21.7 ± 1.0	0.483	0.444	0.697
FL	11.2–14.8	12.9 ± 1.1	12.4–15.6	14.0 ± 2.2	12.3–13.5	12.840 ± 0.5	13.7–14.8	14.3 ± 0.8	0.562	0.946	0.734

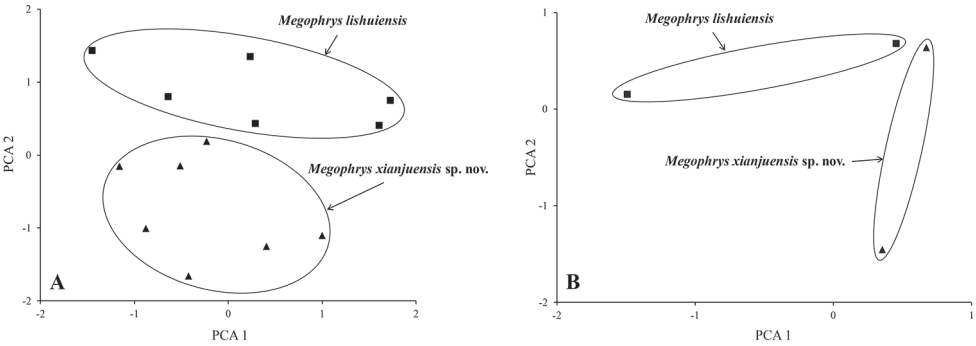

Figure 3. Plots of the first principal component (PC1) versus the second (PC2) for *Megophrys xianjuensis* sp. nov. and *M. lishuiensis* from principal component analyses **A** male **B** female.

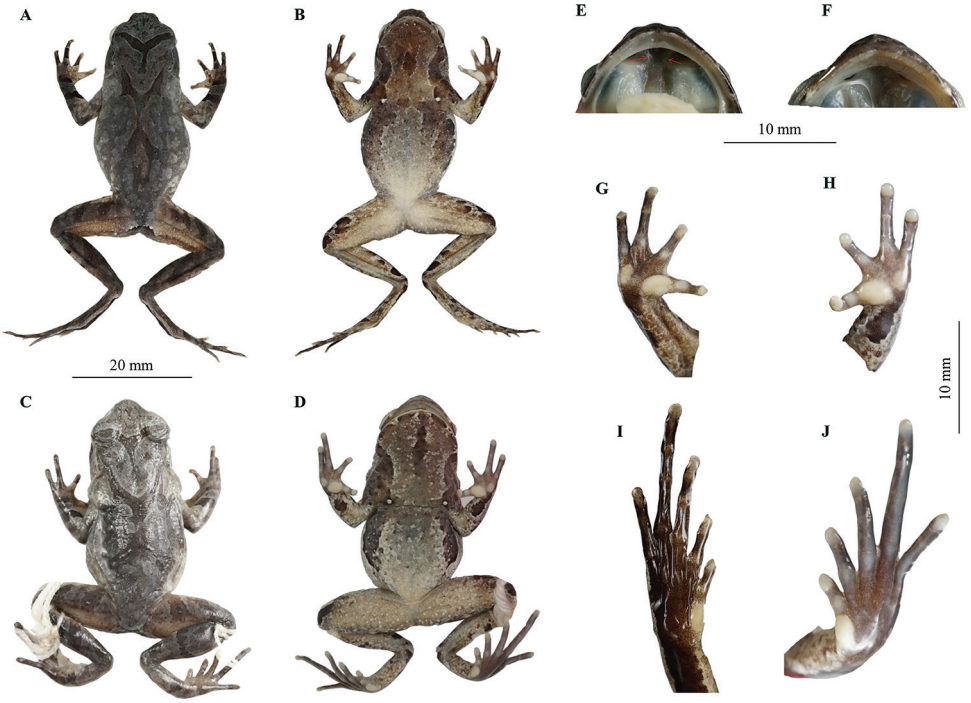

Figure 4. Holotype CIBXJ190503 of *Megophrys xianjuensis* sp. nov. and holotype CIBWYF00164 of *M. lishuiensis* **A, B** dorsal view and ventral of *Megophrys xianjuensis* sp. nov., respectively **C, D** dorsal view and ventral of *M. lishuiensis*, respectively **E** oral of *Megophrys xianjuensis* sp. nov. showing vomerine ridges (red arrows) **F** oral of *M. lishuiensis* showing no vomerine ridge **G** ventral view of hand of *Megophrys xianjuensis* sp. nov. **H** ventral view of hand of *M. lishuiensis* **I** ventral view of foot of *Megophrys xianjuensis* sp. nov. **J** ventral view of foot of *M. lishuiensis*.

Paratype. One adult male CIB20180514007 and one adult female CIB20180514008 collected from the type locality of the new species by Bin Wang on 14 May 2018; one adult male CIBXJ190501 and one adult female CIBXJ190505 collected

from the type locality by Bin Wang on 7 May 2019; five adult males CIBXJ20190801, CIBXJ20190802, CIBXJ20190803, CIBXJ20190804 and CIBXJ20190805 collected from the type locality by Bin Wang on 28 August 2019.

Diagnosis. *Megophrys xianjuensis* sp. nov. is assigned to the genus *Megophrys* based on molecular phylogenetic analyses and the following generic diagnostic characters: snout shield-like; projecting beyond the lower jaw; canthus rostralis distinct; chest gland small and round, closer to the axilla than to midventral line; femoral gland on rear of thigh; vertical pupils.

The new species could be identified from its congeners by a combination of the following morphological characters: (1) small size (SVL 31.0–36.3 mm in males and 41.6 mm in female); (2) vomerine ridge present and vomerine teeth absent; (3) tongue not notched behind; (4) a small horn-like tubercle at the edge of each upper eyelid; (5) tympanum distinctly visible, rounded; (6) two metacarpal tubercles in hand; (7) relative finger lengths: II < I < IV < III; (8) toes with rudimentary webbing at bases; (9) heels overlapping when thighs are positioned at right angles to the body; (10) tibiotarsal articulation reaching tympanum to eye when leg stretched forward; (11) an internal single subgular vocal sac in male; (12) in breeding male, the nuptial pads with black nuptial spines on the dorsal bases of the first and second fingers.

Description of holotype. SVL 34.4 mm; head wider than long (HDW/HDL ratio 1.2); snout obtusely pointed, protruding well beyond the margin of the lower jaw in ventral view; loreal region vertical and concave; canthus rostralis well developed; top of head flat on in dorsal view; an small horn-like tubercle at the edge of the upper eyelid; eye large and convex, eye diameter 40.4% of head length; pupils vertical; nostril orientated laterally, closer to snout than eye; tympanum distinct, TYP/EYE ratio 0.56; vomerine ridges present and vomerine teeth absent; margin of tongue smooth, not notched behind (Fig. 4A, B, E).

Forelimbs slender, the length of lower arm and hand 44.9% of SVL; fingers slender, relative finger lengths: II < I < IV < III; tips of digits globular, without lateral fringes; subarticular tubercle distinct at the base of each fingers; two metacarpal tubercles, prominent, oval-shaped, the inner one bigger than the outer (Fig. 4G).

Hindlimbs slender, heels overlapping when thighs are positioned at right angles to the body, tibiotarsal articulation reaching tympanum to eye when leg stretched forward; tibia length slightly longer than thigh length; relative toe lengths I < II < V < III < IV; tips of toes round, slightly dilated; subarticular tubercle absent; toes with rudimentary webbing at bases; lateral fringe narrow; inner metatarsal tubercle oval-shaped; outer metatarsal tubercle absent (Fig. 4I).

Dorsal rough, with numerous granules; several large warts scattered on flanks; an small horn-like tubercle at the edge of each upper eyelid; a dark brown inverted triangular pattern between anterior corner of eyes, tubercles on the dorsum forming a weak X-shaped ridge and two discontinuous dorsolateral parallel ridges on either side of the X-shaped ridge; several tubercles on the flanks and dorsal surface of thighs and tibias, and limbs barred with dark brown forming four transverse rows; supratympanic fold distinct (Fig. 4A).

Ventral surface with numerous white granules; chest gland distinct and round, closer to the axilla than to midventral line; femoral gland on rear of thigh; posterior end of the body protrudes distinct and appears as an arc-shaped swelling, upper the anal region (Fig. 4B).

Colouration of holotype in life. An inverted triangular brown speckle between the eyes; an X-shaped ridges on the dorsum of body, four transverse bands on the dorsal surface of the hindlimb; several dark brown and white vertical bars on the lower and upper lip; the venter purple and the colour of throat is deeper than belly, flank and middle of throat with black brown spots, numerous white granules on the ventral surface and limbs; palms and soles purple and the metacarpal tubercles are orange, tip of digits greyish white; pectoral and femoral glands white (Fig. 5).

Preserved holotype colouration. Dorsal surface fade to olive; the inverted triangular brown speckle between the eyes, X-shaped ridges on dorsum and transverse bands on limbs and digits and brown spots on flank and middle throat are more distinct; ventral surface greyish white; creamy-white substitutes the orange in metacarpal tubercles; the posterior of ventral surface of body, inner of thigh and upper of tibia creamy-white (Fig. 4).

Variation. In some adult individuals a brown Y-shaped marking on the dorsum of head and disconnected with a X-shaped marking on back (Fig. 6A); an inverted triangular brown speckle between two upper eyelids with Y-shaped marking on back of trunk, the colouration of dorsum is brown with brick-red and the caudal vertebra is pointed in the adult female (Fig. 6B); in some adult individuals the metacarpal tubercles in palm is grey-white but the tip of fingers is orange and the black spots in flank is smaller (Fig. 6C); in some adult individuals the white granules in ventral surface are more intensive (Fig. 6D).

Advertisement calls. Ten advertisement calls from two individuals of the new species were recorded in the Xianju County, Zhejiang Province, China between 21:00–23:00 on 7 May 2019. The call description is based on recordings of the holotype CIBXJ090503 (Fig. 7) from the stone near the streamlet, and the ambient air temperature was 24.5 °C. Each call consists of 22–62 (mean 49.33 ± 14.50, $N = 6$) notes. Call duration was 4.90–14.22 second (mean10.95 ± 3.42, $N = 6$). Call interval was 4.12–7.64 second (mean 6.23 ± 1.56, $N = 5$). Each note had a duration of 0.06– 0.90 second (mean 0.10 ± 0.05, $N = 290$) and the intervals between notes 0.07–0.88 second (mean 0.13 ± 0.05, $N = 284$). Amplitude modulation within note was apparent, beginning with lower energy pulses, increasing slightly to a maximum by approximately mid note, and then decreasing towards the end of each note. The average dominant frequency was 6400 ± 465.79 (5520–6840 Hz, $N = 6$).

Secondary sexual characteristics. Adult females with SVL 41.6 mm, larger than adult males with 31.0–36.3 mm. Adult males have a single subgular vocal sac (Fig. 5E). In breeding males, the brownish red nuptial pads on the dorsal bases of the first finger and second fingers with black nuptial spines under microscope.

Tadpole description. The tadpole was confirmed as *Megophrys xianjuensis* sp. nov. by molecular phylogenetic analyses. The following tadpole description is based on the specimen CIBXJT19050704 at Stage 31 (Fig. 8). Body slender, body and tail yellow-

Figure 5. Photos of the holotype CIBXJ190503 of *Megophrys xianjuensis* sp. nov. in life **A** dorsal view **B** ventral view **C** ventral view of hand **D** ventral view of foot **E** dorsolateral view showing the single external subgular vocal sac (red arrow).

brown in life and fade to light brown and creamy-white of body and tail respectively in preserved specimens; two dotted lines on flank of dorsal from mouth to fin; tail height greater than body height; dorsal fin arising, behind the origin of the tail, height near mid-length, tapering gradually to narrow, tip pointed; tail approximately 1.9 times as long as snout-vent length; tail height 19.9% of tail length; body width slightly longer than body height (BW/BH = 1.1); tail fins lightly coloured, tail muscles with small black spots; eyes large, lateral, nostril near eyes; spiracle on the left side of the body and distinct; oral disk terminal, lips expanded and directed upwardly into a umbelliform oral disk; transverse width of expanded funnel 18.1% of snout-vent length.

Morphological comparisons. By having small size body, *Megophrys xianjuensis* sp. nov. differs from *M. aceras*, *M. auralensis*, *M. binlingensis*, *M. carinense*, *M. caudoprocta*, *M. chuannanensis*, *M. damrei*, *M. edwardinae* (in female), *M. feae*, *M. flavipunctata*, *M. gigantica*, *M. glandulosa*, *M. himalayana*, *M. intermedia*, *M. jingdongensis*, *M. kobayashii*, *M. kalimantanensis*, *M. lekaguli*, *M. liboensis*, *M. ligayae*, *M. longipes*, *M. major*, *M. mangshanensis*, *M. maosonensis*, *M. medogensis*, *M. omeimontis*, *M. oreocrypta*, *M. periosa*, *M. popei*, *M. robusta*, *M.spinata*, *M. sangzhiensis*, *M. shapingensis* and *M.*

Figure 6. Colour variation in *Megophrys xianjuensis* sp. nov. in life **A, B** dorsolateral view of a male (Voucher: CIBXJ190501) and a female (Voucher: CIBXJ190505), respectively **C, D** ventral view of CIBXJ190501 and CIBXJ190505, respectively.

shuichengensis and *M. takensis* (maximum SVL < 42.0 mm in the new species vs. minimum SVL > 45 mm in the latter).

By lacking vomerine teeth, *Megophrys xianjuensis* sp. nov. differs from *M. aceras*, *M. ancrae*, *M. carinense*, *M. baluensis*, *M. caudoprocta*, *M. chuannanensis*, *M. damrei*, *M. daweimontis*, *M. dongguanensis*, *M. fansipanensis*, *M. flavipunctata*, *M. glandulosa*, *M. hoanglienensis*, *M. himalayana*, *M. insularis*, *M. intermedia*, *M. jingdongensis*, *M. jinggangensis*, *M. jiulianensis*, *M. kalimantanensis*, *M. kobayashii*, *M. lancip*, *M. lekaguli*, *M. liboensis*, *M. ligayae*, *M. major*, *M. mangshanensis*, *M. maosonensis*, *M. medogensis*, *M. megacephala*, *M. montana*, *M. nasuta*, *M. nankunensis*, *M. nanlingensis*, *M. omeimontis*, *M. oropedion*, *M. oreocrypta*, *M. palpebralespinosa*, *M. parallela*, *M. parva*, *M. periosa*, *M. popei*, *M. robusta*, *M. rubrimera*, *M. sangzhiensis*, *M. stejnegeri*, *M. takensis*, *M. zhangi* and *M. zunhebotoensis* (vs. present in the latter).

By having a small horn-like tubercle at the edge of each upper eyelid, *Megophrys xianjuensis* sp. nov. differs from *M. binchuanensis*, *M. binlingensis*, *M. damrei*, *M. gigantica*, *M. minor*, *M. nasuta*, *M. nankiangensis*, *M. oropedion*, *M. pachyproctus*,

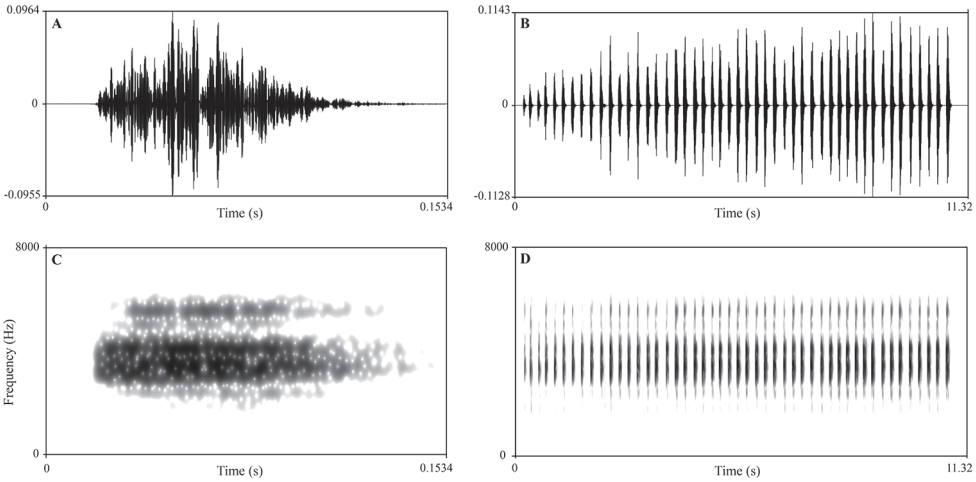

Figure 7. Advertisement call of the holotype CIBXJ190503 of *Megophrys xianjuensis* sp. nov. **A** waveform showing one note **B** waveform showing three notes of one advertisement call **C** sonogram showing one note **D** sonogram showing three notes of one call.

Figure 8. Tadpole specimen CIBXJT19050704 of *Megophrys xianjuensis* sp. nov. **A** dorsal view **B** lateral view **C** ventral view. Arrows indicate two dotted lines on flank of dorsum from mouth to fin.

M. spinata, *M. stejnegeri*, *M. takensis*, *M. wuliangshanensis*, *M. wushanensis*, *M. zhangi*, and *M. zunhebotoensis* (vs. tubercle lacking in the latter) and differs from *M. carinense*, *M. feae*, *M. gerti*, *M. hansi*, *M. intermedia*, *M. kalimantanensis*, *M. koui*, *M. liboensis*, *M.*

microstoma, *M. palpebralespinosa*, *M. popei*, *M. shuichengensis*, and *M. synoria* (vs. having a prominent and elongated tubercle at the edge of each upper eyelid in the latter).

With its tongue not notched behind, *Megophrys xianjuensis* sp. nov. differs from *M. ancrae*, *M. baolongensis*, *M. binlingensis*, *M. boettgeri*, *M. carinense*, *M. cheni*, *M. chuannanensis*, *M. damrei*, *M. dringi*, *M. fansipanensis*, *M. feae*, *M. feii*, *M. flavipunctata*, *M. gerti*, *M. glandulosa*, *M. hoanglienensis*, *M. huangshanensis*, *M. insularis*, *M. jiulianensis*, *M. jingdongensis*, *M. kalimantanensis*, *M. kuatunensis*, *M. liboensis*, *M. mangshanensis*, *M. maosonensis*, *M. medogensis*, *M. minor*, *M. nankiangensis*, *M. nanlingensis*, *M. omeimontis*, *M. oropedion*, *M. pachyproctus*, *M. parallela*, *M. popei*, *M. robusta*, *M. sangzhiensis*, *M. shapingensis*, *M. shuichengensis*, *M. spinata*, *M. vegrandis*, *M. wawuensis*, *M. zhangi*, and *M. zunhebotoensis* (vs. tongue notched behind in the latter).

By toes rudimentary webbing at base, *Megophrys xianjuensis* sp. nov. differs from *M. brachykolos*, *M. carinense*, *M. flavipunctata*, *M. jingdongensis*, *M. jinggangensis*, *M. lini*, *M. major*, *M. palpebralespinosa*, *M. popei*, *M. shuichengensis*, and *M. spinata* (vs. at least one-fourth webbed in the latter).

By heels overlapping when thighs are positioned at right angles to the body, *Megophrys xianjuensis* sp. nov. differs from *M. acuta*, *M. brachykolos*, *M. dongguanensis*, *M. huangshanensis*, *M. kuatunensis*, *M. nankunensis*, *M. obesa*, *M. ombrophila*, and *M. wugongensis* (vs. heels not meeting when thighs are positioned at right angles to the body in the latter).

By tibiotarsal articulation reaching forward to the region between tympanum and eye when hindlimb is stretched along the side of the body, *Megophrys xianjuensis* sp. nov. differs from *M. baolongensis*, *M. nankiangensis*, *M. pachyproctus*, *M. serchhipii*, *M. shuichengensis*, and *M. tuberogranulata* (vs. reaching posterior corner of the eye in the latter); differs from *M. daweimontis*, *M. glandulosa*, *M. lini*, *M. major*, *M. medogensis*, *M. obesa*, and *M. sangzhiensis* (vs. reaching the anterior corner of the eye or beyond eye or nostril and tip of snout in the latter); differs from *M. leishanensis* (vs. reaching middle part of eye); differs from *M. mufumontana* (vs. reaching tympanum in males and to the eye in females).

By having an internal single subgular vocal sac in male, *Megophrys xianjuensis* sp. nov. differs from *M. caudoprocta*, *M. shapingensis*, and *M. shuichengensis* (vs. vocal sac absent in the latter).

By having nuptial pads and nuptial spines on the dorsal base of the first and second fingers in breeding male, *Megophrys xianjuensis* sp. nov. differs from *M. acuta*, *M. feii*, *M. shapingensis*, and *M. shuichengensis* (vs. nuptial pads and nuptial spines lacking in the latter); differs from *M. boettgeri*, and *M. elfina* (vs. nuptial pads and nuptial spines only on the first finger in the latter).

Megophrys boettgeri and *M. kuatunensis* were suggested to be distributed in Zhejiang Province, China and might be sympatric with *Megophrys xianjuensis* sp. nov. (Fei et al. 2016; Wang et al. 2017b). The new species can be distinguished from these species by a series of morphological characters as follows. The new species vs. *M. boettgeri*: vomerine ridges present vs. vomerine ridges absent, tibiotarsal articulation reaching forward to the region between tympanum and eye when hindlimb is stretched along the side of the body vs. tibiotarsal articulation reaching forward to eye, having

nuptial pads and nuptial spines on the dorsal base of the first and second fingers in breeding male vs. nuptial pads and nuptial spines only on the first finger, heels overlapping when thighs are positioned at right angles to the body vs. heels just meeting, light round patches on the shoulder absent vs. present. The new species vs. *M. kuatunensis*: heels overlapping when thighs are positioned at right angles to the body vs. heels not meeting, toes with rudimentary webbing at bases vs. toes without webbing.

Molecular phylogenetic analyses revealed that the new species was genetically closer to *M. lishuiensis*. The new species can be distinguished from *M. lishuiensis* by a series of morphological characters as follows. Vomerine ridges present vs. vomerine ridges absent; heels overlapping when thighs are positioned at right angles to the body vs. heels just meeting or not meeting; light round patches on the shoulder absent vs. present; having significantly lower ratios of UEW, ED, TYD, LW and TW to SVL in males; and having significantly higher ratios of UEW, ED and HAL to SVL in females (all p-values < 0.05; Table 3).

Distribution and habitats. *Megophrys xianjuensis* sp. nov. is known from the type locality, Xianju County, Zhejiang Province, China at elevations between 320–480 m a.s.l. This new species is frequently found on stones in the streams in the subtropical montane forests (Fig. 5E; Fig. 9). Six sympatric amphibian species, i.e., *Amolops wuyiensis*, *Odorrana tianmuensis*, *O. graminea*, *O. tormota*, *Limnonectes fujianensis*, and *Quasipaa spinosa*, were found.

Etymology. The specific epithet *xianjuensis* refers to Xianju County, Zhejiang Province, China, where the type locality of the species is located. We propose the common name "Xianju horned toad" in English and Xian ju Jiao Chan in Chinese.

Discussion

Although *Megophrys xianjuensis* sp. nov. superficially resembles *M. lishuiensis*, our integrative comparisons with morphological and molecular data can clearly identify the new species from the latter. This indicates that conserved morphology could hamper species delineation, requiring the incorporation of detailed morphological, genetic, and bioacoustic data to recognise cryptic species. The discovery of *Megophrys xianjuensis* sp. nov. brings the total number of species in the genus to 93, with 49 of them recorded in China (Fei et al. 2016; Frost 2019). Yet, there remain still dozens of undescribed species just in China (Chen et al. 2017; Liu et al. 2018). As noted, the new species was a newly-found clade which has not been reported in previous phylogenetic works although it belongs to the subgenus *Panophrys* according to our phylogenetic frameworks and previous classifications (Mahony et al. 2017; Liu et al. 2018).

According to records in Fei et al. (2016) and Wang et al. (2017b), *M. boettgeri* is widely distributed in Zhejiang Province, China. However, with two-years' field surveys and detailed comparisons with many *Megophrys* specimens from Xianju County, Zhejiang Province, we have not found *M. boettgeri* in this region. Similarly, in this county, we have also not found *M. kuatunensis* and *M. lishuiensis* even though they were reported to be distributed in western and southern parts of Zhejiang Province, China

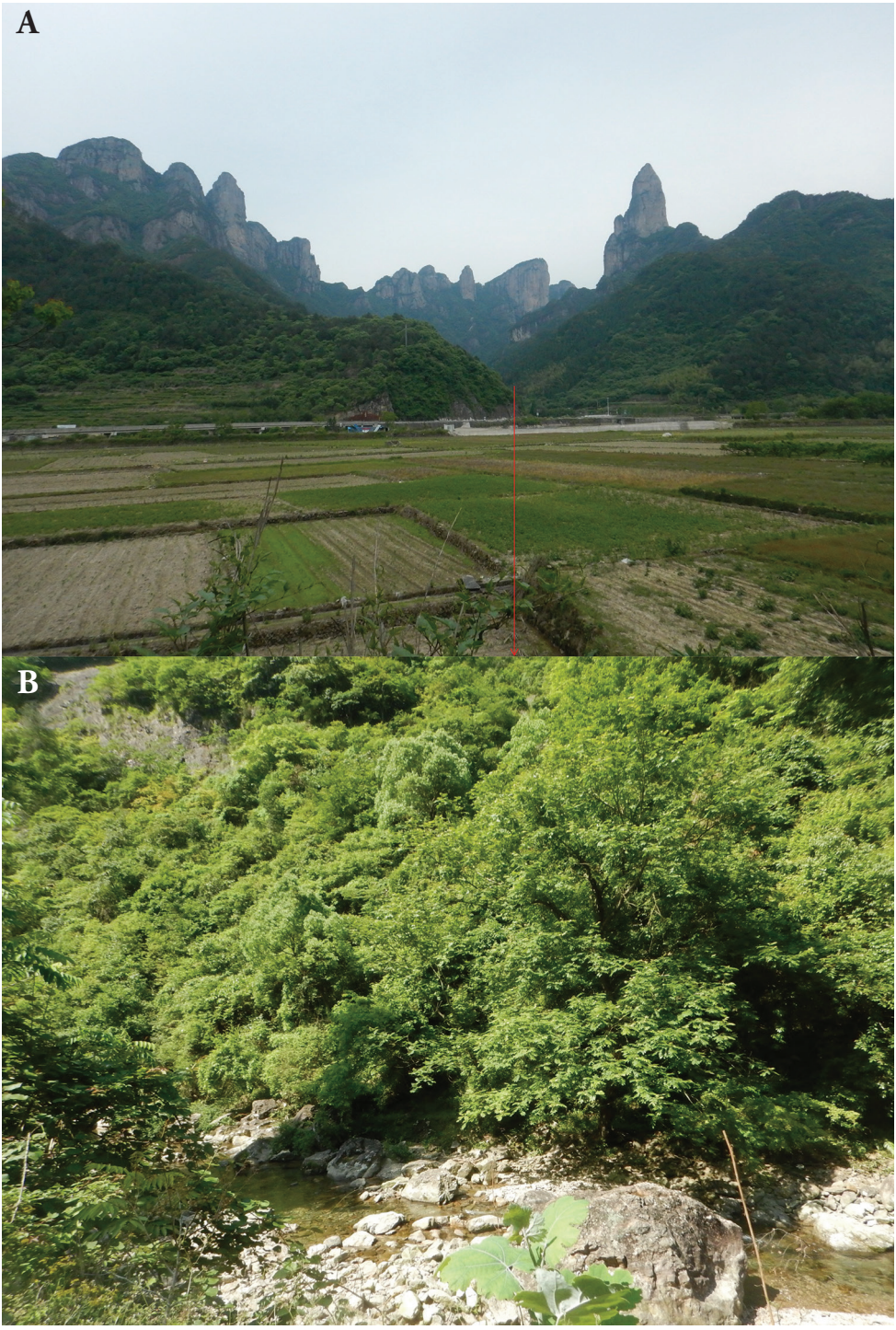

Figure 9. Habitats of *Megophrys xianjuensis* sp. nov. in the type locality, Xianju County, Zhejiang Province, China **A** landscape showing mountain forests **B** a mountain stream where toads of the new species occur.

(Fei et al. 2016; Wang et al. 2017b); therefore, we suggest that probably in Xianju County, Zhejiang Province, China, there is no *M. boettgeri*, *M. kuatunensis* or *M. lishuiensis*. Considering the high underestimated species level and localised diversification in *Megophrys* (Chen et al. 2017; Liu et al. 2018; Wang et al. 2019), wider and in-depth surveys should be conducted in the eastern part of Zhejiang Province and adjacent areas for detecting distributional range of the new species and for finding cryptic species.

Many *Megophrys* species have narrow distributions fitting the "micro-endemism" model of Liu et al. (2018) and Wang et al. (2019). Similarly, according to our surveys, *Megophrys xianjuensis* sp. nov. is probably only distributed in a narrow range in Xianju County and/or adjacent regions. Hence, this species is likely to be threatened as scenic sites in Xianju County harbouring its habitats (Fig. 9) are increasingly impacted by tourists and considerable developments in tourist infrastructure easily leading to habitat loss. Additionally, an increased frequency of extreme weather events in recent years also influenced the species; for example, the super typhoon "Lekima" in August 2019 causing heavy rain seriously broke many channels and forests where the species occurs in Xianju County. It is urgent to conduct more surveys to understand the population status of the new species and to develop appropriate protection strategies.

Acknowledgements

We are grateful to the editors and reviewers for their working on the manuscript. Collections in field were permitted by Administration of Xianju National Park (No. AXJNP2018020801). This study was approved by the animal ethical committee of Chengdu Institute of Biology, Chinese Academy of Sciences, and animal experiments were carried out following the institutional guidelines (No. 2018CIBAEC0345). The work was supported by Demonstration Project on Biodiversity Conservation and Development of Xianju County Project Financed by AFD, Project supported by the biodiversity investigation, observation and assessment program (2019–2023) of Ministry of Ecology and Environment of China, and the Strategic Priority Research Program of the Chinese Academy of Sciences (Grant No. XDPB0202).

References

Beddard FE (1908 "1907") Contributions to the knowledge of the anatomy of the batrachian family Pelobatidae. Proceedings of the Zoological Society of London 1907: 871–911. https://doi.org/10.1111/j.1469-7998.1907.tb06963.x

Bonaparte CLJL (1850) Conspectus Systematum Herpetologiae et Amphibiologiae. Editio altera reformata [Lugduni Batavorum], Brill EJ, Leiden, 1 pp.

Boulenger GA (1886 "1885") Description of a new frog of the genus *Megalophrys*. Proceedings of the Zoological Society of London 1885: 1–850.

Boulenger GA (1887) Description of a new frog of the genus *Megophrys*. Annali del Museo Civico di Storia Naturale di Genova. Serie 2(4): 512–513.

Boulenger GA (1889) Description of a new batrachian of the genus *Leptobrachium*, obtained by M. L. Fea in the Karens Mountains, Burma. Annali del Museo Civico di Storia Naturale di Genova, Serie 2(7): 748–750.

Boulenger GA (1893) Concluding report on the reptiles and batrachians obtained in Burma by Signor L. Fea dealing with the collection made in Pegu and the Karin Hills in 1887–88. Annali del Museo Civico di Storia Naturale di Genova, Serie 2(13): 304–347.

Boulenger GA (1893) Descriptions of three new batrachians from Tonkin. Annals and Magazine of Natural History, Series 7(12): 186–188. https://doi.org/10.1080/00222930308678835

Boulenger GA (1899) Descriptions of three new reptiles and a new batrachian from Mount Kina Balu, North Borneo. Annals and Magazine of Natural History Series 7(4): 1–453. https://doi.org/10.1080/00222939908678228

Boulenger GA (1908) A revision of the oriental pelobatid batrachians (genus *Megophrys*). Proceedings of the Zoological Society of London 78(2): 407–430. https://doi.org/10.1111/j.1096-3642.1908.tb01852.x

Bourret R (1937) Notes herpétologiques sur l'Indochine française. XIV. Les batraciens de la collection du Laboratoire des Sciences Naturelles de l'Université. Descriptions de quinze espèces ou variétés nouvelles. Annexe au Bulletin Général de l'Instruction Publique. Hanoi 1937: 5–56.

Castresana J (2000) Selection of conserved blocks from multiple alignments for their use in phylogenetic analysis. Molecular Biology and Evolution 17: 540–552. https://doi.org/10.1093/oxfordjournals.molbev.a026334

Che J, Chen HM, Yang JX, Jin JQ, Jiang K, Yuan ZY, Murphy RW, Zhang YP (2012) Universal COI primers for DNA barcoding amphibians. Molecular Ecology Resource 12: 247–258. https://doi.org/10.1111/j.1755-0998.2011.03090.x

Chen JM, Zhou WW, Poyarkov NA, Stuart BL, Brown RM, Lathrop A, Wang YY, Yuan ZY, Jiang K, Hou M, Chen HM, Suwannapoom C, Nguyen SN, Duong TV, Papenfuss TJ, Murphy RW, Zhang YP, Che J (2017) A novel multilocus phylogenetic estimation reveals unrecognized diversity in Asian horned toads, genus *Megophrys sensu lato* (Anura: Megophryidae). Molecular Phylogenetics and Evolution 106: 28–43. https://doi.org/10.1016/j.ympev.2016.09.004

Dubois A (1983) Classification et nomenclature supragenerique des amphibiens anoures. Bulletin Mensuel de la Société Linnéenne de Lyon 52: 270–276. https://doi.org/10.3406/linly.1983.10607

Dubois A (1987) Miscellanea taxinomica batrachologica (I). Alytes 1987[1986]: 7–95.

Dubois A, Ohler A (1998) A new species of *Leptobrachium* (Vibrissaphora) from northern Vietnam, with a review of the taxonomy of the genus *Leptobrachium* (Pelobatidae, Megophyinae). Dumerilia 4(14): 1–32.

Delorme M, Dubois A, Grosjean S, Ohler A (2006) Une nouvelle ergotaxinomie des Megophryidae (Amphibia, Anura). Alytes 24: 6–21.

Fei L, Ye CY, Huang YZ (1983) Two new subspecies of *Megophrys omeimontis* Liu from China (Amphibia, Pelobatidae). Acta Herpetologica Sinica 2(2): 49–52. [In Chinese with English abstract]

Fei L, Ye CY, Huang YZ (1990) Key to Chinese Amphibians. Publishing House for Scientific and Technological, Chongqing. [In Chinese]

Fei L, Ye CY, Huang YZ (2001) Colour Handbook Amphibians. Science Press, Beijing. [In Chinese]

Fei L, Ye CY (2005) Two new species of *Megophryidae* from China. In: Fei L, Ye CY, Huang YZ, Jiang JP, Xie F (Ed.) The Key and Illustration of Chinese. Sichuan Publishing House of Science and Technology, Chongqing, 253–255. [In Chinese]

Fei L, Hu SQ, Ye CY, Huang YZ (2009) Fauna Sinica. Amphibia (Vol. 2) Anura. Science Press, Beijing, 328–481. [In Chinese]

Fei L, Ye CY, Jiang JP (2012) Colored Atlas of Chinese Amphibians and Their Distributions. Sichuan Publishing House of Science & Technology, Chengdu, 135–247. [In Chinese]

Fei L, Ye CY (2016) Amphibians of China (Vol. 1). Science Press, Beijing, 611–735.

Frost DR (2019) Amphibian Species of the World: an Online Reference. Version 6.0. Electronic Database. American Museum of Natural History, New York. http://research.amnh.org/herpetology/amphibia/index.html [accessed 17 Oct 2019]

Frost DR, Grant T, Faivovich J, Bain RH, Haas A, Haddad CFB, De SA, Rafael O, Channing A, Wilkinson M, Donnellan SC, Raxworthy CJ, Campbell JA, Blotto BL, Moler P, Drewes RC, Nussbaum RA, Lynch JD, Green DM, Wheeler WC (2006) The amphibian tree of life. Bulletin of the American Museum of natural History 297: 1–370. https://doi.org/10.1206/0003-0090(2006)297[0001:TATOL]2.0.CO;2

Günther ACLG (1864) The Reptiles of British India. Ray Society by R. Hardwicke, London.

Gosner KL (1960) A simplified table for staging anuran embryos and larvae with notes on identification. Herpetologica 16(3):183–190.

Guindon S, Dufayard JF, Lefort V, Anisimova M, Hordijk W, Gascuel O (2010) New algorithms and methods to estimate maximum-likelihood phylogenies: assessing the performance of PhyML 3.0. Systematic Biology 59(3): 307–321. https://doi.org/10.1093/sysbio/syq010

Hall TA (1999) BIOEDIT: a user-friendly biological sequence alignment editor and analysis program for Windows 95/98/NT. Nucleic Acids Symposium Series 41: 95–98.

Hu SQ, Zhao EM, Liu CZ (1966) A herpetological survey of the Tsinling and Ta-Pa Shan region. Acta Zoologica Sinica 18: 57–89. [In Chinese with English abstract]

Hu SX, Zhao EM, Liu CZ (1973) A survey of amphibians and reptiles in Kweichow province, including a herpetofauna analysis. Acta Zoologica Sinica 19(2): 149–171. [In Chinese]

Huang YZ, Fei L (1981) Two new species of amphibians from Xizang. Acta Zootaxonomica Sinica 6: 211–215.

Inger RF, Romer JD (1961) A new pelobatid frog of the genus *Megophrys* from Hong Kong. Fieldiana: Zoology 39(46): 533–538. https://doi.org/10.5962/bhl.title.3373

Inger RF (1989) Four new species of frogs from Borneo. Malayan Nature Journal, Kuala Lumpur 42: 229–243.

Inger RF, Stuebing RB, Lian TF (1995) New species and new records of Anurans from Borneo. Raffles Bulletin of Zoology 43(1): 115–131.

Inger RF, Iskandar DT (2005) A collection of amphibians from West Sumatra, with description of a new species of *Megophrys* (Amphibia: Anura). Raffles Bulletin of Zoology 53: 133–142.

Jiang JP, Ye CY, Fei L (2008) A new horn toad *Megophrys sangzhiensis* from Hunan, China (Amphibia, Anura). Zoological Research 29(2): 219–222. [In Chinese with English abstract] https://doi.org/10.3724/SP.J.1141.2008.00219

Jiang JP, Yuan FR, Xie F, Zheng ZH (2003) Phylogenetic relationships of some species and genera in megophryids inferred from partial sequences of mitochondrial 12S and 16S rRNA genes. Zoological Research 24: 241–248. [In Chinese with English abstract]

Kuhl H, Van Hasselt JC (1822) Uittreksels uit breieven van de Heeren Kuhl en van Hasselt, aan de Heeren C. J. Temminck, Th. van Swinderen en W. de Haan. Algemeene Konst-en Letter-Bode 7: 99–104.

Lathrop A (1997) Taxonomic review of the megophryid frogs (Anura: Pelobatoidea). Asiatic herpetological Research 7: 68–79. https://doi.org/10.5962/bhl.part.18857

Li YL, Jin MJ, Zhao J, Liu ZY, Wang YY, Pang H (2014) Description of two new species of the genus *Xenophrys* (Amphibia: Anura: Megophryidae) from Heishiding Natural Reserve, Fengkai, Guangdong, China, based on molecular and morphological data. Zootaxa 3795: 449–471. https://doi.org/10.11646/zootaxa.3795.4.5

Li SZ, Xu N, Liu J, Jiang JP, Wei G, Wang B (2018) A new species of the Asian toad genus *Megophrys sensu lato* (Amphibia: Anura: Megophryidae) from Guizhou Province, China. Asian Herpetological Research 9(4): 224–239.

Liu CZ (1950) Amphibians of western China. Fieldiana. Zoology Memoires 2: 1–397. https://doi.org/10.5962/bhl.part.4737

Liu CZ, Hu SQ, Yang FH (1960) Amphibia of Yunnan collected in 1958. Acta Zoologica Sinica 12: 149–174.

Liu ZY, Chen GL, Zhu TQ, Zeng ZC, Lyu ZT, Wang J, Messenger K, Greenberg AJ, Guo ZX, Yang ZH, Shi SH, Wang YY (2018) Prevalence of cryptic species in morphologically uniform taxa-fast speciation and evolutionary radiation in Asian frogs. Molecular Phylogenetics and Evolution 127: 723–731. https://doi.org/10.1016/j.ympev.2018.06.020

Mahony S (2011) Two new species of *Megophrys* Kuhl & van Hasselt (Amphibia: Megophryidae), from western Thailand and southern Cambodia. Zootaxa 2734: 23–39. https://doi.org/10.11646/zootaxa.2734.1.2

Mahony S, Sengupta S, Kamei RG, Biju SD (2011) A new low altitude species of *Megophrys* Kuhl and van Hasselt (Amphibia: Megophryidae), from Assam, Northeast India. Zootaxa 3059: 36–46. https://doi.org/10.11646/zootaxa.3059.1.2

Mahony S, Teeling EC, Biju SD (2013) Three new species of horned frogs, *Megophrys* (Amphibia: Megophryidae), from northeast India, with a resolution to the identity of *Megophrys boettgeri* populations reported from the region. Zootaxa 3722(2): 143–169. https://doi.org/10.11646/zootaxa.3722.2.2

Mahony S, Foley NM, Biju SD, Teeling EC (2017) Evolutionary history of the Asian Horned Frogs (Megophryinae): integrative approaches to Timetree dating in the absence of a fossil record. Molecular Biology and Evolution 34(3): 744–771. https://doi.org/10.1093/molbev/msw267

Mahony S, Kamei RG, Teelin EC, Biju SD (2018) Cryptic diversity within the *Megophrys major* species group (Amphibia: Megophryidae) of the Asian Horned Frogs: Phylogenetic perspectives and a taxonomic revision of South Asian taxa, with descriptions of four new species. Zootaxa 4523: 1–96. https://doi.org/10.11646/zootaxa.4523.1.1

Mathew R, Sen N (2007) Description of two new species of *Megophrys* (Amphibia: Anura: Megophryidae) from North-east India. Cobra, Chennai 1: 18–28.

Malkmus R, Matsui M (1997) *Megophrys kobayashii*, ein neuer pelobatider Frosch vom Mount Kinabalu. Sauria, Berlin 19: 31–37.

Messenger KR, Dahn HA, Liang Y, Xie P, Wang Y, Lu C (2019) A new species of the genus *Megophrys* Gunther, 1864 (Amphibia: Anura: Megophryidae) from Mount Wuyi, China. Zootaxa 4554: 561–583. https://doi.org/10.11646/zootaxa.4554.2.9

McGuire JA, Witt CC, Altshule DL, Remsen JV (2007) Phylogenetic systematics and biogeography of hummingbirds: Bayesian and maximum likelihood analyses of partitioned data and selection of an appropriate partitioning strategy. Systematic Biology 56: 837–856. https://doi.org/10.1080/10635150701656360

Mo XY, Shen YH, Li HH, Wu XS (2010) A new species of *Megophrys* (Amphibia: Anura: Megophryidae) from the northwestern Hunan Province, China. Current Zoology 56(4): 432–436. https://doi.org/10.1093/czoolo/56.4.432

Munir M, Hamidy A, Farajallah A, Smith EN (2018) A new *Megophrys* Kuhl and Van Hasselt (Amphibia: Megophryidae) from southwestern Sumatra, Indonesia. Zootaxa 4442: 389–412. https://doi.org/10.11646/zootaxa.4442.3.3

Munir M, Hamidy A, Matsui M, Iskandar DT, Sidik I, Shimada T (2019) A new species of *Megophrys* Kuhl & Van Hasselt (Amphibia: Megophryidae) from Borneo allied to *M. nasuta* (Schlegel, 1858). Zootaxa 4679: 1–24. https://doi.org/10.11646/zootaxa.4679.1.1

Ohler A, Swan SR, Daltry JC (2002) A recent survey of the amphibian fauna of the Cardamom Mountains, Southwest Cambodia with descriptions of three new species. Raffles Bulletin of Zoology 50(2): 465–481

Ohler H (2003) Revision of the genus *Ophryophryne* Boulenger, 1903 (Megophryidae) with description of two new species. Alytes21: 23–44.

Pope CH (1929) Four new frogs from Fukien Province, China. American Museum Novitates 352: 1–5.

Poyarkov NA, Duong Jr TV, Orlov NL, Gogoleva SI, Vassilieva AB, Nguyen LT, Nguyen VDH, Nguyen SN, Che J, Mahony S (2017) Molecular, morphological and acoustic assessment of the genus *Ophryophryne* (Anura, Megophryidae) from Langbian Plateau, southern Vietnam, with description of a new species. ZooKeys 672: 49–120. https://doi.org/10.3897/zookeys.672.10624

R Development Core Team (2008) R: a language and environment for statistical computing. Vienna: R Foundation for Statistical Computing. http://www.Rproject.org.

Rao DQ, Yang DT (1997) The karyotypes of Megophryinae (Pelobatinae) with a discussion on their classification and phylogenetic relationships. Asiatic Herpetological Research 7: 93–102. https://doi.org/10.5962/bhl.part.18858

Robert L, Brett C, Simon YWH, Stephane G (2012) PartitionFinder: Combined Selection of Partitioning Schemes and Substitution Models for Phylogenetic Analyses. Molecular Phylogenetics and Evolution 29(6): 1695–1701. https://doi.org/10.1093/molbev/mss020

Ronquist FR, Huelsenbeck JP (2003) MrBayes3: Bayesian phylogenetic inference under mixed models. Bioinformatics 19(12): 1572–1574. https://doi.org/10.1093/bioinformatics/btg180

Sambrook J, Fritsch EF, Maniatis T (1989) Molecular Cloning: A Laboratory Manual. Cold Spring Harbor Laboratory Press, New York, 1659 pp.

Schlegel H (1858) Handleiding tot de Beoefening der Dierkunde (Vol. 2). Koninklijke Militaire Akademie, Breda, 57 pp. https://doi.org/10.5962/bhl.title.11648

Shen YH (1994) A new Pelobatid Toad of the Genus *Megophrys* from China (Anura: Pelobatidae). Collection of Articles for the 60th Anniversary of the Foundation of the Zoological Society of China, 603–606.

Simon C, Frati F, Beckenbach A, Crespi B, Liu H, Flook P (1994) Evolution, weighting, and phylogenetic utility of mitochondrial gene sequences and a compilation of conserved polymerasechain reaction primers. Annals of the Entomological Society of America 87: 651–701. https://doi.org/10.1093/aesa/87.6.651

Sjöander K, Beskow J (2000) Wavesurfer (Anura: Pelobatidae). Collection of Articles for the International Conference on Spoken Language Processing, Beijing, 464–467.

Smith MA (1921) New or little-known reptiles and batrachians from southern Annam (Indo-China). Proceedings of the Zoological Society of London 1921: 423–440. https://doi.org/10.1111/j.1096-3642.1921.tb03271.x

Stejneger L (1926) Two new tailless amphibians from western China. Proceedings of the Biological Society of Washington 39: 53–54.

Stuart BL, Sok K, Neang T (2006) A collection of amphibians and reptiles from hilly eastern Cambodia. Raffles Bulletin of Zoology, Singapore 54: 129–155.

Tamura K, Stecher G, Peterson D, Filipski A, Kumar S (2013) MEGA6: molecular evolutionary genetics analysis, version 6.0. Molecular Biology and Evolution 30: 2725–2729. https://doi.org/10.1093/molbev/mst197

Tapley B, Cutajar TP, Mahony S, Chung NT, Dau VQ, Nguyen TT, Luong HV, Rowley JJL (2017) The Vietnamese population of *Megophrys kuatunensis* (Amphibia: Megophryidae) represents a new species of Asian horned frog from Vietnam and southern China. Zootaxa 4344: 465–492. https://doi.org/10.11646/zootaxa.4344.3.3

Tapley B, Cutajar TP, Mahony S, Nguyen CT, Dau VQ, Luong AM, Le DT, Nguyen TT, Nguyen TQ, Portway C, Luong HV, Rowley JJL (2018) Two new and potentially highly threatened *Megophrys* Horned frogs (Amphibia: Megophryidae) from Indochina's highest mountains. Zootaxa 4508: 301–333. https://doi.org/10.11646/zootaxa.4508.3.1

Taylor EH (1920) Philippine Amphibia. Philippine Journal of Science 16: 213–359. https://doi.org/10.5962/bhl.part.4751

Taylor EH (1962) The amphibian fauna of Thailand. University of Kansas Science Bulletin 43: 265–599. https://doi.org/10.5962/bhl.part.13347

Tian WS, Hu QX (1983) Taxonomic study on genus *Megophrys*, with descriptions of two genera. Acta Herpetologica Sinica 2: 41–48. [In Chinese]

Tian YZ, Sun A (1995) A new species of *Megophrys* from China (Amphibia: Pelobatidae). Journal of Liupanshui Teachers College 52(3): 11–15. [In Chinese]

Wang J, Liu ZY, Lyu ZT, Zeng ZC, Wang YY (2017a) A new species of the genus *Xenophrys* (Amphibia: Anura: Megophryidae) from an offshore island in Guangdong Province, southeastern China. Zootaxa 4324: 541–556. https://doi.org/10.11646/zootaxa.4324.3.8

Wang YF, Liu BQ, Jiang K, Jin W, Xu JN, Wu CH (2017b) A new species of the horn toad of the genus *Xenophrys* from Zhejiang, China (Amphibia: Megophryidae). Chinese Journal of Zoology 52(1): 19–29. [in Chinese with English abstract]

Wang YY, Zhang TD, Zhao J, Sung YH, Yang JH, Pang H, Zhang Z (2012) Description of a new species of the genus *Xenophrys* Günther, 1864 (Amphibia: Anura: Megophryidae) from Mount Jinggang, China, based on molecular and morphological data. Zootaxa 3546: 53–67. https://doi.org/10.11646/zootaxa.3546.1.4

Wang YY, Zhao J, Yang JH, Zhou ZX, Chen GL, Liu Y (2014) Morphology, molecular genetics, and bioacoustics support two new sympatric *Xenophrys* (Amphibia: Anura: Megophryidae) species in Southeast China. PLoS ONE 9: e93075. https://doi.org/10.1371/journal.pone.0093075

Wang J, Lyu ZT, Liu ZY, Liao CK, Zeng ZC, Li YL, Wang YY (2019) Description of six new species of the subgenus *Panophrys* within the genus *Megophrys* (Anura, Megophryidae) from southeastern China based on molecular and morphological data. ZooKeys 851: 113–164. https://doi.org/10.3897/zookeys.851.29107

Yang JH, Wang J, Wang YY (2018) A new species of the genus *Megophrys* (Anura: Megophryidae) from Yunnan Province, China. Zootaxa 4413(2): 325–338. https://doi.org/10.11646/zootaxa.4413.2.5

Ye CY, Fei L (1992) A new Pelobatid toad of the genus *Megophrys* from Xizang, China. Acta Herpetologica Sinica 1–2: 50–52. [In Chinese]

Ye CY, Fei L (1995) Taxonomic studies on the small type *Megophrys* in China including descriptions of the new species (subspecies) (Pelobatidae: genus *Megophrys*). Acta Herpetologica Sinica 4–5: 72–81. [In Chinese]

Ye CY, Fei L, Xie F (2007) A new species of Megophryidae – *Megophrys baolongensis* from China (Amphibia, Anura). Herpetologica Sinica 11: 38–41. [In Chinese]

Zhang YG, Li N, Xiao JL, Pan T, Wang H, Zhang B, Zhou J (2017) A new species of the genus *Xenophrys* (Amphibia: Anura: Megophryidae) from Libo County, Guizhou, China. Asian Herpetological Research 8: 75–85.

Zhao J, Yang J, Chen G, Chen C, Wang Y (2014) Description of a new species of the genus *Brachytarsophrys* Tian and Hu, 1983 (Amphibia: Anura: Megophryidae) from southern China based on molecular and morphological data. Asian Herpetological Research 5: 150–160. https://doi.org/10.3724/SP.J.1245.2014.00150

Supplementary material 1

Table S1. Measurements of the adult specimens of *Megophrys xianjuensis* sp. nov. and *M. lishuiensis*

Authors: Bin Wang, Yan-Qing Wu, Jun-Wei Peng, Sheng-Chao Shi, Ning-Ning Lu, Jun Wu

Data type: measurements

Link: https://doi.org/10.3897/zookeys.904.47354.suppl1

Supplementary material 2

Table S2. Measurements of the tadpole specimens of *Megophrys xianjuensis* sp. nov.

Authors: Bin Wang, Yan-Qing Wu, Jun-Wei Peng, Sheng-Chao Shi, Ning-Ning Lu, Jun Wu

Data type: measurements

Link: https://doi.org/10.3897/zookeys.904.47354.suppl2

Supplementary material 3

Table S3. Uncorrected *p*-distance between *Megophrys* species based on the 16S gene sequences

Authors: Bin Wang, Yan-Qing Wu, Jun-Wei Peng, Sheng-Chao Shi, Ning-Ning Lu, Jun Wu

Data type: molecular data

Link: https://doi.org/10.3897/zookeys.904.47354.suppl3

ZooKeys 904: 63–87 (2020)
doi: 10.3897/zookeys.904.39161
http://zookeys.pensoft.net

RESEARCH ARTICLE

A peer-reviewed open-access journal
ZooKeys
Launched to accelerate biodiversity research

A new species of the Music frog *Nidirana* (Anura, Ranidae) from Guizhou Province, China

Gang Wei[1*], Shi-Ze Li[2,3*], Jing Liu[3], Yan-Lin Cheng[3], Ning Xu[1], Bin Wang[1,2]

1 *Biodiversity Conservation Key Laboratory, Guiyang College, Guiyang, 550002, China* **2** *CAS Key Laboratory of Mountain Ecological Restoration and Bioresource Utilization and Ecological Restoration Biodiversity Conservation Key Laboratory of Sichuan Province, Chengdu Institute of Biology, Chinese Academy of Sciences, Chengdu 610041, China* **3** *Department of Food Science and Engineering, Moutai Institute, Renhuai 564500, China*

Corresponding author: *Bin Wang* (wangbin@cib.ac.cn)

Academic editor: *A. Crottini* | Received 16 August 2019 | Accepted 29 November 2019 | Published 16 January 2020

http://zoobank.org/43BDAFC7-8D85-45A5-8B05-2CC5EAAEE048

Citation: Wei G, Li S-Z, Liu J, Cheng Y-L, Xu N, Wang B (2020) A new species of the Music frog *Nidirana* (Anura, Ranidae) from Guizhou Province, China. ZooKeys 904: 63–87. https://doi.org/10.3897/zookeys.904.39161

Abstract

The Music frog genus *Nidirana* is widely distributed in East and South Asia. Here, a new species of the genus is described from southwestern China. Phylogenetic analyses based on the mitochondrial 16S rRNA and COI gene sequences supported the new species as a clade closely related to *N. leishanensis*, *N. hainanensis*, *N. chapaensis*, *N. daunchina*, and *N. yaoica*. The new species could be distinguished from its congeners by a combination of the following characters: body of medium size (SVL 41.2–43.5 mm in males and 44.7 mm in female); lateroventral groove only present on toes; relative finger lengths: II < IV < I < III; three metatarsal tubercles on palm; heels overlapping when hindlimbs flexed at right angles to axis of body; tibiotarsal articulation reaching the level of eye when leg stretched forward; a pair of subgular internal vocal sacs at corners of throat in male; nuptial pad present on the inner side of base of fingers I in breeding male; tadpole labial tooth row formula with 1:1+1/1+1:2; in males, the advertisement call contains two kinds of notes and one call contains 2–6 repeated regular notes.

Keywords

Call, molecular phylogenetic analyses, morphology, *Nidirana yeae* sp. nov., taxonomy

* Contributed equally as the first authors

Introduction

The Music frogs of the genus *Nidirana* Dubois, 1992 are widely distributed in East and Southeast Asia, from Japan westwards to southern China, and southwards to northern Thailand, northern Vietnam, and Laos (Frost 2019). Systematic arrangements of the group have been controversial for a long time (Dubois 1992; Chen et al. 2005; Frost et al. 2006; Fei et al. 2009, 2010, 2012; Chuaynkern et al. 2010). Lyu et al. (2017) confirmed it as a distinct genus based on comprehensive species sampling with molecular, morphological, and bioacoustics evidence. To date, *Nidirana* contained ten species: the type species *N. okinavana* (Boettger, 1895) occurring from Yaeyama of southern Ryukyu, and eastern Taiwan Island; *N. adenopleura* (Boulenger, 1909) from Taiwan Island to south-eastern mainland China; *N. hainanensis* (Fei, Ye & Jiang, 2007) from Diaoluo Mountain of Hainan Island of China; *N. daunchina* (Chang, 1933) from southwestern China; *N. pleuraden* (Boulenger, 1904) from southwestern China; *N. chapaensis* (Bourret, 1937) from the north-eastern Indochinese peninsula to south-eastern Yunnan Province, China; *N. lini* (Chou, 1999) from southern Yunnan Province, China, north-western Vietnam and Thailand; *N. nankunensis* (Lyu, Zeng, Wang, Lin, Liu & Wang, 2017) from Nankun Mountain, Guangdong Province, China; *N. leishanebsis* (Li, Wei, Xu, Cui, Fei, Jiang, Liu & Wang, 2019) from Leishan Mountain, Guizhou Province, China; and *N. yaoica* (Lyu, Mo, Wan, Li, Pang & Wang, 2019) from Dayao Mountain, Guangxi Province, China.

In all *Nidirana* species, *N. adenopleura* and *N. daunchina* were reported to have the widest distributional ranges in southwestern China and south-eastern China, respectively (Fei et al. 2009, 2012). Recently, two species (*N. yaoica* and *N. leishanebsis*) were recognised from two populations which had been identified as *N. adenopleura* although they were not phylogenetically sister taxa to *N. adenopleura* (Lyu et al. 2019a; Li et al. 2019a). As well, it is expected that there are cryptic species in populations being recognised as *N. daunchina* in its wide distributional range. Wu et al. (1986) found that the population classified as *N. adenopleura* from Suiyang County, Guizhou Province, China (later classified as *N. daunchina* by Fei et al. 2009) had some morphological differences with the population of the species from its type locality (E'mei Mountain, Sichuan Province, China). Hence, deeper investigations using molecular phylogenetic approaches are necessary to evaluate the taxonomic status of these populations.

In recent years, we carried out a series of biodiversity surveys in Tongzi County, Guizhou Province, China, and collected eleven specimens of *Nidirana*. Molecular phylogenetic analyses, morphological comparisons, and bioacoustics comparisons indicated the specimens as an unnamed species of *Nidirana*. We describe it herein as a new species.

Materials and methods

Specimens

Nine adult males, one adult female, and one tadpole of the new species were collected from Huanglian Town, Tongzi County, Guizhou Province, China from 2015 to 2019

(for voucher information see Table 1, Fig. 1, Suppl. material 1: Table S1). After taking photographs, the animals were euthanised using isoflurane, and the specimens were then fixed in 10 % buffered formalin. Tissue samples were taken and preserved separately in 95 % ethanol prior to fixation. Specimens were deposited in Chengdu Institute of Biology, Chinese Academy of Sciences (**CIB, CAS**).

Molecular data and phylogenetic analyses

Four male specimens, one female specimen, and one tadpole of the new species were included in the molecular analyses (for voucher information see Table 1). For phylogenetic comparisons, the corresponding sequences for other *Nidirana* species, two *Babina* species, and one *Odorrana margaretae* for which comparable sequences were available were downloaded from GenBank (Table 1). *Odorrana margaretae* was used as the outgroup following previous studies (Lyu et al. 2017, 2019a; Li et al. 2019a).

Total DNA was extracted using a standard phenol-chloroform extraction protocol (Sambrook et al. 1989). Two fragments of the mitochondrial 16S rRNA and cytochrome oxidase subunit I (COI) genes were amplified. For 16S, the primers P7 (5'-CGCCTGTTTACCAAAAACAT-3') and P8 (5'-CCGGTCTGAACTCAGATCACGT-3') were used following Simon et al. (1994), and for COI, Chmf4 (5'-TYTCWACWAAYCAYAAAGAYATCGG-3') and Chmr4 (5'-ACYTCRGGRTGRCCRAARAATCA-3') were used following Che et al. (2012). Gene fragments were amplified under the following conditions: an initial denaturing step at 95 °C for 4 min; 36 cycles of denaturing at 95 °C for 30 s, annealing at 52 °C (for 16S)/47 °C (for COI) for 40 s and extending at 72 °C for 70 s. Sequencing was conducted using an ABI3730 automated DNA sequencer in Shanghai DNA BioTechnologies Co., Ltd. (Shanghai, China). New sequences were deposited in GenBank (for GenBank accession numbers see Table 1).

Sequences were assembled and aligned using the Clustalw module in BioEdit v. 7.0.9.0 (Hall 1999) with default settings. Alignments were checked by eye and revised manually if necessary. For phylogenetic analyses of mitochondrial DNA, the dataset concatenated with 16S and COI gene sequences. To avoid under- or over-parameterisation (Lemmon and Moriarty 2004; McGuire et al. 2007), the best partition scheme and the best evolutionary model for each partition were chosen for the phylogenetic analyses using PARTITIONFINDER v. 1.1.1 (Robert et al. 2012). In this analysis, 16S gene and each codon position of COI gene were defined, and Bayesian Inference Criteria was used. As a result, the analysis suggested that the best partition scheme is16S gene/each codon position of COI gene, and selected GTR + G + I model as the best model for each partition. Phylogenetic analyses were conducted using maximum likelihood (ML) and Bayesian Inference (BI) methods, implemented in PhyML v. 3.0 (Guindon et al. 2010) and MrBayes v. 3.12 (Ronquist and Huelsenbeck 2003), respectively. For the ML tree, branch supports were drawn from 10,000 nonparametric bootstrap replicates. In BI, two runs each with four Markov chains were simultaneously run for 50 million generations with sampling every 1,000 generations. The first 25% trees were removed as the "burn-in" stage followed by calculations of Bayesian

Table 1. Information for samples used in molecular phylogenetic analyses in this study.

ID	Species	Locality (* the type locality)	Voucher number	16S	CO1
1	*Nidirana yeae* sp. nov.	*Huanglian Town, Tongzi County, Guizhou Province, China	CIBTZ20190608004	MN295227	MN295233
2	*Nidirana yeae* sp. nov.	*Huanglian Town, Tongzi County, Guizhou Province, China	CIBTZ20190608005	MN295228	MN295234
3	*Nidirana yeae* sp. nov.	*Huanglian Town, Tongzi County, Guizhou Province, China	CIBTZ20190608019	MN295229	MN295235
4	*Nidirana yeae* sp. nov.	*Huanglian Town, Tongzi County, Guizhou Province, China	CIBTZ20190608006	MN295230	MN295236
5	*Nidirana yeae* sp. nov.	*Huanglian Town, Tongzi County, Guizhou Province, China	CIBTZ20160714016	MN295231	MN295237
6	*Nidirana yeae* sp. nov.	*Huanglian Town, Tongzi County, Guizhou Province, China	CIBTZ20190608003	MN295232	MN295238
7	*Nidirana daunchina*	*Emei Mountain, Sichuan Province, China	SYS a004595	MF807823	MF807862
8	*Nidirana daunchina*	*Emei Mountain, Sichuan Province, China	CIB2011081603	MK293821	MK293839
9	*Nidirana daunchina*	*Emei Mountain, Sichuan Province, China	CIB2011081601	MK293819	MK293837
10	*Nidirana daunchina*	*Emei Mountain, Sichuan Province, China	SYS a004594	MF807822	MF807861
11	*Nidirana daunchina*	*Emei Mountain, Sichuan Province, China	CIB2011081602	MK293820	MK293838
12	*Nidirana daunchina*	*Emei Mountain, Sichuan Province, China	CIB20110629001	MK293822	MK293840
13	*Nidirana daunchina*	Hejiang County, Sichuan Province, China	SYS a004930	MF807824	MF807863
14	*Nidirana daunchina*	Hejiang County, Sichuan Province, China	SYS a004931	MF807825	MF807864
15	*Nidirana daunchina*	Hejiang County, Sichuan Province, China	SYS a004932	MF807826	MF807865
16	*Nidirana yaoica*	*Daoyao Mountain, Guangxi Zhuang Autonomous Region, China	SYS a007009	MK882271	MK895036
17	*Nidirana yaoica*	*Daoyao Mountain, Guangxi Zhuang Autonomous Region, China	SYS a007011	MK882272	MK895037
18	*Nidirana yaoica*	*Daoyao Mountain, Guangxi Zhuang Autonomous Region, China	SYS a007012	MK882273	MK895038
19	*Nidirana yaoica*	*Daoyao Mountain, Guangxi Zhuang Autonomous Region, China	SYS a007013	MK882274	MK895039
20	*Nidirana yaoica*	*Daoyao Mountain, Guangxi Zhuang Autonomous Region, China	SYS a007014/CIB 110013	MK882275	MK895040
21	*Nidirana yaoica*	*Daoyao Mountain, Guangxi Zhuang Autonomous Region, China	SYS a007020	MK882276	MK895041
22	*Nidirana yaoica*	*Daoyao Mountain, Guangxi Zhuang Autonomous Region, China	SYS a007021	MK882277	MK895042

ID	Species	Locality (* the type locality)	Voucher number	16S	CO1
23	*Nidirana yaoica*	*Daoyao Mountain, Guangxi Zhuang Autonomous Region, China	SYS a007022	MK882278	MK895043
24	*Nidirana chapaensis*	*Sapa, Lao Cai, Vietnam	ROM 28070	AF206460	/
25	*Nidirana chapaensis*	*Sapa, Lao Cai, Vietnam	1999.5871	KR827710	/
26	*Nidirana chapaensis*	Gia Lai, Vietnam	AMSR176027	KU840598	/
27	*Nidirana chapaensis*	*Sapa, Lao Cai, Vietnam	T2483/2000.4850	KR827711	KR827711
28	*Nidirana hainanensis*	*Diaoluo Mountain, Lingshui County, Hainan Province, China	CIB20110629003	MK293807	MK293825
29	*Nidirana leishanensis*	*Leigong Mountain, Leishan County, Guizhou Province, China	CIBLS20150627003	MK293810	MK293828
30	*Nidirana lini*	*Jiangcheng County, Yunnan Province, China	SYS a003967	MF807818	MF807857
31	*Nidirana adenopleura*	*New Taipei City, Taiwan Province, China	UMMZ 189963	DQ283117	/
32	*Nidirana adenopleura*	Nanping City, Fujian Province, China	SYS a005911	MF807844	MF807883
33	*Nidirana okinavana*	*Iriomote Island, Okinawa, Japan	/	NC022872	NC022872
34	*Nidirana nankunensis*	*Nankun Mountain, Guangdong Province, China	SYS a003618	MF807828	MF807867
35	*Nidirana pleuraden*	Gaoligong Mountain, Yunnan Province, China	SYS a003775	MF807816	MF807855
36	*Babina holsti*	*Okinawa, Japan	/	NC022870	NC022870
37	*Babina subaspera*	*Amami Island, Kagoshima, Japan	/	NC022871	NC022871
38	*Odorrana margaretae*	China	HNNU1207003	NC024603	/

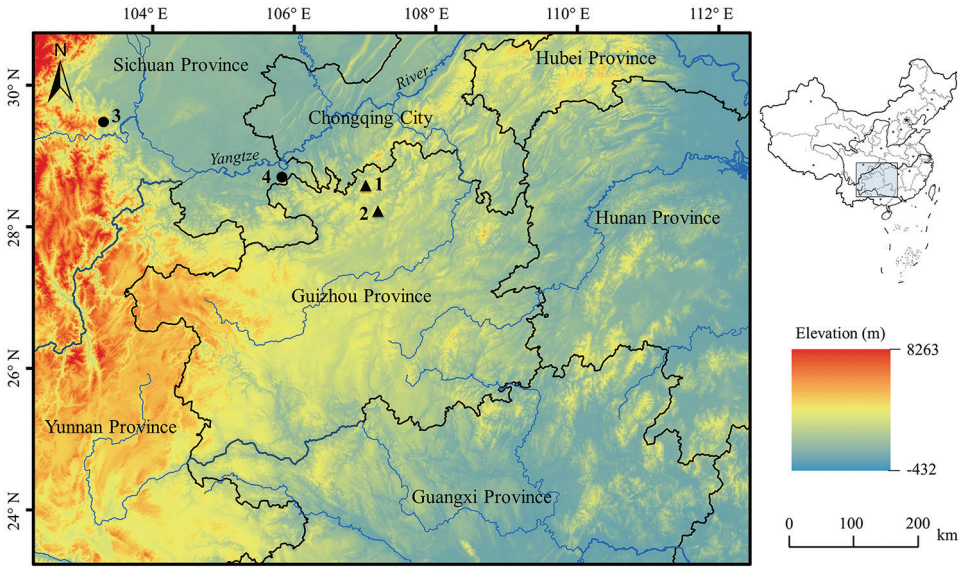

Figure 1. Type locality of *Nidirana yeae* sp. nov. and sampling localities of *N. daunchina*. **1**, the type locality of *Nidirana yeae* sp. nov., Huanglian town, Tongzi County, Guizhou Province, China; **2**, Kuankuoshui National Nature Reserve, Suiyang County, Guizhou Province, China as the potential distribution area deduced from Wu et al. (1986); **3**, the type locality of *N. daunchina*, E'mei Mountain, Sichuan Province, China; **4**, Hejiang County, Sichuan Province, China.

posterior probabilities and the 50% majority-rule consensus of the post burn-in trees sampled at stationarity. Finally, mean genetic distance between *Nidirana* species based on uncorrected *p*-distance model was estimated on the 16S gene using MEGA v. 6.06 (Tamura et al. 2011).

Morphological comparisons

All ten adults (Suppl. material 1: Table S1) and one tadpole of the new species were measured. For comparisons, three adult male specimens of *N. daunchina* freshly collected from its type locality (E'mei Mountain, Sichuan Province, China) were measured (Suppl. material 1: Table S1), and measurements of *N. yaoica* were retrieved from Lyu et al. (2019a). The terminology and methods followed Fei et al. (2005), Mahony et al. (2011), and Lyu et al. (2019a). Measurements were made with a dial caliper to the nearest 0.1 mm. Twenty-four morphometric characters of adult specimens were measured:

SVL snout-vent length (distance from the tip of the snout to the posterior edge of the vent);
HDL head length (distance from the tip of the snout to the articulation of jaw);
HDW head width (greatest width between the left and right articulations of jaw);
SL snout length (distance from the tip of the snout to the anterior corner of the eye);
ED eye diameter (distance from the anterior corner to the posterior corner of the eye);
IOD interorbital distance (minimum distance between the inner edges of the upper eyelids);
IND internasal distance (minimum distance between the inner margins of the external nares);
UEW upper eyelid width (greatest width of the upper eyelid margins measured perpendicular to the anterior-posterior axis);
TYD maximal tympanum diameter;
TED tympanum-eye distance (from anterior edge of tympanum to posterior corner of the eye);
LAL length of lower arm and hand (distance from the elbow to the distal end of the finger IV);
LW lower arm width (maximum width of the lower arm);
HND hand length (from distal end of radioulna to tip of distal finger III);
RAD radioulna length (from the flexed elbow to the base of the outer palmar tubercle);
FIL first finger length (measured from the base of the second finger to the tip of the first finger);
FIIL second finger length (measured from the base of the first finger to the tip of the second);
FIIIL third finger length (measured from the base of the second finger to the tip of the third);

FIVL fourth finger length (measured from the base of the third finger to the tip of the fourth);
HLL hindlimb length (maximum length from the vent to the distal tip of the toe IV);
TL tibia length (distance from knee to tarsus);
TW maximal tibia width;
THL thigh length (distance from vent to knee);
TFL length of foot and tarsus (distance from the tibiotarsal articulation to the distal end of the toe IV);
FL foot length (distance from tarsus to the tip of the fourth toe).

The stage of the tadpole was identified following Gosner (1960). Ten morphometric characters of tadpole specimen were measured:

TOL total length;
SVL snout-vent length (distance from the tip of the snout to the posterior edge of the vent);
BH maximum body height;
BW maximum body width;
SL snout length (distance from the tip of the snout to the anterior corner of the eye);
SS snout to spiraculum (distance from spiraculum to the tip of the snout);
IOD interorbital distance (minimum distance between the inner edges of the upper eyelids);
TBW maximum width of tail base;
TAL tail length (distance from base of vent to the tip of tail);
TAH tail height (maximum height between upper and lower edges of tail).

In order to reduce the impact of allometry, the correct value from the ratio of each character to SVL was calculated and was log-transformed for subsequent morphometric analyses. Mann-Whitney *U* tests were conducted to test the significance of differences on morphometric characters between the new species, *N. daunchina*, and *N. yaoica*. The significance level was set at 0.05. Due to only the measurements SVL, HDL, HDW, SL, IND, IOD, ED, TYD, TED, HND, RAD, TL, and FL of male *N. yaoica* being available from Lyu et al. (2019a), the Mann-Whitney *U* tests were conducted based on these 13 morphometric characters for the new species and *N. yaoica*.

The new species was also compared with all other *Nidirana* species based on morphological characters. Comparative morphological data were obtained from the literature for species. *N. adenopleura* (Boulenger 1909; Chuaynkern et al. 2010; Lyu et al. 2017), *N. chapaensis* (Bourret 1937; Chuaynkern et al. 2010), *N. daunchina* (Chang and Hsü 1932; Liu 1950; Fei et al. 2009; Lyu et al. 2017), *N. hainanensis* (Fei et al. 2007; Li et al. 2019a), *N. leishanensis* (Li et al. 2019a), *N. lini* (Chou 1999; Fei et al. 2009; Lyu et al. 2017), *N. nankunensis* (Lyu et al. 2017), *N. okinavana* (Boettger 1895; Matsui 2007), *N. pleuraden* (Boulenger 1904) and *N. yaoica* (Lyu et al. 2019a).

Bioacoustics analyses

The advertisement calls of the new *species* from Huanglian Town, Tongzi County, Guizhou Province, China were recorded from the specimen CIBTZ20190608004 in the field on 8 June 2019. The advertisement calls were recorded from the ridge of a paddy field at ambient air temperature of 20 °C and air humidity of 80 %. For comparisons, the advertisement calls of *N. daunchina* from E'mei Mountain, Sichuan Province, China were recorded from the specimen CIB2011081603 at ambient air temperature of 20 °C and air humidity of 85 % in the ridge of paddy field on 16 August 2011; the advertisement calls of *N. yaoica* were retrieved from Lyu et al. (2019a). SONY PCM-D50 digital sound recorder was used to record within 20 cm of the calling individual. The sound files in wave format were resampled at 48 kHz with sampling depth 24 bits. Calls were recorded and examined as described by Wijayathilaka and Meegaskumbura (2016). Call recordings were visualised and edited with SoundRuler 0.9.6.0 (Gridi-Papp 2003–2007) and Raven Pro 1.5 software (Cornell Laboratory of Ornithology, Ithaca, NY, USA). Ambient temperature of the type and other localities was taken by a digital hygrothermograph.

Results

Aligned sequence matrix of 16S is 523 base pairs (bp) in length and 561 bp for COI. ML and BI analyses based on the 16S + COI matrix resulted in basically identical topologies (Fig. 2). All samples of the new *species* were clustered into one clade nested in the genus *Nidirana*. This new species clade was clustered into a large clade together with *N. leishanensis*, *N. hainanensis*, *N. daunchina*, *N. yaoica*, and *N. chapaensis*, with high supported value of 100 in ML and 1.00 in BI. On 16S gene, the mean genetic distance between the new species and the closely related species *N. daunchina* and *N. yaoica* were 1.2 % and 1.3 %, respectively, at the same level as the distance between *N. adenopleura* and *N. okinavana* (1.2 %; Table 2).

The results of Mann-Whitney *U* tests indicated that in males, the new species was significantly different from *N. daunchina* and *N. yaoica* on many morphometric characters (all *p*-values < 0.05; Table 3). The new species could also be identified from its congeners based on morphological descriptions from the literature and from our examinations of newly collected material (Table 4). More detailed descriptions of results from morphological comparisons between the new species and its congeners are presented in the following sections.

There were many differences in sonograms and waveforms of calls between the new species, *N. daunchina*, and *N. yaoica* (Fig. 3; Table 5). Firstly, in the call duration and the note duration, the two-note call and three-note call of the new species were longer than those of both *N. daunchina* and *N. yaoica*. Secondly, the note interval of two-note call and three-note call of the new species was shorter than those of *N. daunchina* and *N. yaoica*. Thirdly, the dominant frequency of call in the new species was higher than *N. yaoica*.

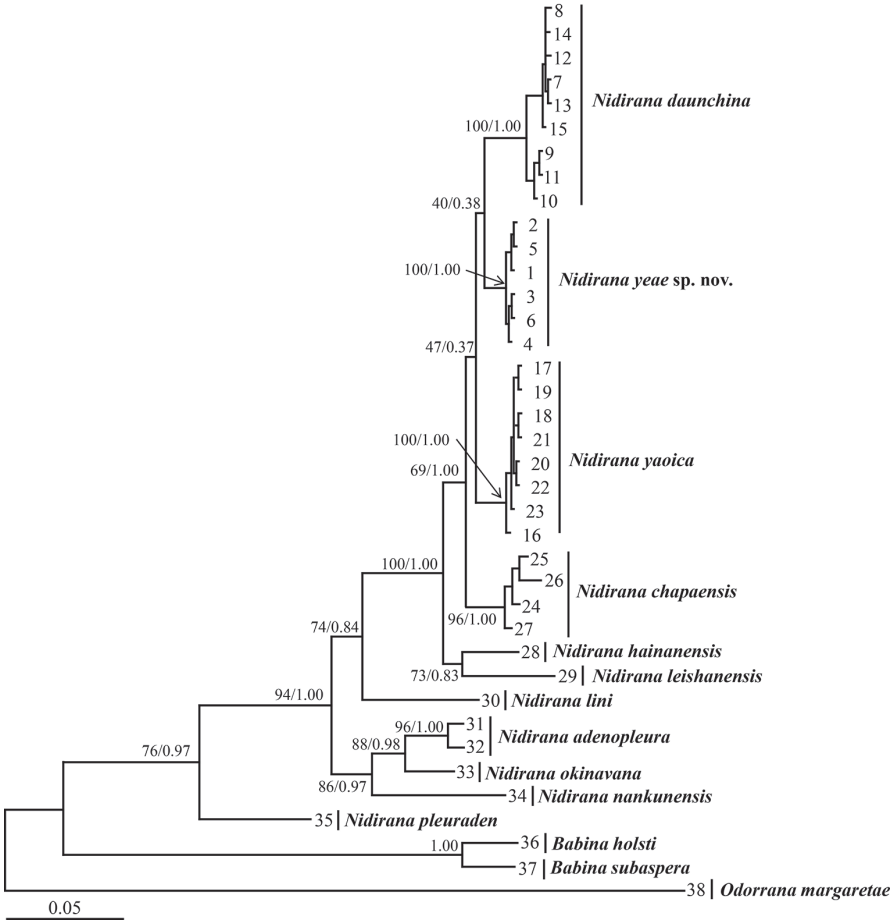

Figure 2. Maximum Likelihood (ML) tree based on the mitochondrial 16S and COI gene sequences. Bootstrap supports from ML analyses/Bayesian posterior probabilities from Bayesian Inference (BI) analyses are labelled beside nodes. Information of samples 1–38 in Table 1.

Table 2. Uncorrected *p*-distance between *Nidirana* species of the 16S rRNA gene. Mean value of genetic distance is given in the lower half of the table.

ID	Species	1	2	3	4	5	6	7	8	9	10
1	*Nidirana yeae* sp. nov.										
2	*Nidirana daunchina*	0.012									
3	*Nidirana yaoica*	0.013	0.016								
4	*Nidirana chapaensis*	0.015	0.017	0.020							
5	*Nidirana hainanensis*	0.028	0.030	0.030	0.032						
6	*Nidirana leishanensis*	0.034	0.036	0.032	0.042	0.029					
7	*Nidirana lini*	0.026	0.035	0.033	0.036	0.035	0.042				
8	*Nidirana adenopleura*	0.031	0.037	0.037	0.036	0.039	0.035	0.030			
9	*Nidirana okinavana*	0.038	0.044	0.044	0.041	0.042	0.044	0.029	0.012		
10	*Nidirana nankunensis*	0.059	0.069	0.069	0.075	0.063	0.065	0.050	0.044	0.040	
11	*Nidirana pleuraden*	0.050	0.054	0.060	0.065	0.062	0.071	0.047	0.052	0.052	0.069

Table 3. Morphometric comparisons between *Nidirana yeae* sp. nov., *N. daunchina* and *N. yaoica*. Units in mm. Abbreviations for the species name: NYE, *Nidirana yeae* sp. nov.; ND, *N. daunchina*; NYA, *N. yaoica*. See abbreviations for morphometric characters in Materials and methods section.

	NYE			ND		NYA		*P*-value from Mann-Whitney *U* test	
	Male (*N* = 9)		Female (*N* = 1)	Male (*N* = 3)		Male (*N* = 13)			
	Range	Mean ± SD	Value	Range	Mean ± SD	Range	Mean ± SD	NYE vs. ND	NYE vs. NYA
SVL	41.2–43.5	42.4 ± 1.8	44.7	46.1–46.3	46.2 ± 0.1	40.4–45.9	43.8 ± 1.7	0.013	0.077
HDL	14.0–15.9	15.0 ± 1.5	16.6	17.7–20.7	19.1 ± 1.5	15.7–18.6	16.9 ± 0.9	0.033	0.021
HDW	14.4–15.5	15.0 ± 0.8	15.1	16.2–17.5	16.8 ± 0.6	15.0–17.2	16.0 ± 0.6	0.309	0.025
SL	6.5–7.0	6.8 ± 0.5	7.1	7.0–7.3	7.2 ± 0.2	6.2–8.7	7.2 ± 0.7	0.116	0.92
IND	5.2–5.6	5.4 ± 0.3	5.6	5.5–6.6	6. 0 ± 0.5	5.4–6.6	5.9 ± 0.3	0.926	0.102
IOD	4.2–4.7	4.5 ± 0.4	4	4.2–4.8	4.4 ± 0.3	3.5–5.1	4.3 ± 0.5	0.644	0.92
ED	3.9–4.6	4.2 ± 0.6	5.1	5.4–6.2	5.8 ± 0.4	4.6–5.4	5.1 ± 0.2	0.033	0.015
UEW	2.8–3.4	3.1 ± 0.5	2.4	3.1–3.3	3.2 ± 0.1	/	/	0.309	/
TYD	3.6–4.2	3.9 ± 0.4	3.7	4.0–4.8	4.4 ± 0.4	3.2–4.5	3.9 ± 0.4	0.926	0.526
TED	1.2–2.0	1.5 ± 0.3	1.6	0.8–1.2	1.0 ± 0.2	1.0–1.6	1.2 ± 0.2	0.013	0.018
LAL	16.9–18.2	17.5 ± 1.0	19.1	19.8–21.1	20.4 ± 0.7	/	/	0.079	/
LW	3.6–3.9	3.8 ± 0.2	3.9	3.6–4.6	4.1 ± 0.5	/	/	0.782	/
HND	10.1–11.9	11.0 ± 0.5	11	11.4–12.1	11.8 ± 0.4	10.2–12.8	11.1 ± 0.9	0.782	0.367
RAD	7.7–9.6	8.6 ± 0.7	9	9.7–9.9	9.8 ± 0.1	7.8–9.4	8.5 ± 0.4	0.166	0.018
FIL	5.0–6.0	5.5 ± 0.4	6	5.7–6.6	6.1 ± 0.4	/	/	0.926	/
FIIL	3.3–4.6	4.1 ± 0.4	4.4	4.3–4.9	4.7 ± 0.3	/	/	0.309	/
FIIIL	5.8–7.6	6.8 ± 0.5	7.1	6.2–7.5	6.9 ± 0.6	/	/	0.405	/
FIVL	4.5–5.0	4.7 ± 0.2	5	4.5–5.3	5.0 ± 0.4	/	/	0.926	/
HLL	62.7–67.4	65.0 ± 3.7	62.4	73.6–75.1	74.3 ± 0.7	/	/	0.033	/
THL	19.6–21.4	20.6 ± 1.5	21.7	20.6–23.0	21.9 ± 1.2	/	/	0.782	/
TL	20.9–22.1	21.5 ± 1.0	22.6	23.8–24.3	24.0 ± 0.3	21.6–25.6	23.1 ± 1.0	0.405	0.018
TW	6.4–6.9	6.6 ± 0.4	6	5.9–7.0	6.6 ± 0.6	/	/	0.033	/
TFL	28.7–30.9	29.8 ± 1.9	33.2	23.9–24.9	24.2 ± 0.6	/	/	0.013	/
FL	21.3–22.7	21.9 ± 1.1	23.3	34.3–36.7	35.4 ± 1.2	31.1–35.7	31.4 ± 9.0	0.013	0.001

Table 4. Diagnostic characters separating *Nidirana yeae* sp. nov. from its congeners.

Species	SVL of male (mm)	SVL of female (mm)	Fingers tips	Lateroventral groove on fingers	Relative finger length	Toe tips	Lateroventral groove on toes	Tibiotarsal articulation reaching level when leg stretched forward	Subgular vocal sacs	Nuptial pad	Tadpole labial tooth row formula	Calling	References
Nidirana yeae sp. nov.	41.2–43.5	44.7	dilated	absent	II < IV < I < III	dilated	present	eye	present	one on first finger	1:1+1/1+1:2	2–6 notes	This study
N. adenopleura	43.1–57.6	47.6–60.7	dilated	present or absent	II < I <IV < III	dilated	present	snout tip or between eye and snout	present	one on first finger	1:1+1/1+1:2 or 1:0 +0/1+1:1	2–4 notes	Pope (1931); Chuaynkern et al. (2010); Lyu et al. (2017)
N. chapaensis	35.5–42.5	41.0–51.8	dilated	present or absent	II < I = IV < III	dilated	present	nostril	present	two on first finger	1:1+2/1+1:2	3 notes	Chuaynkern et al. (2010)
N. daunchina	40.6–51.0	44.0–53.0	dilated	present	II < IV < I < III	dilated	present	nostril	present	one on first finger	1:1+1/1+1:2 or 1:1+1/2+2:1	2–5 notes containing a specific first note	This study; Liu (1950); Fei et al. (2009); Lyu et al. (2017)
N. hainanensis	32.8–33.5	/	dilated	present	II <I < IV < III	dilated	present	nostril	present	absent	/	2–4 fast-repeated double notes	Fei et al. (2009); Lyu et al. (2017); Li et al. (2019a)
N. leishanensis	49.5–56.4	43.7–55.3	dilated	present	II < IV < I < III	dilated	present	between eye and snout	present	two on first two finger	1:1+2/1+1: 2	1 note	Li et al. (2019a)
N. lini	44.1–63.1	57.7–68.6	dilated	present or absent	II < I < IV < III	dilated	present	beyond snout	present	one on first finger	1:1+1/1+1:2	5–7 notes	Chou (1999); Fei et al. (2009); Lyu et al. (2017)
N. nankunensis	33.3–37.1	37.8–39.5	dilated	present or absent	II < I < IV < III	dilated	present	nostril	present	one on first finger	1:1+1/1+1:2	13–15 fast-repeated notes	Lyu et al. (2017)
N. okinavana	35.5–42.8	44.6–48.8	dilated	present or absent	II < I < IV < III	dilated	present	between eye and nostril	absent	poorly one on first finger	1:1+1/1+1:2	17–25 fast-repeated notes	Matsui and Utsunomiya (1983); Chuaynkern et al. (2010)
N. pleuraden	45.4–58.7	45–62.5	not dilated	absent	II < I < IV < III	not dilated	absent	between eye and snout	present	one on first finger	1:1+1/1+1:2 or 1:1+1/2+2:1	4–7 notes	Lyu et al. (2017)
N. yaoica	40.4–45.9	/	dilated	present	II < I < IV < III	dilated	present	nostril	present	one on first finger	/	1–3 fast-repeated notes	Lyu et al. (2019a)

Table 5. Comparisons of characteristics of advertisement calls of *Nidirana yeae* sp. nov., *N. daunchina*, and *N. yaoica*. Units in milliseconds (ms).

Nidirana yeae sp. nov.				*N. daunchina*		*N. yaoica*		
Two-note call (N = 5)	**Three-note call (*N* = 2)**	**Four-note call (*N* = 3)**	**Six-note call (*N* = 1)**	**Two-note call (*N* = 5)**	**Three-note call (*N* = 2)**	**One-note call (*N* = 25)**	**Two-note call (*N* = 59)**	**Three-note call (*N* = 3)**
728–825, 755.4 ± 45.2	988–1135, 1061.5 ± 103.9	1400–1563, 1459.3 ± 90.0	2082	453–462, 457.7 ± 4.5	768–826, 792.0 ± 21.1	37–51, 43.3 ± 2.7	307–454, 355.9 ± 31.1	565–678, 628.0 ± 57.6
1st 342–418, 362.0 ± 31.8	1st 308–443, 375.5 ± 95.4	1st 314–403, 364.0 ± 45.5	1st 440	1st 45–65, 56.0 ± 10.1	1st 43–55, 52.0 ± 5.1	1st 37–51, 43.3 ± 2.7	1st 36–51, 43.5 ± 2.8	1st 42–54, 46.7 ± 6.4
2nd 212–225, 218.6 ± 6.1	2nd 169–220, 194.5 ± 36.1	2nd 203–218, 212.0 ± 79.4	2nd 240	2nd 47–53, 49.3 ± 3.2	2nd 49–60, 55.0 ±4.7		2nd 30–49, 39.6 ± 3.3	2nd 37–40, 38.7 ± 1.5
	3rd 135–205, 170.0 ± 49.5	3rd 166–180, 170.6 ± 8.1	3rd 194		3rd 38–58, 45.0 ± 7.9			3rd 35–52, 42.3 ± 8.7
		145–172, 157.0 ± 13.7	4th 175					
			5th 160					
			6th 166					
151–197, 170.0 ± 19.1	1st 120–194, 157.0 ± 52.3	1st 175–218, 194.6 ± 21.7	1st 132	347–359, 352.0 ± 6.2	1st 320–355, 337.0 ± 15.2	/	215–372, 272.8 ± 31.7	1st 212–250, 234.0 ± 19.7
	2nd 147–178, 162.5 ± 21.9	2nd 155–185, 174.0 ± 16.5	2nd 132		2nd 298–310, 303.0 ± 4.9			2nd 222–302, 266.3 ± 40.7
		3rd 138–228, 190.7 ± 46.9	3rd 135					
			4th 126					
			5th 132					
4200–5040, 4776.0 ± 332.9	4620–5040, 4830.0 ± 296.9	4680–5160, 4880.0 ± 249.7	5280	3629–4240, 3938.0 ± 305.6	3875–4832, 4586.4 ± 402.0	516.8	516.8	516.8
1st 4200–4800, 4440.0 ± 226.2	1st 4320–4440, 4380.0 ± 84.8	1st 4680–5160, 4880.0 ± 249.7	1st 4560	1st 3629–4240, 3899.3 ± 311.5	1st 2624–4448, 3894.4 ± 774.7	516.8	1st 516.8 (98.3%) or 2584 (1.7%)	1st 516.8
2nd 4200–5040, 4776.0 ± 332.9	2nd 4620–5040, 4830 ± 297	2nd 4080–4680, 4400.0 ± 301.9	2nd 5280	2nd 2151–3945, 3187.6 ± 929.0	2nd 3875–4832, 4586.4 ± 402.0			2nd 516.8
	3rd 3840–4560, 4200.0 ± 509.1	3rd 4080–4680, 4440.0 ± 317.5	3rd 4800		3rd 1478–3200, 2241.2 ± 662.8		2nd 516.8	3rd 516.8
		4th 4320–4680, 4466.6 ± 189.0	4th 4560					
			5th 3800					
			6th 4080					

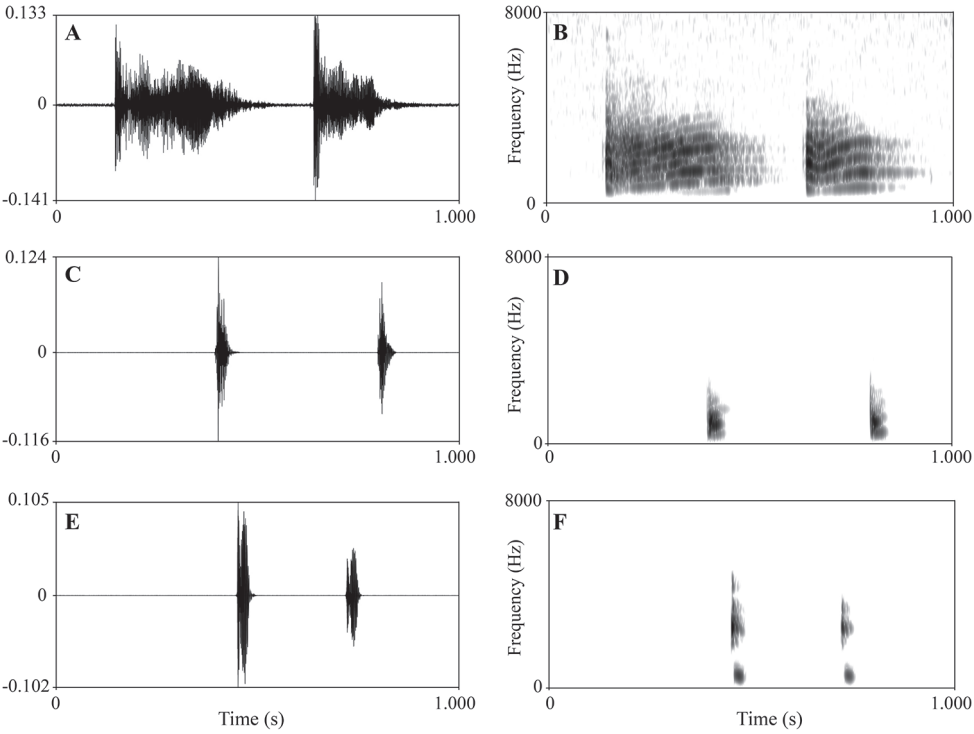

Figure 3. Advertisement calls of *Nidirana yeae* sp. nov. (holotype CIBTZ20190608004), *N. daunchina* (specimen CIB2011081603) and *N. yaoica* (specimen SYS a007009). **A** Waveform showing two-note call of *Nidirana yeae* sp. nov **B** sonogram showing two-note call of *Nidirana yeae* sp. nov **C** waveform showing two-note call of *N. daunchina* **D** sonogram showing two-note call of *N. daunchina* **E** waveform showing two-note call of *N. yaoica* **F** sonogram showing two-note call of *N. yaoica*.

Based on the molecular, morphological, and bioacoustics differences, the specimens from Tongzi County, Guizhou Province, China, represent a new species which is described as *Nidirana yeae* sp. nov.

Taxonomic account

***Nidirana yeae* sp. nov.**
http://zoobank.org/B4E44DFA-4720-4B28-8CF1-DEFC6096D2EF
Figures 4, 5A–C, 6; Table 1, Suppl. material 1: Table S1

Material examined. *Holotype.* CIBTZ20190608004 (Figs 4, 5), adult male, collected by Shi-Ze Li on 6 June 2019 in Huanglian Town (28.44317N, 107.02003E; ca. 1170 m a.s.l.), Tongzi County, Guizhou Province, China.

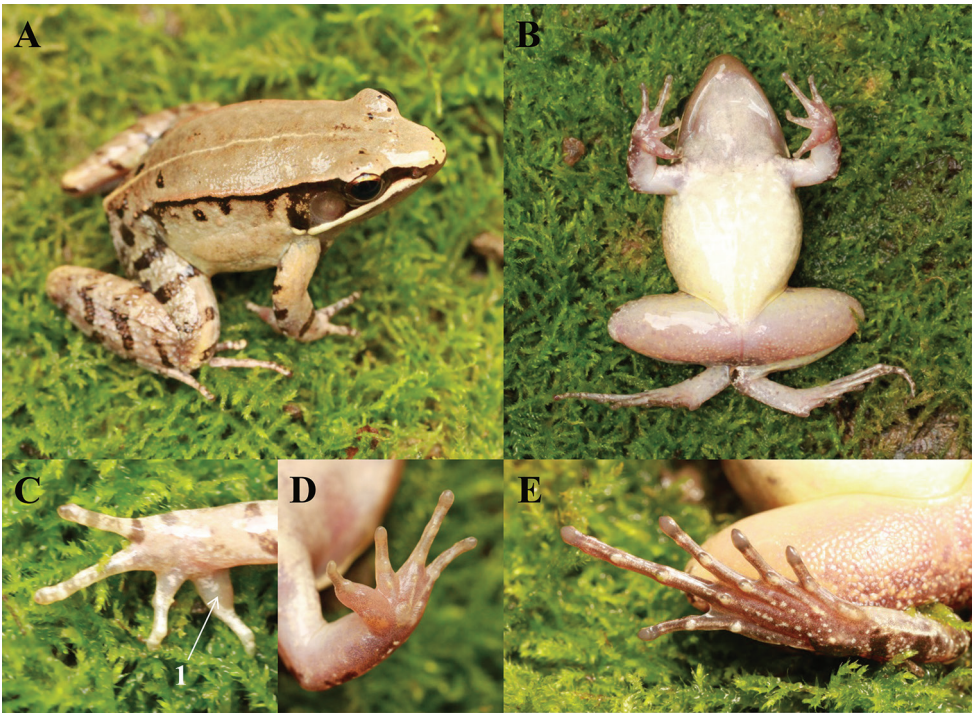

Figure 4. Photos of the holotype CIBTZ20190608004 of *Nidirana yeae* sp. nov. in life. **A** Dorsal view **B** ventral view **C** dorsal view of hand **D** ventral view of hand **E** ventral view of foot. Key: 1 indicates nuptial pad on the inner side of finger I.

Paratypes. A total of nine specimens (eight adult males and one adult female) collected by Shi-Ze Li from Huanglian Town in Tongzi County, Guizhou Province, China. Two male specimens: CIBTZ20160714016 and CIBTZ20160714017 collected on 14 July 2016; one female specimen: CIBTZ20190608005 and six male specimens: CIBTZ20190608001, CIBTZ20190608003, CIBTZ20190608006, CIBTZ20190608010, CIBTZ20190608011, CIBTZ20190608013, CIBTZ20190608016 and CIBTZ20190608017 collected on 8 June 2019.

Other material examined. One tadpole (CIBTZ20190608019) collected by Jing Liu on 8 June 2019.

Diagnosis. *Nidirana yeae* sp. nov. is assigned to the genus *Nidirana* based on molecular data and the following combination of characters: absence of thumb-like structure on finger I; disks of digits dilated, rounded; dorsolateral folds distinct; the presence of large suprabrachial gland in male.

Nidirana yeae sp. nov. could be distinguished from its congeners by a combination of the following characters: (1) body of medium size (SVL 41.2–43.5 mm in males and 44.7 mm in female); (2) lateroventral groove only present on toes; (3) relative finger lengths: II < IV < I < III; (4) three metatarsal tubercles on palm; (5) heels overlapping when hindlimbs flexed at right angles to axis of body; (6) tibiotarsal articulation reaching the level of eye when leg stretched forward; (7) a pair of subgular internal vocal sacs

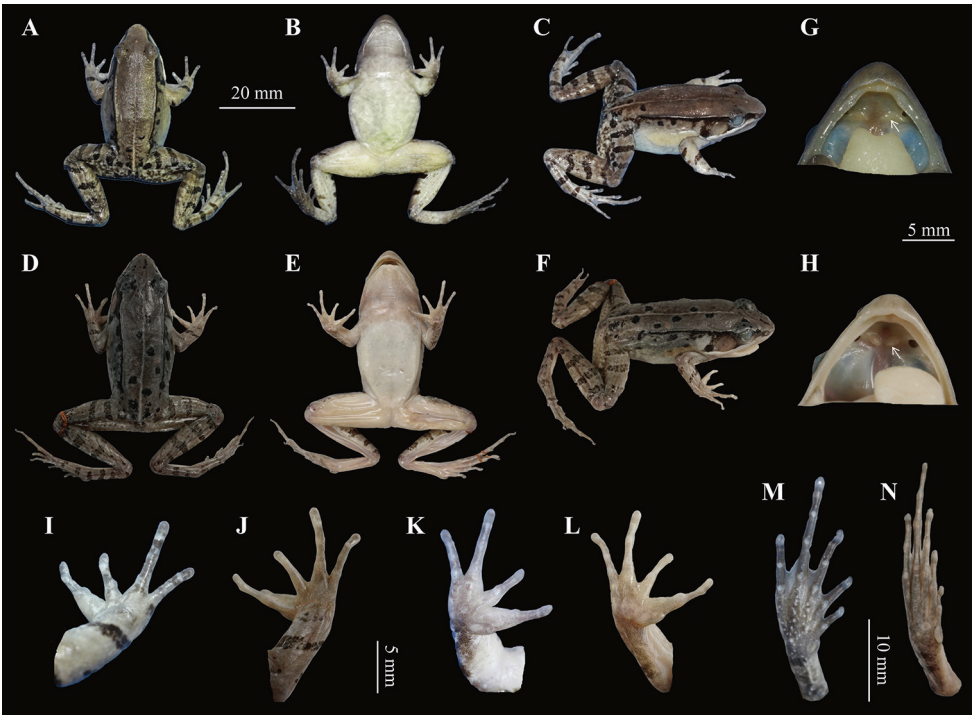

Figure 5. The holotype specimen CIBTZ20190608004 of *Nidirana yeae* sp. nov. and topotype specimen CIB2011081603 of *N. daunchina*. **A–C** Dorsal view, ventral view and dorsolateral view of CIBTZ20190608004 **D–F** dorsal view, ventral view and dorsolateral view of CIB2011081603 **G, H** oral cavity of CIBTZ20190608004 and CIB2011081603 (arrow point to vomerine ridge) **I, J** dorsal view of hand of CIBTZ20190608004 and CIB2011081603 **K, L** ventral view of hand of CIBTZ20190608004 and CIB2011081603 **M, N** ventral view of foot of CIBTZ20190608004 and CIB2011081603.

at corners of throat in male; (8) nuptial pad present on the inner side of base of fingers I in male in breeding season; (9) tadpole labial tooth row formula with 1:1+1/1+1:2; (10) in male, the advertisement call containing two kinds of note and the call containing 2–6 repeated regular notes.

Description of holotype. Body size medium, SVL 40.2 mm; head slightly wider than long (HDW/HDL = 1.03), flat above; snout rounded in dorsal and lateral views, slightly projecting beyond lower jaw; a maxillary gland in posterior corner of mouth from snout to tympanum, behind the gland a shoulder gland present; supratympanic fold absent; interorbital space narrower than internarial distance (IND/IOD = 1.38); eye large and convex, ED 0.76 times of SL; tympanum distinct, large and rounded, 0.76 times of ED, and close to eye; vomerine ridge present, but the outline of vomerine ridges are not sharp and almost connected to the internal nostril; tongue deeply notched posteriorly; paired subgular inner vocal sacs at corners of throat.

Forelimbs moderately robust (LW/SVL = 0.08); lower arm and hand less than a half of body length (LAL/SVL = 0.42); relative finger lengths: II < IV < I < III; tip of fingers weakly dilated, forming elongated and pointed disks; lateroventral grooves on

the disks of finger absent; fingers free of webbing, with lateral fringes on fingers III and IV; subarticular tubercles prominent and rounded; week supernumerary tubercles below the base of fingers III and IV; palmar tubercles three, elliptic, distinct.

Hindlimbs relatively robust, tibia 47% of SVL; tibia longer than thigh (TL/THL = 1.04); heels overlapping when hindlimbs held at right angles to axis of body; tibiotarsal articulation reaching the level of mid-eye when hindlimb is stretched forward; toes long and thin, relative toe lengths: I < II < V < III < IV; tip of toes dilated, forming significantly elongated disks; distinct lateroventral grooves on toes; webbing weak, webbing formula:

$$\text{I}\,2-2\,\text{II}\,1\frac{2}{3}-3\frac{1}{2}\,\text{III}\,2\frac{1}{2}-3\frac{2}{3}\,\text{IV}\,3\frac{2}{3}-2\,\text{V};$$

toes with lateral fringes; subarticular tubercles rounded, prominent; inner metatarsal tubercle elliptic, twice as long as its width; outer metatarsal tubercle indistinct, small and rounded.

Dorsal skin of head and anterior part of body smooth, posterior part and flanks with several tubercles, some tubercles with black spot; a large suprabrachial gland behind base of forelimb; dorsolateral fold extending from posterior margin of upper eyelid to above groin; several granules on the dorsal surfaces of thigh, tibia, and tarsus; ventral surface of head, body, and limbs smooth, several flattened tubercles densely arranged on the rear of thigh and around vent.

Colouration of holotype in life. In life, dorsal surface and suprabrachial gland pale brown; flank relatively smooth with dense tubercles on region nearly the dorsolateral fold; several black spots on flank, dorsum, and head; a discontinuous light yellow streak from posterior head to cloacae; dorsal forelimbs light brown and one brown stripe in front of the base of forelimb; dorsal hindlimb grey-brown with dense tubercles, three brown bands on the thigh, four on the tibia and the tarsus; tympanum and temporal region black; maxillary gland white; ventral surface smooth, throat and ventral of thigh and forelimbs incarnadine, belly and chest light yellow (Fig. 4).

Preserved holotype colouration. Dorsal surface faded to brown; black spots on dorsum and flank more distinct; limbs faded light brown and the crossbars becoming clearer; ventral surface faded to pale cream and throat fade to brownness (Fig. 5).

Variations. All adult specimens were similar in morphology but some individuals differed from the holotype in colour pattern. In some adult males, the colour of tympanum and temporal region pinkish red (Fig. 6A); in some adult males, the colour of dorsum is reddish brown (Fig. 6B); in the adult female, the colour of dorsum was brownish red and the flank was brownish under the dorsolateral fold (Fig. 6C); in some adult males, the colour of dorsum brick-red and the tubercles on flank were obvious (Fig. 6D); in some adult males, the throat was creamy and ventral surface of body was white with brown patches (Fig. 6E); in the adult female, the throat was brown and there were some patchiness on the ventral surface of the body and thigh (Fig. 6F).

Tadpole description. Measurements of specimen CIBTZ20190608019 (in mm): TOL 35.2, SVL 14.0, BW 6.1, BH 5.1, SL 3.1, SS 8.1, IOD 3.3, TAL 20.7, TAH 4.0, TBW 3.0. Body oval, body and tail yellowish brown, flattened above; several brown spots on dorsum and tail; maximum depth near posterior part of tail and more than

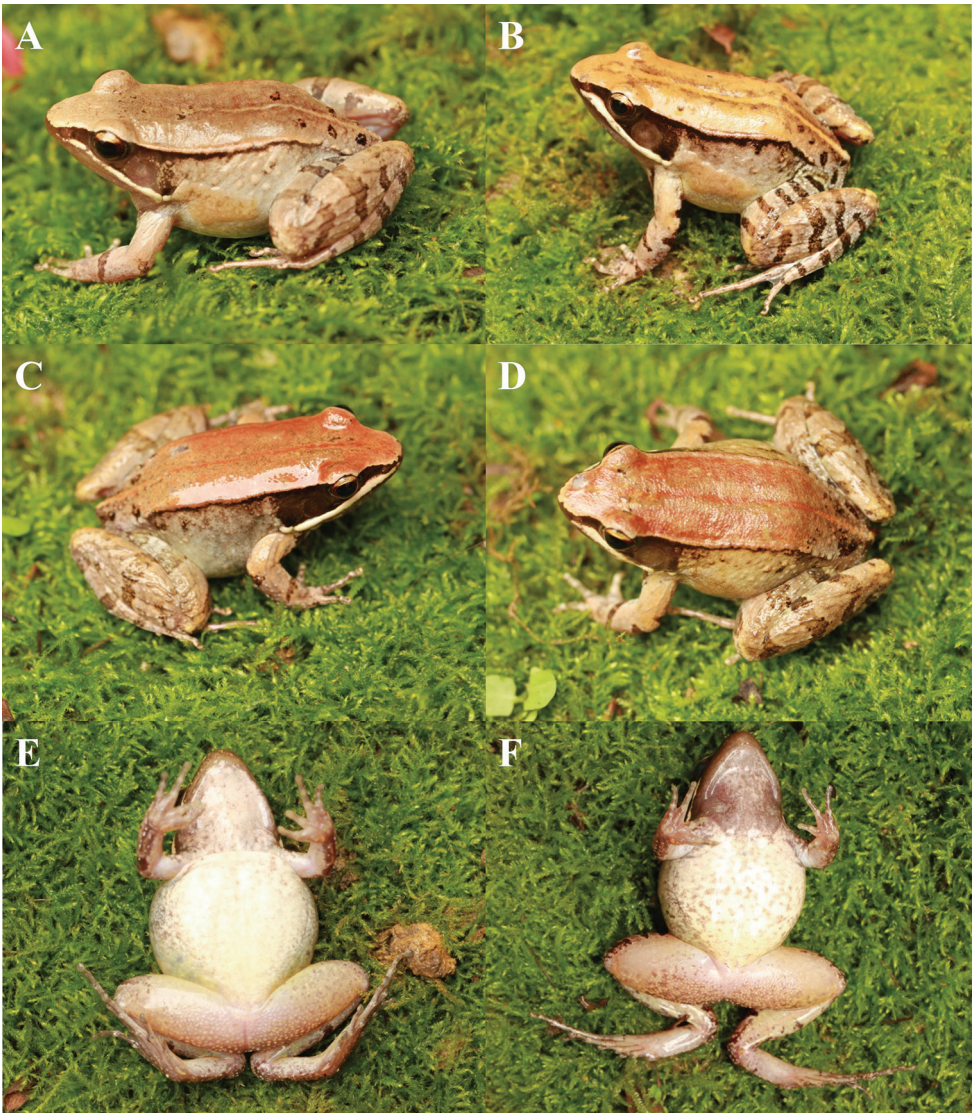

Figure 6. Colour variation in *Nidirana yeae* sp. nov. **A** Dorsal view of male specimen CIBTZ20190608003 **B** dorsal view of male specimen CIBTZ20190608016 **C** dorsal view of female specimen CIBTZ20190608005 **D** dorsal view of male specimen CIBTZ20190608006 **E** ventral view of male specimen CIBTZ20190608006 **F** ventral view of female specimen CIBTZ20190608005.

body depth; body width longer than body height (BW/ BH = 1.53); eyes lateral, nostril near snout; spiracle on left side of body, directed dorsoposteriorly; keratodont formula: 1:1+1/1+1:2; ventral of body oval, creamy white with dense brown spots on flank of body; both upper and lower lips with labial papillae; some additional tubercles at the angles of the mouth, usually with small keratodonts; tail fusiform, approximately 1.5 times as long as snout-vent length, tail height 19.3 % of tail length; dorsal fin arising behind the origin of the tail (Fig. 7).

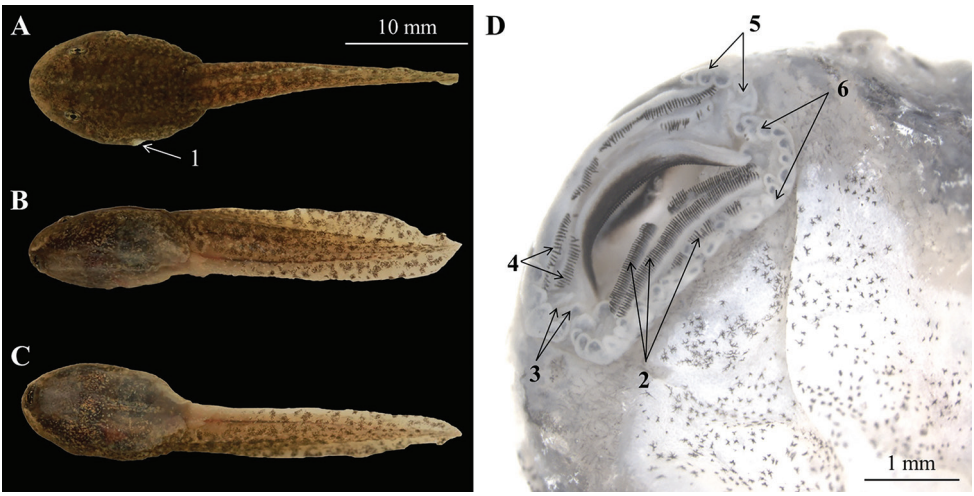

Figure 7. The tadpole CIBTZ20190608019 of *Nidirana yeae* sp. nov. in life. **A** Dorsal view **B** lateral view **C** ventral view **D** mouth structure. Key: **1**, spiracle; **2**, lower keratodonts; **3**, additional tubercles at the angles of mouth; **4**, upper keratodonts; **5**, labial papillae on upper lips; **6**, labial papillae on lower lips.

Advertisement call. Eleven advertisement calls of *Nidirana yeae* sp. nov. were recorded from the holotype CIBTZ20190608004 on the ridge of a paddy field in Huanglian Town, Tongzi County, Guizhou Province, China on 8 June 2019 between 21:00–22:00. The call has two kinds of notes (Fig. 3; Table 5). Call duration was 728–2082 ms (mean 1199 ± 174 ms, N = 11). Call interval was 2000–9435 ms (mean 4586 ± 2659 ms, N = 10). The first type of note is the start note in each call and the other notes in each call are termed the second type. Amplitude modulation within strophe is apparent, beginning with moderate energy pulses, decreasing slightly to a minimum then increasing approximately to the midnote, subsequently increasing to a peak then decreasing rapidly towards the end of each note in the first type; in the second type amplitude beginning with highest pulses and decreasing towards approximately the midnote then increasing slightly then decreasing towards the end of each note. The first type of note has a longer duration than the second type (308–440 ms, N = 10 vs.135–240 ms, N = 23).The two-note call (N = 5) has a duration of 728–825 ms, and dominant frequency is 4200–5040 Hz, three-note call (N = 2) has a duration of 988–1135 ms and dominant frequency is 4620–5040 Hz, four-note call (N = 3) has a duration of 1400–1563 ms and dominant frequency is 4680–5160 Hz, six-note call (N = 1) has a duration of 2082 ms and dominant frequency is 5280 Hz (Table 5).

Secondary sexual characteristics. A pair of subgular inner vocal sacs, a pair of slit-like openings at posterior of jaw; a single light brown nuptial pad on the inner side of dorsal surface of finger I (Fig. 4C); nuptial spicules invisible; suprabrachial gland present.

Morphological comparisons. *Nidirana yeae* sp. nov. differs from *N. leishanensis* and *N. lini* by having smaller body size (SVL < 45 mm in the new species vs. SVL > 49 mm in males of *N. leishanensis* and SVL > 57 mm in females of *N. lini*).

Nidirana yeae sp. nov. differs from *N. daunchina*, *N. hainanensis* and *N. leishanens* by the presence of lateroventral groove only on toes (vs. both fingers and toes present in the latter).

Nidirana yeae sp. nov. differs from *N. pleuraden* by the presence of lateroventral groove only on toes (vs. both fingers and toes absent in the latter).

Nidirana yeae sp. nov. differs from *N. adenopleura*, *N. hainanensis*, *N. lini*, *N. nankunensis*, *N. okinavana*, and *N. pleuraden* by the relative finger lengths II < IV < I < III (vs. II < I < IV < III or II < I = IV < III in the latter).

Nidirana yeae sp. nov. differs from *N. hainanensis*, *N. lini*, and *N. nankunensis* by tibiotarsal articulation reaching the level of eye when leg stretched forward (vs. reaching nostril or beyond snout in the latter).

Nidirana yeae sp. nov. differs from *N. okinavana* by having subgular internal vocal sacs (vs. gular vocal sacs absent in the latter).

Nidirana yeae sp. nov. differs from *N. hainanensis* and *N. leishanensi* by having nuptial pad on the inner side of base of fingers I in males in breeding season (vs. nuptial pad absent in *N. hainanensis* and nuptial pads on both fingers I and II in *N. leishanensis*).

Nidirana yeae sp. nov. differs from *N. nankunensis* and *N. okinavana* by the call containing 2–6 notes (vs. 13–15 notes in *N. nankunensis* and 17–25 notes in *N. okinavana*).

Nidirana yeae sp. nov. is genetically closer to *N. chapaensis*, *N. daunchina*, and *N. yaoica*. It differs from *N. chapaensis* by the following characters: the relative finger lengths II < IV < I < III (vs. II < I = IV < III), tibiotarsal articulation reaching the level of eye when leg stretched forward (vs. reaching nostril), having nuptial pad on the inner side base of finger I in males in breeding season (vs. having two nuptial pads on finger I), tadpole labial tooth row formula of 1:1+1/1+1:2 (vs. 1:1+2/1+1:2); differs from *N. daunchina* by the presence of lateroventral groove only on toes (vs. both fingers and toes present), heels overlapping when hindlimbs flexed at right angles to axis of body (vs. heels meeting), tibiotarsal articulation reaching the level of eye when leg stretched forward (vs. reaching nostril), having significantly lower value of SVL in males and having significantly lower ratios of HDL, ED, TED, HLL, TW, TFL, and FL to SVL in males, the outline of vomerine ridges not sharp and almost connected to the internal nostril (vs. outline of vomerine ridges sharp and distinctly separated from the internal nostril; Fig. 5G, H), having longer call duration in two-note call and three-note call, having shorter note interval in the two-note call and three-note call (Table 4); differs from *N. yaoica* by the presence of lateroventral groove only on toes (vs. both fingers and toes present), relative finger lengths II < IV < I < III (vs. II < I < IV < III), tibiotarsal articulation reaching the level of eye when leg stretched forward (vs. reaching nostril), having significantly lower ratios of HDL, HDW, ED, TED, RAD, TL, and FL of SVL in males, having longer call duration and longer note duration in two-note call and three-note call, having shorter note interval in two-note call and three-note call, and having higher dominant frequency in call (Table 5).

Remarks. Wu et al. (1986) reported that the populations from Kuankuoshui Nature Reserve of Suiyang County, Fanjiang Mountain of Jiangkou County and Leigong Mountain of Leishan County, Guizhou Province, China belonged to *N. adenopleura*. Fei et al. (1990, 2009) suggesting that populations from Kuankuoshui Nature Reserve of Suiyang County together with the populations from north-eastern part of Guizhou Province, China should be *N. daunchina*, and the populations from Fanjiang Mountain of Jiangkou County and Leigong Mountain of Leishan County, Guizhou Province, China should be *N. adenopleura*. Li et al. (2019a) proved

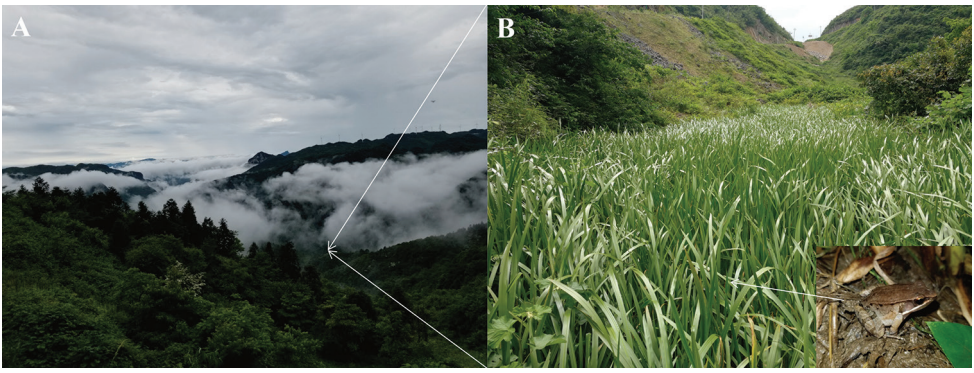

Figure 8. Habitats of *Nidirana yeae* sp. nov. in the type locality, Huanglian Town, Tongzi County, Guizhou Province, China. **A** Landscape of montane forests in the type locality **B** a paddy field occupied by the species in its type locality. *insert*: a male of *Nidirana yeae* sp. nov. in the paddy field.

that the population from Leigong Mountain of Leishan County should be a new species, which they named *N. leishanensis*. From the morphological description and morphometric data of the population from Kuankuoshui Nature Reserve of Suiyang County, some characters is very similar to *Nidirana yeae* sp. nov.: body of medium size (SVL 39.0–46 mm in males and 44–48 mm in females); lateroventral groove on toes present; relative finger lengths II < IV < I < III; three metatarsal tubercles on palm; a pair of subgular internal vocal sacs at corners of throat in males; nuptial pad present on the inner side of base of fingers I in males in breading season; tadpole labial tooth row formula with 1:1+1/1+1:2. This population was probably *Nidirana yeae* sp. nov., and detailed comparisons especially with molecular data should be conducted to establish its identity. The phylogenetic trees in our work and Lyu et al. (2019a) all supported that the population from Hejiang County, Sichuan Province, China was the closest to topotypes of *N. daunchina* but separated from *Nidirana* yeae sp. nov. and other relatives, and so this population in the south-eastern part of Sichuan Province should be *N. daunchina* and not *Nidirana yeae* sp. nov. Although the morphometric data (large body size) of the population from Fanjiang Mountain of Jiangkou County in Wu et al. (1986) indicated that it was similar to *N. leishanensis*, we still need detailed comparisons and molecular data to clarify its taxonomic status.

Ecology. *Nidirana yeae* sp. nov. is currently found from the paddy field (28.44317N, 107.02003E; ca. 1170 m a. s. l.) in Huanglian Town, Tongzi County, Guizhou Province, China. The individuals were found on the paddy field near an evergreen broad-leaved forest (Fig. 8). Tadpoles of the species could be found in the water. Two sympatric amphibians, *Zhangixalus omeimontis* (Stejneger, 1924) and *Polypedates braueri* (Vogt, 1911) were also found in the type locality.

Etymology. The specific name *yeae* is in homage to the famous taxonomist Ye Chang-Yuan for her great contributions to Chinese amphibian research. For the common name, we suggest Ye's Music Frog (English) and Ye Shi Qin Wa (Chinese).

Discussion

Before this work, the taxonomic status for the populations of *Nidirana* in Tongzi County in the north part of Guizhou Province had not been reported, but populations in Suiyang County adjacent to Tongzi County were identified as *N. daunchina* (Fei et al. 1990, 2009, 2012; Fei and Ye 2005). Now, the Tongzi population is revealed as a new species, *Nidirana yeae* sp. nov. based on integrative taxonomy using morphological comparisons, molecular phylogenetic analyses, and bioacoustics. *Nidirana* populations in Suiyang County, to the east of Tongzi County, are probably the new species also. Moreover, Lyu et al. (2017) recognised three specimens (included in our phylogenetic analyses) from Hejiang County, Sichuan Province as *N. daunchina*; of note, the straight-line geographical distance between Hejiang County and Tongzi County is ca. 110 km, much shorter than that (ca. 280 km) between Hejiang County and the type locality of *N. daunchina* (E'mei Mountain, Sichuan Province, China). Therefore, it could be speculated that the two closely related species, *Nidirana yeae* sp. nov. and *N. daunchina*, were probably parapatric in the region between Hejiang and Tongzi counties. Many more surveys of the surrounding areas are needed to clarify the populations of "*N. daunchina*" and the accurate distribution of the two species.

South-western China has long been proposed as biodiversity hotspot (Myers et al. 2000). However, Guizhou Province is an important part of south-western China, especially with the particular environments of karst rocky desertification, and knowledge of biodiversity levels and/or patterns are still seriously lacking. Recently, a series of new amphibian species were described from this province (Zhang et al. 2017; Li et al. 2018a, b, 2019a, b; Lyu et al. 2019b; Wang et al. 2019), indicating that species diversity of amphibians in this region is highly underestimated. It is urgent for herpetologists to conduct comprehensive and in-depth surveys to discover the level of amphibian species diversity in this region under accelerating global changes.

Acknowledgements

We are grateful to editors and reviewers for their work on the manuscript. This work was supported by The laboratory on biodiversity conservation and applied ecology of Guiyang College (GYU-KYZ [2019–2020] PT14–01), Project supported by the Biodiversity investigation, Observation and Assessment Program (2019–2023) of Ministry of Ecology and Environment of China, National Natural Science Foundation of China (No. 31960099), Biodiversity Conservation Key Laboratory of Guizhou Province Education Department, Guiyang College, Guizhou Provincial Department of Education Youth Science and Technology Talents Growth Project (Nos. KY[2018]455, KY[2018]468 and KY[2018]469).

References

Boulenger GA (1892) Descriptions of new reptiles and batrachians from the Loo Choo Islands. Annals and Magazine of Natural History 6(10): 302–304. https://doi.org/10.1080/00222939208677414

Boulenger GA (1904) Descriptions of new frogs and snakes from Yunnan. Annals and Magazine of Natural History(7)13: 130–135. https://doi.org/10.1080/00222930408562447

Boulenger GA (1909) Descriptions of four new frogs and a new snake discovered by Mr. H. Sauter in Formosa. Annals and Magazine of Natural History (8)4: 492–495. https://doi.org/10.1080/00222930908692704

Boettger O (1895) Neue Frösche und Schlangen von den Liukiu-Inseln. Zoologischer Anzeiger 18: 266–270.

Bourret R (1937) Notes herpétologiques sur l'Indochine française. XIV. Les batraciens de la collection du Laboratoire des Sciences Naturelles de l'Université. Descriptions de quinze especes ou variétés nouvelles. Annexe au Bulletin Général de l'Instruction Publique, Hanoi 1937: 5–56.

Chang MLY, Hsü HF (1932) Study of some amphibians from Szechuan. Contributions from the Biological Laboratory of the Science Society of China 8(5): 137–181.

Chang MLY (1933) A preoccupied name in Rana. China Journal of Science and Arts, Shanghai 18: 209.

Chaves JA, Weir JT, Smith TB (2011) Diversification in Adelomyia hummingbirds follows Andean uplift. Molecular Ecology 20(21): 4564–4576. https://doi.org/10.1111/j.1365-294X.2011.05304.x

Che J, Chen HM, Yang JX, Jin JQ, Jiang K, Yuan ZY, Murphy RW, Zhang YP (2012) Universal COI primers for DNA barcoding amphibians. Molecular Ecology Resources 12(2): 247–258. https://doi.org/10.1111/j.1755-0998.2011.03090.x

Chen L, Murphy RW, Lathrop A, Ngo A, Orlov NL, Ho CT, Somorjai IL (2005) Taxonomic chaos in Asian ranid frogs: an initial phylogenetic resolution. Herpetological Journal 15(4): 231–243.

Chou WH (1999) A new frog of the genus *Rana* (Anura: Ranidae) from China. Herpetologica 55(3): 389–400.

Chuaynkern Y, Ohler A, Inthara C, Duengkae P, Makchai S, Salangsingha N (2010) A revision of species in the subgenus *Nidirana* Dubois, 1992, with special attention to the identity of specimens allocated to *Rana adenopleura* Boulenger, 1909, and *Rana chapaensis* (Bourret, 1937) (Amphibia: Anura: Ranidae) from Thailand and Laos. Raffles Bulletin of Zoology 58: 291–310.

Dubois A (1992) Notes sur la classification des Ranidae (Amphibiens anoures). Bulletin Mensuel de la Société Linnéenne de Lyon 61: 305–352. https://doi.org/10.3406/linly.1992.11011

Fei L, Ye CY, Huang YZ (1990) Key to Chinese Amphibians. Publishing House for Scientific and Technological, Chongqing.

Fei L, Ye CY (2005) The Key and Illustration of Chinese. Sichuan Publishing House of Science and Technology, Chongqing.

Fei L, Ye CY, Jiang JP (2007) A new species of Ranidae *Hylarana* (*Nidirana*) *hainanensis* from China (Amphibia: Anura). Herpetologica Sinica 11: 1–4.

Fei L, Hu SQ, Ye CY, Huang YZ (2009) Fauna Sinica, Amphibia 2, Anura Ranidae. Science Press, Beijing.

Fei L, Ye CY, Jiang JP (2010) Phylogenetic systematics of Ranidae. Herpetological Sinica 12: 1–43.

Fei L, Ye CY, Jiang JP (2012) Colored atlas of Chinese amphibians and their distributions. Sichuan Publishing House of Science and Technology, Chengdu.

Frost DR, Grant T, Faivovich J, Bain RH, Haas A, Haddad CF, De Sa RO, Channing A, Wilkinson M, Donnellan SC, Raxworthy CJ, Campbell JA, Blotto BL, Moler P, Drewes RC, Nussbaum RA, Lynch JD, Green DM, Wheeler WC (2006) The amphibian tree of life. Bulletin of the American Museum of Natural History 297: 1–291. https://doi.org/10.1206/0003-0090(2006)297[0001:TATOL]2.0.CO;2

Frost DR (2019) Amphibian species of the world. Version 6.0. New York: American Museum of Natural History. http://research.amnh.org/vz/herpetology/amphibia/index.html [accessed 1 Nov 2019]

Gosner KL (1960) A simplified Table for Staging Anuran Embryos and Larvae with Notes on Identification. Herpetologica 16(3): 183–190.

Guindon S, Dufayard JF, Lefort V, Anisimova M, Hordijk W, Gascuel O (2010) New algorithms and methods to estimate maximum-likelihood phylogenies: assessing the performance of PhyML 3.0. Systematic Biology 59(3): 307–321. https://doi.org/10.1093/sysbio/syq010

Hall TA (1999) BIOEDIT: a user-friendly biological sequence alignment editor and analysis program for Windows 95/98/NT. Nucleic Acids Symposium Series 41(41): 95–98. https://doi.org/10.1021/bk-1999-0734.ch008

Liu CC (1950) Amphibians of western China. Fieldiana: Zoology Memoirs 2: 1–400. https://doi.org/10.5962/bhl.title.2977

Li SZ, Xu N, Lv JC, Jiang JP, Wei G, Wang B (2018a) A new species of the odorous frog genus *Odorrana* (Amphibia, Anura, Ranidae) from southwestern China. PeerJ 6(e5695): 1–28. https://doi.org/10.7717/peerj.5695

Li SZ, Xu N, Liu J, Jiang JP, Wei G, Wang B (2018b) A new species of the Asian Toad genus *Megophrys sensu lato* (Amphibia: Anura: Megophryidae) from Guizhou Province, China. Asian Herpetological Research 9: 224–239.

Li SZ, Wei G, Xu N, Cui JG, Fei L, Jiang JP, Liu J, Wang B (2019a) A new species of the Asian music frog genus *Nidirana* (Amphibia, Anura, Ranidae) from Southwestern China. PeerJ 7: e7157. https://doi.org/10.7717/peerj.5695

Li SZ, Zhang MH, Xu N, Lv JC, Jiang JP, Liu J, Wei G, Wang B (2019b) A new species of the genus *Microhyla* (Amphibia: Anura: Microhylidae) from Guizhou Province, China. Zootaxa 4624: 551–575. https://doi.org/10.11646/zootaxa.4624.4.7

Lyu ZT, Zeng ZC, Wang J, Lin CY, Liu ZY, Wang YY (2017) Resurrection of genus *Nidirana* (Anura: Ranidae) and synonymizing *N. caldwelli* with *N. adenopleura*, with description of a new species from China. Amphibia-Reptilia 38: 483–502. https://doi.org/10.1163/15685381-00003130

Lyu ZT, Mo YM, Wan H, Li YL, Pan H, Wang YY (2019a) Description of a new species of Music frogs (Anura, Ranidae, *Nidirana*) from Mt Dayao, southern China. ZooKeys 858: 109–126. https://doi.org/10.3897/zookeys.858.34363

Lyu ZT, Zeng ZC, Wan H, Yang JH, Li YL, Pang H, Wang YY (2019b) A new species of *Amolops* (Anura: Ranidae) from China, with taxonomic comments on *A. liangshanensis* and Chinese populations of *A. marmoratus*. Zootaxa 4609: 247–268. https://doi.org/10.11646/zootaxa.4609.2.3

Mahony S, Sengupta S, Kamei RG, Biju SD (2011) A new low altitude species of *Megophrys* Kuhl and van Hasselt (Amphibia: Megophryidae), from Assam, Northeast India. Zootaxa 3059: 36–46. https://doi.org/10.11646/zootaxa.3059.1.2

Matsui M, Utsunomiya T (1983) Mating call characteristics of the frogs of the subgenus *Babina* with reference to their relationship with *Rana adenopleura*. Journal of Herpetology 17: 32–37. https://doi.org/10.2307/1563777

Matsui, M (2007) Unmasking *Rana okinavana* Boettger, 1895 from the Ryukyus, Japan (Amphibia: Anura: Ranidae). Zoological Science 24: 199–204. https://doi.org/10.2108/zsj.24.199

McGuire JA, Witt CC, Altshuler DL, Remsen JV (2007) Phylogenetic systematics and biogeography of hummingbirds: Bayesian and maximum likelihood analyses of partitioned data and selection of an appropriate partitioning strategy. Systematic Biology 56(5): 837–856. https://doi.org/10.1080/10635150701656360

Pope CH (1931) Notes on amphibians from Fukien, Hainan and other parts of China. Bulletin of the American Museum of Natural History 61: 397–611.

Robert L, Brett C, Simon YWH, Stephane G (2012) PartitionFinder: Combined Selection of Partitioning Schemes and Substitution Models for Phylogenetic Analyses. Molecular Phylogenetics and Evolution 29(6): 1695–1701. https://doi.org/10.1093/molbev/mss020

Ronquist FR, Huelsenbeck JP (2003) MrBayes3: Bayesian phylogenetic inference under mixedmodels. Bioinformatics 19(12): 1572–1574. https://doi.org/10.1093/bioinformatics/btg180

Sambrook J, Fritsch EF, Maniatis T (1989) Molecular Cloning: A Laboratory Manual. Cold Spring Harbor Laboratory Press, New York.

Simon C, Frati F, Beckenbach A, Crespi B, Liu H, Flook P (1994) Evolution, weighting, and phylogenetic utility of mitochondrial gene sequences and a compilation of conserved polymerase chain reaction primers. Annals of the Entomological Society of America 87: 651–701. https://doi.org/10.1093/aesa/87.6.651

Tamura K, Stecher G, Peterson D, Fiipski A, Kumar S (2011) MEGA6: molecular evolutionary genetics analysis using evolutionary distance. Molecular Biology and Evolution 28: 2725–2729. https://doi.org/10.1093/molbev/msr121

Wang J, Li YL, Li Y, Chen HH, Zeng YJ, Shen JM, Wang YY (2019) Morphology, molecular genetics, and acoustics reveal two new species of the genus *Leptobrachella* from northwestern Guizhou Province, China (Anura, Megophryidae). ZooKeys 848: 119–154. https://doi.org/10.3897/zookeys.848.29181

Wijayathilaka N, Meegaskumbura M (2016) An acoustic analysis of the genus *Microhyla* (Anura: Microhylidae) of Sri Lanka. PloS ONE 11: e0159003. https://doi.org/10.1371/journal.pone.0159003

Wu L, Dong Q, Xu RH (1986) Amphibians of Guizhou province. Guizhou People Press, Guiyang.

Zhang Y, Li G, Xiao N, Li J, Pan T, Wang H, Zhang B, Zhou J (2017) A new species of the genus *Xenophrys* (Amphibia: Anura: Megophryicae) from Libo County, Guizhou, China. Asian Herpetological Research 8: 75–85.

Supplementary material 1

Table S1. Measurements of *Nidirana yeae* sp. nov. and *N. daunchina*

Authors: Gang Wei, Shi-Ze Li, Jing Liu, Yan-Lin Cheng, Ning Xu, Bin Wang

Data type: species data

Explanation note: Units in mm. See abbreviations for characters in the Materials and methods section.

Link: https://doi.org/10.3897/zookeys.904.39161.suppl1

ZooKeys 904: 89–101 (2020)
doi: 10.3897/zookeys.89.47721
http://zookeys.pensoft.net

SHORT COMMUNICATION

A peer-reviewed open-access journal
ZooKeys
Launched to accelerate biodiversity research

Fish rubbings, 'gyotaku', as a source of historical biodiversity data

Yusuke Miyazaki[1], Atsunobu Murase[2,3]

1 *Department of Child Studies and Welfare, Shiraume Gakuen College, 1-830 Ogawa-chou, Kodaira, Tokyo 187-8570, Japan* **2** *Nobeoka Marine Science Station, Field Science Center, University of Miyazaki, 376-6 Akamizu, Nobeoka, Miyazaki 889-0517, Japan* **3** *Department of Marine Biology and Environmental Sciences, Faculty of Agriculture, University of Miyazaki, 1-1 Gakuen-Kibanadai-Nishi, Miyazaki 889-2192, Japan*

Corresponding author: *Yusuke Miyazaki* (miyazaki@shiraume.ac.jp)

Academic editor: *Nina Bogutskaya* | Received 29 October 2019 | Accepted 10 December 2019 | Published 16 January 2020

http://zoobank.org/EE0A76AC-A3CD-444F-A2FC-D5D9A4F3A0B4

Citation: Miyazaki Y, Murase A (2020) Fish rubbings, 'gyotaku', as a source of historical biodiversity data. ZooKeys 904: 89–101. https://doi.org/10.3897/zookeys.904.47721

Abstract

Methods for obtaining historical biodiversity information are mostly limited to examining museum specimens or surveying past literature. Such materials are sometimes time limited due to degradation, discarding, or other loss. The Japanese cultural art of 'gyotaku', which means "fish impression" or "fish rubbing" in English, captures accurate images of fish specimens, and has been used by recreational fishermen and artists since the Edo Period (the oldest known 'gyotaku' was made in 1839). 'Gyotaku' images often include distributional information, i.e., locality and sampling date. To determine the extent and usefulness of these data, field and questionnaire surveys targeting leisure fishing and boating stores were conducted in the following regions where threatened or extinct fishing targets exist (four regions including the northernmost to the southernmost regions). As a result, 261 'gyotaku' rubbings were digitally copied with their owners' consents. From these, distributional data were extracted for 218 individuals, which roughly represented regional fish faunas and common fishing targets. The peak number of 'gyotaku' stocked at the surveyed shops was made in 2002, while ones made before 1985 were much fewer. The number of 'gyotaku' rubbings made in recent years shows a recovery trend after 2011–2012. The present study demonstrates the validity of examining 'gyotaku' for historical biodiversity information.

Keywords

biogeography, citizen science, data mining, fish rubbing, red list

Introduction

Access to historical biodiversity information is limited, being mainly obtained via museum specimens, past literature, movies, photographs/images and/or other historical materials such as classic monographs (e.g., Hayashi 2014; Rocha et al. 2014; Schilthuizen et al. 2015). These potential data sources, in particular historical materials, are sometimes lost by deliberate or accidental disposal or, for example, by fire or an estate liquidation where materials are scattered far from their origin. There are other similar examples where biodiversity information can be lost over time: seeds in seed banks can die within decades of their collection (e.g., Telewski and Zeevaart 2002; Nishihiro et al. 2016), and environmental DNA cannot be detected several hours or days after sampling (e.g., Thomsen et al. 2012; Bohmann et al. 2014). Thus, it is important for historical biodiversity information to be accessed and recorded as a matter of urgency. Copying or extracting information from privately owned materials is of highest priority.

Biodiversity observations have been made not only by researchers but also by citizens, even prior to the recent rise of citizen science projects (Miller-Rushing et al. 2012; Kobori et al. 2016). Although data mining from citizens' observation records is a legitimate method of citizen science (Fink and Hochachka 2012), limitations on data availability have not been well documented except for online data (e.g., Miyazaki et al. 2015).

In Japan, many recreational fishers have recorded their memorable catches as 'gyotaku' (魚拓), which means fish impression or fish rubbing in English (Fig. 1), since the last Edo Period (the current oldest known 'gyotaku' dates back to late February 1839) (Hiyama 1964a, b; Shimizu 1975; Nakajima 2005). 'Gyotaku' is made directly from fish specimen(s), and usually includes information such as sampling date and locality, the name(s) of the fisher(s), its witness(es), the fish species (frequently its local name), and fishing tackle used. In recent decades, color versions of 'gyotaku' have become well developed, and used for art and educational purposes (Hiyama 1964a, b; Shimizu 1972, 1975; Yamamoto 1998; Stokes 2001; Baggett and Shaw 2008). In contrast, the traditional method is printed by using black writing ink. Generally, color prints for art rarely include specimen data including sampling locality and date (e.g., Hiyama 1964a, b; Shimizu 1975; Yamamoto 1998).

We hypothesized that historical biodiversity data attached to 'gyotaku' prints are at risk of being lost, and that the number of 'gyotaku' prints is generally declining, being replaced with photographs from digital cameras and/or smart phones. The number of fishing-related shops that are personally managed (rather than the large chain stores) and therefore likely to stock original 'gyotaku' prints may be decreasing in recent years due to their owners retiring, an increase in chain store numbers, and/or a decrease in recreational fishers (Miyazaki in press).

In the present study, we attempt to validate these hypotheses by collecting data of 'gyotaku' from recreational fishing shops where threatened fish species are distributed according to both the national and regional Red Lists. The potential use of 'gyotaku' for historical biodiversity information (Miyazaki and Fukui 2018; Miyazaki in press) is discussed.

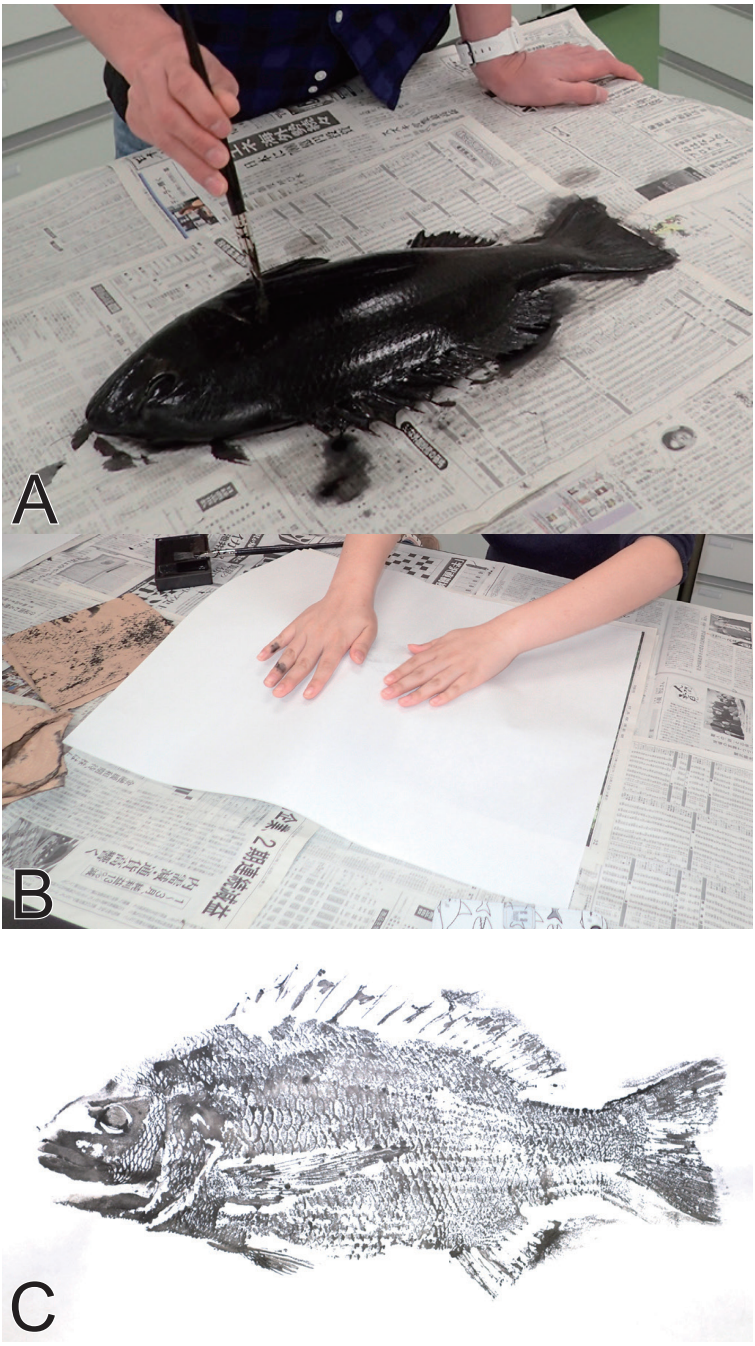

Figure 1. An explanation of fish rubbing ('gyotaku', in Japanese). **A** 1st step – the fish specimen is painted using ink **B** 2nd step – the specimen is covered with a sheet of paper **C** the finished image of the fish specimen on the paper. This is known as the direct method of 'gyotaku'; there is also an indirect method whereby a sheet of paper is placed on the fish specimen, then the sheet is painted by hand using ink. See also Hiyama (1964a, b) and Shimizu (1972, 1975).

Materials and methods

First, preliminary field surveys were conducted at three fishing shops in Miyazaki Prefecture, and one recreational boating shop in Chiba Prefecture where we found 'gyotaku' of threatened species were stocked via a reference (Onoue 2004) and by chance during in August 2016 (Miyazaki Pref.), and in March 2017 (Chiba Pref.). Second, we also conducted preliminary surveys of recreational fishing shops at the northernmost and southernmost regions of Japan in order to understand the 'gyotaku' information available at the latitudinal limits of Japan (from the subarctic to the tropics). Referencing the *Town Page* (yellow pages by the Nippon Telegraph and Telephone Corporation) of the Souya (northernmost) and the Yaeyama (southernmost) regions, we identified relevant shops (six for Souya in November 2017, and ten for Yaeyama in May 2017). In these surveys, we asked for information on the presence/absence of 'gyotaku' and the possibility of photographing them, and other relevant data. Where possible, we photographed 'gyotaku' stocks, and sought permission to use the images for research.

Our questionnaires mainly surveyed three regions of Japan where threatened fish species are distributed according to the national Red List (Ministry of the Environment, Japan 2017): the Sakhalin taimen, *Hucho perryi* (Brevoort, 1856) for Hokkaido (234 shops and stores); the small-scale sillago, *Sillago parvisquamis* Gill, 1861 for Tokyo Bay (274 shops and stores); and the Japanese lates, *Lates japonicus* Katayama & Taki, 1984 for Miyazaki Prefecture (80 shops and stores). The Souya region, which had been previously surveyed and no 'gyotaku' with distributional data were recorded from there, was excluded from this.

An explanation of the aim of our research and an answer sheet, which covered fifteen items for informed consent based on a research ethics review at the first author's institution, were attached to the questionnaire. In the surveys conducted during July–September 2018, we asked for information on the presence/absence of 'gyotaku', and the possibility of copying relevant data. When possible, we conducted field surveys to photograph 'gyotaku' in March 2019.

We pooled the collected 'gyotaku' data, and statistically analyzed the dataset by a state space model using R v. 3.6.0 (R Core Team 2019) and the *dlm* package (Petris 2010) that applies a local level model with filtering and smoothing.

Results and discussion

Of the stores and shops targeted by our second preliminary surveys, none (of six) in the northernmost (Souya) region and three (of ten) in the southernmost (Yaeyama) region stocked 'gyotaku' rubbings with distributional information.

Regarding the questionnaires, fourteen surveys were returned unopened due to stores being closed down, and 56 responses were received from others, indicating that the questionnaire response rate was 9.5%. Our field surveys were permitted by nine stores and shops that stocked 'gyotaku' rubbings, based on the questionnaire surveys,

while 82% of the responses recorded no stock of 'gyotaku'. This low response rate was possibly caused by us not paying to have the surveys completed and by a high perceived workload to complete the answers.

In total, 261 'gyotaku' rubbings, with 325 printed individual specimens (i.e., a part of 'gyotaku' has multiple individuals on a single sheet), were found among the targeted shops (Table 1; Suppl. material 1). All data recorded were integrated to the 'gyotaku' database (https://zukan.com/gyotaku/) using the same system as *WEB sakana-zukan* (see Miyazaki et al. 2014). Among the data obtained in the present study, we extracted distributional data for 221 individuals. Distributional data for an additional 14 individuals were obtained through interviewing the holders of the 'gyotaku' regarding date and/or locality information, resulting in a total of 235 individuals with distributional data (Table 1). Among the prints, 68 Japanese fish and three cephalopod species were represented, but 65 of these (14.9%) did not include a fish name (Tables 1, 2; Suppl. material 1). In general, a limited number of species are targeted by recreational fishers. Anglers and shop staff accurately identify the main fishing targets, and misidentifications are quickly corrected by other fishers in the local community. A pertinent example is the common octopus, *Octopus vulgaris* Cuvier, 1797, which is identified as a main fishing target by one fishing shop in Yokohama City, Tokyo Bay. 'Gyotaku' images of an octopus from this shop is likely to be *O. vulgaris* even if there is no name on the specific 'gyotaku'. However, this study did not validate such identifications based on external morphology and/or molecular analyses.

The observed species compositions reflected the biogeography of the regions (Table 2; Suppl. material 1). For example, prints of seven individuals of *Hucho perryi* were recorded from only Hokkaido. Similarly, one individual of *Sillago parvisquamis* was recorded from only around Tokyo Bay, while three individuals of *Lates japonicus* were recorded from only Miyazaki Prefecture (Fig. 2). These three species are listed as threatened in national and prefectural Red Lists. In particular, populations of *S. parvisquamis* are probably extinct in Tokyo Bay. The last reliable record from Tokyo Bay is from 1975–1976 (Shigeta and Usuki 2011). Additionally, the populations of *L. japonicus* at Miyazaki Prefecture were listed on the Specified Prefectural Endangered Species of Wild Fauna and Flora on 21 December 2012; this prohibits the capture, holding, receiving, and giving of, and other interactions with, the species without the prefectural governor's permission (Miyazaki Prefecture 2012; Murase et al. 2019). Given the rarity of these threatened species in some regions, 'gyotaku' are probably important vouchers for estimating historical population status, and factors of decline or extinction.

Species belonging to other families such as Salmonidae and Pleuronectidae, which originate in cold waters, were mostly recorded from Hokkaido rather than the other surveyed regions (Table 2; Suppl. material 1). On the other hand, several carangid fishes (*Caranx* spp.), the Okinawa seabream (*Acanthopagrus sivicolus* Akazaki, 1962), the spangled emperor [*Lethrinus nebulosus* (Forsskål, 1775)], the orange-spotted spinefoot [*Siganus guttatus* (Bloch, 1787)] and others originating from warm waters were recorded from only the Yaeyama region (Table 2). Another seabream species, *Acanthopagrus latus* (Houttuyn, 1782), which shares a similar distributional

Table 1. Details of 'gyotaku' rubbings surveyed from the shops in the present study.

Shops surveyed	Region	Shop style	The number of			
			'gyotaku'	individuals printed	distributional data[1]	species (potential)[2]
A	Hokkaido	Tackles and bait shops	23	23	20	4
B	Hokkaido	Tackles and bait shops	11	11	11	9
C	Hokkaido	Tackles and bait shops	44	53	37 + 8	8
D	Hokkaido	Tackles and bait shops	4	4	3 + 1	4
E	Hokkaido	Tackles and bait shops	1	1	0	1
Sub-total in the Hokkaido area			83	92	71 + 9	18
F	Tokyo Bay	Tackles and bait shops	27	31	31	17
G	Tokyo Bay	Tackles and bait shops	22	23	16 + 3	8
H	Tokyo Bay	Tackles and bait shops	9	9	7 + 1	8
I	Tokyo Bay	Ship shops	39	41	32	7
J	Tokyo Bay	Ship shops	9	15	4	6
Sub-total around the Tokyo Bay area			106	119	90 + 4	32
K	Miyazaki	Tackles and bait shops	12	12	10	4
L	Miyazaki	Tackles and bait shops	8	8	6 + 1	3
M	Miyazaki	Tackles and bait shops	6	6	5	5
Sub-total in the Miyazaki area			26	26	21 + 1	9
N	Yaeyama	Tackles and bait shops	10	11	10	4
O	Yaeyama	Tackles and bait shops	8	8	8	6
P	Yaeyama	Tackles and bait shops	28	69	21	18
Sub-total in the Yaeyama area			46	88	39	21
Total			261	325	221 + 14	68

[1]Where two numbers are provided (e.g., 37 + 8) the second number refers to data obtained from the owner rather than indicated on the 'gyotaku' rubbings.

[2]The number reflects expert opinions provided by the current authors, but more rigorous identifications have not yet been conducted.

pattern with *L. japonicus*, was recorded from only Miyazaki Prefecture. Furthermore, our list (Table 2) also included exotic non-native species, i.e., the rainbow trout, *Oncorhynchus mykiss* (Walbaum, 1792) and the brown trout, *Salmo trutta* Linnaeus, 1758, from the fishing tackle stores at Hokkaido, and *O. mykiss* and the largemouth bass, *Micropterus salmoides* (Lacepède, 1802), from a fishing tackle store in Tokyo Metropolis. Furthermore, some images printed of 'gyotaku' were found at stores well outside the pictured species' known range; generally, these resources had been provided by customers who had traveled to other regions for leisure fishing trips. Overall, the species composition displayed in the 'gyotaku' approximately reflected the fish faunas of each biogeographic region.

We also obtained a statistically estimated result using a state space model (Fig. 3). This estimation showed very few 'gyotaku' available from before 1985, with a peak in 2002. These results suggest that using this technique to gather historical data is valid for perhaps the last 30 years or so and not prior to that. Obtaining useful 'gyotaku' more than 30 years old is unlikely. A decline in number was observed during 2011 and 2012, which probably reflects an indirect effect of the catastrophic tsunamis and the nuclear accidents caused by the Great East Japan Earthquake on 11 March 2011 (see also Kataoka 2013). Our data does not support the hypothesis that the use of 'gyotaku' will be decreasing over recent years due to the rise of digital photography. We suggest that Japanese recreational fishers may be continuing to use the 'gyotaku' method in addition to digital photography to record their memorable catches.

Table 2. The composition of the species name given for various individual 'gyotaku'.

Species	Number of Individual(s)				Remarks
	Hokkaido	Tokyo Bay	Miyazaki	Yaeyama	
Loliginidae					
Sepia esculenta Hoyle, 1885	0	0	0	1	
Sepioteuthis lessoniana Férussac, 1831	0	1	0	3	
PISCES					
Cyprinidae					
Carassius cuvieri Temminck & Schlegel, 1846	0	2	0	0	
Cyprinus carpio Linnaeus, 1758	0	2	0	0	
Tribolodon hakonensis (Günther, 1880)	1	0	0	0	
Plecoglossidae					
Plecoglossus altivelis altivelis (Temminck & Schlegel, 1846)	1	0	0	0	
Salmonidae					
Hucho perryi (Brevoort, 1856)	7	0	0	0	
Oncorhynchus keta (Walbaum, 1792)	4	0	0	0	
Oncorhynchus masou masou (Brevoort, 1856)	18	1	1	0	
Oncorhynchus mykiss (Walbaum, 1792)	5	2	0	0	
Salmo trutta Linnaeus, 1758	14	0	0	0	
Salvelinus leucomaenis leucomaenis (Pallas, 1814)	11	0	0	0	
Sebastidae					
Sebastes cheni Barsukov, 1988	0	1	0	0	
Sebastes schlegelii Hilgendorf, 1880	1	0	0	0	
Sebastiscus marmoratus (Cuvier, 1829)	0	1	0	0	
Sebastes sp.	2	0	0	0	'Soi' or 'Mazoi' in Japanese
Platycephalidae					
Platycephalus sp. 2 *sensu* Nakabo (2002)	0	4	0	0	
Serranidae					
Epinephelus lanceolatus (Bloch, 1790)	0	0	0	1	
Niphon spinosus Cuvier, 1828	0	1	0	0	
Plectropomus leopardus (Lacepède, 1802)	0	0	0	2	
Centrarchidae					
Micropterus salmoides (Lacepède, 1802)	0	2	0	0	
Lateolabracidae					
Lateolabrax japonicus (Cuvier, 1828)	0	7	8	0	
Latidae					
Lates japonicus Katayama & Taki, 1984	0	0	3	0	
Carangidae					
Caranx ignobilis (Forsskål, 1775)	0	0	0	12	
Caranx melampygus Cuvier, 1833	0	0	0	1	
Caranx sp.	0	0	0	2	'Gāra' in Japanese
Pseudocaranx dentex (Bloch & Schneider, 1801)	0	1	0	0	
Seriola lalandi Valenciennes, 1833	0	2	0	0	
Seriola rivoliana Valenciennes, 1833	0	0	0	1	
Sparidae					
Acanthopagrus latus (Houttuyn, 1782)	0	0	2	0	
Acanthopagrus schlegelii (Bleeker, 1854)	1	12	6	0	
Acanthopagrus sivicolus Akazaki, 1962	0	0	0	2	
Pagrus major (Temminck & Schlegel, 1844)	0	3	0	0	
Lethrinidae					
Lethrinus nebulosus (Forsskål, 1775)	0	0	0	4	
Branchiostegidae					
Branchiostegus japonicus (Houttuyn, 1782)	0	1	0	0	
Oplegnathidae					
Oplegnathus fasciatus (Temminck & Schlegel, 1844)	0	2	0	0	

Species	Number of Individual(s)				Remarks
	Hokkaido	Tokyo Bay	Miyazaki	Yaeyama	
Oplegnathus punctatus (Temminck & Schlegel, 1844)	0	2	1	0	
Sciaenidae					
Argyrosomus japonicus (Temminck & Schlegel, 1844)	0	1	1	0	
Sillaginidae					
Sillago japonica Temminck & Schlegel, 1843	0	1	0	0	
Sillago parvisquamis Gill, 1861	0	1	0	0	
Rachycentridae					
Rachycentron canadum (Linnaeus, 1766)	0	0	0	1	
Coryphaenidae					
Coryphaena hippurus Linnaeus, 1758	0	0	0	3	
Kyphosidae					
Kyphosus cinerascens (Forsskål, 1775)	0	0	0	1	
Girellidae					
Girella leonina (Richardson, 1846)	0	0	2	0	
Girella punctata Gray, 1835	0	8	0	0	
Haemulidae					
Plectorhinchus cinctus (Temminck & Schlegel, 1843)	0	0	1	0	
Labridae					
Cheilinus undulatus Rüppell, 1835	0	1	0	0	
Semicossyphus reticulatus (Valenciennes, 1839)	1	0	0	0	
Scaridae					
Calotomus japonicus (Valenciennes, 1840)	0	1	0	0	
Hexagrammidae					
Hexagrammos otakii Jordan & Starks, 1895	0	4	0	0	
Siganidae					
Siganus guttatus (Bloch, 1787)	0	0	0	2	
Scombridae					
Katsuwonus pelamis (Linnaeus, 1758)	0	1	0	0	
Thunnus albacares (Bonnaterre, 1788)	0	0	0	1	
Sphyraenidae					
Sphyraena barracuda (Edwards, 1771)	0	0	0	2	
Trichiuridae					
Trichiurus sp.	0	0	0	1	'Tachiuo' in Japanese
Istiophoridae					
Istiophorus platypterus (Shaw & Nodder, 1792)	0	0	0	1	
Pleuronectidae					
Kareius bicoloratus (Basilewsky, 1855)	1	0	0	0	
Pleuronectes herzensteini (Jordan & Snyder, 1901)	1	0	0	0	
Pleuronectes schrenki (Schmidt, 1904)	2	0	0	0	
Verasper moseri Jordan & Gilbert, 1898	1	0	0	0	
Paralichthyidae					
Paralichthys olivaceus (Temminck & Schlegel, 1846)	2	3	0	0	
Monacanthidae					
Stephanolepis cirrhifer (Temminck & Schlegel, 1850)	0	4	0	0	
NO NAME GIVEN*	19	55	2	46	

*The individuals have been given no name in the 'gyotaku'.

Currently, the oldest 'gyotaku' material is a collection of the Tsuruoka City Library made in 1839 (Nakajima 2005). Others from the 19th Century were made in 1850s–1860s and are now collections of the Homma Museum of Art and the Chido Museum (Hiyama 1964a, b; Shimizu 1972, 1975). The oldest material found in the present study was made in 1936, indicating that it is difficult to find very old 'gyotaku'

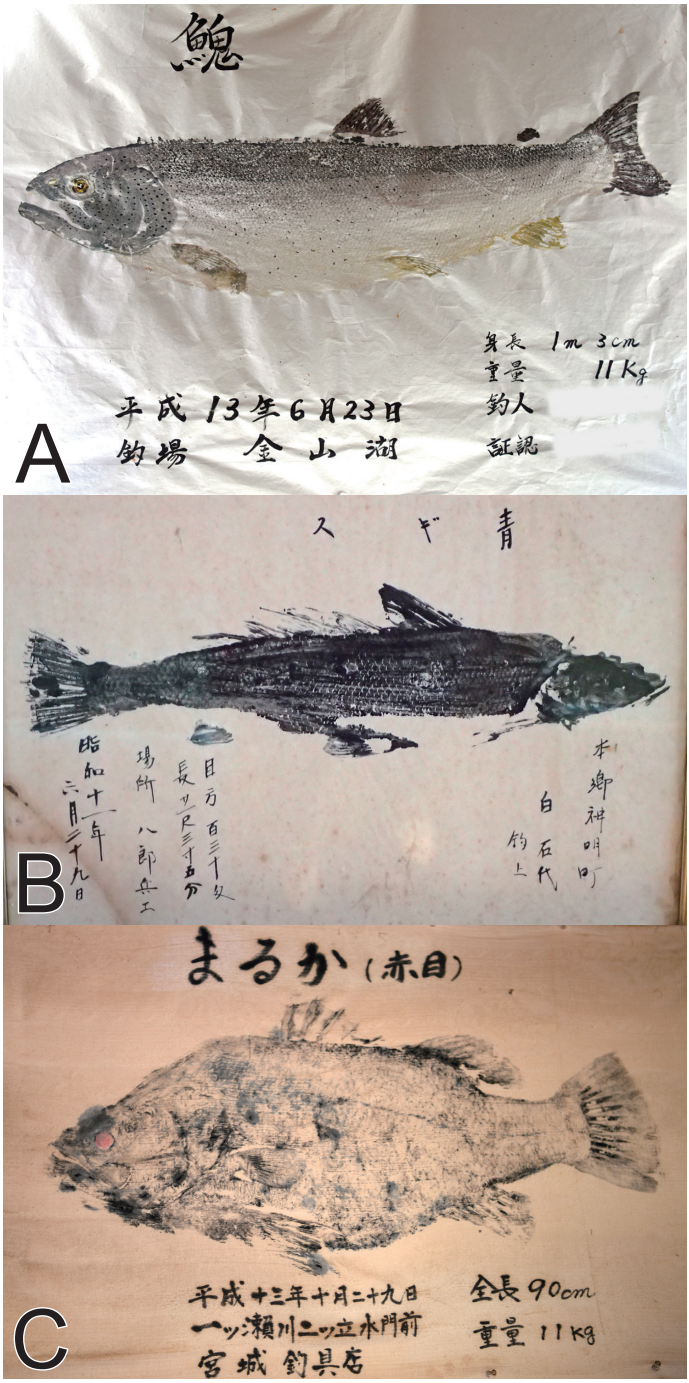

Figure 2. Three species targeted in leisure fishing and listed as threatened species in the Japanese national Red List. **A** *Hucho perryi* (Brevoort, 1856) from a shop in Hokkaido **B** *Sillago parvisquamis* Gill, 1861 from a shop facing Tokyo Bay **C** *Lates japonicus* Katayama & Taki, 1984 from a shop in Miyazaki Prefecture.

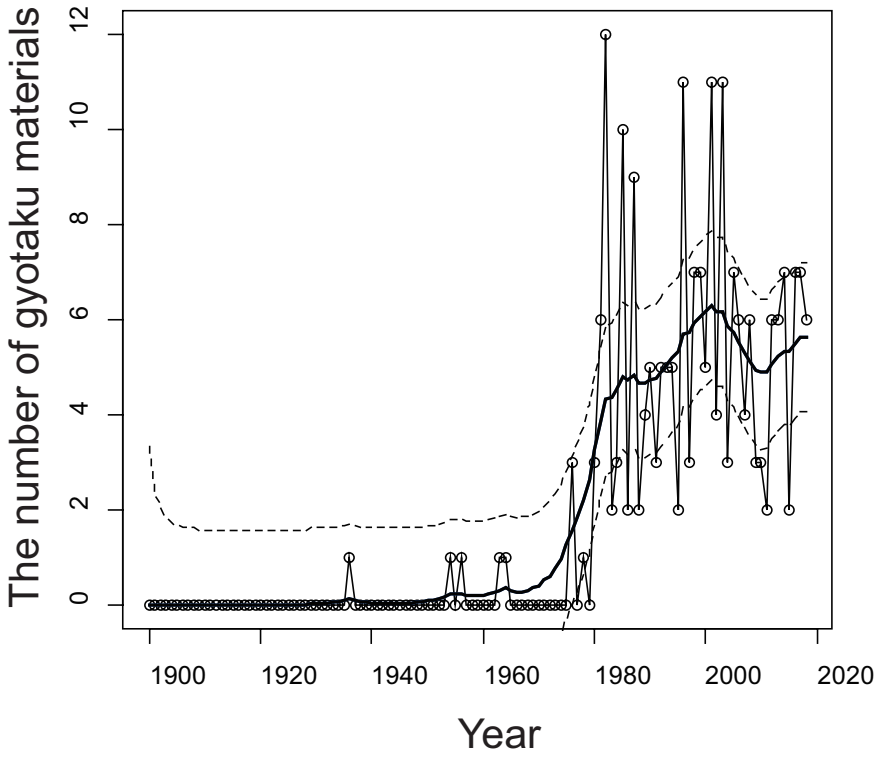

Figure 3. The number of 'gyotaku' rubbings stocked at the 16 fishing shops targeted by the present study based on the year of creation. The bold and dotted lines indicate the estimation and the 95% CI (upper and lower limits) based on the statistical analysis using a state space model.

rubbings at leisure fishing stores and shops. Storage of 'gyotaku' in the public areas of shops and stores is usually less than ideal, with exposure to tobacco smoke, sunlight, and moisture. This is the main reason for deteriorating 'gyotaku'. In fact, some shop owners reported disposing of older damaged materials. Further field surveys of, for example, museum and private collections are required to discover older 'gyotaku' and extract relevant data.

In conclusion, distributional data related to fish diversity records were able to be mined from 'gyotaku'. However, this method is time limited with respect to data rescue from the general public. The volume of data obtained in this study is too small to analyze statistically from the perspective of ecology, biogeography, or other similar disciplines. Additionally, validation of the identifications sourced from the 'gyotaku' is required via taxonomic evaluations. This could be done by examining the external morphology captured in the printed image and possibly by trying to obtain biological material from the print for molecular analysis (i.e., based on the residuum of dried DNA on the sheet). Overall, further research is required into the use of 'gyotaku' rubbings for acquiring historical biodiversity data.

Acknowledgements

We express our deepest gratitude to O. Adachi (Casting Shinagawa Seaside Branch), H. Egami (Egami Tsuriguten), Y. Hayasaka (Yokohama Sao-no-Shioyoshi), M. Kinjou (Yaeyama Tsurigu), K. Miyagi (Miyagi Tsuriguten), S. Shimabukuro (Umi-no-Sougou Super Shima), S. Yoshino (Funayado Yoshinoya), and other all staff of the fishing shops and stores for their kind cooperation, and to G. Yearsley (Ellipsis Editing, Australia) for English technical editing of the manuscript. We also thank Y. Nagashima (Uonofu), and Y. Ogawa (Tatsumi Publishing) for guiding to the leisure fishing shops and stores, and K. Naoe and J. Yamaide (zukan.com, Inc.) for setting up the database. This research was partly supported by the JSPS KAKENHI Grant-in-Aid for Young Scientists (B) (No. 16K16225).

References

Baggett PV, Shaw EL (2008) The art and science of gyotaku: there's somethin' fishy goin' on here… Science Activities: Classroom Projects and Curriculum Ideas 45(1): 3–8. https://doi.org/10.3200/SATS.45.1.3-8

Bohmann K, Evans A, Gilbert MTP, Carvalho GR, Creer S, Knapp M, Yu DW, de Bruyn M (2014) Environmental DNA for wildlife biology and biodiversity monitoring. Trends in Ecology & Evolution 29(6): 358–367. https://doi.org/10.1016/j.tree.2014.04.003

Fink D, Hochachka WM (2012) Using data mining to discover biological patterns in citizen science observations. In: Dickinson JL, Bonney R (Eds) Citizen Science: Public Participation in Environmental Research. Cornel University Press, Ithaca, 125–138. https://doi.org/10.7591/cornell/9780801449116.003.0009

Hayashi R (2014) Past biodiversity: historical Japanese illustrations document the distribution of whales and their epibiotic barnacles. Ecological Indicators 45: 687–691. https://doi.org/10.1016/j.ecolind.2014.05.031

Hiyama H (1964a) Gyotaku. University of Tokyo Press, Tokyo, 66 pp. [in Japanese]

Hiyama H (1964b) Gyotaku: The Art and Technique of the Japanese Fish Print. University of Washington Press, Seattle, 68 pp.

Kataoka T (2013) Dramatically changed consumptions: How is 2013 going on? The keywords are safety, family, and leisure. Nikkei Consumption Insight 1: 36–39. [in Japanese]

Kobori H, Dickinson JL, Washitani I, Sakurai R, Amano T, Komatsu N, Kitamura W, Takagawa S, Koyama K, Ogawara T, Miller-Rushing AJ (2016) Citizen science: a new approach to advance ecology, education, and conservation. Ecological Research 31(1): 1–19. https://doi.org/10.1007/s11284-015-1314-y

Miller-Rushing A, Primack R, Bonney R (2012) The history of public participation in ecological research. Frontiers in Ecology and the Environment 10(6): 285–290. https://doi.org/10.1890/110278

Ministry of the Environment, Japan (2017) About the publication of the red list for marine species, version Ministry of the Environment. https://www.env.go.jp/press/103813.html [Accessed on 24.10.2019; in Japanese]

Miyazaki Prefecture (2012) Summary of the Specified Prefectural Endangered Species of Wild Fauna and Flora (*Lates japonicus*). https://www.pref.miyazaki.lg.jp/shizen/kurashi/shizen/akame.html [Accessed on 24.10.2019; in Japanese]

Miyazaki Y (in press) Scientific applications of citizen science data obtained via information media. Japanese e-Journal of Species Biology 2. [in Japanese]

Miyazaki Y, Fukui A (2018) Ichthyology for beginners: an introduction to fish diversity. Ohmsha, Tokyo, 154 pp. [in Japanese]

Miyazaki Y, Murase A, Shiina M, Masui R, Senou H (2015) Integrating and utilizing citizen biodiversity data on the web for science: an example of a rare triggerfish hybrid image provided by a sport fisherman. Journal of Coastal Research 31(4): 1035–1039. https://doi.org/10.2112/JCOASTRES-D-14-00170.1

Miyazaki Y, Murase A, Shiina M, Naoe K, Nakashiro R, Honda J, Yamaide J, Senou H (2014) Biological monitoring by citizens using Web-based photographic databases of fishes. Biodiversity and Conservation 23(9): 2383–2391. https://doi.org/10.1007/s10531-014-0724-4

Murase A, Miki R, Wada M, Senou H (Eds) (2019) Coastal and Market Fishes around Kadogawa Bay, northern part of Miyazaki Prefecture, southern Japan. Nobeoka Marine Science Station, University of Miyazaki, Nobeoka, 208 pp. [in Japanese]

Nakajima M (2005) Fourth exhibition of citizens' collections: enchanted by the fish caught. A•Museum 45: 2. [in Japanese]

Nishihiro J, Akasaka M, Yamanouchi T, Takamura N (2016) Time-declining potential of aquatic plant recovery from the propagule banks of lake sediments. Japanese Journal of Conservation Ecology 21(2): 147–154. https://doi.org/10.18960/hozen.21.2_147 [in Japanese with English abstract]

Onoue K (2004) Recreation of *aogisu* fishing. In: Urayasu Local Museum (Ed.) The sea where *aogisu* inhabited. Urayasu Local Museum, Urayasu, 11–18. [in Japanese]

Petris G (2010) An R package for Dynamic Linear Models. Journal of Statistical Software 36(12): 16 pp. https://doi.org/10.18637/jss.v036.i12

R Core Team (2019) R: a language and environment for statistical computing: R Foundation for Statistical Computing. https://www.R-project.org [Accessed on 24.10.2019]

Rocha LA, Aleixo A, Allen G, Almeda F, Baldwin CC, Barclay MV, Bates JM, Bauer AM, Benzoni F, Berns CM, Berumen ML, Blackburn DC, Blum S, Bolaños F, Bowie RC, Britz R, Brown RM, Cadena CD, Carpenter K, Ceríaco LM, Chakrabarty P, Chaves G, Choat JH, Clements KD, Collette BB, Collins A, Coyne J, Cracraft J, Daniel T, de Carvalho MR, de Queiroz K, Di Dario F, Drewes R, Dumbacher JP, Engilis Jr A, Erdmann MV, Eschmeyer W, Feldman CR, Fisher BL, Fjeldså J, Fritsch PW, Fuchs J, Getahun A, Gill A, Gomon M, Gosliner T, Graves GR, Griswold CE, Guralnick R, Hartel K, Helgen KM, Ho H, Iskandar DT, Iwamoto T, Jaafar Z, James HF, Johnson D, Kavanaugh D, Knowlton N, Lacey E, Larson HK, Last P, Leis JM, Lessios H, Liebherr J, Lowman M, Mahler DL, Mamonekene V, Matsuura K, Mayer GC, Mays Jr H, McCosker J, McDiarmid RW, McGuire J, Miller MJ, Mooi R, Mooi RD, Moritz C, Myers P, Nachman MW, Nussbaum RA, Foighil DÓ, Parenti LR, Parham JF, Paul E, Paulay G, Pérez-Emán J, Pérez-Matus A, Poe S, Pogonoski J, Rabosky DL, Randall JE, Reimer JD, Robertson DR, Rödel MO,

Rodrigues MT, Roopnarine P, Rüber L, Ryan MJ, Sheldon F, Shinohara G, Short A, Simison WB, Smith-Vaniz WF, Springer VG, Stiassny M, Tello JG, Thompson CW, Trnski T, Tucker P, Valqui T, Vecchione M, Verheyen E, Wainwright PC, Wheeler TA, White WT, Will K, Williams JT, Williams G, Wilson EO, Winker K, Winterbottom R, Witt CC (2014) Specimen collection: An essential tool. Science 344(6186): 814–815. https://doi.org/10.1126/science.344.6186.814

Schilthuizen M, Vairappan CS, Slade EM, Mann DJ, Miller JA (2015) Specimens as primary data: museums and 'open science'. Trends in Ecology and Evolution 30(5): 237–238. https://doi.org/10.1016/j.tree.2015.03.002

Shigeta T, Usuki H (2011) Small-scale sillago (*Sillago parvisquamis*): a symbol of tidal flat ecosystems. Japanese Journal of Ichthyology 58(1): 104–107. https://doi.org/10.11369/jji.58.104 [in Japanese]

Shimizu Y (1972) Gyotaku: methods for making, and appreciation. Takahashi Shoten, Tokyo, 160 pp. [in Japanese]

Shimizu Y (1975) Gyotaku—methods for viewing and making—. Hoikusha, Tokyo, 152 pp. [in Japanese]

Stokes NC (2001) The fin art of science: Japanese fish printing brings interdisciplinary science and culture to the classroom. The Science Teacher 68(3): 22–24.

Telewski FW, Zeevaart AD (2002) The 120-yr period for Dr. Beal's seed viability experiment. American Journal of Botany 89(8): 1285–1288. https://doi.org/10.3732/ajb.89.8.1285

Thomsen PF, Kielgast J, Iversen LL, Wiuf C, Rasmussen M, Gilbert MTP, Orlando L, Willerslev E (2012) Monitoring endangered freshwater biodiversity using environmental DNA. Molecular Ecology 21(11): 2565–2573. https://doi.org/10.1111/j.1365-294X.2011.05418.x

Yamamoto R (1998) Fish feel satisfaction with becoming gyotaku. Kyoto Shoin, Kyoto, 256 pp. [in Japanese]

Supplementary material 1

The attributional information of the 'gyotaku' materials observed by the present study

Authors: Yusuke Miyazaki, Atsunobu Murase

Data type: species data

Explanation note: Although the identifications of each individual have not still validated via scientifc evaluations, the scientific names are provisional based on the fish names given by creaters with our suggestions.

Link: https://doi.org/10.3897/zookeys.904.47721.suppl1

ZooKeys 904: 103–115 (2020)
doi: 10.3897/zookeys.904.48592
http://zookeys.pensoft.net

RESEARCH ARTICLE

A peer-reviewed open-access journal
ZooKeys
Launched to accelerate biodiversity research

A new genus and species of Staphylininae rove beetle from the Peruvian Amazon (Coleoptera, Staphylinidae)

Josh Jenkins Shaw[1], Igor Orlov[2], Alexey Solodovnikov[2]

1 *Key Laboratory of Zoological Systematics and Evolution, Institute of Zoology, Chinese Academy of Sciences, Beijing, 100101, China* **2** *Natural History Museum of Denmark, Zoological Museum, Universitetsparken 15, Copenhagen 2100, Denmark*

Corresponding author: *Josh Jenkins Shaw* (joshjenkins@btinternet.com)

Academic editor: *J. Klimaszewski* | Received 19 November 2019 | Accepted 11 December 2019 | Published 16 January 2020

http://zoobank.org/4D09D3D4-3C8E-4CE7-B038-44957A423E55

Citation: Jenkins Shaw J, Orlov I, Solodovnikov A (2020) A new genus and species of Staphylininae rove beetle from the Peruvian Amazon (Coleoptera, Staphylinidae). ZooKeys 904: 103–115. https://doi.org/10.3897/zookeys.906.48592

Abstract

A new monotypic genus of Staphylininae Latreille, 1802 tribe *incertae sedis* is proposed based on *Amazonothops aslaki* **gen. et sp. nov.** from the Peruvian Amazon. Descriptions and illustrations of the new genus and species are provided. Its systematic placement and phylogenetic significance are discussed.

Keywords

Hyptiomini, Neotropical Region, Peru, South America, Tanygnathinini, taxonomy

Introduction

During a field trip to the Amazonian region of Peru, members of the Natural History Museum of Denmark Coleoptera section collected several conspecific specimens of a small rove beetle which strongly resembled the widespread, polyphyletic genus *Heterothops* Stephens, 1829 from the tribe Amblyopinini (Jenkins Shaw et al. 2019). One of these specimens was included in the molecular phylogenetic analysis of Jenkins Shaw et al. (2019). Whilst that study primarily sought to investigate the phylogeny of the tribe Amblyopinini, it also included a broad sample of representative Staphylininae and other subfamilies of

Staphylinidae as outgroups. The results of that phylogeny recovered the Amazonian taxon as sister to the tribes Tanygnathinini and Hyptiomini with strong support, far away from *Heterothops* and even Amblyopinini as a whole (Fig. 1). Further morphological study revealed numerous unusual characters that confirmed it indeed did not belong to the genus *Heterothops* or even the tribe Amblyopinini. At the same, it was morphologically distinct from either Tanygnathinini or Hyptiomini. Without hesitation we describe *Amazonothops aslaki* gen. et sp. nov. Even though we place this new genus as *incertae sedis* in the subfamily Staphylininae pending further inquiry, we provide comparisons and discussion to explain why *Amazonothops* is an important discovery for understanding evolution of the morphologically heterogeneous and still rather enigmatic clade it belongs to.

Material and methods

Specimens studied are deposited in the following institutions:

NHMD Natural History Museum of Denmark, University of Copenhagen, Denmark (Curator Alexey Solodovnikov)

SEMC Snow Entomological Museum Collection, University of Kansas, USA (Collection Manager Zack Falin)

One specimen was prepared for scanning electron microscopy (SEM) by initial immersion in soapy water, followed by 1 hour in 10% KOH, resting overnight in 70% alcohol, then successive immersion in 96% alcohol for 15 minutes, in 99.9% alcohol for 15 minutes and in acetone for 15 minutes. SEM photographs were taken using a JEOL JSM-6335F SEM at the NHMD. One specimen was slide mounted using the method described in Hanley and Ashe (2003): slide photographs were taken using a Canon EOS 6D DSLR (Canon Inc.) digital camera mounted on a Zeiss Axioskop 50 via a LM Digital SLR Universal Adapter. Images were captured from multiple focal planes with the help of Canon EOS utility 3.4.30.0 software (Canon Inc.), combined with Zerene Stacker (Zerene Systems LLC, Richland, USA) software and edited with Adobe Photoshop CS6 and Adobe Illustrator CS6 (Adobe Systems, San Jose, CA, U.S.A) afterwards. The map in Fig. 6 was generated using SimpleMappr (Shorthouse 2010). Holotype or paratype labels have been added to all type specimens, respectively. Measurements were taken using ImageJ and calibrated based on the scale bar in the images. Measurements were based on a single specimen as all individuals studied exhibited very little or no variation in size or proportions.

The following measurements were taken (all in mm):

HW Head width, at widest point

PL Pronotum length, at middle

PW Pronotum width, at widest point

FB Forebody length, from anterior edge of frons to posterior end of elytral suture

EW Elytral width, at widest point

TL Total length, from anterior edge of frons to apex of abdominal segment IX

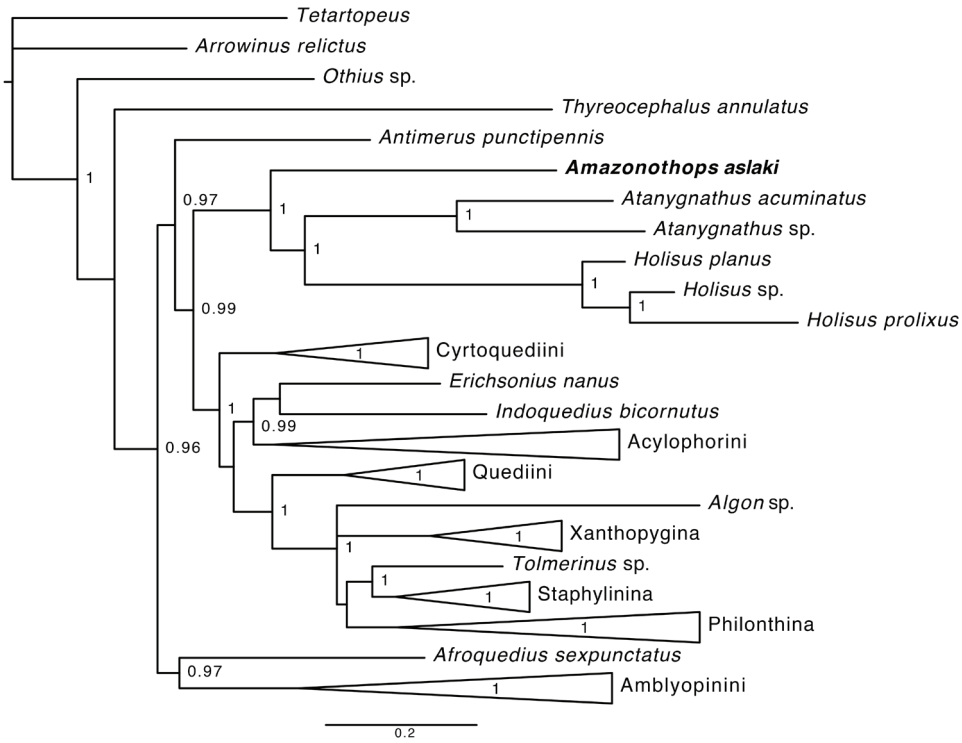

Figure 1. Majority-rule consensus tree from the Bayesian analysis of Jenkins Shaw et al. (2019), showing the position of *Amazonothops aslaki*. Major clades have been collapsed. Posterior probabilities of 0.96 and higher are provided.

Results

Family Staphylinidae Latreille, 1802
Subfamily Staphylininae Latreille, 1802
Tribe *incertae sedis*

Genus *Amazonothops* gen. nov.
http://zoobank.org/36850046-A545-4133-8ECB-8D6357BFAC53
Figs 2–5

Type species. *Amazonothops aslaki* gen. et sp. nov.

Diagnosis. From all other genera of Staphylininae the new genus can be recognized based on the following characters: antennomere 2 1.6× wider than antennomere 3; antennomere 11 3× longer than antennomere 10; penultimate segment of maxillary palpi large, covered in short setae, approximately 2× the length of apical segment; apical segment of maxillary and labial palpi aciculate. Head with 'infraorbital ridges' straight, extended to base of mandibles; postgenal ridge absent; frontoclypeal suture present; mesoventrite with transverse ridge present (incomplete medially); mesotrochanter and

Figure 2. Habitus of *Amazonothops aslaki* gen. et sp. nov. Scale bar: 1 mm.

first mesotarsomere of males with black combs; tarsal formula 5-5-5; empodial setae long and parallel-sided; apical edge of sternites III to VI with randomly distributed acute projections; tergites VII and VIII with broader, foliose setae in addition to the usual acuminate, simple setae; apparent fusion of tergite X to lateral tergal sclerites in males.

Differential diagnosis. The differential diagnosis is based on the recovered phylogenetic position of *Amazonothops* and its strong resemblance to the Amblyopinini genus *Heterothops*. *Amazonothops* differs from *Atanygnathus* Jacobson, 1909 (Tanygnathinini) in the number of tarsal segments (5-4-4 in *Atanygnathus*); short genae and normal shape of the apical labial and maxillary palpomere (extremely elongate and distinctly converging to apex in *Atanygnathus*); absence of dorsal setae on the apical tarsomere (present in *Atanygnathus*). It should be noted that some species of *Atanygnathus* have combs on the profemora (Adam Brunke, personal communication). *Amazonothops* differs from species of *Holisus* Erichson, 1839 (Hyptiomini) in the pronotal hypomeron strongly inflexed, not visible in lateral view and without longitudinal middle carina (visible in lateral view and with middle carina in *Holisus*), presence of empodial setae (absent in *Holisus*) and general appearance and habitus (*Holisus* is distinctly dorsoventrally flattened with coarse punctation). *Amazonothops* differs from the genus *Natalignathus* Solodovnikov, 2005, a hitherto unrecognized possible member of the same clade (see Discussion below) in the smaller body, short genae and much lesser elongate mouthparts, absence of dorsal setae on the apical tarsomere (present in *Natalignathus*) and presence of the combs. *Amazonothops* differs from *Heterothops* and other genera of Amblyopinini in presence of the frontoclypeal suture; antennomere 3 distinctly smaller than antennomeres 2 and 4; mesosternum with transverse ridge present (incomplete medially); apical edge of sternites III to VI with randomly distributed acute projections; tergites VII and VIII with broader, foliose setae in addition to the usual acuminate, simple setae; and apparent fusion of tergite X to lateral sclerites in males.

Description. Habitus as in Fig. 2. Body dark brown-black; antennae and legs yellowish. Measurements (all in mm): HW = 0.31; PL = 0.38; PW = 0.48; FB = 1.00; EW = 0.55; TL = 2.19.

Head. Dorsal surface with weak transverse microsculpture. Neck indistinct; nuchal ridge absent dorsally, present laterally, extended as 'infraorbital ridge' towards base of mandibles. Frontoclypeal suture present. Frontoclypeal puncture present (Brunke et al. 2019: fig. 1). Anterior and posterior frontal punctures present (Brunke et al. 2019: fig. 1). Single basal puncture present (Brunke et al. 2019: fig. 1). Eyes occupying two thirds of the side of head; temples indistinct. Antennae (Fig. 3A) inserted close to margin of eye. Antennomeres 1 to 3 setiferous; 4 to 11 setiferous and with tomentose pubescence. Antennomere 2 1.6× the width of antennomere 3; antennomere 3 half the size of antennomere 2; antennomere 11 elongate, three times as long as antennomere 10. Gula widest in anterior half; gular sutures separated along entire length; postgenal ridge absent. Maxillary palpi four-segmented (Fig. 3B; apical segment acicular, about a third of the length of the penultimate palpomere; penultimate segment widest at middle; covered with setae. Labial palpi three-segmented (Fig. 3C); apical segmented acicular. Labrum transverse, complete, without emargination. Mandibles simple, crossing in resting position, without large teeth.

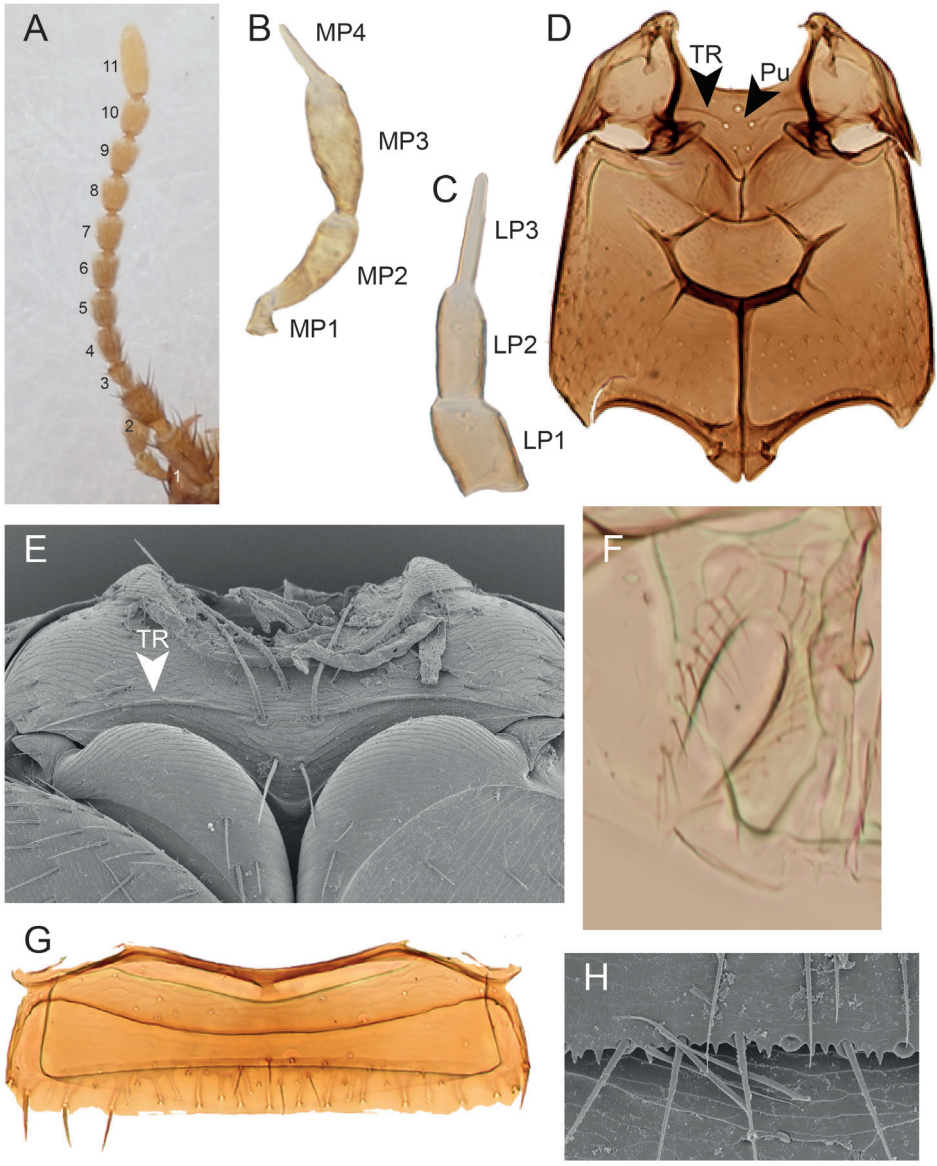

Figure 3. Morphology of *Amazonothops aslaki* gen. et sp. nov. **A** antennae **B** maxillary palpi **C** labial palpi **D** meso- and metathorax **E** mesothorax **F** protergal gland **G** tergite II **H** sternite III (apical edge). LP, Labial palpomere; MP, Maxillary palpomere; Pu, punctures; TR, Transverse ridge.

Prothorax. Pronotum widest in posterior third. Dorsal surface with weak transverse microsculpture and two pairs of punctures in dorsal series (one puncture near posterior margin and one distad of that); hypomeron strongly inflexed (not visible in lateral view). Basisternum with weak longitudinal ridge in posterior half, without punctures or setae. Post-coxal process absent.

Scutellum with anterior transverse ridge only, impunctate, glabrous. Elytra widest posteriorly. Hind wings fully developed, posterior edge with fringe of setae; veins CuA and MP4 fused; vein MP3 present. Mesoventrite (Fig. 3D) with five large punctures medially (Fig. 3D; Pu), with rounded ventral process and with transverse ridge, incomplete medially (Fig. 3E).

Abdomen. Protergal glands elongate, fringed by setae (Fig. 3F). Tergites with anterior transverse carina only. Tergite II as in Fig. 3G. Sternite III with evenly curved transverse carina, slightly projected medially. Tergite VII with white fringe along posterior edge. Apical edge of sternites III to VI with randomly distributed acute projections (Fig. 3H). Tergites VII and VIII with broader, foliose setae in addition to the usual acuminate, simple setae (Fig. 4A–C).

Legs. Tarsal formula 5-5-5. Both sexes with protarsomeres 1 to 4 transverse. All tarsal empodia with long, parallel-sided setae (Fig. 4D, E).

Male. Protarsomeres 1 to 4 with white adhesive setae ventrally. First mesotarsomere with black comb comprising 11–14 articles (Fig. 4F, H). Mesotrochanter with black comb comprising 7–11 articles (Fig. 4G, H). The number of articles within each comb varies between individuals.

Female. Protarsomeres 1 to 4 only with usual setae ventrally, white adhesive setae absent. No combs.

Distribution. Based on the specimens studied here, the new genus is restricted to the lowland areas of the Amazonian basin of Peru.

Bionomics. Based on the available label data, the genus occurs in forested areas (100–420 m elevation) and has so far only been collected by flight intercept traps.

Etymology. The genus name is a combination of 'Amazon' and the genus name *Heterothops*, which the new genus strongly resembles superficially.

Remarks. The new genus is certainly morphologically distinct among other members of the subfamily Staphylininae and family Staphylinidae. Noteworthy is the secondary sexual dimorphism exhibited by *Amazonothops*. In males, the mesotrochanter and first mesotarsomere have distinct black combs which are completely lacking in females (Fig. 4F, G, H). The function, if any, of the combs remains unknown but very similar combs are commonly found within Amblyopinini, e.g., recently illustrated for *Myotyphlus* Fauvel, 1883 (Solodovnikov and Jenkins Shaw 2017).

Amazonothops aslaki sp. nov.

http://zoobank.org/1B5BA8C2-CD02-428D-A21B-FFD807C74724
Figs 2–5

Material examined. ***Holotype.*** Male 'PERU: Amazonia, Loreto region, Requena Province, 3km E of Jenaro Herrera, 100–200 m, 4°53.914'S, 73°38.689'W, 24–28. VIII.2017, rainforest, FIT close to logs, A. Hansen, D. Zyla, M. Chani-Posse PER17-11i' (NHMD). ***Paratypes.*** 2 males (of them 1 DNA vouchered), 1 female, same locality but 4°53.210'S, 73°38.921'W, 7–10.IX.2017, rainforest, FIT near wetland/*Mauritia flexuosa* L.f. palms, leg. A. Hansen, J. Kypke, A. Solodovnikov (PER 17-22f) (NHMD).

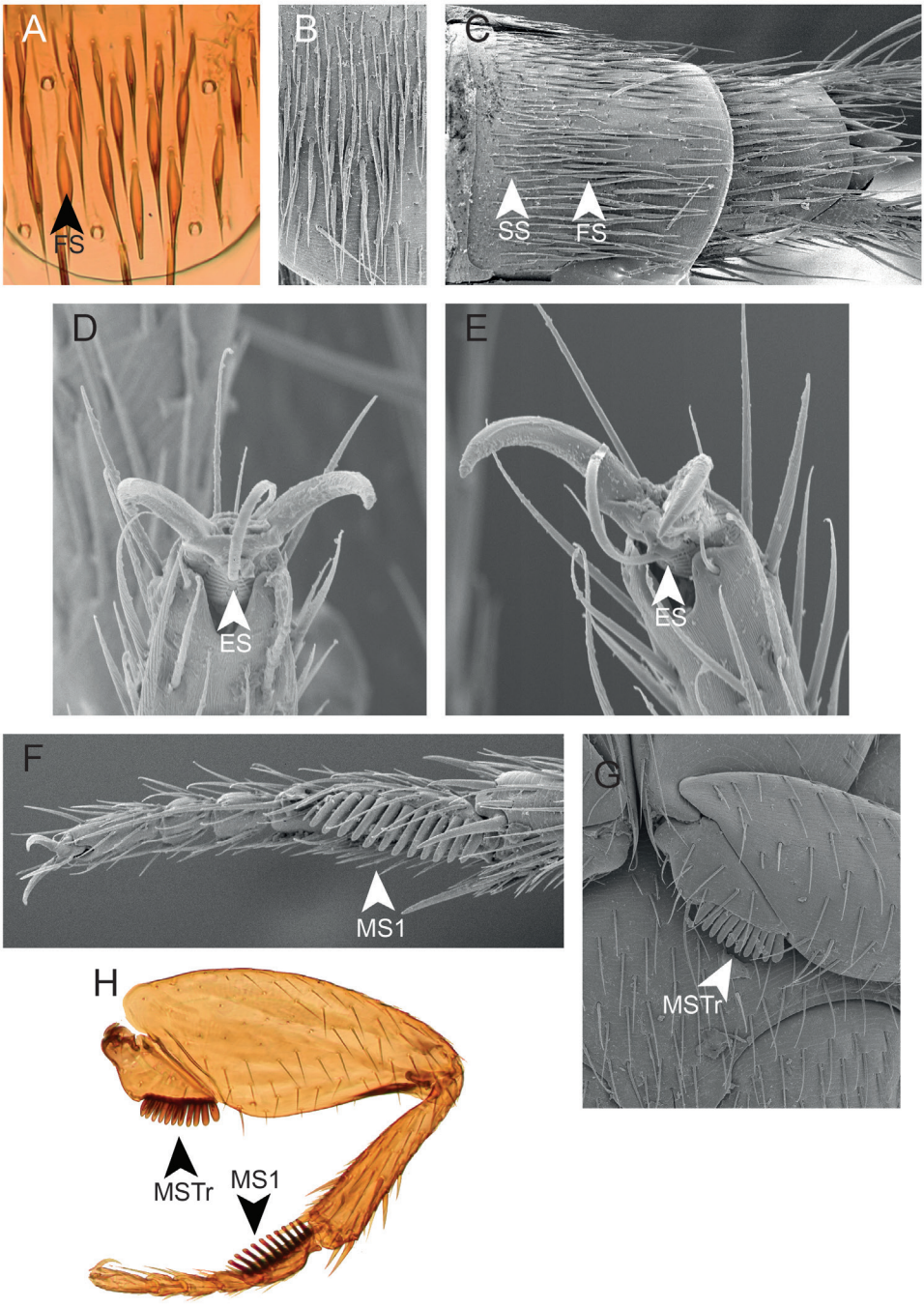

Figure 4. Morphology of *Amazonothops aslaki* gen. et sp. nov. **A** tergite VII **B** tergite VII **C** abdominal apex (tergites VII and VIII) **D** empodium of mesotarsi **E** empodium of metatarsi **F** mesotarsi (male) **G** mesotrochanter (male) **H** mesoleg (male). ES, Empodial setae; FS, Foliose setae; MS, Mesotarsomere; MSTr, Mesotrochanter; SS, Simple setae.

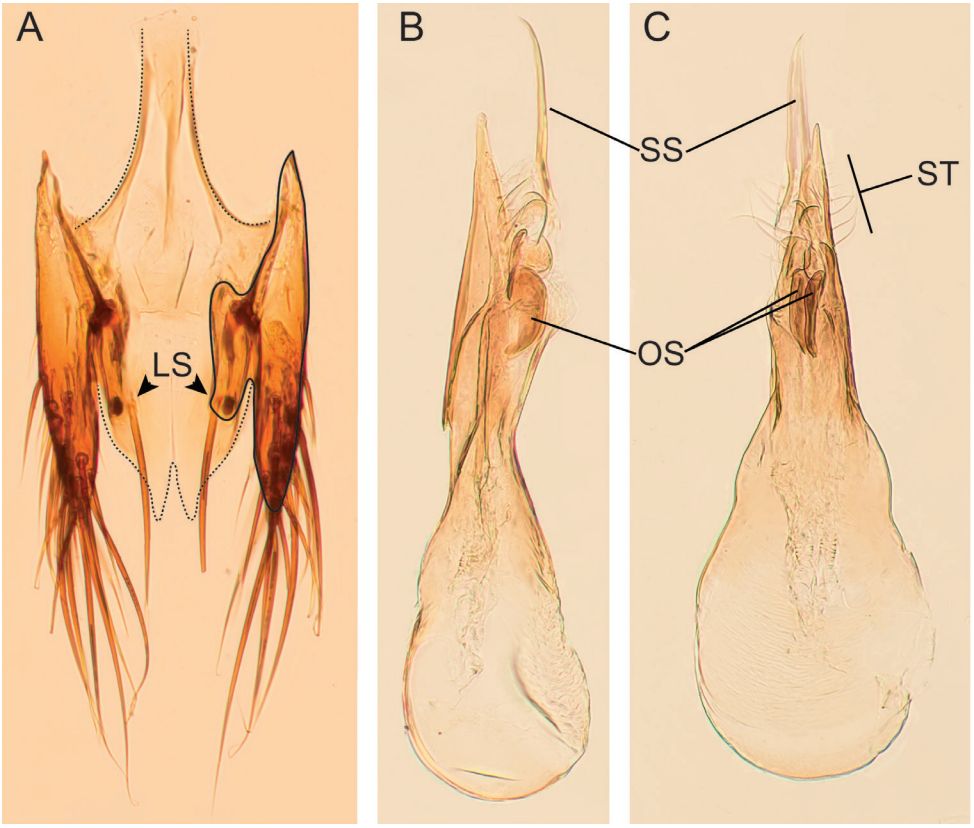

Figure 5. Morphology of *Amazonothops aslaki* gen. et sp. nov. **A** male terminalia (abdominal segments IX, X) **B** aedeagus in lateral view **C** aedeagus in antiparameral view (slightly lateral). LS, Long setae. OS, Oblong sclerite. SS, Slender sclerite. ST, setae.

Male (coated for SEM and mounted on two stubs), same data, but FIT near creek (PER17-22l) (NHMD). 1 male, disarticulated and slide mounted, 'PERU: Dept. Madre de Dios: Pantiacolla Lodge, Alto Madre de Dios R. 12°39.3'S, 71°13.9'W 420m 14-19-XI-2007 D. Brzoska ex. flight intercept trap PER1B07 004 / SEMC0874476 KUNHM-ENT' (SEMC).

Description. In addition to characters in the genus description, the species is characterized by the following primary and secondary male sexual characters. Sternite VIII without apical incision. Tergite X apparently fused to internal face of lateral sclerites (Fig. 5A, solid line), with two large setae situated at apical third of length (Fig. 5A; LS). Sternite IX emarginate apically, with symmetrical basal stem (Fig. 5A, dashed line). Lateral tergal sclerites and tergite X of approximately equal length. Aedeagus (Fig. 5B, C); paramere longer than and closely attached to, median lobe (Fig. 5B); lateral apical area of paramere with setae of varying length (Fig. 5C; ST); internal sac consisting of a pair of heavily sclerotized oblong-shaped sclerites (Fig. 5C; OS) and pair of weakly sclerotised longer, more slender sclerites extruding from apical area of median lobe under pressure (Fig. 5C, SS).

Figure 6. Known distribution of *Amazonothops aslaki* gen. et sp. nov. in Peru.

Distribution. Based on the specimens studied here, the new genus is restricted to the lowland areas of the Amazonian basin of Peru (Fig. 6). As a fully winged species known only from six specimens from two areas approximately 1000 kilometres apart from each other, it seems to be a widespread species, perhaps much more than it appears now.

Bionomics. Same as above.

Etymology. The species is named in honour of Aslak Kappel Hansen (NHMD) who was one of the collectors of this new genus and who brought our attention to its unusual nature compared to *Heterothops*.

Comments. It is notable that a species of *Heterothops* (Amblyopinini) was obtained during the same collecting event as one of the *Amazonothops* specimens. This shows that these two similar looking, yet phylogenetically distant (Fig. 1) taxa co-occur, probably in similar or the same microhabitats in the Amazon basin.

Discussion

The molecular phylogeny of Jenkins Shaw et al. (2019) placed *Amazonothops* sister to a peculiar clade formed by the tribes Tanygnathinini and Hyptiomini with maximal support (Fig. 1). As Jenkins Shaw et al. (2019) noted, the recovery of *Amazonothops* in a clade with Tanygnathinini and Hyptiomini also makes the somewhat similar South African endemic genus *Natalignathus* relevant when considering the sister relationships of *Amazonothops*. *Natalignathus* was originally placed in Tanygnathinini (Solodovnikov 2005) and later moved to Amblyopinini (then Amblyopinina) by Chatzimanolis et al. (2010). Although the phylogenetic study by Chatzimanolis et al. (2010) was molecular, *Natalignathus* was reclassified based on a morphological character assessment and not included in the analysis as DNA-grade material was not available. Besides, previous morphological studies considered it to be sister to *Atanygnathus*, itself considered a highly autapomorphic lineage nested within Amblyopinini, a pattern repeatedly revealed in morphology-based phylogenetic analyses since Solodovnikov (2006). Tanygnathinini were not sunk in synonymy to Amblyopinini by these authors because of their very clear morphological diagnosis and a lack of knowledge of the internal phylogeny of Amblyopinini. Chatzimanolis et al. (2010) were the first to link *Holisus* and *Atanygnathus* in an isolated clade within Staphylininae, though they are so different morphologically that this was suspected to be an artefact. However, this sister group relationship between Tanygnathinini and Hyptiomini, persisted through several later molecular (Brunke et al. 2016; Żyła and Solodovnikov 2019; Jenkins Shaw et al. 2019) and total evidence (Chani-Posse et al. 2018) phylogenetic studies with better and more diverse taxon and gene sampling. Unfortunately, *Natalignathus* remains unsampled for molecular phylogeny due to a lack of DNA-grade material. In view of the continued corroboration of the Tanygnathinini + Hyptiomini clade, and now with *Amazonothops* discovered as a sister group to that, it seems plausible that *Natalignathus* should belong to the Tanygnathinini + Hyptiomini clade as well, probably as a sister to *Atanygnathus* as was initially noted at the time of its description (Solodovnikov 2005). Even though peculiar, the morphology of *Amazonothops* seems less derived than either *Holisus* or *Atanygnathus*, showing some resemblance, and sharing some characters with, *Natalignathus*. Like *Natalignathus*, *Amazonothops* resembles and shares some characters with the early-diverging and plesiomorphy-rich 'Quediine-looking' lineages of Staphylininae, much more so than the derived *Atanygnathus* or *Holisus*. *Amazonothops* is clearly an important taxon for understanding of the origin the entire Tanygnathinini + Hyptiomini clade. Once the molecular data from *Natalignathus* is obtained, both it and *Amazonothops* should be included in a total evidence phylogenetic analysis to explore the early evolution of Staphylininae. Discovery of *Amazonothops* further highlights the rich and unknown biodiversity of the Peruvian Amazon and suggests a high probability that more species of this genus, or even new genera of this lineage maybe discovered there in the future.

With the recently updated classification of the subfamily Staphylininae (Żyła and Solodovnikov 2019) and the recovered phylogenetic position of *Amazonothops* (Jenkins Shaw et al. 2019), it is plausible that *Amazonothops* should be placed in its own tribe. Here we refrain from doing so pending further molecular and morphological exploration of the (*Amazonothops* (*Atanygnathus* + *Holisus*)) clade with broad outgroup sampling that would also include sampling many more ingroup species for the latter two sizeable genera, and revisiting *Natalignathus*.

Acknowledgements

We are much obliged to all collectors of the new genus and to Zack Falin for the loan of the SEMC specimen. Particular thanks are due to Aslak Kappel Hansen for noticing these specimens and bringing them to the attention of JJS. Thanks to Anders Illum (NHMD) for assistance using the SEM. This project has received funding from the European Union's Horizon 2020 research and innovation program under the Marie Skłodowska-Curie Grant Agreement No. 642241 and the Chinese Academy of Sciences President's International Fellowship Initiative for Postdoctoral Fellows. Grant No. 2019PB0090. Thanks to Adam Brunke and Maria Salnitska for providing constructive reviews that led to the improvement of this manuscript. The authors have declared that no competing interests exist.

References

Brunke AJ, Chatzimanolis S, Schillhammer H, Solodovnikov A (2016) Early evolution of the hyperdiverse rove beetle tribe Staphylinini (Coleoptera: Staphylinidae: Staphylininae) and a revision of its higher classification. Cladistics 32: 427–451. https://doi.org/10.1111/cla.12139

Brunke AJ, Żyła D, Yamamoto S, Solodovnikov A (2019) Baltic amber Staphylinini (Coleoptera: Staphylinidae: Staphylininae): a rove beetle fauna on the eve of our modern climate. Zoological Journal of the Linnean Society 187: 166–197. https://doi.org/10.1093/zoolinnean/zlz021

Chani-Posse MR, Brunke AJ, Chatzimanolis S, Schillhammer H, Solodovnikov A (2018) Phylogeny of the hyper-diverse rove beetle subtribe Philonthina with implications for classification of the tribe Staphylinini (Coleoptera: Staphylinidae). Cladistics 34: 1–40. https://doi.org/10.1111/cla.12188

Chatzimanolis S, Cohen IM, Schomann A, Solodovnikov A (2010) Molecular phylogeny of the mega-diverse rove beetle tribe Staphylinini (Insecta, Coleoptera, Staphylinidae). Zoologica Scripta 39: 436–449. https://doi.org/10.1111/j.1463-6409.2010.00438.x

Hanley RS, Ashe JS (2003) Techniques for dissecting adult aleocharine beetles (Coleoptera: Staphylinidae). Bulletin of Entomological Research 93: 11–18. https://doi.org/10.1079/BER2002210

Herman LH (2001) Catalog of the Staphylinidae (Insecta: Coleoptera) – 1758 to the end of the second Millennium. VI. Staphylinine Group (Part 3). Staphylininae: Staphylinini (Quediina, Staphylinina, Tanygnathinina, Xanthopygina), Xantholinini. Staphylinidae: Incertae Sedis fossils, Protactinae. Bulletin of the American Museum of Natural History 265: 3021–3840. https://doi.org/10.1206/0003-0090.265.1.6

Jenkins Shaw J, Żyła D, Solodovnikov A (2019) Molecular phylogeny illuminates Amblyopinini (Coleoptera: Staphylinidae). Systematic Entomology. [Early view] https://doi.org/10.1111/syen.12405

Newton A (2019) StaphBase: Staphyliniformia world catalog database (version Nov. 2018). In: Roskov Y, Ower G, Orrell T, Nicolson D, Bailly N, Kirk PM, Bourgoin T, DeWalt RE, Decock W, Nieukerken E van, Zarucchi J, Penev L (Eds) Species 2000 & ITIS Catalogue of Life, 26th February 2019. Species 2000: Naturalis, Leiden, the Netherlands. www.catalogueoflife.org/col

Shorthouse DP (2010) SimpleMappr, an online tool to produce publication-quality point maps. https://www.simplemappr.net [Accessed May 24, 2019]

Solodovnikov A (2005) *Natalignathus*, gen. nov. and larvae of *Atanygnathus*: a missing phylogenetic link between subtribes Quediina and Tanygnathinina (Coleoptera: Staphylinidae: Staphylininae: Staphylinini). Invertebrate Systematics 19: 75–98. https://doi.org/10.1071/IS04031

Solodovnikov A (2006) Revision and phylogenetic assessment of *Afroquedius* gen. nov. from South Africa: toward new concepts of the genus *Quedius*, subtribe Quediina and reclassification of the tribe Staphylinini (Coleoptera: Staphylinidae: Staphylininae). Annals of the Entomological Society of America 99: 1064–1084. https://doi.org/10.1603/0013-8746(2006)99[1064:RAPAOA]2.0.CO;2

Solodovnikov A, Jenkins Shaw J (2017) The remarkable Australian rove beetle genus *Myotyphlus*: its cryptic diversity and significance for exploring mutualism among insects and mammals (Coleoptera: Staphylinidae). Austral Entomology 56: 311–321. https://doi.org/10.1111/aen.12233

Żyła D, Solodovnikov A (2019) Multilocus phylogeny defines a new classification of Staphylininae (Coleoptera, Staphylindiae), a rove beetle group with high lineage diversity. Systematic Entomology. [Early view] https://doi.org/10.1111/syen.12382

ZooKeys 904: 117–130 (2020)
doi: 10.3897/zookeys.904.46790
http://zookeys.pensoft.net

SHORT COMMUNICATION

A peer-reviewed open-access journal
ZooKeys
Launched to accelerate biodiversity research

Molecular evidences confirm the taxonomic separation of two sympatric congeneric species (Mollusca, Gastropoda, Neritidae, *Neritina*)

Cristiane Xerez Barroso[1,2], João Eduardo Pereira de Freitas[1,3], Helena Matthews-Cascon[1,2], Luis Ernesto Arruda Bezerra[1,4], Tito Monteiro da Cruz Lotufo[5]

1 *Graduate Program on Marine Tropical Sciences, Instituto de Ciências do Mar -LABOMAR, Universidade Federal do Ceará, Av. da Abolição, 3207, Meireles, CEP: 60165-081, Fortaleza, CE, Brazil* **2** *Laboratório de Invertebrados Marinhos do Ceará - LIMCE, Departamento de Biologia, Centro de Ciências, Universidade Federal do Ceará, Rua Campus do Pici, s/n, Bloco 909, Pici, CEP: 60440-900, Fortaleza, CE, Brazil* **3** *Marine Vertebrate Evolution and Conservation Lab - EvolVe, Departamento de Biologia, Centro de Ciências, Universidade Federal do Ceará, Rua Campus do Pici, s/n, Bloco 909, Pici, CEP: 60440-900, Fortaleza, CE, Brazil* **4** *Laboratório de Zoobentos, Instituto de Ciências do Mar - LABOMAR, Universidade Federal do Ceará, Av. da Abolição, 3207, Meireles, CEP: 60165-081, Fortaleza, CE, Brazil* **5** *Laboratório de Biologia Recifal - BIOREC, Instituto Oceanográfico, Universidade de São Paulo, Praça do Oceanográfico, 191, CEP: 05508-120, São Paulo, SP, Brazil*

Corresponding author: *Cristiane Xerez Barroso* (cristianexb@gmail.com)

Academic editor: *T. Backeljau* | Received 23 September 2019 | Accepted 5 December 2019 | Published 16 January 2020

http://zoobank.org/C9DAB612-6235-4088-ABAE-4410DC01C93B

Citation: Barroso CX, Freitas JEP, Matthews-Cascon H, Bezerra LEA, Lotufo TMC (2020) Molecular evidences confirm the taxonomic separation of two sympatric congeneric species (Mollusca, Gastropoda, Neritidae, *Neritina*). ZooKeys 904: 117–130. https://doi.org/10.3897/zookeys.904.46790

Abstract

A reliable taxonomy, together with more accurate knowledge of the geographical distribution of species, is a fundamental element for the study of biodiversity. Multiple studies on the gastropod family Neritidae record three species of the genus *Neritina* in the Brazilian Province: *Neritina zebra* (Bruguière, 1792), *Neritina virginea* (Linnaeus, 1758), and *Neritina meleagris* Lamarck, 1822. While *N. zebra* has a well-established taxonomic status and geographical distribution, the same cannot be said regarding its congeners. A widely cited reference for the group in Brazil considers *N. meleagris* a junior synonym of *N. virginea*. Using a molecular approach (phylogenetic, species delimitation, and statistical parsimony network analyses), based on two mitochondrial markers (COI and 16S), this study investigated if *N. virginea* and *N. meleagris* are distinct species. The molecular results confirmed the existence of two strongly

supported distinct taxonomic entities in the Brazilian Province, which is consistent with the morphological descriptions previously proposed for *N. virginea* and *N. meleagris*. These species occur in sympatry in the intertidal sandstone formations of Northeastern Brazil. Despite the great variation in the colour patterns of the shells, the present study reinforced previous observations that allowed the differentiation of these two species based on these patterns. It also emphasized the importance of the separation of these two clades in future studies, especially those conducted in the Brazilian Province, since these species may cohabit.

Keywords
Brazilian Province, Caribbean Province, geographic distribution, neritids, species delimitation

Introduction

Molluscs from the gastropod family Neritidae are the most diverse members of Neritimorpha (Kano et al. 2002), with some groups within this family having variable shell colouration patterns (e.g., Russell 1941; Tan and Clements 2008; Eichhorst 2016). Due to the great variety of colour patterns, the delimitation of different species could be hampered, especially if they are closely related and live in sympatry (e.g., Huang 1997; Blanco et al. 2014). This may explain the disparate estimates in the literature of the number of species of *Neritina* reported for the Brazilian Province.

Several studies report three species of the genus *Neritina* on the Brazilian coast: *Neritina zebra* (Bruguière, 1792), *Neritina virginea* (Linnaeus, 1758), and *Neritina meleagris* Lamarck, 1822 (e.g., Baker 1923; Russell 1941; Rios 1975; Matthews-Cascon et al. 1990; Díaz and Puyana 1994; Quintero-Galvis and Castro 2013; Eichhorst 2016). While *N. zebra* has a well-established taxonomic status and geographical distribution (Matthews-Cascon et al. 1990; Rios 2009; Barroso et al. 2012; Eichhorst 2016), there is uncertainty regarding its congeners. The shell catalogues of Rios (1985, 1994, 2009), a widely cited reference in studies conducted in Brazil, state that only two species occur in the Brazilian Province: *N. virginea* and *N. zebra*. In these compendia, *N. meleagris* is considered a junior synonym of *N. virginea* without any justification. Quintero-Galvis and Castro (2013), using a molecular phylogenetic approach to analyse specimens from the Colombian coast (Caribbean Province), concluded that *N. meleagris* and *N. virginea* are phylogenetically close, but different species. Since these species have a wide geographic distribution, encompassing the Caribbean and Brazilian Provinces (Barroso et al. 2016; Eichhorst 2016), that are separated by a recognized biogeographic barrier (the Amazon-Orinoco outflow) (Floeter et al. 2008; Barroso et al. 2016), the inclusion of specimens from both biogeographical provinces in phylogenetic analyses is desirable.

Since a reliable taxonomy, together with a more accurate knowledge about the geographical distribution of species, is fundamental to the study of biodiversity (Wheeler et al. 2004), the present study aims to investigate if *N. virginea* and *N. meleagris* are two distinct species, using molecular data (phylogenetic, species delimitation, and statistical parsimony network analyses).

Methods

We collected specimens from Barra Grande beach (Piauí State) (2°54.125'S, 41°24.573'W) and Camocim beach (Ceará State) (02°51.778'S, 41°51.57'W), both located in Northeastern Brazil, and preserved them in 95% ethanol. We identified the species using the literature (Russell 1941; Matthews-Cascon et al. 1990; Eichhorst 2016), primarily based on the shape and colour patterns of the shells. Specimens were collected under SISBIO permit no. 57473-3 and deposited in the malacological collection "Prof. Henry Ramos Matthews" – series B (CMPHRM-B) of Universidade Federal do Ceará (UFC). A total of 17 specimens, eight newly sequenced and nine already published by Quintero-Galvis and Castro (2013) and available on GenBank, were used for phylogenetic reconstruction (Table 1). All sequences used were attributed to nominal species considered valid in the literature (see Aktipis and Giribet 2010; Cook et al. 2010; Page et al. 2013; Quintero-Galvis and Castro 2013).

We extracted whole genomic DNA from the foot muscle of specimens, using the Qiagen DNeasy Blood & Tissue Kit (Qiagen, Valencia, CA, USA). The quality and integrity of the DNA obtained were evaluated in a micro-volume spectrophotometer. Amplification of double-stranded fragments from the cytochrome c oxidase I (COI) and 16S mitochondrial genes was achieved by polymerase chain reaction (PCR) using newly developed neritid-specific custom primers for the 16S gene [(16SNer_F 5'ACTACTCCGCCTGTTTATCAAA3') and (16SNer_R 5'GGGCTTAAACCTAATGCACTT3')] and modified versions of Folmer et al. (1994) primers for the COI gene [(LCO1490_mod 5'ATTCTACGAATCAYAAAGAYATTGG3') and (HCO2198_mod 5'TAWACTTCAGGATGACCRAAAAATCA3')]. The PCR was carried out using GoTaq Green Master Mix (Promega Corporation), 1.25 µL of each primer (10 µM stock), and 100 ng of DNA template in a 25 µL reaction volume. The PCR cycles for COI and 16S amplification consisted of an initial denaturation step at 95 °C for 2 min, followed by 35 cycles of denaturation at 95 °C for 30 s, annealing at 48–49 °C for 45 s and extension at 72 °C for 1 min, and a final extension at 72 °C for 5 min. The PCR products were then examined using gel electrophoresis on 1.3% Tris-Borate-EDTA-agarose gel stained with SYBR Safe DNA Gel Stain (Invitrogen). The PCR products showing strong bands in gel electrophoresis were purified with IllustraExoProStar - 1 Step (GE Healthcare Life Sciences), following its standard protocol, and sent for Sanger sequencing (Macrogen Inc., South Korea).

The forward and reverse sequences for each gene fragment were edited using Geneious v. 7.1 (Biomatters). The concatenated alignments of COI and 16S were conducted using the MAFFT program with the G-INS-I algorithm (Katoh and Standley 2013) using the default parameters, with additional inspection by eye for accuracy (see Suppl. material 1). As our 16S sequences (650 bp for *N. virginea* and 651 bp for *N. meleagris*) were longer than those available on GenBank, we used a minor homologous region in the alignment of this gene. However, we deposited the full 650–651 bp 16S sequences in GenBank. The combined dataset contained 1124 bp (639 bp for COI and 485 bp for 16S). Evolutionary relationships were estimated

for the concatenated genetic markers using Bayesian inference (BI) and maximum likelihood (ML) analyses. The best-fit evolution models were determined using PartitionFinder (Lanfear et al. 2012), considering the positions of the codon for the COI gene, which codes for protein, and a single partition for the 16S gene. The corrected Bayesian Information Criterion (BIC) was used to select among the options. PartitionFinder selected respectively GTR + I, F81, and HKY + G as the best model for the three positions of the codon in COI, and GTR + G for 16S. Bayesian inference, using the previously mentioned partitions and models, was performed using the MrBayes program (Ronquist et al. 2012) and the dataset was run for 3×10^7 generations, with Markov chains sampled every 1000 generations, and the standard 25% burn-in calculated. Convergence was checked using Tracer 1.6 (http://beast.bio.ed.ac.uk/Tracer). Tree branches were considered strongly supported if posterior probabilities were ≥ 0.90. Randomized accelerated maximum likelihood (RAxML) (Stamatakis 2006) was used to generate a ML tree with partitions under the evolution model GTR + G and with 1×10^4 replications. Branches with bootstrap values greater than 70 were considered strongly supported. Phylogenetic trees were drawn and edited in FigTree 1.4.3 (http://tree.bio.ed.ac.uk/software/figtree/).

For the species delimitation analyses, we initially constructed a distance matrix based on the Kimura 2-parameter (K2P) model, using the COI sequences, in the MEGA 6.0.6 software (Tamura et al. 2013). This matrix was analysed with the default settings of the Automatic Barcode Gap Discovery method (ABGD) (Puillandre et al. 2012) (available at http://www.abi.snv.jussieu.fr/public/abgd/abgdweb.html). We also used the Species Delimitation plugin v1.04 for Geneious v. 7.1 (Masters et al. 2011) with two data sets: (1) the results of our Bayesian concatenated phylogenetic analysis (COI + 16S), and (2) the results of a neighbor-joining tree based on the K2P model with 10,000 bootstrap replicates using COI sequences generated in MEGA 6.0.6. In this analysis, we calculated (1) the mean distance between the members within the clade (Intra Dist), (2) the mean distance of those individuals to the nearest clade (Inter Dist-closest), (3) the ratio between Intra Dist and Inter Dist-closest, and (4) the P ID, which represents the mean probability (95% confidence interval) of correctly identifying an unknown member of the putative species to fit inside (Strict P ID), or at least to be the sister group of (Liberal P ID), the species clade in a tree (Masters et al. 2011).

A statistical parsimony network analysis was conducted with COI sequences (347 bp), using the TCS algorithm (Clement et al. 2002) implemented in PopART v. 1.7.2 (Leigh and Bryant 2015). The sequence alignment step followed the same procedures already described in our phylogenetic analysis protocol (see Suppl. material 1). In addition to the *N. virginea* and *N. meleagris* sequences generated in this study, we included 55 sequences of *N. virginea* from island (Puerto Rico: 44 sequences) and continental (Panama: 10; Colombia: 1) locations in the Caribbean Province (Aktipis and Giribet 2010; Cook et al. 2010; Page et al. 2013; Quintero-Galvis and Castro 2013) (Table 1). Along with phylogenetic and species delimitation analyses, we also included the only COI sequence available on GenBank attributed to *N. meleagris* from Colombia (Quintero-Galvis and Castro 2013) (Table 1).

Table 1. List of species included in the phylogenetic, species delimitation, and statistical parsimony network analyses. The voucher number of species collected in NE Brazil and the accession numbers of the sequences obtained in the present study and from GenBank are indicated. The numbers in parentheses next to the GenBank accession number correspond to each of the specimens analysed in the present study (see Figs 1, 3).

Family/Species	Locality	Voucher No.	Accession No.		References[b]
			COI	16S[a]	
Outgroups					
Phenacolepadidae					
Thalassonerita naticoidea (A. H. Clarke, 1989)	Gulf of Mexico	–	FJ977768	FJ977721	1
Neritidae					
Nerita fulgurans Gmelin, 1791	Colombia	–	JX646664	JX646655	2
Nerita tessellata Gmelin, 1791	Colombia	–	JX646663	JX646654	2
Nerita peloronta Linnaeus, 1758	Colombia	–	JX646665	JX646656	2
Nerita versicolor Gmelin, 1791	Colombia	–	JX646666	JX646658	2
Neritina piratica Russell, 1940	Colombia	–	JX646669	JX646660	2
Neritina usnea (Röding, 1798)	Colombia	–	JX646670	JX646661	2
Neritina punctulata Lamarck, 1816	Colombia	–	JX646667	JX646657	2
Ingroup					
Neritina meleagris Lamarck, 1822	Colombia	–	JX646671	JX646662	2
	Camocim, Ceará, Brazil	CMPHRM 6408B	MK628548 (1)	MK628556 (1)	3
	Barra Grande, Piauí, Brazil	CMPHRM 6409B	MK628549 (2), MK628550, (3) MK628551 (4)	MK628557 (2), MK628558 (3), MK628559 (4)	3
Neritina virginea (Linnaeus, 1758)	Colombia	–	JX646668	JX646659	2
	Panama	–	JF810998 to JF811004[c] and FJ977766	–	1, 4
	Puerto Rico	–	FJ348932 to FJ348975	–	5
	Camocim, Ceará, Brazil	CMPHRM 6410B	MK628552 (1)	MK628560 (1)	3
	Barra Grande, Piauí, Brazil	CMPHRM 6411B	MK628553 (2), MK628554 (3), MK628555 (4)	MK628561 (2), MK628562 (3), MK628563 (4)	3

[a]Our 16S sequences deposited in GenBank are longer than those used for the construction of the molecular phylogenetic hypothesis. [b]1. Aktipis and Giribet (2010); 2. Quintero-Galvis and Castro (2013); 3. present study; 4. Page et al. (2013); and 5. Cook et al. (2010). [c]For the statistical parsimony network analysis, the haplotypes JF811001 and JF811002 had frequency 2 (Page et al. 2013).

The shells and opercula of the specimens of *N. virginea* and *N. meleagris* submitted to molecular analyses were observed and photographed under a stereomicroscope. A scanning electron microscope (SEM) was used to view their radulae (two females of *N. virginea* and two males and one female of *N. meleagris*) in the Analytical Facility of UFC (Central Analítica, UFC). This information was collected in order to compare our results with the information available in the literature.

Results and discussion

The results of our molecular analyses (phylogeny, species delimitation, and statistical parsimony network) confirmed the existence of two strongly supported clades living in sympatry in the intertidal beachrocks of Northeastern Brazil (Brazilian Province). The Bayesian and maximum likelihood trees showed the same topology, with the formation of four clades within *Neritina*: Group I (*Neritina piratica* + *Neritina usnea*), Group II (*Neritina meleagris*, collected in NE Brazil), Group III (*Neritina virginea*, collected in NE Brazil and Colombia, + "*Neritina meleagris*", from Colombia), and Group IV (*Neritina punctulata*) (Fig. 1). The Groups II and III were also observed in the ABGD analysis. Intraspecific distances in these groups were at least one order of magnitude smaller than the interspecific distances. Our minimum interspecific genetic distance values (COI region only), involving groups II and III, were 8.4 and 9.6%, respectively (Table 2). These values are higher than the minimum value assumed by Abdou et al. (2017) to characterize distinct Indo-Pacific *Neritina* species. In addition, the probabilities of a new sequence fitting inside P ID (Strict) or at least the sister group P ID (Liberal) of these clades were equal to, or in most cases, greater than 84% (Table 2). These results are compatible with the values found to delimit species in different groups of gastropods (e.g. Churchill et al. 2014; Cooke et al. 2014; Espinoza et al. 2014).

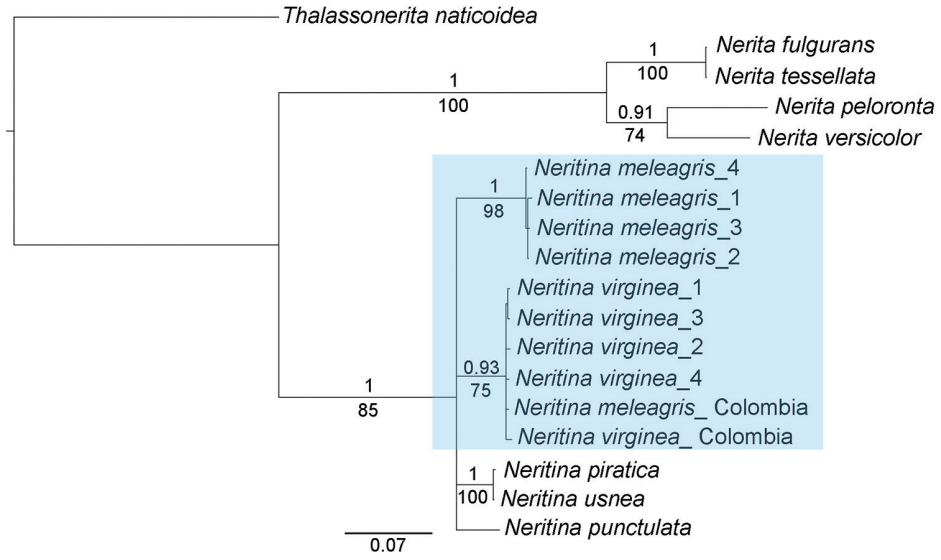

Figure 1. Molecular phylogenetic hypothesis (Bayesian tree) of some species of Neritidae of the Western Atlantic. The Bayesian tree was based on partial mitochondrial COI and 16S sequences. The *Neritina meleagris* and *Neritina virginea* clades (ingroup) are highlighted. The other taxa were used as outgroup. Numbers on and below the main branches represent the posterior Bayesian probabilities (BP) (>0.90) and bootstrap values for maximum likelihood (ML) (>70%), respectively. Specimens with the number "1" are from Camocim beach (Ceará State, NE Brazil) and those with numbers "2", "3", and "4" are from Barra Grande beach (Piauí State, NE Brazil). The numbered specimens of *N. virginea* (1, 2, 3, and 4) and *N. meleagris* (1, 2, 3, and 4) are the same specimens shown in Figure 3.

Table 2. Species delimitation results from the Bayesian concatenated and Neighbor-Joining trees. These analyses were performed with the Species Delimitation plugin for Geneious.

Bayesian concatenated tree (COI + 16S)						
Species	**Monophyly**	**Intra Dist**	**Inter Dist-closest**	**Intra/Inter**	**P ID(Strict)**	**P ID(Liberal)**
Neritina virginea	yes	0.006	0.073	0.08	0.88 (0.76, 1.0)	0.97 (0.87, 1.0)
Neritina meleagris	yes	0.004	0.088	0.04	0.84 (0.70, 0.98)	0.97 (0.86, 1.0)
Neighbor-Joining K2P COI tree						
Species	**Monophyly**	**Intra dist**	**Inter Dist-closest**	**Intra/Inter**	**P ID(Strict)**	**P ID(Liberal)**
Neritina virginea	yes	0.008	0.084	0.09	0.87 (0.75, 1.00)	0.97 (0.87, 1.0)
Neritina meleagris	yes	0.002	0.096	0.02	0.86 (0.72, 1.00)	0.98 (0.87, 1.0)

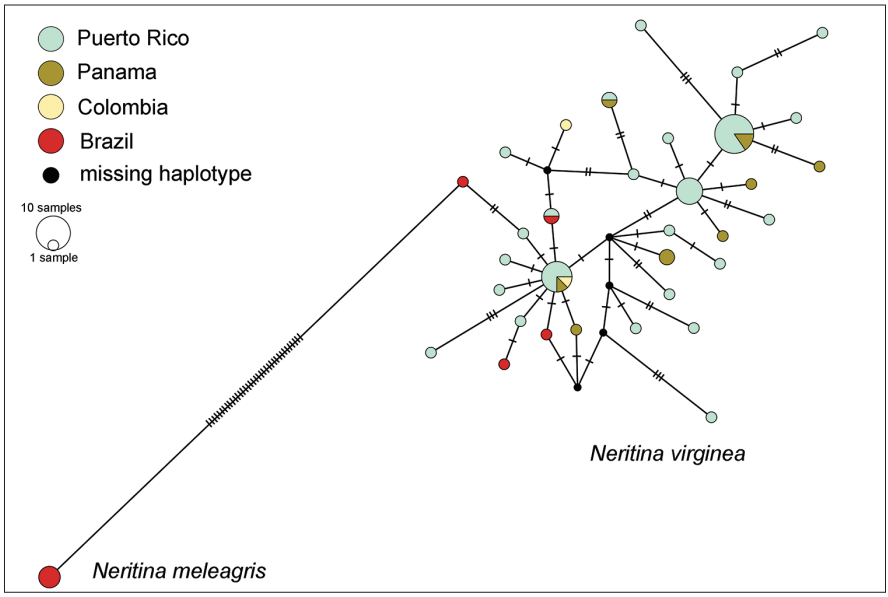

Figure 2. Statistical parsimony network analysis (TCS algorithm) based on 64 partial mitochondrial COI sequences (347 bp). This analysis included specimens of *Neritina meleagris* and *Neritina virginea* from the Caribbean and Brazilian Provinces. Size of the circle is proportional to frequency of the haplotype and colours inside the circles designate geographical locations to which the samples belong. Black circles correspond to hypothetical haplotypes. The number of mutational steps is indicated by dashes on branches. We highlighted the 36 mutational steps that separate the two species haplotypes.

Although the distinction between clades showed high support values, the phylogenetic relationship between them could not be recovered. As we did not have access to the specimens, it was not possible to check the shell colour patterns of the *Neritina meleagris* from Colombia (obtained from GenBank) that was included in the same clade as *Neritina virginea*. Thus, we suspect that an error may have occurred at the time of submission of the sequences to GenBank, since, in the study of Quintero-Galvis and Castro (2013), *N. virginea* and *N. meleagris* appeared in very distinct branches of the phylogenetic tree.

Despite the geographical distance, all *N. virginea* sequences from Brazil and the Caribbean were very similar, with all haplotypes grouped within a few mutational steps (Fig. 2). This result reinforces the validity of *N. virginea* and confirms its presence in the

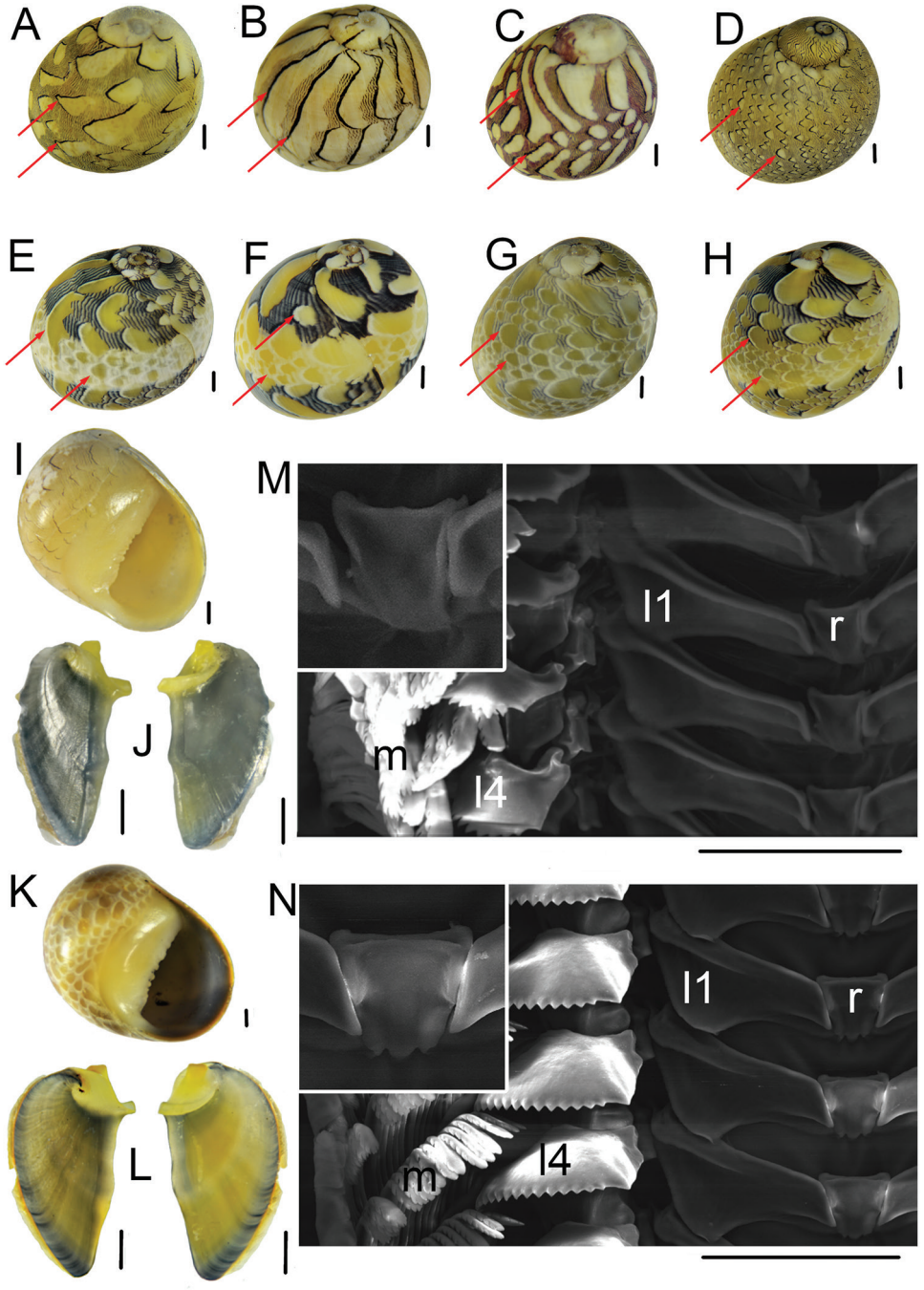

Figure 3. Colour patterns of shells, opercula, and radulae of the *Neritina virginea* and *Neritina meleagris* analysed. The red arrows highlight the differences between the leading edges of colour patterns of both species: *N. virginea* has the leading edges outlined in heavy black, while *N. meleagris* has the leading edge outlined in white or black and white. **A** *Neritina virginea*_1 **B** *Neritina virginea*_2 **C** *Neritina virginea*_3.

Brazilian Province. As also observed in the phylogenetic analysis, the only sequence assigned as *N. meleagris* from the Caribbean Province is positioned within one of the most frequent *N. virginea* haplotypes for this region (Fig. 2). With respect to our *N. meleagris* sequences, although this species is found in sympatry with its congener in the Brazilian Province, it is separated from the *N. virginea* haplogroups by at least 36 mutational steps.

Figure 3 shows the colour patterns, opercula, and radulae of the *N. meleagris* and *N. virginea* specimens collected from the Barra Grande and Camocim beaches. Our molecular results are consistent with the morphological descriptions previously proposed for each species (Russell 1941; Matthews-Cascon et al. 1990; Eichhorst 2016). Russell (1941) described, for both species, a colour pattern consisting of dark zigzag lines and lighter spots. However, this author emphasized that while *N. virginea* has a leading edge outlined in heavy black, *N. meleagris* instead has a leading edge outlined with white, white and black, or white and red, resembling imbricating scales. The imbricating scales pattern was emphasized in the original description of *N. meleagris* (Lamarck 1822), whereas Matthews-Cascon et al. (1990) and Eichhorst (2016) highlighted the differences in the leading edges of the colour pattern for each species. Although did not examine the type specimens, individuals of *N. virginea* from the Linnean Collection at the Natural History Museum, London (see http://linnean-online.org/17152/), and *N. meleagris*, from the type locality (Dominican Republic) (see http://data.biodiversitydata.nl/naturalis/specimen/ZMA.MOLL.313038), had the same leading edge patterns as described earlier. All analysed specimens of *N. meleagris* had the leading edge outlined with white or white and black, while *N. virginea* specimens had the leading edge outlined in black (Fig. 3A–H). Despite the great variation in their shell colour patterns, a more detailed observation of the leading edges of the *N. virginea* and *N. meleagris* shells allows the separation of the two species, even in the field. Warmke and Abbott (1962) also emphasized the use of leading edges to separate the two species. Williams (2017) argued that the colours and patterns of gastropod shells could be genetically determined, influenced directly by environmental factors, or a combination of both. Specifically, the patterns of leading edges (leading edge outlined with white or white and black in *N. meleagris* and outlined in black in *N. virginea*) appear to be under genetic control rather than be influenced directly by environmental factors, since the patterns for each species are consistent regardless of the location studied (e.g. Russell 1941; Eichhorst 2016;

Figure 3. Continued. **D** *Neritina virginea*_4 **E** *Neritina meleagris*_1 **F** *Neritina meleagris*_2 **G** *Neritina meleagris*_3 **H** *Neritina meleagris*_4 **I** ventral view of shell of *Neritina virginea* **J** operculum (outer and inner views) of *Neritina virginea* **K** ventral view of shell of *Neritina meleagris* **L** operculum (outer and inner views) of *Neritina meleagris* **M** radula of *Neritina virginea* (SEM), with rachidian tooth enlarged in the upper left quadrant **N** radula of *Neritina meleagris* (SEM), with rachidian tooth enlarged in the upper left quadrant. Abbreviations: l1 first lateral tooth, l4 fourth lateral tooth, m marginal teeth, r rachidian tooth. The specimens with the number "1" are from Camocim beach (Ceará State, NE Brazil) and those with numbers "2", "3", and "4" are from Barra Grande beach (Piauí State, NE Brazil). The numbered specimens of *N. virginea* (1, 2, 3, and 4) and *N. meleagris* (1, 2, 3, and 4) are the same specimens used in the phylogenetic analysis of Figure 1. Scale bars: 1.0 mm (**A–L**); 100 μm (**M, N**).

present study). This observation is reinforced by the clades obtained in our phylogenetic analysis, corroborating the diagnostic colour patterns previously described (Fig. 1).

Besides the shell colour patterns, *N. virginea* and *N. meleagris* differ from each other in subtle ways. The inner lips of the shells of the two species are denticulated. However, in *N. virginea* there are several small denticles interspersed by two larger teeth, while in *N. meleagris* the teeth are larger, more prominent in the central region, and less numerous when compared to *N. virginea* (Fig. 3I, K). Russell (1941), Matthews-Cascon et al. (1990), and Eichhorst (2016) also highlighted these differences regarding the number of teeth on the inner lip. Both species have a calcareous and smooth operculum, with a bifurcated apophysis. Comparing the opercula, *N. virginea* has a darker (bluish-black) and more elongated operculum, with the apophysis elements thinner and more separated from each other. On the other hand, the operculum of *N. meleagris* presents a lighter coloration (yellowish-black) and a semi-circular shape, with the apophysis elements much stouter and closer to each other (Fig. 3J, L). In the present study, *Neritina virginea* and *N. meleagris* have a very similar morphology of the radula: a rhipidoglossate radula, with one rachidian tooth, five pairs of lateral teeth, and many denticulated marginal teeth arranged in transverse rows (Fig. 3M, N; see also Suppl. material 2). The most striking difference between these radulae is the rectangular rachidian tooth, which has three cusps in *N. meleagris* (both male and female) but is cuspless in *N. virginea*. The first lateral tooth of *N. virginea* is more slender than that of *N. meleagris*. Previous studies have shown that the radula teeth pattern of neritids is very stable, the most variable character being the number of cusps on the fifth lateral tooth, which is likely correlated with age (Baker 1923; Huang 1997; Haynes 2001). This characteristic makes it difficult to define intra- and interspecific differences. Further studies are needed to better define the differences between the radulae of the two species.

Our molecular data show that *N. virginea* and *N. meleagris* are two distinct species, thus confirming the *N. meleagris* record for the Brazilian coast. In summary, our results, along with the already well-established record of *Neritina zebra* (Matthews-Cascon et al. 1990; Rios 2009; Barroso et al. 2012, 2016; Eichhorst 2016), demonstrate that there are three species of the genus *Neritina* registered for the Brazilian Province to date. We emphasize the importance of the separation of *N. virginea* and *N. meleagris* in future studies, especially those conducted in the Brazilian Province, since these species may cohabit. In the field, these species can be identified with a detailed observation of the leading edge patterns of their shells, assisting ecological studies. Further research is needed in other areas along the Brazilian Province to determine the geographic distribution of *N. virginea* and *N. meleagris*, highlighting the locations where they co-occur.

Acknowledgements

Coordenação de Aperfeiçoamento de Pessoal de Nível Superior (CAPES) provided a postdoctoral fellowship to C.X. Barroso (PNPD process number 88882.306440/2018-01) and J.E.P Freitas (PNPD process number 88887.466769/2019-00). H. Matthews-

Cascon and T.M.C. Lotufo are research fellows from Conselho Nacional de Desenvolvimento Científico e Tecnológico (CNPq). This work was partially funded by Fundação de Amparo à Pesquisa do Estado de São Paulo (FAPESP), projects # 2015/17177-6 and 2017/11948-6. The authors would like to thank the Central Analítica-UFC/CT-INFRA/MCTI-SISANO/Pró-Equipamentos CAPES for the support. The authors are also indebted to Patricia N. Bordallo (Embrapa), Vicente V. Faria (UFC), and Diego V. Wilke (UFC) for making laboratory infrastructure available in part of the research. Finally, we are indebted to Dr. Thierry Backeljau, Dr. Ahmed Abdou and the anonymous referees for their careful reviews.

References

Abdou A, Galzin R, Lord C, Denys GPJ, Keith P (2017) Revision of the species complex "*Neritina pulligera*" (Gastropoda, Cycloneritimorpha: Neritidae) using taxonomy and barcoding. Vie et Milieu 67: 149–161.

Aktipis SW, Giribet G (2010) A phylogeny of Vetigastropoda and other "archaeogastropods": re-organizing old gastropod clades. Invertebrate Biology 129: 220–240. https://doi.org/10.1111/j.1744-7410.2010.00198.x

Baker HB (1923) Notes on the radula of the Neritidae. Proceedings of the Academy of Natural Sciences of Philadelphia 75: 117–178. https://doi.org/10.1016/0016-0032(77)90769-4

Barroso CX, Matthews-Cascon H, Simone LRL (2012) Anatomy of *Neritina zebra* from Guyana and Brazil (Mollusca: Gastropoda: Neritidae). Journal of Conchology 41: 49–64.

Barroso CX, Lotufo TMC, Matthews-Cascon H (2016) Biogeography of Brazilian prosobranch gastropods and their Atlantic relationships. Journal of Biogeography 43: 2477–2488. https://doi.org/10.1111/jbi.12821

Blanco JF, Tamayo S, Scatena FN (2014) Variación fenotípica de la concha en Neritinidae (Gastropoda: Neritimorpha) en ríos de Puerto Rico. Revista de Biología Tropical 62: 53–68. https://doi.org/10.15517/rbt.v62i0.15778

Churchill CKC, Valdés Á, Foighil DÓ (2014) Molecular and morphological systematics of neustonic nudibranchs (Mollusca: Gastropoda: Glaucidae: *Glaucus*), with descriptions of three new cryptic species. Invertebrate Systematics 28: 174–195. https://doi.org/10.1071/IS13038

Clement M, Snell Q, Walker P, Posada D, Crandall K (2002) TCS: estimating gene genealogies. In: Proceedings 16th International Parallel and Distributed Processing Symposium 2, 184. https://doi.org/10.1109/IPDPS.2002.1016585

Cook BD, Pringle CM, Hughes JM (2010) Immigration history of amphidromous species on a Greater Antillean island. Journal of Biogeograhy 37: 270–277. https://doi.org/10.1111/j.1365-2699.2009.02215.x

Cooke S, Hanson D, Hirano Y, Ornelas-Gatdula E, Gosliner TM, Chernyshev AV, Valdés Á (2014) Cryptic diversity of *Melanochlamys* sea slugs (Gastropoda, Aglajidae) in the North Pacific. Zoologica Scripta 43: 351–369. https://doi.org/10.1111/zsc.12063

Díaz JM, Puyana M (1994) Moluscos del Caribe Colombiano: un catálogo ilustrado. Colciencias y Fundacion Natura Colombia, Bogota, 291 pp.

Eichhorst TE (2016) Neritidae of the World – Volume One. 1st edition. ConchBooks, Hackenheim, Germany, 694 pp.

Espinoza E, DuPont A, Valdés Á (2014) Molecular data reveal an undescribed cryptic species of *Costasiella* Pruvot-Fol, 1951 (Euthyneura: Sacoglossa: Limapontidae) in the Bahamas. American Malacological Bulletin 32: 173–182. https://doi.org/10.4003/006.032.0208

Floeter SR, Rocha LA, Robertson DR, Joyeux JC, Smith-Vaniz WF, Wirtz P, Edwards AJ, Barreiros JP, Ferreira CEL, Gasparini JL, Brito A, Falcón JM, Bowen BW, Bernardi G (2008) Atlantic reef fish biogeography and evolution. Journal of Biogeography 35: 22–47. https://doi.org/10.1111/j.1365-2699.2007.01790.x

Folmer O, Black M, Hoeh W, Lutz R, Vrijenhoek R (1994) DNA primers for amplification of mitochondrial cytochrome c oxidase subunit I from diverse meta- zoan invertebrates. Molecular Marine Biology and Biotechnology 3: 294–299.

Haynes A (2001) A revision of the genus *Septaria* Férussac, 1803 (Gastropoda: Neritimorpha). Annalen des Naturhistorischen Museums in Wien: Serie B für Botanik und Zoologie 103B: 177–229.

Huang Q (1997) Morphological, allozymic, and karyotypic distinctions between *Neritina* (*Dostia*) *violacea* and *N.* (*D.*) *cornucopia* (Gastropoda: Neritoidea). Journal of Zoology 241: 343–369. https://doi.org/10.1111/j.1469-7998.1997.tb01964.x

Kano Y, Chiba S, Kase T (2002) Major adaptive radiation in neritopsine gastropods estimated from 28S rRNA sequences and fossil records. Proceedings of the Royal Society of London B 269: 2457–65. https://doi.org/10.1098/rspb.2002.2178

Katoh K, Standley DM (2013) MAFFT multiple sequence alignment software version 7: Improvements in performance and usability. Molecular Biology and Evolution 30: 772–780. https://doi.org/10.1093/molbev/mst010

Lamarck JBM (1822) Histoire naturelle des animaux sans vertèbres. Tome sixième, 2me partie. published by the Author, Paris, 232 pp.

Lanfear R, Calcott B, Ho SYW, Guindon S (2012) PartitionFinder: Combined Selection of Partitioning Schemes and Substitution Models for Phylogenetic Analyses. Molecular Biology and Evolution 29: 1695–1701. https://doi.org/10.1093/molbev/mss020

Leigh JW, Bryant D (2015) POPART: Full-feature software for haplotype network construction. Methods in Ecology and Evolution 6: 1110–1116. https://doi.org/10.1111/2041-210X.12410

Masters BC, Fan V, Ross HA (2011) Species delimitation-a geneious plugin for the exploration of species boundaries. Molecular Ecology Resources 11: 154–157. https://doi.org/10.1111/j.1755-0998.2010.02896.x

Matthews-Cascon H, Pinheiro PR, Matthews HR (1990) A família Neritidae no norte e nordeste do Brasil Mollusca: Gastropoda. Caatinga 7: 44–56.

Page TJ, Torati LS, Cook BD, Binderup A, Pringle CM, Reuschel S, Schubart CD, Hughes JM (2013) Invertébrés Sans Frontières: Large Scales of Connectivity of Selected Freshwater Species among Caribbean Islands. Biotropica 45: 236–244. https://doi.org/10.1111/j.1744-7429.2012.00900.x

Puillandre N, Lambert A, Brouillet S, Achaz G (2012) ABGD, Automatic Barcode Gap Discovery for primary species delimitation. Molecular Ecology 21: 1864–1877. https://doi.org/10.1111/j.1365-294X.2011.05239.x

Quintero-Galvis J, Castro LR (2013) Molecular phylogeny of the Neritidae (Gastropoda: Neritimorpha) based on the mitochondrial genes cytochrome oxidase I (COI) and 16S rRNA. Acta Biológica Colombiana 18: 307–318.

Rios EC (1975) Marine Iconography. Fundação da Universidade do Rio Grande, Rio Grande, 331 pp.

Rios EC (1985) Seashells of Brazil. Fundação Universidade do Rio Grande, Rio Grande, 328 pp.

Rios EC (1994) Seashells of Brazil. 2nd edn. Fundação da Universidade do Rio Grande, Rio Grande, 331 pp.

Rios EC (2009) Compendium of Brazilian Sea Shells. Editora Evangraf, Rio Grande, 668 pp.

Ronquist F, Teslenko M, Van Der Mark P, Ayres DL, Darling A, Höhna S, Larget B, Liu L, Suchard MA, Huelsenbeck JP (2012) Mrbayes 3.2: Efficient bayesian phylogenetic inference and model choice across a large model space. Systematic Biology 61: 539–542.

Russell HD (1941) The recent mollusks of the family Neritidae of the Western Atlantic. Bulletin of the Museum of Comparative Zoology at Harvard College 88: 347–404.

Stamatakis A (2006) RAxML-VI-HPC: Maximum likelihood-based phylogenetic analyses with thousands of taxa and mixed models. Bioinformatics 22: 2688–2690. https://doi.org/10.1093/bioinformatics/btl446

Tamura K, Stecher G, Peterson D, Filipski A, Kumar S (2013) MEGA 6: molecular evolutionary genetics analysis, version 6.0. Molecular Biology and Evolution 30: 2725–2729. https://doi.org/10.1093/molbev/mst197

Tan SK, Clements R (2008) Taxonomy and distribution of the Neritidae (Mollusca: Gastropoda) on Singapore. Zoological Studies 47: 481–494.

Warmke GL, Abbott RT (1962) Caribbean seashells: A guide to the marine mollusks of Puerto Rico and other West Indian islands, Bermuda and the Lower Florida Keys. Livingston Publishing Company, Wynnewood, 348 pp.

Wheeler QD, Raven PH, Wilson EO (2004) Taxonomy: Impediment or Expedient? Science 303: 285. https://doi.org/10.1126/science.303.5656.285

Williams ST (2017) Molluscan shell colour. Biological Reviews 92: 1039–1058. https://doi.org/10.1111/brv.12268

Supplementary material 1

Alignments used to construct the phylogenetic trees and statistical parsimony network analysis

Authors: Cristiane Xerez Barroso, João Eduardo Pereira de Freitas, Helena Matthews-Cascon, Luis Ernesto Arruda Bezerra, Tito Monteiro da Cruz Lotufo

Link: https://doi.org/10.3897/zookeys.904.46790.suppl1

Supplementary material 2

Radulae of the *Neritina meleagris* (A) and *Neritina virginea* (B) analysed

Authors: Cristiane Xerez Barroso, João Eduardo Pereira de Freitas, Helena Matthews-Cascon, Luis Ernesto Arruda Bezerra, Tito Monteiro da Cruz Lotufo

Link: https://doi.org/10.3897/zookeys.904.46790.suppl2

ZooKeys 904: 131–146 (2020)
doi: 10.3897/zookeys.904.46547
http://zookeys.pensoft.net

RESEARCH ARTICLE

A peer-reviewed open-access journal
ZooKeys
Launched to accelerate biodiversity research

A new *Diplolepis* Geoffroy (Hymenoptera, Cynipidae, Diplolepidini) species from China: a rare example of a rose gall-inducer of economic significance

Juli Pujade-Villar[1], Yiping Wang[2], Wenli Zhang[2,3], Noel Mata-Casanova[1], Irene Lobato-Vila[1], Avar-Lehel Dénes[4], Zoltán László[4]

1 *Department of Animal Biology, University of Barcelona, Barcelona 08028, Catalonia, Spain* **2** *College of Forest and Biotechnology, Zhejiang Agricultural and Forestry University, Lin'an 311300, China* **3** *Lanzhou Agro-technical research and Popularization Center, Lanzhou, 730010, China* **4** *Hungarian Department of Biology and Ecology, Babeș-Bolyai University, Cluj-Napoca 400006, Romania*

Corresponding author: *Zoltán László* (laszlozoltan@gmail.com)

Academic editor: *A. Köhler* | Received 13 September 2019 | Accepted 2 December 2019 | Published 17 January 2020

http://zoobank.org/49036F44-5497-44C4-A0E7-77BC87099A44

Citation: Pujade-Villar J, Wang Y, Zhang W, Mata-Casanova N, Lobato-Vila I, Dénes A-L, László Z (2020) A new *Diplolepis* Geoffroy (Hymenoptera, Cynipidae, Diplolepidini) species from China: a rare example of a rose gall-inducer of economic significance. ZooKeys 904: 131–146. https://doi.org/10.3897/zookeys.904.46547

Abstract

A new species of the genus *Diplolepis* Geoffroy, *Diplolepis abei* Pujade-Villar & Wang **sp. nov.** is described on host plant *Rosa sertata* Rolfe × *R. rugosa* Thunb. from China with an integrative approach based on molecular and morphological data. Diagnosis, distribution and biology of the new species are included and illustrated. This species is the first known rose gall-inducer of economic importance. A review of Eastern Palearctic species of *Diplolepis* is given and a key to the Chinese fauna is presented.

Keywords

gall wasp, Kushui rose, new species, phytophagous, taxonomy

Introduction

The family Cynipidae (Hymenoptera, Cynipoidea) includes around 1400 species, all of them exclusively phytophagous and divided into 12 tribes (Ronquist 1999; Ronquist et al. 2015). The tribe Diplolepidini induces galls exclusively on *Rosa* spp. L. and

is distributed in the Holarctic Region. Diplolepidini is a monophyletic group characterized by a unique autapomorphy within Cynipidae: the presence of a longitudinal furrow on the mesopleuron of the mesosoma. Only two genera, *Diplolepis* Geoffroy, 1762 and *Liebelia* Kieffer, 1903, are currently included in this tribe, together comprising 58–62 species (Melika 2006; Ronquist et al. 2015). *Diplolepis* and *Liebelia* can be easily distinguished on the basis of the following diagnostic morphological characters (Melika 2006): in *Diplolepis*, antennae of females and males are 12–15-segmented, the radial cell of the forewing is closed along the wing margin and the hypopygium is plough-shaped, while in *Liebelia* antennae are 16-segmented, the radial cell is open and the hypopygium is not plough-shaped.

The genus *Diplolepis* includes six European species (Pujade-Villar 1993; Pujade-Villar and Plantard 2002), some of them also occurring in Western Asia and North Africa (Morocco) (Mimeur 1949; Melika 2006); eight Eastern Palaearctic species (Abe et al. 2007; Wang et al. 2013) and 31 North American species (Burks 1979; Shorthouse and Ritchie 1984). The relatively low number of species recorded from the Eastern Palaearctic could be due to a lack of sampling efforts; herein we describe a new species for the Eastern Palaearctic fauna.

Guo et al. (2013) and Wang et al. (2013) published the first record of *D. rosae* in China, which later has been proved to be a misidentification. The eastern boundary of *D. rosae*'s distribution range may be the Ural, Altay, Tianshan, Pamir, Hindukush Mountains (Belizin 1957). However, a single mention of a more eastern location: India, appears in the key of Belizin (1957: 11), a record that has not been confirmed since then. Therefore, we presume that *D. rosae* does not occur in China.

Diplolepis is morphologically characterized by having both the head and the mesosoma black or reddish brown; antennae 14–15 segmented (except *D. hunanensis* with only 12) in both sexes and with relatively large, cylindrical flagellomeres; pronotum dorsomedially short; pronotal plate not pronounced; scutellar foveae faint or absent; mesopleuron with a broad, crenulate mesopleural furrow; propodeum rugose and lateral propodeal carinae usually indistinct; metanotal trough broad, apically truncate; forewings moderately or strongly uniformly or partially infuscate, margins with short but distinct cilia; radial cell closed along the wing margin; 2r of forewings usually with a prominent median vein stump anterolaterally projected; nucha dorsally short; hypopygium plough-shaped and hypopygial spine slightly longer than broad, with some sparse short setae (Melika 2006; Ronquist et al. 2015).

Diplolepis are known to cause galls mainly on feral roses. Accidental infections on cultivated *Rosa rugosa* and its hybrids were reported from North America, but neither of the *Diplolepis* species became serious pests of rose cultivars (Shorthouse 2001). There are no published data on the large-scale economic importance of *Diplolepis*.

Material and methods

The terminology for the morphology of cynipid gall wasps used in this work follows Liljeblad and Ronquist (1998) and Melika (2006). Abbreviations for the forewing

venation are taken from Ronquist and Nordlander (1989), and the cuticular surface terminology, from Harris (1979). Measurements and abbreviations used in this work are: F1–F12, first and subsequent flagellomeres; post-ocellar distance (POL), the distance between the inner margins of the posterior ocelli; ocellar-ocular distance (OOL), the distance from the outer margin of the posterior ocellus to the inner margin of the compound eye; LOL, the distance between lateral and frontal ocelli. The width of the forewing radial cell was measured from the margin of the wing to the Rs vein.

Scanning electron microscope (SEM) images of the described species were taken with a FEI Quanta 200 ESEM at high voltage (15 kV) without gold coating in the "Serveis de Microscopia Electrònica" of the University of Barcelona.

Specimens of the new species were collected in Lanzhou City of Gansu Province and they are deposited in the Hymenoptera Collection of Zhejiang Agricultural and Forest University (**ZAFU**) and in the University of Barcelona (UB, Col. JP-V).

Genomic DNA was extracted from two individuals using an ISOLATE II Genomic DNA Kit (Bioline, Germany), following the protocol provided by the manufacturer. The mitochondrial cytochrome c oxidase subunit I (COI) sequences were amplified using the standard LCO1490 and HCO2198 primer pair (Folmer et al. 1994) in a 50 µl reaction volume at a 42 °C annealing temperature. PCR products were purified with the Wizard SV Gel and PCR Clean-Up System (Promega, USA) and sent for sequencing to Macrogen Inc. (Europe).

Sequences were downloaded and verified with the BLAST (Johnson et al. 2008). Further, sequences for all available *Diplolepis* species were also downloaded from the NCBI database and the BOLD System (see Fig. 5 for reference numbers). The sequences were aligned using a Clustal W algorithm (Thompson et al. 1994) in BioEdit (Hall 1999). A Bayesian inference (BI) tree was generated in MrBayes (Ronquist et al. 2012) for 1,000,000 generations, sampled every 1000th step, until the average standard deviation of split frequencies fell below 0.01. The first 25% of the sampled trees were discarded as burn-in. The GTR+G+I model of molecular evolution was selected as most suitable for this analysis, based on the Bayesian information criterion in jModelTest2 (Darriba et al. 2012). Interspecific *p*-distances were calculated in MEGA X (Kumar et al. 2018).

Results

Diplolepis abei **Pujade-Villar & Wang sp. nov.**
http://zoobank.org/E35C7053-8145-4CAC-B453-C6A657A11330
Figs 1, 2

Type material. ***Holotype*****:** ♀ deposited in UB with the following labels: 'Lanzhou (Gansu Province), ex *Rosa sertata* × *R. rugosa*, (03.ii.2011) 15.iii.2011, col. Sheng Maoling' (white label); '*Diplolepis abei* Pujade-Villar & Wang, desig. JP-V-2017' (red label). ***Paratypes*****:** 11♀♀ with the same labels as the holotype: 8♀♀ in ZAFU, 3♀♀ in UB.

Diagnosis. This species is characterized by having the following morphological characters: head smooth to alutaceous, mesoscutum alutaceous with piliferous punctures, scutellum rugose with a more delicate sculpture in the centre of the disk; legs, including coxae, reddish; forewings hyaline but slightly smoky in both the radial and the 3rd cubital cells, never with a dusky cloud around veins; second metasomal tergite short. It differs from the rest of species known from China because veins of its forewings are not infuscate. In addition, the deciduous galls have numerous long stout sharp-pointed spines unlike other known species. Molecular results: the two sequenced individuals represent one haplotype (GeneBank accession number: MN434062). Based on the BI tree the species is part of a polytomous clade with a group consisting of *D. fructuum*, *D. mayri* and *D. rosae*, and with *D. spinosissimae* (Fig. 5). The average *p*-distance compared to the other species is 9.73% (Table 1), with the lowest values shown when compared to *D. fructuum* (6.38%) and *D. spinosissimae* (6.39%).

Description. Female. *Length*. Body length 3.3–3.6 mm ($N = 4$).

Color (Fig. 2g). Head and mesosoma uniformly black. Antenna black; pedicel, and sometimes also the scapus, lighter. Tegulae brown. Mandibles reddish, with black tips, maxillary and labial palpi brown. Legs reddish, including coxae; last tarsi (and sometimes the 4th tarsomere) darker. Metasoma reddish; basal and posterior parts and hypopygium, brown. Wings hyaline but slightly smoky in both the radial and the 3rd cubital cells; wing veins distinct, dark brown, never with infuscate clouds.

Head (Fig. 1a, b). Head trapezoidal in frontal view, transverse, as wide as the mesosoma, shiny, with short sparse white setae, 1.3 times as broad as high in frontal view and 2.1 times as broad as long seen from above. Lower face smooth to alutaceous, with distinct piliferous punctures; median elevated area alutaceous. Clypeus quadrangular, broader than high, smooth to alutaceous, flattened; anterior tentorial pits, epistomal sulcus and clypeo-pleurostomal line, distinct, ventral margin straight. Gena smooth to alutaceous, with piliferous punctures and basally with some weak carinae, not broadened behind the compound eye (not visible in frontal view) and 2.0 times as broad as the cross diameter of the compound eye in lateral view. Malar space smooth to coriaceous, around 0.5 times as long as height of compound eye. Transfacial distance 1.5 times as long as height of compound eye; diameter of antennal toruli 1.4 times as long as the distance between them, and distance between torulus and eye margin 1.2 times longer than torulus diameter. Inner margins of compound eyes divergent. Frons and vertex shiny, alutaceous; occiput dull, coriaceous. POL 0.75 times as long as OOL; OOL 2.0 times longer than the diameter of the lateral ocelli and 6.6 times longer than LOL.

Antenna (Fig. 1c). 14-segmented, 1.5 times longer than head plus mesosoma; pedicel slightly longer than broad; F1 very long, 4.0 times longer than pedicel and nearly 1.8 times longer than F2; F2 as long as F3; F12 slightly longer than F11; placodeal sensilla present in all the funicular segments, but only apically in F1 and in the anterior half in F2. Antennal formula: 6: 4(x3): 16: 9: 9: 8: 8: 8: 7: 7: 7: 7: 7: 9.

Mesosoma (Fig. 1d–g). Mesosoma curved and slightly longer than high in lateral view, with short white setae. Pronotum very narrow, coarsely punctured, sparsely

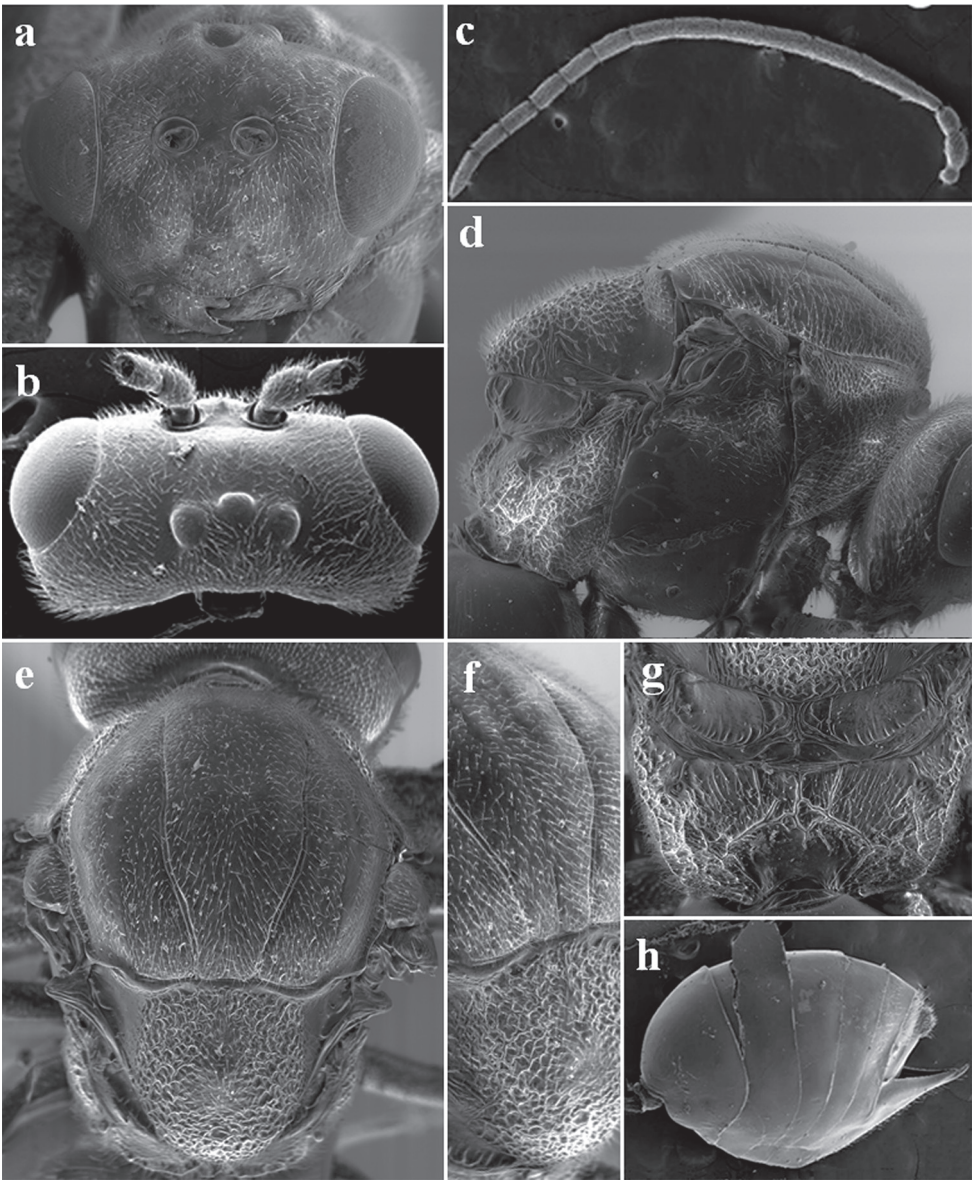

Figure 1. *Diplolepis abei* Pujade-Villar & Wang ♀ sp. nov. **a** head in frontal view **b** genae in dorsal view **c** antenna **d** mesosoma in lateral view **e** mesosoma in dorsal view **f** mesosoma in dorso-lateral view **g** propodeum **h** metasoma in lateral view.

haired in the middle and coriaceous with some carinae in the basal part. Scutum wider than long and at least 1.7 times longer than the scutellum, alutaceous, with distinct punctures. Notauli complete, convergent posteriorly; median mesoscutal line very shallow, reaching at least the level of tegulae; parapsidal lines visible but poorly impressed, narrow, shining, reaching tegulae level; anterior parallel lines distinct,

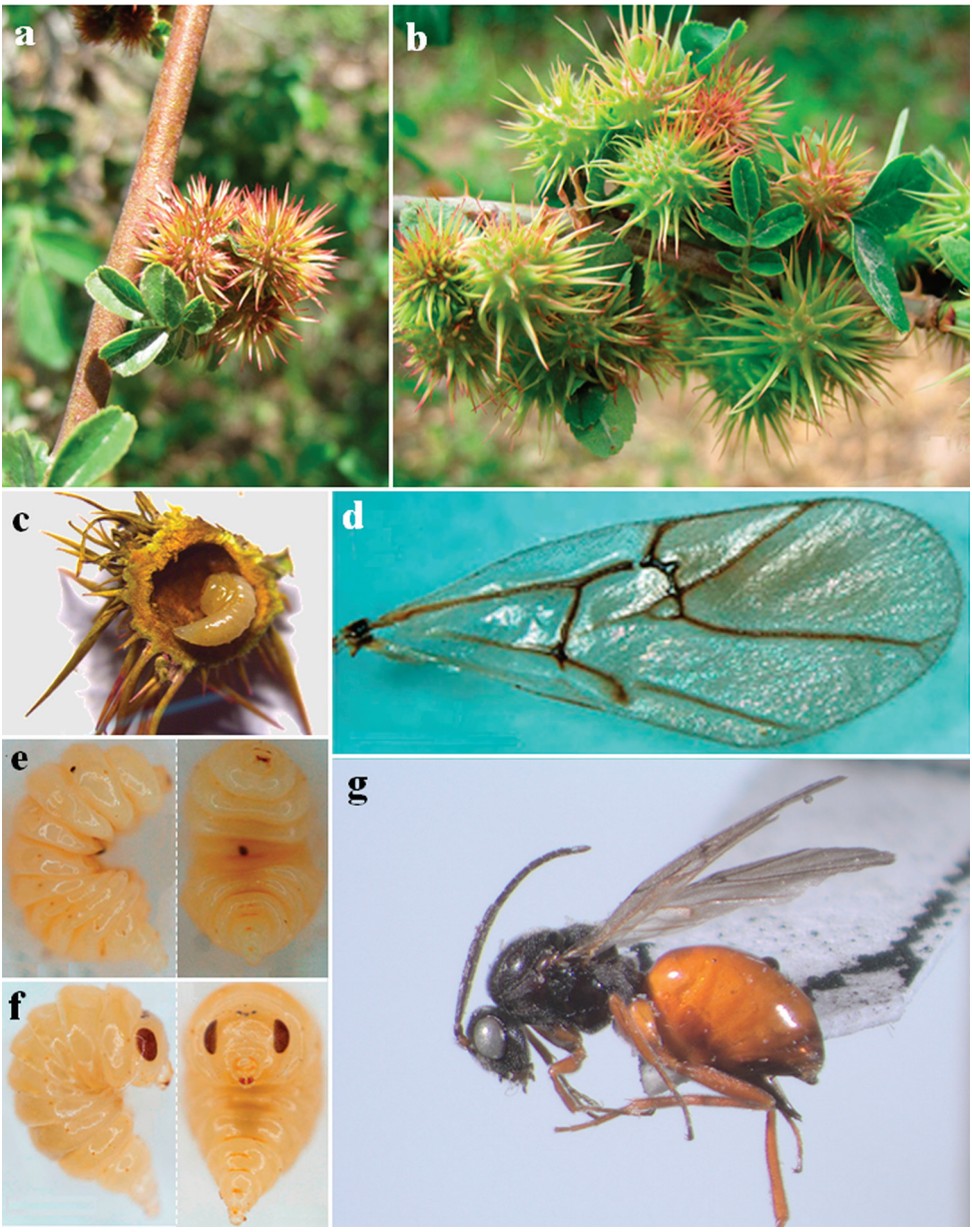

Figure 2. *Diplolepis abei* Pujade-Villar & Wang ♀ sp. nov. **a–b** galls **c** dissected gall with last instar larva **d** forewing **e** lateral and ventral view of the 3rd instar larva **f** lateral and ventral view of the last instar larva **g** lateral habitus.

smooth, extending to half the length of the scutum. Scutellum as long as wide, with parallel lateral margins, rounded posteriorly, dull, rugose, with a more delicate sculpture in the centre of the disk. Scutellar foveae short, transversal, inconspicuous, rugose,

not delimited posteriorly. Mesopleuron smooth and shiny, with a strong transverse dull rugose furrow; mesopleural triangle with numerous delicate wrinkles. Metapleural sulcus reaching the mesopleuron slightly above half of its height; axillula ovate, smooth, distally with some short rugae, without setae; subaxillular bar coriaceous, with very delicate carinae. Dorsellum smooth with some carinae, inferiorly convex. Metanotal trough smooth, shining, with some longitudinal parallel weak wrinkles and without setae; ventral impressed area alutaceous, without delicate longitudinal wrinkles, shining. Propodeum laterally rugose, medially smooth; lateral propodeal carinae anteriorly with three straight carinae and strongly curved outwards in posterior 2/3, delimiting a closed area.

Legs. Tarsal claws simple, without a basal lobe.

Forewing (Fig. 2d). Radial cell partially closed and margin pigmented, 2.3 times longer than wide, first abscissa of radius nearly straight, 2r with an additional median prolongation into the radial cell. Areolet distinct, large. Rs+M well-marked and reaching basalis in the lower third.

Metasoma (Fig. 1h). Slightly longer than head plus mesosoma length (1.1×); in lateral view, 1.4 times longer than high. Second metasomal tergite short, reaching 1/3 if the metasoma; metasomal tergites 2 to 5 without punctures, subsequent tergites alutaceous. Hypopygium plough-shaped, shiny, smooth and large; prominent part of the ventral spine of the hypopygium very thin, 3.0 times longer than broad, with sparse white setae, apical setae short, not extending behind apex of the spine.

Male: unknown.

Gall (Fig. 2a–c). Resembles the North American gall *Diplolepis bicolor* (Harris, 1841), but the new species has more abundant spines and a different coloration. It also resembles *D. japonica* (Walker, 1874), but the shape and the length of the spines are very different. The galls of the new species are spherical-shaped, appearing as monothalamous or one-celled swellings bearing numerous long, stout and sharp-pointed spines that are longer than the diameter of the galls. Their surface is smooth and glabrous. Galls arise on branches, buds or leaf veins of *Rosa sertata* Rolfe × *R. rugosa* Thunb., usually in groups. Young galls are pea green or reddish green and soft, gradually turning greyish green and harder when maturing. The inner cell is large, and the delimiting wall of parenchymatous cells is thick, usually 1.5 mm thick. Mature galls are deciduous.

Host. The new species was collected on the Chinese Kushui rose, a hybrid of *Rosa sertata* Rolfe × *R. rugosa* Thunb. which is cultivated mainly in Gansu Province (China) for its oil. *Rosa rugosa* also occurs at the collection site (a Kushui rose plantation) but no galls were found on them despite growing only a few meters from Kushui roses supporting large numbers of galls. To the best of our knowledge this may be the first known *Diplolepis* species that causes significant agricultural loss. In Gansu Province (China) the *R. sertata* × *R. rugosa* hybrid is commonly planted for its high yields of flowers and oil. The infected shrubs may suffer up to 70% yield loss according to rose oil farmers (We et al. 2014). In infected plantations, *D. abei* is considered a significant pest which reduces rose flower numbers and subsequent rose oil yields.

Table 1. P-distance values for sequences of *Diplolepis abei* sp. nov. and all available *Diplolepis* species. Abbreviations: *dradi*: *Diplolepis radicum*, *drosfol*: *D. rosaefolii*, *dfusif*: *D. fusiformans*, *dtrif*: *D. triforma*, *dspinsa*: *D. spinosa*, *degla*: *D. eglanteriae*, *dbic*: *D. bicolor*, *dbass*: *D. bassetti*, *doreg*: *D. oregonensis*, *dignot*: *D. ignota*, *dvari*: *D. variabilis*, *dgrac*: *D. gracilis*, *dpoli*: *D. polita*, *dnodu*: *D. nodulosa*, *dnebu*: *D. nebulosa*, *dfruc*: *D. fructuum*, *dcalif*: *D. californica*, *dmayr*: *D. mayri*, *drosa*: *D. rosae*, *dnerv*: *D. nervosa*, *dspinsi*: *D. spinosissimae*, *dspnov*: *D. abei* sp. nov.

	dradi	***drosfol***	***dfusif***	***dtrif***	***dspinsa***	***degla***	***dbic***	***dbass***	***doreg***	***dignot***	***dvari***	***dgrac***	***dpoli***	***dnodu***	***dnebu***	***dfruc***	***dcalif***	***dmayr***	***drosa***	***dnerv***	***dspinsi***
dradi																					
drosfol	13.14																				
dfusif	11.81	4.55																			
dtrif	6.54	11.98	10.87																		
dspinsa	6.60	12.59	11.87	7.15																	
degla	15.25	13.90	12.81	13.81	14.31																
dbic	14.17	11.54	9.57	13.56	14.73	12.06															
dbass	14.59	11.36	9.48	13.14	14.98	12.31	6.24														
doreg	6.99	12.63	10.62	7.82	8.90	13.56	11.81	12.48													
dignot	11.59	10.93	9.32	10.48	11.98	11.98	10.40	11.81	10.15												
dvari	11.92	10.75	9.15	10.48	11.98	11.98	10.40	11.81	10.15	0.83											
dgrac	13.09	9.97	8.65	11.48	12.31	12.65	10.40	10.65	10.98	5.66	5.49										
dpoli	14.14	11.13	8.71	12.65	13.70	12.42	5.68	2.61	11.56	10.59	10.59	9.93									
dnodu	7.04	11.68	10.76	5.71	7.60	15.09	13.84	13.87	8.21	10.87	10.87	11.20	12.92								
dnebu	11.76	10.75	9.15	10.32	12.15	11.81	10.23	11.65	9.98	0.17	0.67	5.49	10.43	10.70							
dfruc	11.76	9.62	8.32	10.82	12.48	12.81	9.40	9.15	9.48	8.65	8.65	9.48	7.82	10.21	8.49						
dcalif	5.75	12.38	11.13	6.58	6.66	14.24	14.32	14.32	7.70	11.49	11.74	11.49	13.43	6.86	11.66	10.99					
dmayr	11.00	8.60	7.54	10.39	12.23	12.06	9.13	8.88	9.38	8.71	8.71	9.38	7.76	10.44	8.54	2.35	10.39				
drosa	11.33	9.21	8.21	10.80	12.81	12.40	9.72	9.72	10.18	8.71	8.71	9.55	8.71	10.78	8.54	3.02	10.90	2.09			
dnerv	13.46	10.27	9.76	12.39	13.69	10.23	10.83	11.44	13.78	11.09	11.09	12.48	10.80	13.06	10.92	10.23	12.40	9.71	10.14		
dspinsi	12.27	9.36	8.67	11.48	13.52	12.50	8.84	8.50	12.25	7.91	8.08	9.61	7.71	10.85	7.91	6.03	11.91	5.61	6.29	9.62	
dspn	12.89	10.13	8.89	12.00	13.03	12.26	9.15	10.10	11.05	8.81	8.63	8.80	8.49	11.54	8.63	6.38	12.19	6.90	7.94	10.11	6.39

Biology. Only females are known (Fig. 2g). Galls appear in mid-April and larvae occupy the most part of the larval chamber (Fig. 2c, e, f). Adults emerge in early March of the following year.

Comment. In Wang et al. (2013) and Guo et al. (2013), the material corresponding to this new species is determined as *D. rosae*. In Wang et al. (2013) seven males and nine females were cited. The reason why there are more females (12) in the present paper than those mentioned in Wang et al. (2013) is that the sexes were confused in Wang et al. (2013): four of the specimens were considered males, although they were females. The other four specimens of the 16 mentioned in Wang et al. (2013) are lost.

Distribution. China (Gansu Province).

Etymology. Named in honour of the Japanese cynipidologist and friend, Prof. Yoshihisa Abe (Biosystematics Laboratory, Graduate School of Social and Cultural Studies, Kyushu University, Fukuoka, Japan).

Discussion

According to Abe et al. (2007), *D. brunneipes* (Ashmead, 1904) from Japan has an uncertain status, and *D. kunugi* Shinji, 1938, also from Japan, is not a *Diplolepis*. Thus, based on Abe et al. (2007) a total of 11 species occur in the Palaearctic Region of which five are distributed in the Eastern Palearctic (Fig. 3). Wang et al. (2013) subsequently described three new *Diplolepis* species from China, increasing the number of recorded species present in the Eastern Palaearctic to eight: *D. japonica* (Walker, 1874) from Japan and possibly also from China (see comments below); *D. nigriceps* Vyrzhikovskaja, 1963, *D. nitidus* Vyrzhikovskaja, 1963 and *D. variegatus* Vyrzhikovskaja, 1963 from Kazakhstan; *D. radoszkowskii* Kieffer, 1904 from Uzbekistan and Tajikistan; and *D. flaviabdomenis* Wang, Liw & Chen, 2013, *D. hunanensis* Wang, Liw & Chen, 2013 and *D. minoriabdomenis* Wang, Liw & Chen, 2013 from China). From Asia Minor and Western Palearctic region six species are known: *D. fructuum* (Rübsaamen, 1895) from Turkmenistan; *D. mayri* (Schlechtendal, 1876) from Siberia, Kazakhstan, Turkmenistan, Uzbekistan, Tajikistan and Kyrgyzstan; *D. nervosa* (Curtis, 1838) (= *D. centifoliae* (Hartig, 1840)) from Western Kazakhstan; *D. rosae* (Linnaeus, 1758) from Southern Kazakhstan, Turkmenistan, Uzbekistan, Tajikistan and Kyrgyzstan; *D. spinosissimae* (Giraud, 1859) from Kazakhstan; and a single species, *D. eglanteriae* (Hartig, 1840), from Europe and North Africa (Morocco).

Diplolepis rosae is also recorded from India (Belizin 1957), which must be confirmed, and erroneously from China (Guo et al. 2013; Wang et al. 2013) – this record was a misidentification of the new species described here. Records of *D. nervosa* and *D. spinosissimae* by Kovalev (1965) must be confirmed too. The only *D. japonica* specimen mentioned from China (Wang et al. 2013) collected in Malaise trap presents some differences in the sculpture with respect the redescription of *D. japonica* provided by Yasumatsu and Taketani (1967) (see taxonomic key below); for this reason, we consider

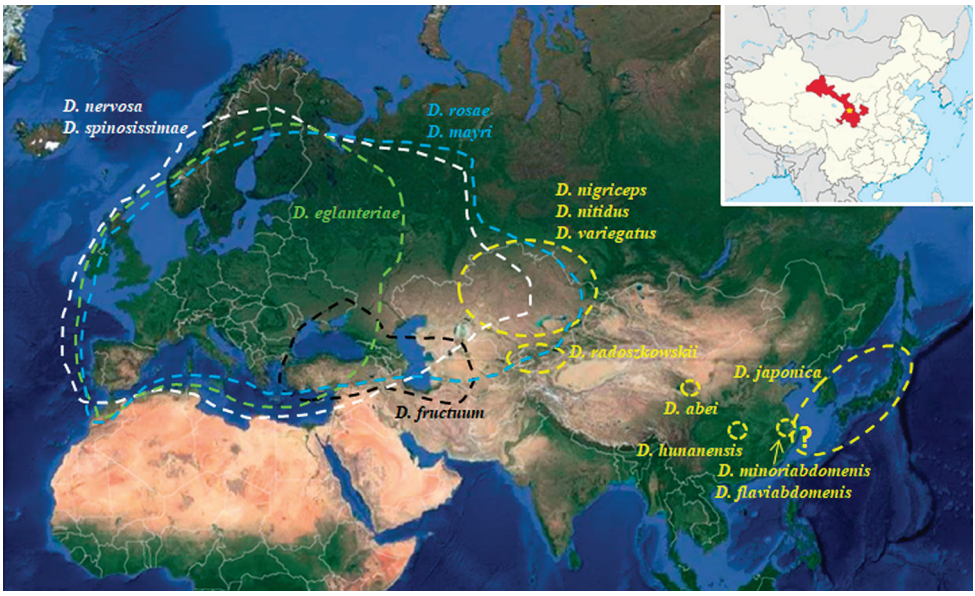

Figure 3. Distribution of the 11 species of *Diplolepis* of the Palearctic; in yellow, the species distributed exclusively in the Eastern Palearctic. Palaearctic map obtained from https://www.google.com/maps/@57.7164944,49.0396796,9792440m/data=!3m1!1e3. The inset image pointing out in red the Gansu Province (and thus the collecting location) was obtained from https://en.wikipedia.org/wiki/Gansu.

this specimen here as *Diplolepis* nr *japonica*, pending collection of more specimens and its gall. *Diplolepis* nr *japonica* could be an undescribed species.

The new species, *D. abei* Pujade-Villar & Wang induces spherical galls with spines resembling *D. japonica* and, some forms of *D. nervosa* in the Palaearctic Region. However, *D. abei* differs from these species by producing galls with relatively longer, pointed, hard and woody spines. Adults of *D. nervosa* differ from the new species by having POL slightly longer than OOL, the scutum coriaceous, the scutellum strongly elongated (nearly 2.0 times longer than wide) with subparallel margins and slightly constricted basally, the scutellar foveae present (large, transversely ovate and smooth) and forewings are hyaline (neither with infuscate areas nor smoky marks); on the other hand, in *D. japonica* the radial cell is shorter (around 2.0 times as long as wide), forewings are hardly infuscate around radial cell, the face is coarsely rugose, the mesoscutum is smooth and the 2nd tergite occupies more than half the length of metasoma.

The species of *Diplolepis* present in China can be differentiated from each other according to the following key:

1 Radial cell relatively long, longer than 2.5 times as long as broad (Figs 2d, 4a)....**2**
– Radial cell shorter, around 2.0 times as long as broad (Fig. 4b–d) **3**

2 Radial cell closed, with infuscate veins and 2r vein without projection into the radial cell (Fig. 4a). Malar distance long, around 0.75 times as long as compound eye height..... ***D. flaviabdomenis***

– Radial cell partially open in margin, without infuscate veins and 2r vein with a projection into the radial cell (Fig. 2d). Malar distance shorter, around 0.5 times as long as compound eye height ..... ***D. abei* sp. nov.**

3 Head strongly transverse in frontal view, 1.7 times wider than high (Fig. 4e) and slightly wider than mesosoma. Median mesoscutal line faintly present posteriorly over 1/4 of the entire length of mesoscutum. Occiput sculptured but never with striae. Propodeum sparsely setose **4**

– Head trapezoid-shaped in frontal view, around 1.5 times wider than high (Fig. 4g) and distinctly narrower than mesosoma. Median mesoscutal line absent or only present by a very short depression (extending over 1/10 of mesoscutum length). Occiput smooth and shiny with striae. Propodeum densely pubescent (Fig. 4h)....**5**

4 Vertex and mesoscutum smooth and shiny. Occiput coarsely punctured. From Japan and Korea..... ***D. japonica***

– Vertex (Fig. 4f) and mesoscutum (Fig. 4i) distinctly alutaceous to coriaceous. Occiput coriaceous. From China ..... ***D. japonica***

5 Antennae 12-segmented, with scapus and pedicel yellowish-brown. POL around 2.0 times longer than OOL. Parapsidal lines absent, almost invisible. Radial cell closed (Fig. 4b). Third and following metasomal tergites with distinct punctures dorso-laterally ..... ***D. hunanensis***

– Antennae 14-segmented, with scapus and pedicel black. POL around 3.0 times longer than OOL. Parapsidal lines distinct and extending almost the entirely length of mesoscutum. Radial cell completely open in margin (Fig. 4c). All metasomal tergites without punctures..... ***D. minoriabdomenis***

Diplolepis abei is the first *Diplolepis* associated with a gall from China; *D. flaviabdomenis*, *D. hunanensis* and *D. minoriabdomenis* were described from material collected by Malaise traps (Wang et al. 2013). This new species occurs on *R. sertata* × *rugosa*, and there are around 100 described species of *Rosa* in China (Wu et al. 2003) of which at least 65 species are endemic (eFloras 2008); therefore, the richness of Diplolepidini (*Diplolepis* and *Liebelia*) is probably greater. As an example of how poorly understood *Diplolepis* is in Eastern Palaearctic, a species of *Periclistus* Förster, 1869, which are obligate inquilines of *Diplolepis*, was recently described from China (Pujade-Villar et al. 2015). Its host remains unidentified, but the gall morphology differs from that of *D. abei*.

Finally, *D. abei* Pujade-Villar & Wang is morphologically closely related to '*rosae*' clade according to Pujade-Villar and Plantard (2002). This clade includes four Western Palaearctic species: *D. rosae*, *D. mayri*, *D. fructuum* and *D. spinosissimae*. It is defined morphologically, according to Pujade-Villar (1993), by the following characters: scutellum rounded, medial sulcus absent or rudimentary (in species with smoky wing

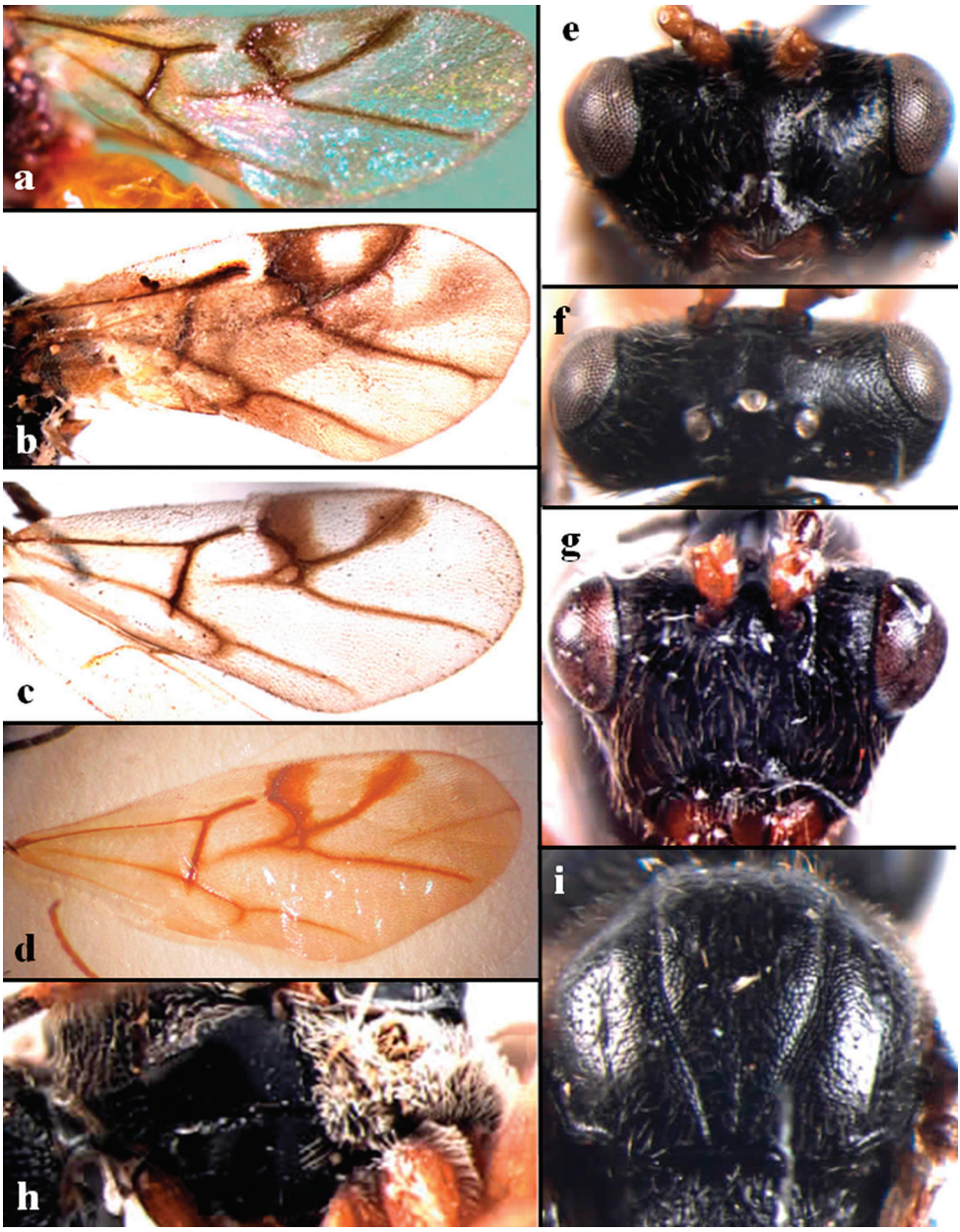

Figure 4. a forewing of *D. flaviabdomenis* **b** forewing of *D. hunanensis* **c** forewing of *D. minoriabdomenis*, and **d** forewing of *D.* nr *japonica* **e** head in frontal view of *D.* nr *japonica* (reused from Wang et al. 2013) **f** head in dorsal view of *D.* nr *japonica* (reused from Wang et al. 2013) **g** head in frontal view of *D. hunanensis* **h** lateral mesosoma of *D. minoriabdomenis* **i** mesoscutum of *D.* nr *japonica*.

areas) or present (in species without strongly smoky areas), F1 at least 1.7 times F2, straight in females (curved and shortly expanded in males), head in frontal view oval and galls not detachable from plant tissues. The '*rosae*' clade has been also confirmed

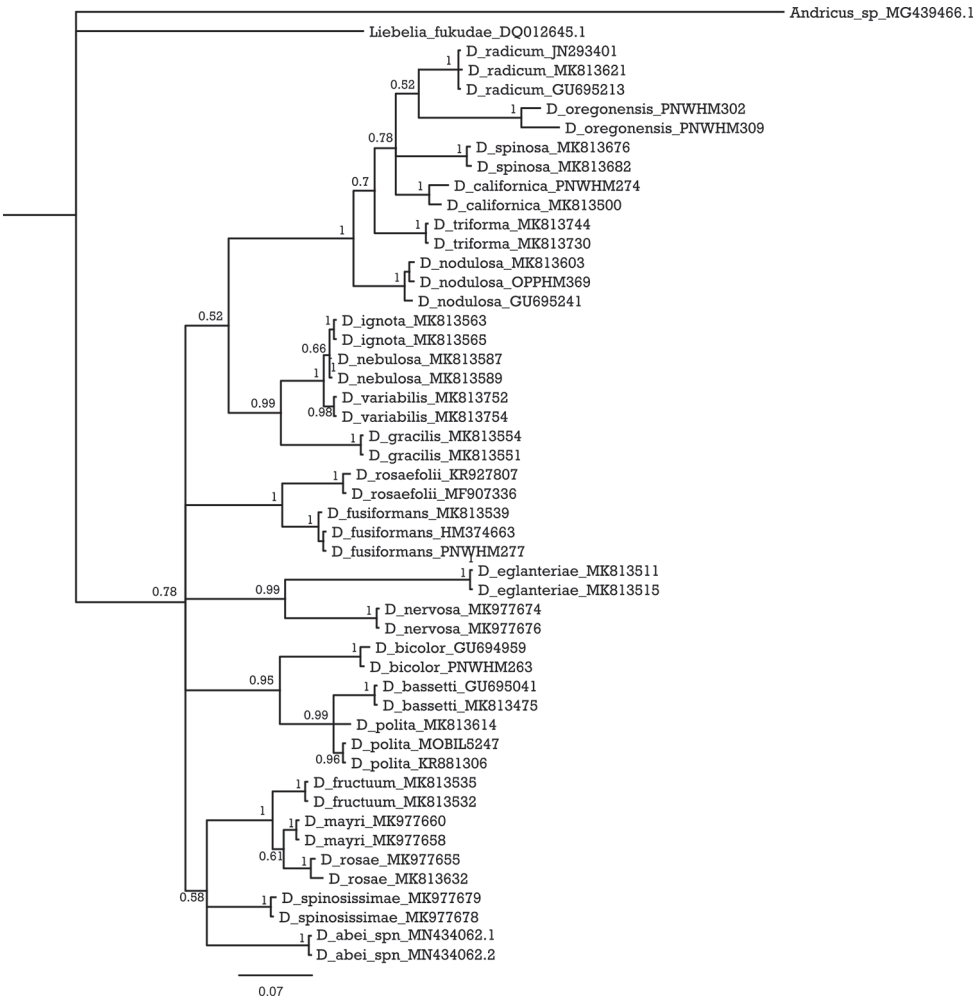

Figure 5. Bayesian inference (BI) tree of the *Diplolepis* species that have available mitochondrial COI sequences. Numbers on the branches represent posterior probabilities (PP).

by Zhang et al. (2019) as the 'Palaearctic multi-chamber subclade'. The closeness of *D. abei* to the '*rosae*' clade is also confirmed by the molecular genetic results based on COI sequences. It is the first species of this group present in China.

Acknowledgments

We are grateful to Yoshihisa Abe (Kyushu University, Fukuoka, Japan) for his comments regarding *Diplolepis japonica* and the gall of the species described here. The authors are grateful to Chris Looney (Washington State Department of Agriculture, Olympia, United States) for his review, comments and suggestions of the manuscript.

The authors are also thankful for Jessica Awad, Yuanmeng M. Zhang and Evandson J. dos Anjos-Silva for their reviews on the submitted manuscript. The molecular work was done at the Interdisciplinary Research Institute on Bio-Nano-Sciences of Babeş-Bolyai University, Treboniu Laurian 42, 400271, Cluj-Napoca Romania. The study was supported by the National Natural Science Foundation of China (31472032 and 31071970) and Zhejiang Provincial Natural Science Foundation for Distinguished Young Scholars (LR14C040002).

References

Abe Y, Melika G, Stone GN (2007) The diversity and phylogeography of cynipid gallwasps (Hymenoptera: Cynipidae) of the Oriental and Eastern Palaearctic Regions, and their associated communities. Oriental Insects 41: 169–212. https://doi.org/10.1080/00305316.2007.10417504

Belizin VI (1957) Rose gall wasps (Hymenoptera, Cynipidae) in the Fauna of the USSR. Entomologicheskoje Obozrenije 36: 925–934. [in Russian]

Burks BD (1979) Superfamily Cynipoidea. In: Krombein KV, Hurd Jr PD, Smith DR, Burks BD (Eds) Catalog of Hymenoptera in America North of Mexico. Symphyta and Apocrita (Parasitica) (Vol. 1). Smithsonian Institution Press, Washington, DC, 1045–1059.

Darriba D, Taboada GL, Doallo R, Posada D (2012) jModelTest 2: more models, new heuristics and parallel computing. Nature Methods 9: 1–772. https://doi.org/10.1038/nmeth.2109

eFloras (2008) Published on the Internet. http://www.efloras.org [accessed 13 January 2019] Missouri Botanical Garden, St. Louis, MO & Harvard University Herbaria, Cambridge, MA.

Folmer O, Black M, Hoeh W, Lutz R, Vrijenhoek R (1994) DNA primers for amplification of mitochondrial cytochrome c oxidase subunit I from diverse metazoan invertebrates. Molecular Marine Biology and Biotechnology 3: 294–299.

Guo R, Wu BM, Zhang WL, Wang YQ, Wang YP (2013) First discovery of an invasive gall-former insect pest, *Diplolepis rosae*, in China. Chinese Journal of Applied Entomology 50(2): 500–504.

Hall T (1999) BioEdit: a user-friendly biological sequence alignment editor and analysis program for Windows 95/98/NT, Nucleic Acids Symposium Series 41: 95–98.

Harris R (1979) A glossary of surface sculpturing. State of California, Department of Food and Agriculture. Occasional Papers of Entomology 28: 1–31.

Johnson M, Zaretskaya I, Raytselis Y, Merezhuk Y, McGinnis S, Madden TL (2008) NCBI BLAST: a better web interface. Nucleic acids research 36: 5–9. https://doi.org/10.1093/nar/gkn201

Kovalev OV (1965) Gall wasps (Hymenoptera, Cynipidae) from the south of the Soviet Far East. Entomologicheskoye Obozrenije 44(1/2): 46–73. [In Russian] [English translation in Entomological Review 44: 25–38]

Kumar S, Stecher G, Li M, Knyaz C, Tamura K (2018) MEGA X: Molecular Evolutionary Genetics Analysis across computing platforms. Molecular Biology and Evolution 35:1547–1549. https://doi.org/10.1093/molbev/msy096

Liljeblad J, Ronquist F (1998) A phylogenetic analysis of higher-level gall wasp relationships (Hymenoptera: Cynipidae). Systematic Entomology 23: 229–252. https://doi.org/10.1046/j.1365-3113.1998.00053.x

Melika G (2006) Gall Wasps of Ukraine. Cynipidae. Vestnik zoologii, supplement 21(1): 1–300.

Mimeur JM (1949) Contribution a l'etude des zoocecidies du Maroc. Encyclopedie Entomologique 24 P. LeChevalier, Paris, 259 pp.

Pujade-Villar J (1993) Revisió de les espécies del génere *Diplolepis* de l'Europa centro occidental (Hym., Cynipidae) amb una especial atenció a la Península Ibérica. Historia Animalium 2: 57–76.

Pujade-Villar J, Plantard O (2002) About the validity of *Diplolepis fructuum* (Rübsaamen) and some new synonyms in *Diplolepis nervosa* (Curtis). In: Melika G, Thuróczy C (Eds) Parasitic Wasps: Evolution, Systematics, Biodiversity and Biological Control. Agroinform, Budapest, 135–142.

Pujade-Villar J, Wang YP, Guo R, Chen XX (2015) Revision on Palaearctic species of *Periclistus* Förster with description of a new species and its host plant gall (Hymenoptera, Cynipidae). ZooKeys 596: 65–75. https://doi.org/10.3897/zookeys.596.5945

Ronquist F (1999) Phylogeny, classification and evolution of the Cynipoidea. Zoologica Scripta 28: 139–164. https://doi.org/10.1046/j.1463-6409.1999.00022.x

Ronquist F, Nordlander G (1989) Skeletal morphology of an archaic cynipoid, *Ibaliarufipes* (Hymenoptera: Ibaliidae). Entomologica Scandinavica, supplement 33: 1–60.

Ronquist F, Teslenko M, Van Der Mark P, Ayres DL, Darling A, Höhna S, Larget B, Liu L, Suchard MA, Huelsenbeck JP (2012) Mrbayes 3.2: Efficient bayesian phylogenetic inference and model choice across a large model space. Systematic Biology 61: 539–542. https://doi.org/10.1093/sysbio/sys029

Ronquist F, Nieves-Aldrey JL, Buffington ML, Liu Z, Liljeblad J, Nylander JAA (2015) Phylogeny, Evolution and Classification of Gall Wasps. The Plot Thickens. PLoS ONE 10(5): e0123301. https://doi.org/10.1371/journal.pone.0123301

Shorthouse JD (2001) Galls induced by cynipid wasps of the genus *Diplolepis* (Cynipidae, Hymenoptera) on cultivated shrub roses in Canada. Acta horticulturae 547: 91–92. https://doi.org/10.17660/ActaHortic.2001.547.10

Shorthouse JD, Ritchie AJ (1984) Description and biology of *Diplolepis triforma*, new species (Hymenoptera: Cynipidae) inducing galls on the stems of *Rosa acicularis*. The Canadian Entomologist 116(12): 1623–1636. https://doi.org/10.4039/Ent1161623-12

Thompson JD, Higgins DG, Gibson TJ (1994) ClustalW: improving the sensitivity of progressive multiple sequence alignment through sequence weighting, position specific gap penalties and weight matrix choice. Nucleic Acids Research 22: 4673–4680. https://doi.org/10.1093/nar/22.22.4673

Wang YP, Guo R, Liu ZW, Chen XX (2013) Taxonomic study of the genus *Diplolepis* Geoffroy (Hymenoptera, Cynipidae, Diplolepidini) in China, with descriptions of three new species. Acta Zootaxonomica Sinica 38(2): 317–327.

We BM, Wang YQ, Zhang WL, Xu Q, Ma H, Wang X (2014) Preliminary report of investigation on *Torymus bedeguaris*. Plant protection 40(5): 148–151. [in Chinese]

Wu C, Li C, Lu L, Jiang S, Alexander V, Bartholomew B, Brach AR, Boufford DE, Ikeda H, Ohba H, Robertson KR, Spongberg SA (2003) Rosaceae AL Jussieu. In: Wu ZY, Raven PH, Hong DY (Eds) Flora of China (Vol. 9). (Pittosporaceae through Connaraceae). Science Press, Beijing, and Missouri Botanical Garden Press, St. Louis.

Yasumatsu K, Taketani A (1967) Some remarks on the commonly known species of the genus Diplolepis in Japan. Esakia 6: 77–86.

Zhang Y, László Z, Looney C, Dénes AL, Hanner R, Shorthouse JD (2019) DNA barcodes reveal inconsistent species boundaries in Diplolepis rose gall wasps and their Periclistus inquilines (Hymenoptera: Cynipidae). The Canadian Entomologist 151(6): 717–727. https://doi.org/10.4039/tce.2019.59